สารที่มีฤทธิ์ทางชีวภาพจากหางไหลขาว, หนามแดง และหนามพรม

นางสาว รุจิรา หวังธีระประเสริฐ

วิทยานิพนธ์นี้เป็นส่วนหนึ่งของการศึกษาตามหลักสูตรปริญญาวิทยาศาสตรดุษฎีบัณฑิต
สาขาวิชาเภสัชเวท ภาควิชาเภสัชเวทและเภสัชพฤกษศาสตร์
คณะเภสัชศาสตร์ จุฬาลงกรณ์มหาวิทยาลัย
ปีการศึกษา 2552

BIOACTIVE COMPOUNDS FROM *DERRIS MALACCENSIS*, *CARISSA CARANDAS* AND *CARISSA SPINARUM*

Miss Ruchira Wangteeraprasert

A Dissertation Submitted in Partial Fulfillment of the Requirements
for the Degree of Doctor of Philosophy in Pharmacognosy
Department of Pharmacognosy and Pharmaceutical Botany
Faculty of Pharmaceutical Sciences
Chulalongkorn University
Academic Year 2009

Thesis Title	BIOACTIVE COMPOUNDS FROM *DERRIS MALACCENSIS*, *CARISSA CARANDAS* AND *CARISSA SPINARUM*
By	Miss Ruchira Wangteeraprasert
Field of Study	Pharmacognosy
Thesis Advisor	Associate Professor Kittisak Likhitwitayawuid, Ph.D.

Accepted by the Faculty of Pharmaceutical Sciences, Chulalongkorn University in Partial Fulfillment of the Requirements for the Doctoral Degree

..... Dean of the Faculty of Pharmaceutical Sciences
(Associate Professor Pintip Pongpech, Ph.D.)

THESIS COMMITTEE

..... Chairman
(Associate Professor Nijsiri Ruangrungsi, Ph.D.)

..... Thesis Advisor
(Associate Professor Kittisak Likhitwitayawuid, Ph.D.)

..... Examiner
(Associate Professor Vimolmas Lipipun, Ph.D.)

..... Examiner
(Associate Professor Rutt Suttisri, Ph.D.)

..... Examiner
(Assistant Professor Boonchoo Sritularak, Ph.D.)

..... External Examiner
(Assistant Professor Lalita Wirasathien, Ph.D.)

รุจิรา หวังธีระประเสริฐ : สารที่มีฤทธิ์ทางชีวภาพจากหางไหลขาว, หนามแดง และหนามพรม (BIOACTIVE COMPOUNDS FROM *DERRIS MALACCENSIS CARISSA CARANDAS* AND *CARISSA SPINARUM*.) อาจารย์ที่ปรึกษาวิทยานิพนธ์หลัก: รศ. ดร. กิตติศักดิ์ ลิขิตวิทยาวุฒิ, 254 หน้า

การศึกษาทางพฤกษเคมีของรากหางไหลขาว สามารถแยกสารใหม่ในกลุ่ม rotenoid ได้ 1 ชนิด คือ 6-oxo-dehydroelliptone และอีก 6 ชนิดเป็นสารที่เคยมีรายงานมาแล้ว คือ 12-deoxo-12α-acetoxyelliptone, 12a-hydroxyelliptone, tephrosin, dehydroelliptone, deguelin และ elliptone การศึกษาทางพฤกษเคมีของลำต้นหนามแดง สามารถแยกสารใหม่ 2 ชนิด คือ (6*S*,7*R*,8*R*)-7a-[(β-glucopyranosyl)oxy]lyoniresinol และ carandoside นอกจากนี้ยังพบสารที่มีรายงานมาแล้วอีก 3 ชนิด ได้แก่ (6*R*,7*S*,8*S*)-7a-[(β-glucopyranosyl)oxy]lyoniresinol, (−)-carissanol และ (−)-nortrachelogenin. ส่วนการศึกษาทางพฤกษเคมีของลำต้นหนามพรม พบสารที่มีรายงานมาแล้ว 12 ชนิด ได้แก่ (−)-carissanol, (−)-nortrachelogenin, scopoletin, (−)-carinol, (+)-cycloolivil, (+)-8-hydroxypinoresinol, (−)-olivil, (−)-secoisolariciresinol, (+)-pinoresinol, carissone, digitoxigenin 3-*O*-β-D-digitalopyranoside และ evomonoside การพิสูจน์โครงสร้างทางเคมีของสารที่แยกได้นี้ อาศัยการวิเคราะห์สเปคตรัมของ UV, IR, MS และ NMR ร่วมกับการเปรียบเทียบข้อมูลของสารที่ทราบโครงสร้างแล้ว ได้ทำการทดลองฤทธิ์จับอนุมูลอิสระ, ฤทธิ์ต้านไวรัสเริม, ฤทธิ์ต้านแบคทีเรียและฤทธิ์ความเป็นพิษต่อเซลล์ของสารที่สกัดแยกได้ พบว่าสารจำพวก lignan จำนวน 10 ชนิดมีฤทธิ์ปานกลางในการจับอนุมูลอิสระ ขณะที่สารอีก 2 ชนิดมีฤทธิ์อ่อน มีสาร 2 ชนิดคือ tephrosin และ elliptone ที่มีฤทธิ์ปานกลางในการต้านไวรัสเริมทั้งสองชนิด และในการทดลองทั้งแบบ post-treatment และ inactivation ส่วน evomonoside นั้นมีฤทธิ์ปานกลางในการต้านไวรัสเริมทั้งสองชนิดเฉพาะในการทดลองแบบ inactivation เท่านั้น นอกจากนี้ไม่มีสารใดเลยที่มีฤทธิ์ต้านแบคทีเรีย อย่างไรก็ตาม พบว่ามีสารบางชนิดมีฤทธิ์ความเป็นพิษต่อเซลล์ สารที่น่าสนใจ คือ elliptone ที่มีฤทธิ์ความเป็นพิษต่อเซลล์เฉพาะเจาะจงในเซลล์มะเร็งชนิด A549 และ MCF7 เมื่อเปรียบเทียบกับเซลล์ปกติชนิด WI-38

ภาควิชา : เภสัชเวทและเภสัชพฤกษศาสตร์ ลายมือชื่อนิสิต .....

สาขาวิชา : เภสัชเวท ลายมือชื่อ. ที่ปรึกษาวิทยานิพนธ์หลัก .....

ปีการศึกษา :2552 .....

4876954133 : MAJOR PHARMACOGNOSY
KEYWORDS : *DERRIS MALACCENSIS* / *CARISSA CARANDAS* / *CARISSA SPINARUM* / FREE RADICAL SCAVENGING ACTIVITY / ANTI-HERPES SIMPLEX VIRUS/ ANTIBACTERIAL ACTIVITY/ CYTOTOXIC ACTIVITY

RUCHIRA WANGTEERAPRASERT : BIOACTIVE COMPOUNDS FROM *DERRIS MALACCENSIS*, *CARISSA CARANDAS* AND *CARISSA SPINARUM*. THESIS ADVISOR : ASSOCIATE PROFESSOR KITTISAK LIKHITWITAYAWUID, Ph. D, 254 pp.

Phytochemical study of the roots of *Derris malaccensis* Prain. led to the isolation of a new rotenoid, namely, 6-oxo-dehydroelliptone, along with six known compounds, 12-deoxo-12α-acetoxyelliptone, 12a-hydroxyelliptone, tephrosin, dehydroelliptone, deguelin and elliptone. Chemical examination of the stems of *Carissa carandas* L. led to the isolation of two new compounds, namely, (6*S*,7*R*,8*R*)-7a-[(β-glucopyranosyl)oxy]lyoniresinol and carandoside, along with three known compounds. The known compounds are (6*R*,7*S*,8*S*)-7a-[(β-glucopyranosyl)oxy]lyoniresinol, (−)-carissanol and (−)-nortrachelogenin. From the stems of *C. spinarum* L., twelve known compounds were isolated, including (−)-carissanol, (−)-nortrachelogenin, scopoletin, (−)-carinol, (+)-cycloolivil, (+)-8-hydroxypinoresinol, (−)-olivil, (−)-secoisolariciresinol, (+)-pinoresinol, carissone, digitoxigenin 3-*O*-β-D-digitalopyranoside and evomonoside. The structures of all of these isolates were determined on the basis of spectroscopic evidence, including comparison of their UV, IR, MS and NMR properties with previously reported data. These isolated compounds were evaluated for their free radical scavenging, anti-herpes simplex virus (HSV-1 and HSV-2), antibacterial and cytotoxic activities. Ten lignans were found to posses moderate free radical scavenging activity whereas two compounds showed weak activity. Two compounds, tephrosin and elliptone, exhibited moderate activity against HSV-1 and HSV-2 in post-treatment and inactivation assays while evomonside showed moderate activity against both types of virus only in the inactivation method. In addition, no compounds showed antibacterial activity at the concentration 128 μg/mL. Interestingly, elliptone possessed cytotoxicity against cancerous cells A549 and MCF7 but showed no toxicity against WI-38 normal cells.

Department : Pharmacognosy and Pharmaceutical Botany
Student's Signature S. Wong

Field of Study : Pharmacognosy
Advisor's Signature K. Likhitwitayawuid

Academic Year : 2009

Acknowledgements

The author would like to express her deepest gratitude to her thesis advisor, Associate Professor Dr. Kittisak Likhitwitayawuid of the Department of Pharmacognosy and Pharmaceutical botany, Faculty of Pharmaceutical Sciences, Chulalongkorn University, for his invaluable advice, useful guidance, endless support, concern, patience and encouragement throughout the course of this study.

The author wishes to express her sincere thanks to Professor Dr. Simon Gibbons of the Department of Pharmaceutical and Biological Chemistry, School of Pharmacy, University of London for providing research opportunities and invaluable suggestions during her stay in the United Kingdom.

The author would like to thank Associate Professor Dr. Vimolmas Lipipun of the Department of Biochemistry and Microbiology and Assistant Professor Dr. Boonchoo Sritularak of the Department of Pharmacognosy and Pharmaceutical botany, Faculty of Pharmaceutical Sciences, Chulalongkorn University, for her kind assistance in the determination of the anti-herpes simplex virus activity and for his beneficial guidance and encouragements, respectively.

The author would like to acknowledge the thesis committee for their constructive suggestions and critical review of her thesis.

The author would like to thank the Thailand Research Fund for a 2005 Royal Golden Jubilee Scholarship and the 90th Anniversary Chulalongkorn University (Ratchadaphiseksomphot) Endowment Fund for financial support.

The author would also like to thank all lecturers and staff members of the Department of Pharmacognosy and Pharmaceutical Botany, and Pharmaceutical Research Instrument Center, Faculty of Pharmaceutical Sciences, Chulalongkorn University for their support and facilities.

The author would like to thank Dr. Mukhlesur Rahman and Miss Khadijo Osman of the Department of Pharmaceutical and Biological Chemistry, School of Pharmacy, University of London for their friendly cooperation and advice.

The author is grateful to all students of the Department of Pharmacognosy and Pharmaceutical Botany, Faculty of Pharmaceutical Sciences, Chulalongkorn University, for their unforgettable friendship and warmth.

Finally, the author wishes to express her infinite gratitude to her family for their love, understanding, assistance and encouragement.

CONTENTS

Page

Page

Page

Page

LIST OF TABLES

TABLE Page

LIST OF FIGURES

FIGURE Page

FIGURE Page

FIGURE Page

FIGURE Page

FIGURE Page

FIGURE Page

FIGURE Page

FIGURE Page

LIST OF SCHEMES

ABBREVIATIONS

$[\alpha]_D^{20}$	=	Specific rotation at 20° and sodium D line (589 nm)
α	=	Alpha
A549	=	Lung cancer cell line
Acetone-d_6	=	Deuterated acetone
ATCC 25943	=	*Staphylococcus aureus* standard strain
β	=	Beta
br	=	Broad (for NMR spectra)
C	=	Concentration
ºC	=	Degree Celsius
calcd	=	Calculated
CD	=	Circular Dichroism
$CDCl_3$	=	Deuterated chloroform
CH_2Cl_2	=	Dichloromethane
$CHCl_3$	=	Chloroform
CH_3CN	=	Acetonitrile
cm	=	Centimeter
^{13}C NMR	=	Carbon-13 Nuclear Magnetic Resonance
1-D	=	One dimensional (for NMR spectra)
2-D	=	Two dimensional (for NMR spectra)
d	=	Doublet (for NMR spectra)
dd	=	Doublet of doublets (for NMR spectra)
δ	=	Chemical shift
DEPT	=	Distortionless Enhancement by Polarization Transfer
DMSO-d_6	=	Deuterated dimethylsulfoxide
DPPH	=	1,1-Diphenyl-2-picrylhydrazyl
EIMS	=	Electron Impact Mass Spectrometry
EMRSA15 and EMRSA16	=	*Staphylococcus aureus* methicillin resistant strain
ESIMS	=	Electrospray Ionization Mass Spectrometry
EtOAc	=	Ethyl acetate

FCC	=	Flash Column Chromatography
g	=	Gram
GF	=	Gel Filtration Chromatography
Hr	=	Hour
HIV	=	Human immunodeficiency virus
^{1}H-NMR	=	Proton Nuclear Magnetic Resonance
HMBC	=	^{1}H-detected Heteronuclear Multiple Bond Correlation
HMQC	=	^{1}H-detected Heteronuclear Multiple Quantum Coherence
H_2O	=	Water
HPLC	=	High Pressure Liquid Chromatography
HRESIMS	=	High Resolution Electrospray Ionization Mass Spectrrmetry
HSV-1	=	Herpes Simplex Virus type 1
HSV-2	=	Herpes Simplex Virus type 2
Hz	=	Hertz
IC_{50}	=	Concentration showing 50% inhibition
IR	=	Infrared
J	=	Coupling constant
Kg	=	Kilogram
L	=	Liter
μL	=	Microliter
λ_{max}	=	Wavelength at maximal absorption
ε	=	Molar absorptivity
M^+	=	Molecular ion
m	=	Multiplet (for NMR spectra)
MCF7	=	Breast cancer cell line
MeOH	=	Methanol
MeOH-d_4	=	Deuterated methanol
mg	=	Milligram
μg	=	Microgram
μL	=	Microliter
μM	=	Micromolar
MHB	=	Mueller-Hinton broth

MHz	=	Mega Hertz
MIC	=	Minimum inhibitory concentration
Min	=	Minute
mL	=	Milliliter
mm	=	Millimeter
MS	=	Mass spectrum
MTT	=	3-[4,5-Dimethylthiazol-2-yl]-2,5-diphenyltetrazolium bromide
MW	=	Molecular weight
m/z	=	Mass to charge ratio
nm	=	Nanometer
NMR	=	Nuclear Magnetic Resonance
NOESY	=	Nuclear Overhauser Effect Spectroscopy
ppm	=	Part per million
Prep TLC	=	Preparative Thin Layer Chromatography
pyridine-d_5	=	Deuterated pyridine
q	=	Quartet (for NMR spectra)
RN4220	=	*Staphylococcus aureus* which possesses the MsrA macrolide efflux protein
ROESY	=	Rotating-Frame Overhauser Enhancement Spectroscopy
s	=	Singlet (for NMR spectra)
SA1199B	=	*Staphylococcus aureus* which overexpresses the norA gene encoding the NorA MDR efflux pump)
S. aureus	=	*Staphylococcus aureus*
SPE	=	Solid Phase Extraction
spp.	=	Species
t	=	Triplet (for NMR spectra)
TLC	=	Thin Layer Chromatography
UV-VIS	=	Ultraviolet and Visible spectrophotometry
VLC	=	Vacuum Liquid Column Chromatography
WI-38	=	Normal human lung fibroblast line
XU212	=	*Staphylococcus aureus* tetracycline resistant strain

CHAPTER I

INTRODUCTION

Oxidation, which is the transfer of electrons from one atom to another, represents an essential part of aerobic life and our metabolism, since oxygen is the ultimate electron acceptor in the electron flow system that produces energy in the form of ATP. However, problems may arise when the electron flow becomes uncoupled, generating free radicals. Examples of oxygen-centered free radical, known as reactive oxygen species (ROS), include superoxide ($O_2^{\bullet -}$), peroxyl ($ROO^{\bullet}$), alkoxyl ($RO^{\bullet}$), hydroxyl ($HO^{\bullet}$) and nitric oxide ($NO^{\bullet}$) (Pietta, 2000).

At high concentrations, ROS can be important mediators of damage to cell structures, including lipids and membranes, proteins and nucleic acids. The harmful effects of ROS are balanced by the antioxidant action of non-enzymatic antioxidants in addition to antioxidant enzymes. Despite the presence of the cell's antioxidant defence system to counteract oxidative damage from ROS, oxidative damage accumulates during the life cycle, and radical-related damage to DNA, proteins and lipids has been proposed to play a key role in the development of age-dependent diseases such as cancer, arteriosclerosis, arthritis, neurodegenerative disorders and other conditions (Valko *et al*., 2006).

The growing interest in natural antioxidants of plant origin is due to the fact that epidemiological studies have indicated, although with some controversial results, that the dietary intake of phenolic compounds is associated with a lower risk of age-related health problems including cancer and coronary heart diseases. Also, the demand for natural antioxidants has increased because of questions about the long-term safety and negative consumer perception of the commonly used synthetic antioxidants BHT (butylated hydroxytoluene) and BHA (butylated hydroxyanisol) (Eklund *et al*., 2005). Over the past decade evidence has been accumulated that plant polyphenols are an important class of defense antioxidants. These compounds are widespread virtually in all plant foods, often at high levels, and include phenols, phenolic acids, flavonoids, tannins, and lignans (Pietta, 2000).

Herpes simplex viruses (both types, HSV-1 and-2) are pathogenic to humans. Among HSV-related pathology, genital herpes is an important sexually transmitted

disease (STD) commonly caused by HSV-2, with the exception of a minority of cases caused by HSV-1. The clinical manifestation of the disease exhibits different severity in normal and immuno-competent hosts; in addition, several patients always encounter recurrent attacks and in immuno-compromised patients and neonates. HSV infections can cause serious systemic illnesses. Moreover, HSV-2 has been reported to be a high risk factor for HIV infection. Therefore, the discovery of novel anti-HSV drugs deserves great efforts (Khan *et al*., 2005).

Multidrug-resistant *Staphylococcus aureus* (MRSA) infections, particularly those caused by methicillin-resistant *S. aureus*, have been a major threat to public health in hospitals and the community during the past decade. In the UK, the number of MRSA infections rose by nearly 5% between 2003 and 2004. Despite new advances in antibiotic development, MRSA infections remain a considerable concern owing to the anticipated resistance to these new drugs. In 2002, MRSA strains fully resistant to vancomycin were isolated in the US. Resistance to linezolid has also been reported in some patients receiving prolonged antibiotic treatment in the US. Therefore, there is an urgent need to develop new classes of antibiotics to fight the problem of drug resistance (Shiu and Gibbons, 2006).

Plants have a long history of use in the treatment of cancer. There are more than 3,000 plant species in Hartwell (1982) lists that have reportedly been used in the treatment of cancer, but in many instances, the “cancer” is undefined, or reference is made to conditions such as “hard swellings”, abscesses, calluses, corns, warts, polyps, or tumors, to name a few. Such symptoms would generally apply to skin, “tangible”, or visible conditions, and may indeed sometimes correspond to a cancerous condition, but many of the claims for efficacy should be viewed with some skepticism because cancer, as a specific disease entity, is likely to be poorly defined in terms of folklore and traditional medicine. Nevertheless, despite these observations, plants have played an important role as a source of effective anti-cancer agents, and it is significant that over 60% of currently used anti-cancer agents are derived in one way or another from natural sources, including plants, marine organisms and micro-organisms (Cragg and Newman, 2005).

The search for anti-cancer agents from plant sources started in earnest in the 1950s with the discovery and development of the vinca alkaloids, vinblastine and vincristine, and the isolation of the cytotoxic podophyllotoxins. As a result, the United States National Cancer Institute (NCI) initiated an extensive plant collection program

in 1960, focused mainly in temperate regions. This led to the discovery of many novel chemotypes showing a range of cytotoxic activities including the taxanes and camptothecins, but their development into clinically active agents spanned a period of some 30 years, from the early 1960s to the 1990s. This plant collection program was terminated in 1982, but the development of new screening technologies led to the revival of collections of plants and other organisms in 1986, with a focus on the tropical and sub-tropical regions of the world. It is interesting to note, however that no new plant derived clinical anti-cancer agents have, as yet, reached the stage of general use, but a number of agents are in preclinical development (Cragg and Newman, 2005).

The genus *Derris* belongs to the family Leguminosae, the second-largest family of flowering plants (Evans, 2002). This genus consists of about 80 species generally distributed in the tropical regions of Asia and East Africa and is widely used in cattle and sheep dips for the control of ticks and other ectoparasites (Thasana, Chuankamnerdkarn and Ruchirawat, 2001).

The species of *Derris* in Thailand, according to Smitinand (2001), are as follows.

Derris alborubra Hemsl.	เถาตาปลา Thao tap la (Nakhon Ratchasima).
D. amoena Benth.	ย่านสาวคำ Yan sao kham (Peninsular); ยานะเละ Ya-na-le (Malay-Narathiwat).
D. dalbergioides Baker (*D. microphylla* Hassk.)	ค่างเต้น Khang ten (Prachuap Khiri Khan); ดีงู Di ngu (Surat Thani); แปรงปืน Praeng puen, มะนามจาย Ma nam chai (Chumphon); พันแต Phan tae (Narathiwat); มะตาฮะจิง Ma-ta-ha-ching, มะแตฮาจิง Ma-tae-ha-ching (Malay-Narathiwat).
D. elliptica (Roxb.) Benth.	กะลำเพาะ Kalam pho (Phetchaburi); เครือไหลน้ำ Khruea lai nam, หางไหลแดง Hang lai daeng, ไหล Lai, ไหลน้ำ Lai nam (Northern); โพตะโกส้า Pho-ta-ko-sa (Karen-Mae Hong Son); อวดน้ำ Uat nam (Surat Thani); Tuba root, Derris.

D. indica Bennet.	กายี Ka yi (Peninsular); ขยี้ Kha yi (CHumphon); เพาะดะปากี้ Pho-da-pa-ki (Malay-Songkhla); ปารี Pa-ri (Malay-Narathiwat); มะปากี Ma-pa-ki (Malay-Pattani); ราโยด Ra yot (Pattani); หยีน้ำ Yi nam (Peninsular).
D. kerrii Craib	กางขี้มอด Kang khi mot (Northern).
D. malaccensis Prain	ยานาเละ Ya-na-lae (Malay-Narathiwat).
D. reticulata Craib	ชะเอมเหนือ Cha em nuea (Kanchanaburi).
D. robusta (DC.) Benth.	ขางไส้ช้าง Khang sai chang, คุ่ Khu, เดื่อคู่ Duea khu (Phitsanulok); ขี้มอด Khi mot (Saraburi); พี้จั่น Phi chan, มะเล้น Malen (Chanthaburi); ระวิดตัวผู้ Ra-wit-tua-phu, ระวิดตัวเมีย Ra-wit-tua-mia, ลาวิด La-wit (Chong-Chanthaburi, Trat); ฮางคาว Hang khao (Northern).
D. scandens (Roxb.) Benth.	เครือเขาหนัง Khruea khao nang, เถาตาปลา Thao ta pla (Nakhon Ratchasima); เถาวัลย์เปรียง Thao wan priang (Central); พานไสน Phan sanai (Chumphon).
D. thorelii Craib	ขี้ช้างเฒ่า Khi chang thao, เครือตับปลา Khruea tap pla (Northern); เครือตาปลา Khruea tap la, เครือไหล Khruea lai (Chiang Rai); ออดอ้อ Ot o (Loei).
D. thyrsiflora (Benth.) Benth.	= *Aganope thyrsiflora* (Benth.) Polhill
D. trifoliate Lour. (*D. uliginosa* (Willd.) Benth.)	แควบทะเล Khwaep thale, ถอบแถบน้ำ Thop thaep nam, ผักแถบ Phak thaep (Central); ถอบแถบทะเล Thop thaep thale, (Phetchaburi); ถั่วน้ำ Tuan am (Narathiwat); ทับแถบ Thap thaep (Samut Songkhram).

Derris malaccensis Prain is a climber known in Thailand as “Haang-lai-khao,” with its roots locally used as insecticidal and piscicidal agents (Thasana,

Chuankamnerdkarn, and Ruchirawat, 2001). It is found throughout Malaysia and cultivated outside Malaysia in India, southern China and tropical America. It is a liana up to at least 15 meters long. Root: grayish brown, young shoots adpressed pubescent. Leaves: leaflets 5-9, glabrous above, adpressed pubescent beneath. Flowers: glabrous pink calyx and whitish or pinkish corolla, standard with basal callosities, glabrous. Fruits: oblong with a narrow wing along both sides, rarely without wings (Padua, Bunyapraphatsara, and lemmens, 1999).

The genus *Carissa* (Apocynaceae) comprises about 35 species (Evans, 2002) distributed in Africa, Asia and Australia (Hooker, 1882). They are spinous, densely branch and usually erect shrubs. Leaves are opposite, small and coriaceous. Flowers are in terminal and axillary peduncled 3-chotomous cymes. Calyx is 5-partite, glandular within or not, segments acute. Corolla-tube is cylindric, throat naked and lobes overlapping to the right (in the Indian species). Stamens are at the top of the tube, included, anthers lanceolate, cells rounded at the base. Ovary has 2-celled, style filiform, stigma fusiform or columnar, minutely 2-fid, ovules 1-4 in each cell, rarely more. Berry is ellipsoid or globose, 2-(or by abortion 1-) celled. Seeds are usually 2, peltately attached to the septum, albumen fleshy, cotyledons ovate.

The species of *Carissa* in Thailand, according to Smitinand (2001), are as follows.

Carissa carandas L.	มะนาวไม่รู้โห่ Manao mairu ho (Central); มะนาวโห่ Manao ho (Peninsular); หนามขี้แฮด Nam khi haet (Chiang Mai); หนามแดง Nam daeng (Bangkok); Carunda, Christ's thorn
C. spinarum L. (*C. Cochinchinensis* Pit.) (*C. laotica* Pitard *var. ferruginea* Kerr)	ขี้แฮด Khi haet (Northern); พรม Phrom, หนามพรม Nam phrom (Central).

C. carandas L. is a shrub usually reaching 2-3 m in height, rich in white latex and branched sharp spines. The leaves are simple, opposite, elliptic or obovate, 3-7 cm x 1.5-4.5 cm. The inflorescences develop in the axil of leaves. The color of the corolla is white and that of the corolla tube is pale rose. Fruits are ellipsoid, purplish black when ripe (Faculty of Pharmaceutical Sciences, Mahidol University. 1995).

C. spinarum L. is a shrub reaching 4-5 m with white latex and branched sharp spines. The leaves are simple, opposite, elliptic, 2.5-4 cm x 1.5-2.5 cm. The

inflorescences develop in the terminal branch. The corolla tube is white. The flowers are fragrant. Fruits are fusiform, purplish black when ripe (Faculty of Pharmaceutical Sciences, Mahidol University. 1995).

A number of chemical investigations of *D. malaccensis* have shown the presence of rotenoids (Thasana *et al*., 2001; Takashima *et al*., 2002) whilst lignans and terpenoids were found in *C. carandas* (Pal, Kulshreshtha and Rastogi, 1975; Siddiqui *et al.*, 2002) and *C. spinarum* (Rao *et al*., 2005).

The main objectives in this study were as follows.

1. To isolate secondary metabolites from the root of *D. malaccensis* and the stems of *C. carandas* and *C. spinarum*.

2. To determine the structures of the isolated compounds.

3. To evaluate the free radical scavenging, anti-herpes simplex virus, antibacterial and cytotoxic activity of the isolated compounds.

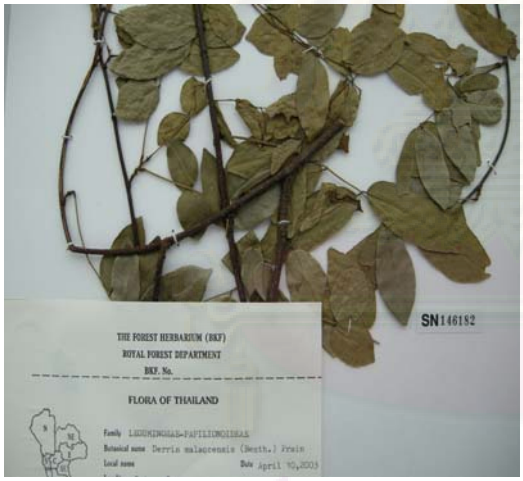

Figure 1 *Derris malaccensis* Prain

Figure 2 *Carissa carandas* L.

Figure 3 *Carissa spinarum* L.

CHAPTER II

HISTORICAL

1. Chemical constituents of *Derris* spp.

Most of isolated compounds from the genus *Derris* can be classified as flavonoids, which include rotenoids, isoflavones and chalcones. In addition, other classes of natural compounds such as coumarins and miscellaneous substances have been found (Table 1).

Table 1 Distribution of chemical constituents in the genus *Derris*

Plant and compound	Category	Plant part	Reference
Derris araripensis			
3,4,5,6-Tetramethoxy-(7,8,2″,3″)-furanoflavan [**1**] 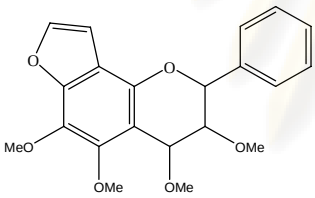	Flavan	Root	Nascimento and Mors, 1981
3,5,6-Trimethoxy-(7,8,2″,3″)-furanoflavone [**2**] 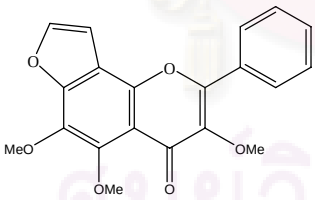	Flavone	Root	Nascimento and Mors, 1981
3,6-Dimethoxy-6″,6″-dimethyl-(7,8,2″,3″)-chromenoflavone [**3**] 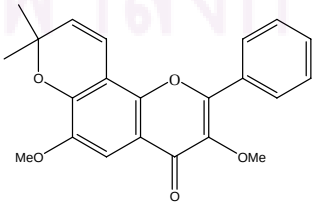	Flavone	Root	Nascimento and Mors, 1981

Table 1 (continued)

Plant and compound	Category	Plant part	Reference
3′,4′-Methylenedioxy-3,5,6-trimethoxy-(7,8,2′′,3′′)-furanoflavanone [**4**] 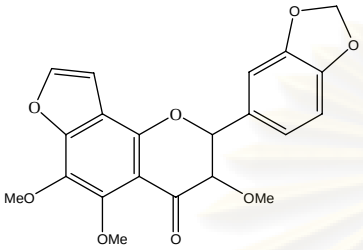	Flavanone	Root	Nascimento and Mors, 1981
3′,4′-Methylenedioxy-3,5,6-trimethoxy-(7,8,2′′,3′′)-furanoflavone [**5**] 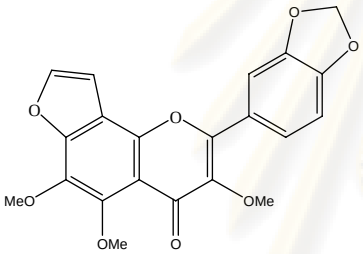	Flavone	Root	Nascimento and Mors, 1981
3′,4′-Methylenedioxy-3,6-dimethoxy-6′′,6′′-dimethyl-(7,8,2′′,3′′)-chromenoflavone [**6**] 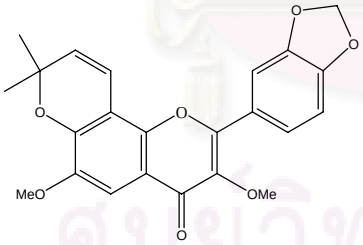	Flavone	Root	Nascimento and Mors, 1981
3′,4′-Methylenedioxy-5,6-dimethoxy-(7,8,2′′,3′′)-furanoflavone [**7**] 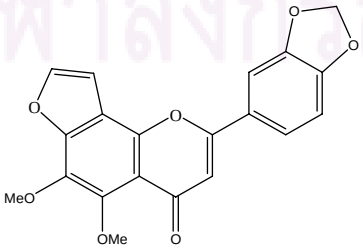	Flavone	Root	Nascimento and Mors, 1981

Table 1 (continued)

Plant and compound	Category	Plant part	Reference
3,4-Methylenedioxy-5′-hydroxy-2′,3′-methoxy-(3′,4′,2′′,3′′)-furanodihydrochalcone [**8**] 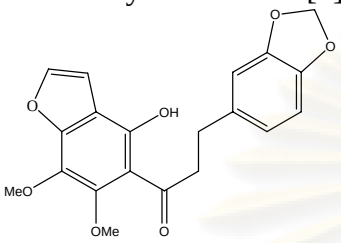	Chalcone	Root	Nascimento and Mors, 1981
3′,4′-Methylenedioxy-5-hydroxy-6-methoxy-(7,8,2′′,3′′)-furanoflavanone [**9**] 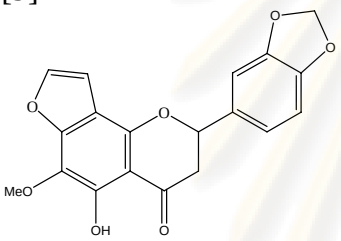	Flavanone	Root	Nascimento and Mors, 1981
Derris elliptica			
(−)-Deguoic acid [**10**] 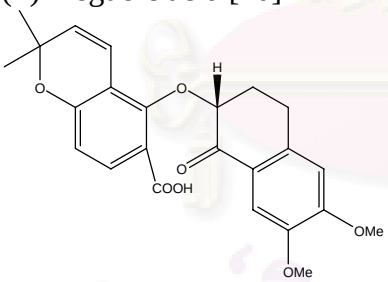	Rotenoid	Root	Lu *et al*., 2009b
(−)-Rotoic acid [**11**] 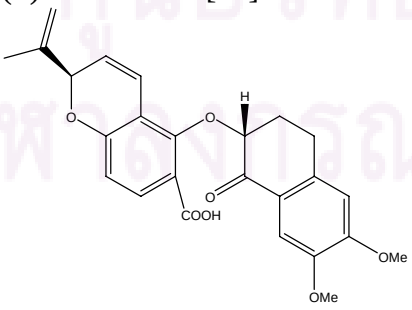	Rotenoid	Root	Lu *et al*., 2009b

Table 1 (continued)

Plant and compound	Category	Plant part	Reference
(6a*R*,12a*R*,4′*R*,5′*S*)-4′,5′-Dihydro-4′,5′-dihydroxytephrosin [**12**] 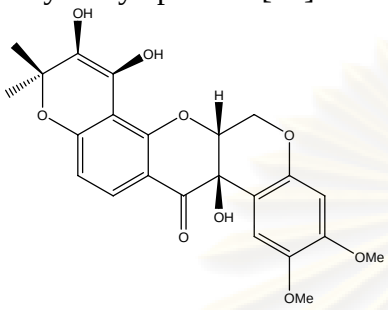	Rotenoid	Root	Lu *et al*., 2009b
11,4′,5′-Trihydroxy-6a,12a-dehydrodeguelin [**13**] 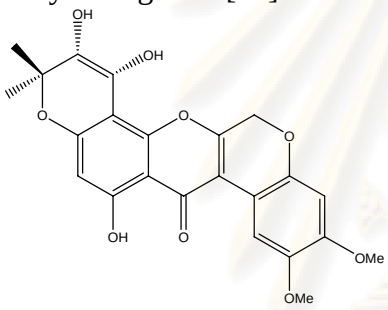	Rotenoid	Root	Lu *et al*., 2008b
12-Deoxo-12a-acetoxyelliptone [**14**] 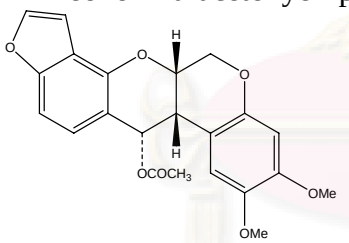	Rotenoid	Root	Lu *et al*., 2009b
2,5-Dihydroxymethyl-3,4-dihydroxypyrrolidine [**15**] 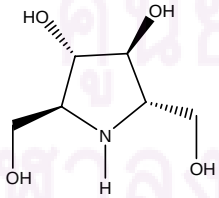	Imino-alcohol	Leaves	Welter and Jadot, 1976

Table 1 (continued)

Plant and compound	Category	Plant part	Reference
2-Hydroxy-5-aminorotenonone [**16**] 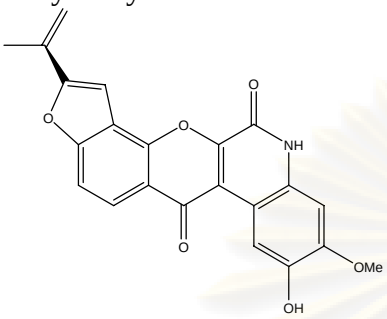	Rotenoid	Root	Lu and Liang, 2009a
3′-Methoxydaidzein [**17**] 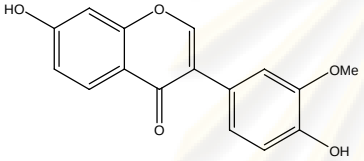	Rotenoid	Root	Lu *et al*., 2008a
4′,5′-Dihydroxy-6a,12a-dehydrodeguelin [**18**] 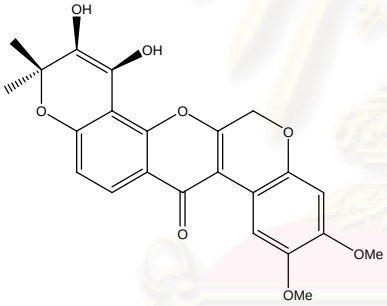	Rotenoid	Root	Lu *et al*., 2008b
6′-Hydroxy-6a,12a-dehydrorotenone [**19**] 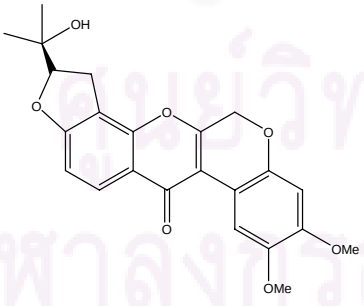	Rotenoid	Root	Lu *et al*., 2009b

Table 1 (continued)

Plant and compound	Category	Plant part	Reference
6-Hydroxy-6a,12a-dehydrodeguelin [**20**] 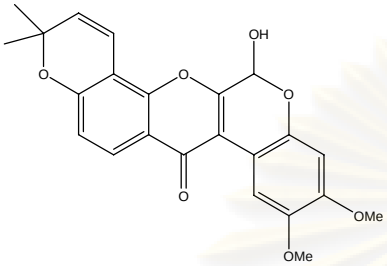	Rotenoid	Root	Lu *et al*., 2009b
7′-Hydroxy-6a,12a-dehydrodeguelin [**21**] 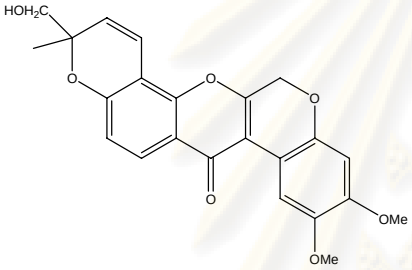	Rotenoid	Root	Lu *et al*., 2009b
Daidzein [**22**] 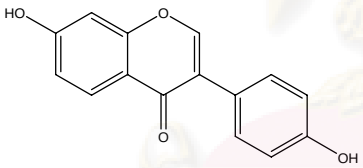	Isoflavone	Root	Lu *et al*., 2008a
Deguelin [**23**] 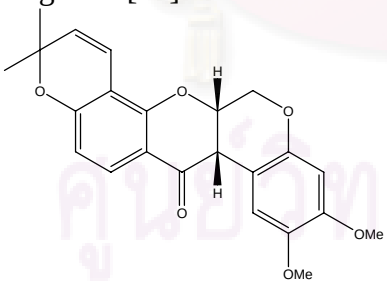	Rotenoid	Root	Lu *et al*., 2008b
Demethylvestitol [**24**] 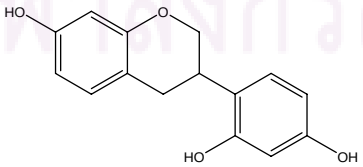	Isoflavan	Root	Lu *et al*., 2008a

Table 1 (continued)

Plant and compound	Category	Plant part	Reference
Dihydrodaidzein [**25**] 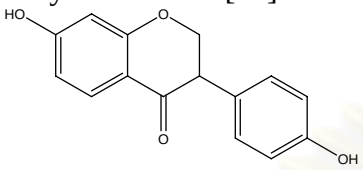	Isoflavan	Root	Lu *et al*., 2008a
Elliptoic acid [**26**] 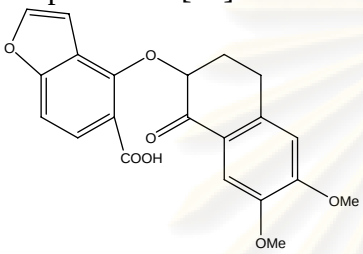	Rotenoid	Root	Lu *et al*., 2009a
Formononetin [**27**] 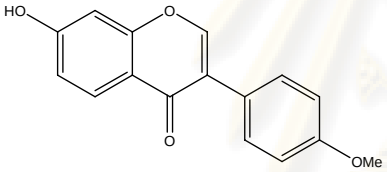	Isoflavone	Root	Lu *et al*., 2008a
Genistein [**28]** 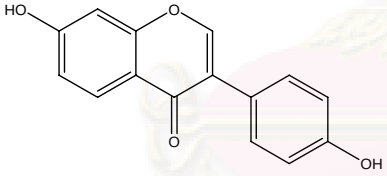	Isoflavone	Root	Lu *et al*., 2008a
Prunetin [**29**] 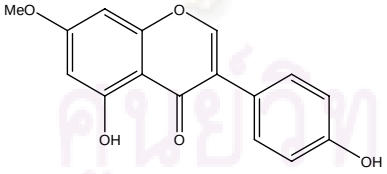	Isoflavone	Root	Lu *et al*., 2008a
Rotenone [**30**] 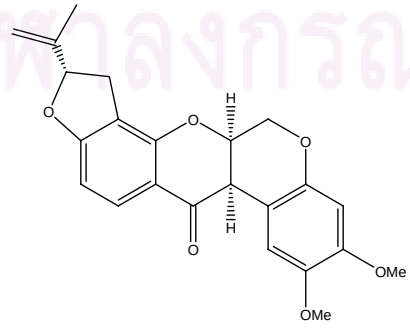	Rotenoid	Root	Lu *et al*., 2008b; Sae-Yun *et al*., 2006

Table 1 (continued)

Plant and compound	Category	Plant part	Reference
Derris indica			
2′-Methoxy-4′,5′-methylenedioxy (7,8:2″,3″)-furanoflavone [**31**] 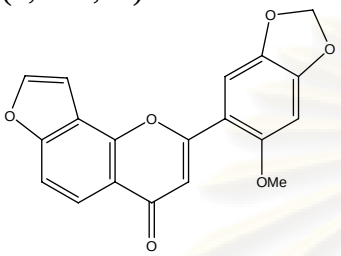	Flavone	Stem, Root	Koysomboon *et al*., 2006
3,3′,4′-Trihydroxy-4H-furo(2,3-h)chromen-4-one [**32**] 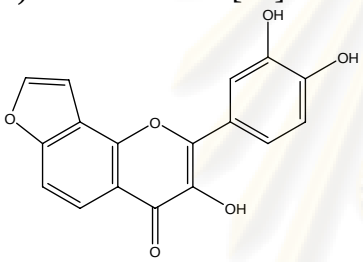	Flavonol	Root	Rao *et al*., 2009
3′,4′-Dihydroxy-4H-furo(2,3-h)chromen-4-one [**33**] 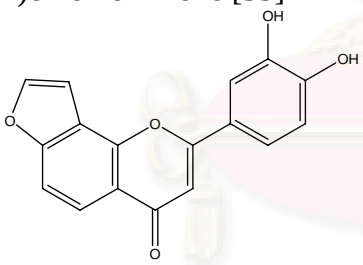	Flavone	Root	Rao *et al*., 2009
3′,4′-Methylenedioxy-10-methoxy-7-oxo(2)benzopyrano(4,3-b)benzopyran [**34**] 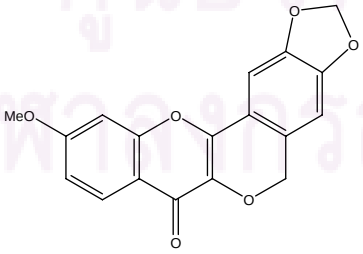	Flavone	Stem, Root	Koysomboon *et al*., 2006

Table 1 (continued)

Plant and compound	Category	Plant part	Reference
3,7-Dimethoxyflavone [**35**] 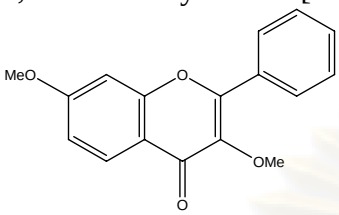	Flavone	Stem, Root	Koysomboon *et al*., 2006
3-Methoxy-(3″,4″-dihydro-3″,4″-diacetoxy)-2″,2″-dimethyl-(7,8:5″,6″)-pyranoflavone [**36**] 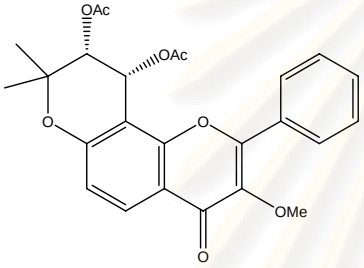	Flavone	Stem, Root	Koysomboon *et al*., 2006
3-Methoxy-7-hydroxy-3′,4′-methylenedioxyflavone [**37**] 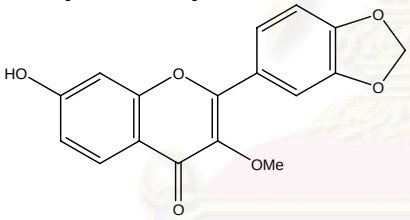	Flavone	Root	Rao *et al*., 2009
7,4′-Dimethoxy-5-hydroxyflavone [**38**] 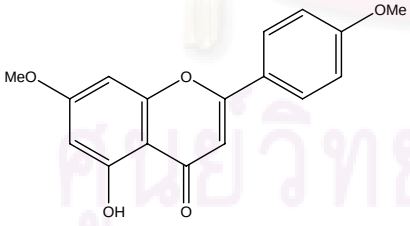	Flavone	Root	Rao *et al*., 2009

Table 1 (continued)

Plant and compound	Category	Plant part	Reference
7-*O*-Methylchrysin [**39**] 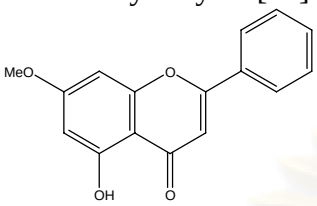	Flavone	Root	Rao *et al*., 2009
8,4′-Dimethoxy-7-*O*-γ,γ-dimethylallylisoflavone [**40**] 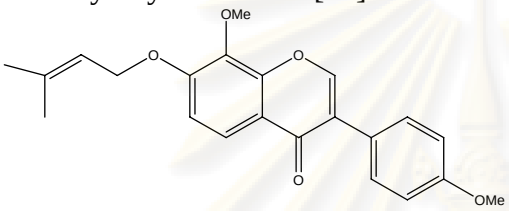	Isoflavone	Stem, Root	Koysomboon *et al*., 2006
Desmethoxy kanugin [**41**] 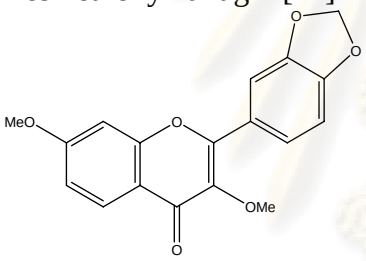	Flavone	Stem, Root	Koysomboon *et al*., 2006
Fisetin tetramethyl ether [**42**] 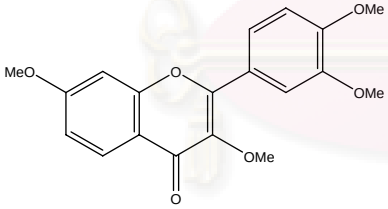	Flavone	Root	Rao *et al*., 2009
Karanjachromene [**43**] 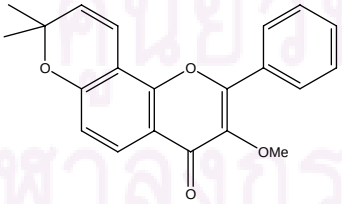	Flavone	Stem, Root	Koysomboon *et al*., 2006

Table 1 (continued)

Plant and compound	Category	Plant part	Reference
Karanjin [**44**] 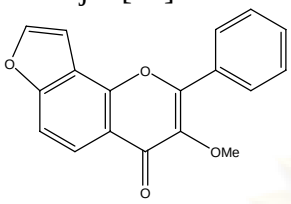	Flavone	Stem, Root	Koysomboon *et al*., 2006; Rao *et al*., 2009
Laceolatin B [**45**] 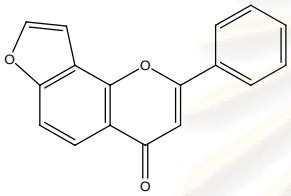	Flavone	Stem, Root	Koysomboon *et al*., 2006
Maackiain [**46**] 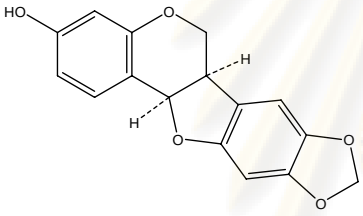	Pterocarpan	Stem, Root	Koysomboon *et al*., 2006
Medicarpin [**47**] 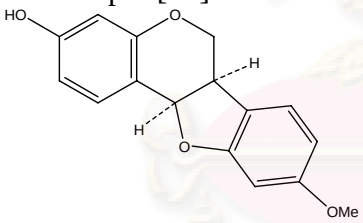	Pterocarpan	Stem, Root	Koysomboon *et al*., 2006
Ovalitenone [**48**] 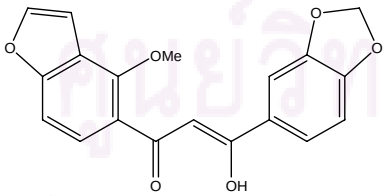	Chalcone	Root	Rao *et al*., 2009

Table 1 (continued)

Plant and compound	Category	Plant part	Reference
Pachycarin D [**49**] 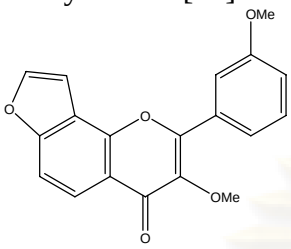	Flavone	Stem, Root	Koysomboon *et al*., 2006
Pinnatin [**50**] 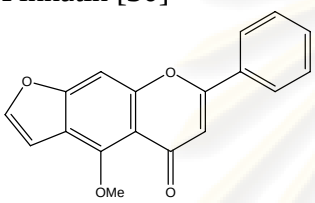	Flavone	Stem, Root	Koysomboon *et al*., 2006; Rao *et al*., 2009
Piperonylic acid [**51**] 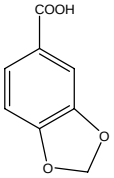	Benzoic acid	Root	Rao *et al*., 2009
Pongachromene [**52**] 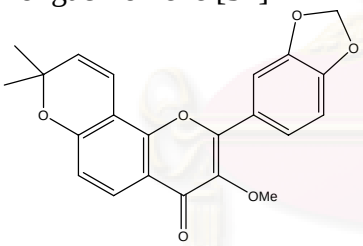	Flavone	Stem, Root	Koysomboon *et al*., 2006; Rao *et al*., 2009
Pongaglabrone [**53**] 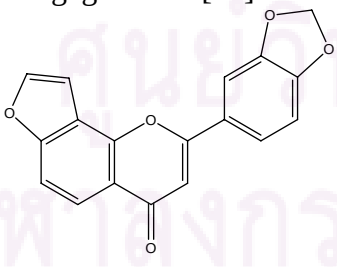	Flavone	Root	Rao *et al*., 2009

Table 1 (continued)

Plant and compound	Category	Plant part	Reference
Pongamol [**54**] 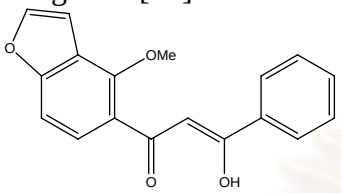	Chalcone	Root	Rao *et al*., 2009
Pongapin [**55**] 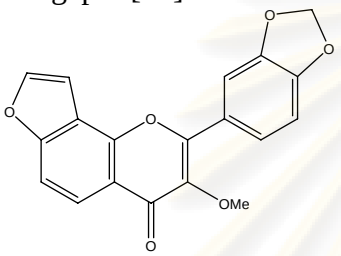	Flavone	Root	Rao *et al*., 2009
Pongapinone-B [**56**] 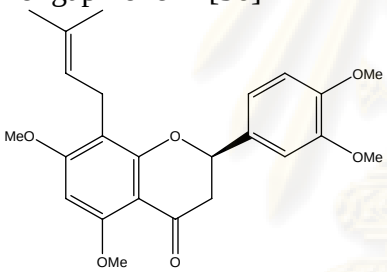	Flavanone	Root	Rao *et al*., 2009
Derris malaccensis			
2′,4′-Dihydroxy-4-methoxy-3′-prenylchalcone [**57**] 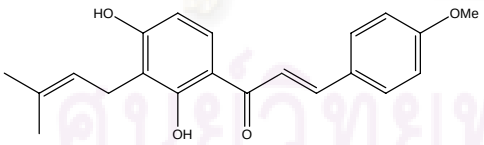	Chalcone	Leaves	Siripaisarnpipat, Kongjinda and Techasakul, 2007
(6a*R*,12a*R*,4′*R*,5′*S*)-4′,5′-Dihydro-4′,5′-dihydroxytephrosin [**12**] 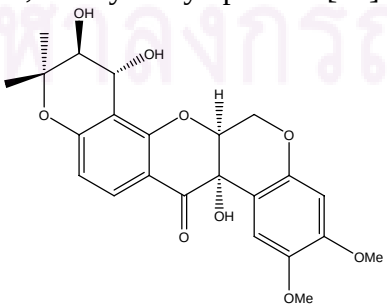	Rotenoid	Root	Takashima *et al*., 2002

Table 1 (continued)

Plant and compound	Category	Plant part	Reference
12a-Hydroxyelliptone [**58**] 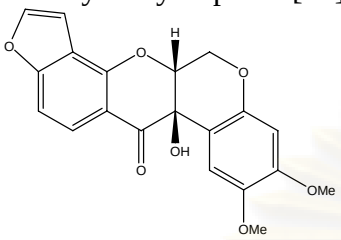	Rotenoid	Stem	Thasana, Chuankamnerdkarn and Ruchirawat, 2001
12-Deoxo-12α-acetoxyelliptone [**14**] 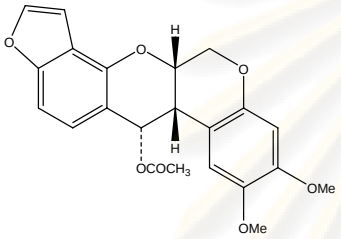	Rotenoid	Stem	Thasana *et al*., 2001
13-Homo-13-oxa-6a,12a-dehydrodeguelin [**59**] 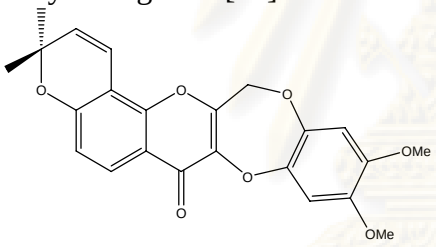	Rotenoid	Root	Takashima *et al*., 2002
Deguelin [**23**] 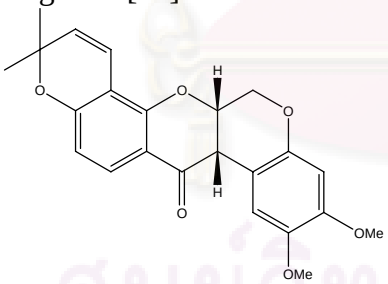	Rotenoid	Root	Takashima *et al*., 2002
Dehydrodeguelin [**60**] 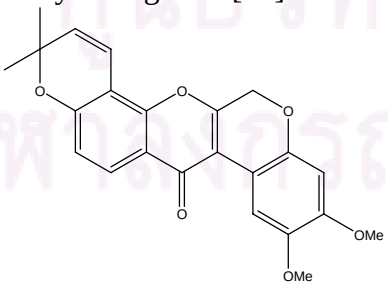	Rotenoid	Root	Takashima *et al*., 2002

Table 1 (continued)

Plant and compound	Category	Plant part	Reference
Dehydrorotenone [**61**] 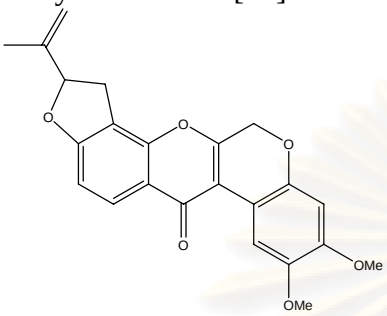	Rotenoid	Root	Takashima *et al*., 2002
Derrisin [**62**] 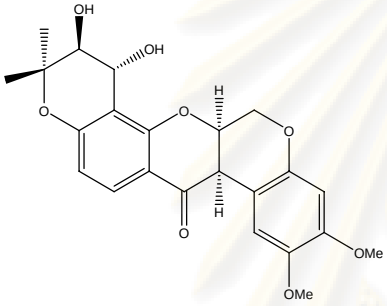	Rotenoid	Root	Takashima *et al*., 2002
Elliptone [**63**] 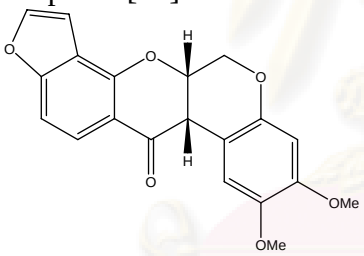	Rotenoid	Root	Takashima *et al*., 2002
Rotenone [**30**] 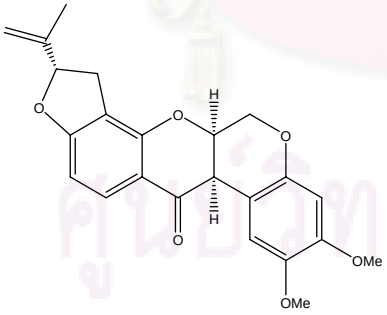	Rotenoid	Root	Takashima *et al*., 2002; Sae-Yun, *et. al*., 2006
Tephrosin [**64**] 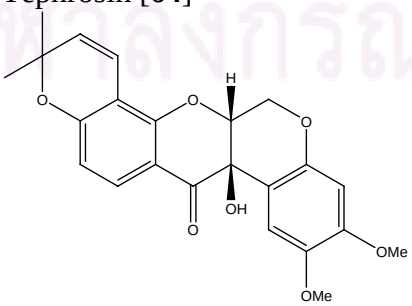	Rotenoid	Root	Takashima *et al*., 2002

Table 1 (continued)

Plant and compound	Category	Plant part	Reference
Toxicarol [**65**] 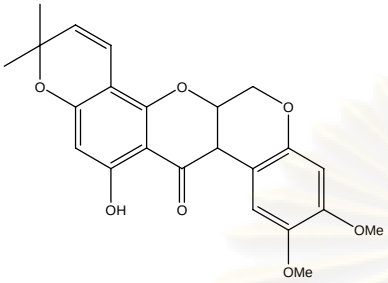	Rotenoid	Root	Takashima *et al*., 2002
Derris reticulata			
2‴,3‴-Epoxylupinifolin [**66**] 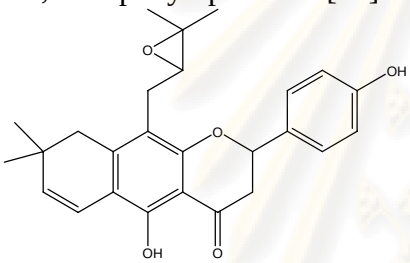	Flavanone	Stem	Mahidol *et al*., 1997
Dereticulatin [**67**] 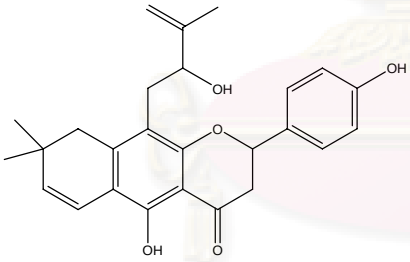	Flavanone	Stem	Mahidol *et al*., 1997
Lupinifolin [**68**] 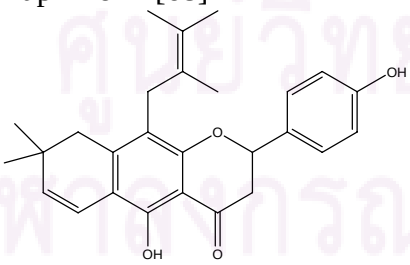	Flavanone	Stem	Mahidol *et al*., 1997

Table 1 (continued)

Plant and compound	Category	Plant part	Reference
Derris robusta			
Derrone [**69**] 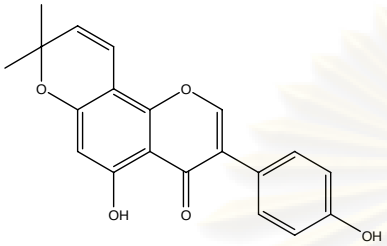	Isoflavone	Seed	Chibber and Sharma, 1980
Derrubone [**70**] 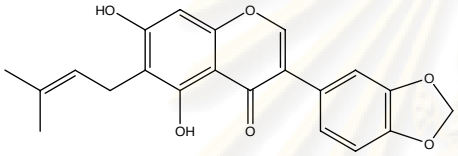	Isoflavone	Root	East, Ollis and Wheller, 1967
Derrugenin [**71**] 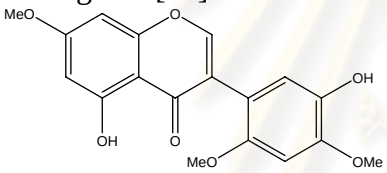	Isoflavone	Seed shell	Chibber and Sharma, 1979a
Derrusnin [**72**] 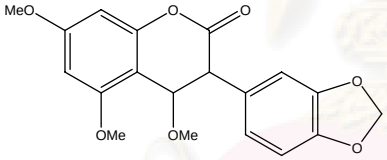	Coumarin	Root	East *et al*., 1967
Derrustone [**73**] 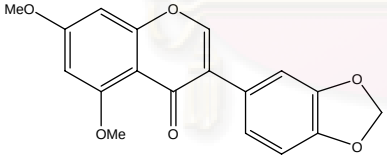	Isoflavone	Root	East *et al*., 1967
Robustic acid [**74**] 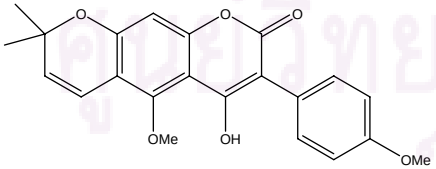	Coumarin	Root	East *et al*., 1967
Robustigenin [**75**] 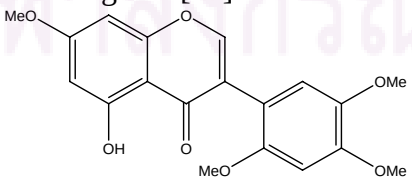	Isoflavone	Seed shell	Chibber and Sharma, 1979b

Table 1 (continued)

Plant and compound	Category	Plant part	Reference
Robustone [**76**] 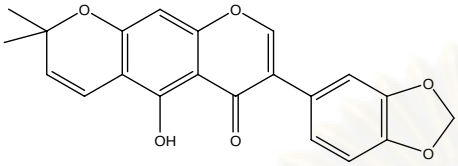	Isoflavone	Root	East *et al*., 1967
Rubone [**77**] 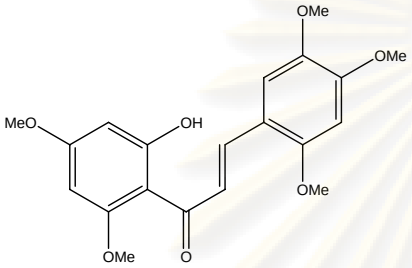	Chalcone	Seed	Chibber, Sharma and Dutt, 1979c
Derris scandens			
3′-γ-γ-Dimethylallylwighteone [**78**] 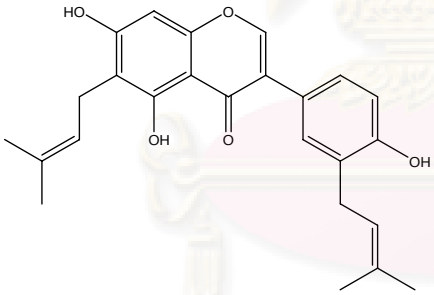	Isoflavone	Stem	Rao, Krupadanam and Srimannarayana, 1994; Laupattarakasem, Houghton and Hoult, 2004
3′-Methylorobol [**79**] 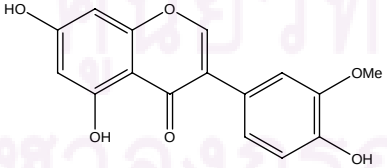	Isoflavone	Stem	Mahabusarakam *et al*., 2004

Table 1 (continued)

Plant and compound	Category	Plant part	Reference
4,4′-Di-*O*-methyl scandenin [**80**] 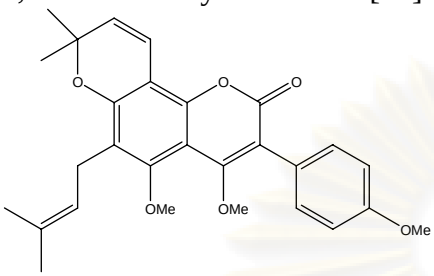	Coumarin	Stem	Rao *et al*.,1994
		Whole plant	Rao *et al*., 2007
4′,5,7-Trihydroxybiprenyl-isoflavone [**81**] 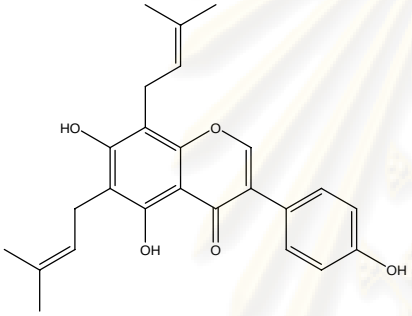	Isoflavone	Stem	Rao *et al*.,1994 ; Sekine *et al*., 1999
		Whole Plant	Rao *et al*., 2007
4′-*O*-Methylosajin [**82**] 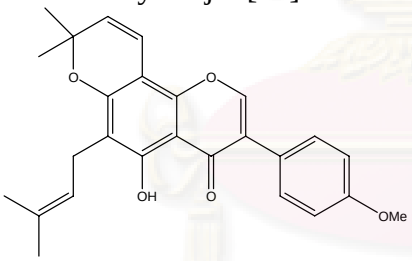	Isoflavone	Whole plant	Rao *et al*., 2007
4′-*O*-Methylscandinone [**83**] 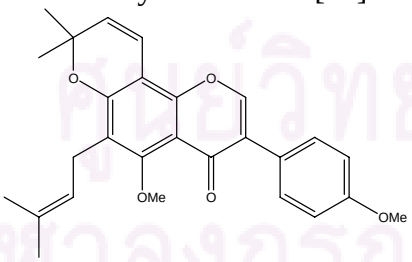	Isoflavone	Whole plant	Rao *et al*., 2007

Table 1 (continued)

Plant and compound	Category	Plant part	Reference
5-Hydroxy-2′′,2′′–dimethyl chromeno-(6,7:5′′,6′′)-2′′′,2′′′-dimethylchromeno(3',4':5′′′,6′′′) isoflavone [**84**] 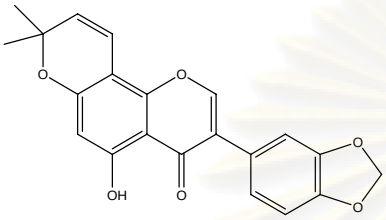	Isoflavone	Stem	Mahabusarakam *et al*., 2004
7-Hydroxy-4′,8-dimethoxyisoflavone 7-*O*-β-glucopyranoside [**85**] 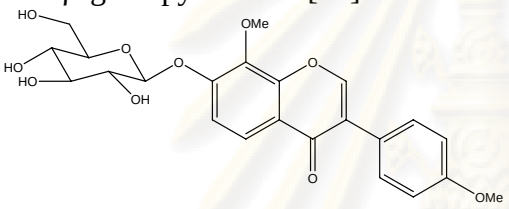	Isoflavone glycoside	Stem	Rukachaisirikul *et al*., 2002
7-*O*-α-Rhamno(1→6)-β-glucosyl glycosidegenistein [**86**] 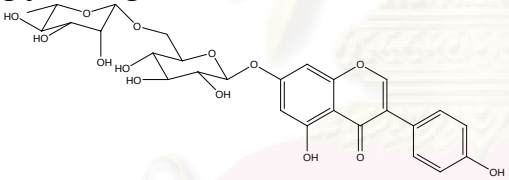	Isoflavone glycoside	Stem	Laupattarakasem *et al*., 2004
8-Hydroxy-4′,7-dimethoxyisoflavone-8-*O*-β-glucopyranoside [**87**] 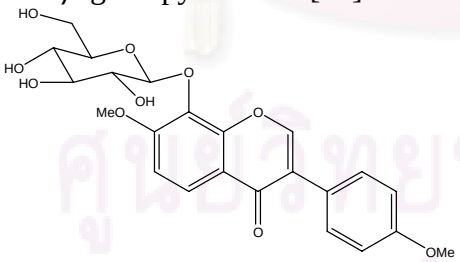	Isoflavone glycoside	Stem	Rukachaisirikul *et al*., 2002
Chandalone [**88**] 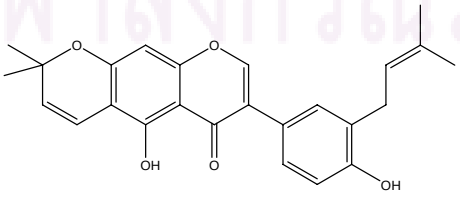	Isoflavone	Stem	Mahabusarakam *et al*., 2004

Table 1 (continued)

Plant and compound	Category	Plant part	Reference
Derriscandenosides A [**89**] 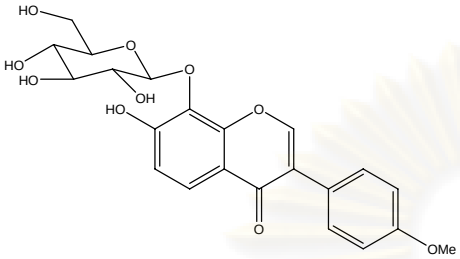	Isoflavone glycoside	Stem	Rukachaisirikul *et al*., 2002
Derriscandenosides B [**90**] 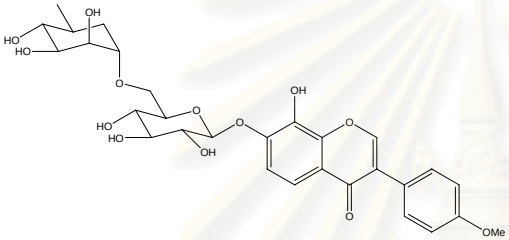	Isoflavone glycoside	Stem	Rukachaisirikul *et al*., 2002
Derriscandenosides C [**91**] 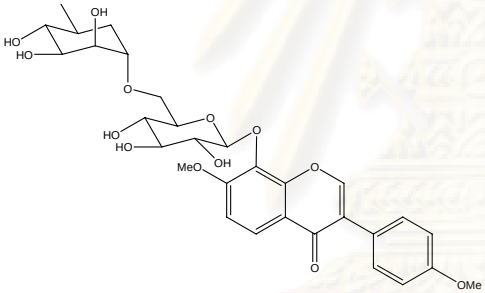	Isoflavone glycoside	Stem	Rukachaisirikul *et al*., 2002
Derriscandenosides D [**92**] 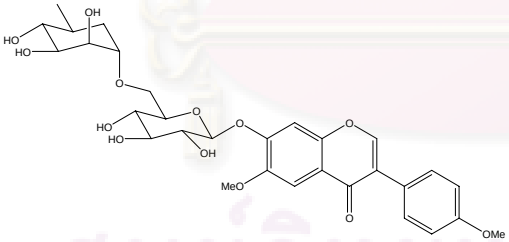	Isoflavone glycoside	Stem	Rukachaisirikul *et al*., 2002
Derriscandenosides E [**93**] 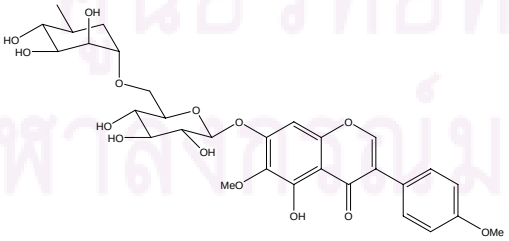	Isoflavone glycoside	Stem	Rukachaisirikul *et al*., 2002

Table 1 (continued)

Plant and compound	Category	Plant part	Reference
Derriscanosides A [**94**] 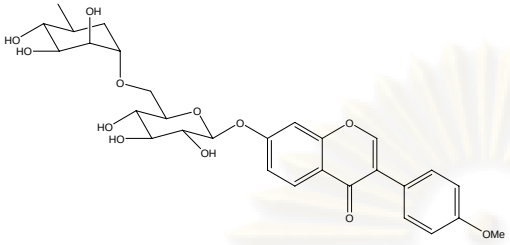	Isoflavone glycoside	Stem	Rukachaisirikul *et al*., 2002
Derriscanosides B [**95**] 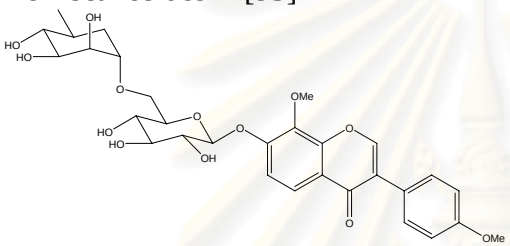	Isoflavone glycoside	Stem	Rukachaisirikul *et al*., 2002
Derrisisoflavone A [**96**] 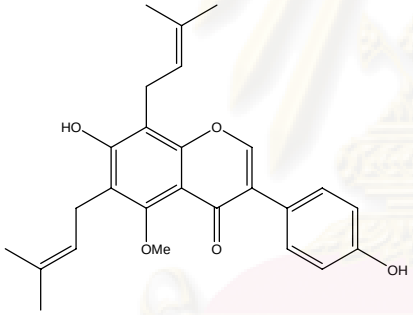	Isoflavone	Stem Whole Plant	Mahabusarakam *et al*., 2004; Sekine *et al*., 1999 Rao *et al*., 2007
Derrisisoflavone B [**97**] 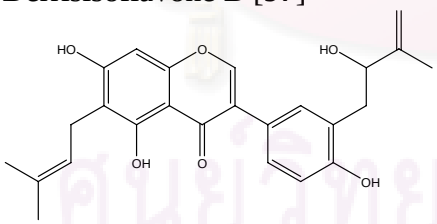	Isoflavone	Stem	Sekine *et al*., 1999
Derrisisoflavone C [**98**] 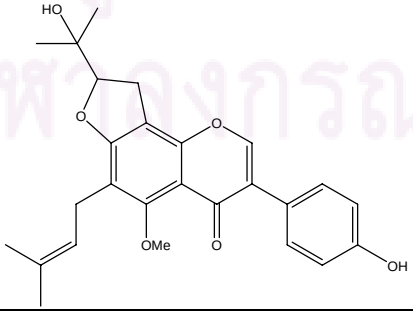	Isoflavone	Stem Whole plant	Sekine *et al*., 1999 Rao *et al*., 2007

Table 1 (continued)

Plant and compound	Category	Plant part	Reference
Derrisisoflavone D [**99**] 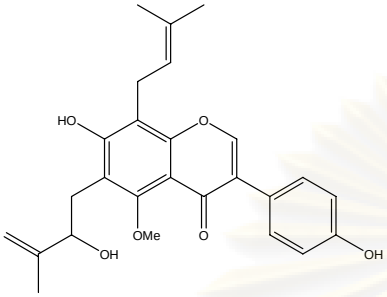	Isoflavone	Stem	Sekine *et al*., 1999
Derrisisoflavone E [**100**] 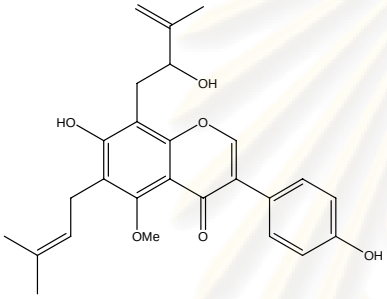	Isoflavone	Stem	Sekine *et al*., 1999
Derrisisoflavone F [**101**] 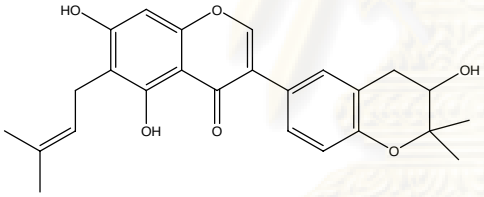	Isoflavone	Stem	Sekine *et al*., 1999
Daidzein 7-*O*-[α-rhamnopyranosyl-(1→6)]-β-glucopyranoside [**102**] 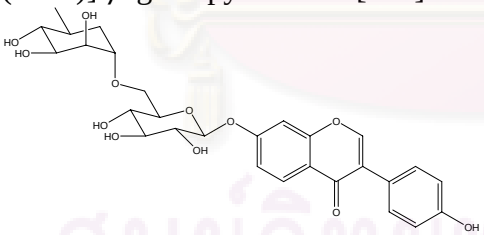	Isoflavone glycoside	Stem	Rukachaisirikul *et al*., 2002
Erysenegalensein E [**103**] 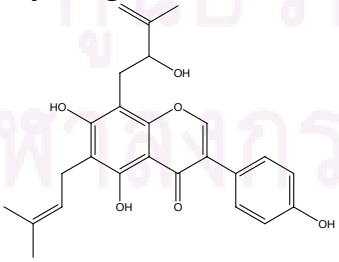	Isoflavone	Stem	Sekine *et al*., 1999

Table 1 (continued)

Plant and compound	Category	Plant part	Reference
Flemichapparin B [**104**] 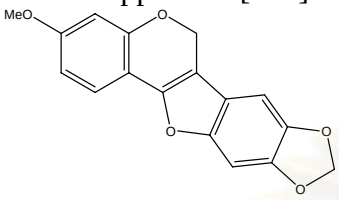	Pterocarpan	Stem	Mahabusarakam *et al*., 2004
Flemichapparin C [**105**] 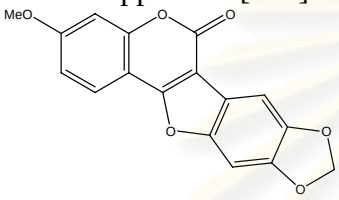	Pterocarpan	Stem	Mahabusarakam *et al*., 2004
Formononetin 7-*O*-[α-rhamnopyranosyl-(1→6)]-*β*-glucopyranoside [**106**] 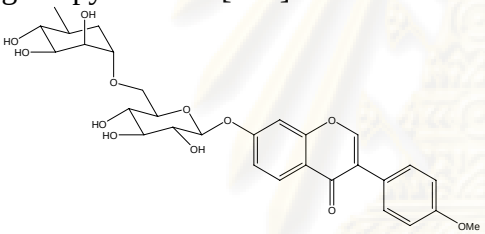	Isoflavone glycoside	Stem	Rukachaisirikul *et al*., 2002
Formononetin 7-*O*-*β*-glucopyranoside [**107**] 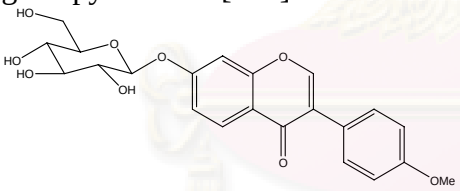	Isoflavone glycoside	Stem	Rukachaisirikul *et al*., 2002
Genistein [**28]** 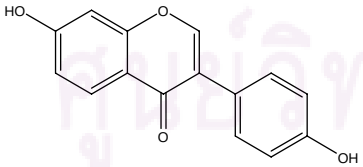	Isoflavone	Stem	Laupattarakasem *et al*., 2004; Mahabusarakam *et al*., 2004

Table 1 (continued)

Plant and compound	Category	Plant part	Reference
Genistein 7-*O*-[α-rhamnopyranosyl-(1→6)]-β-glucopyranoside [**108**] 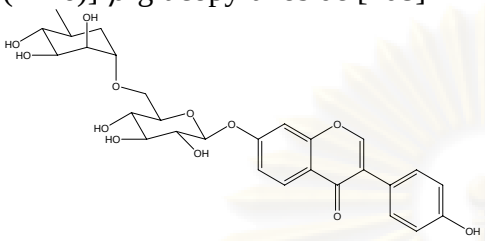	Isoflavone glycoside	Stem	Rukachaisirikul *et al*., 2002
Isochandalone [**109**] 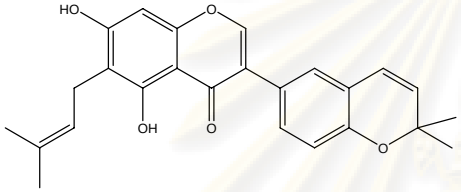	Isoflavone	Stem	Mahabusarakam *et al*., 2004
Isorobustone [**110**] 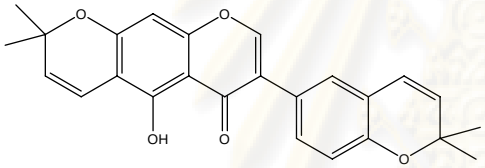	Isoflavone	Stem	Mahabusarakam *et al*., 2004
Isoscandinone [**111**] 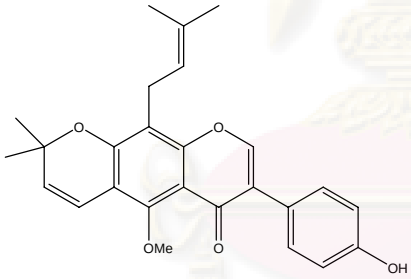	Isoflavone	Whole plant	Rao *et al*., 2007
Lupalbigenin [**112**] 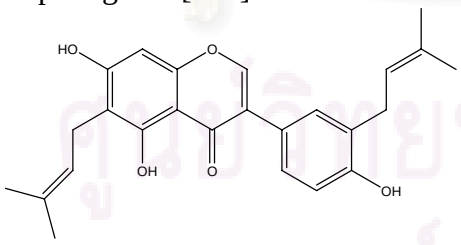	Isoflavone	Stem	Sekine *et al*., 1999; Mahabusarakam *et al*., 2004
		Whole plant	Rao *et al*., 2007

Table 1 (continued)

Plant and compound	Category	Plant part	Reference
Lupinisoflavone G [**113**] 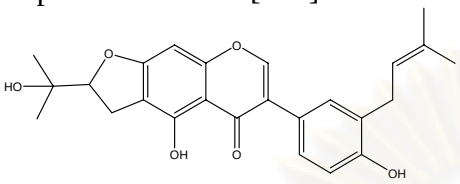	Isoflavone	Stem	Sekine *et al.*, 1999
Lupinisol A [**114**] 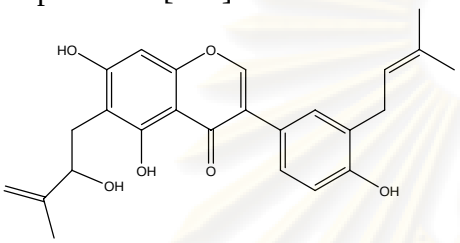	Isoflavone	Stem	Sekine *et al.*, 1999
Lupiwighteone [**115**] 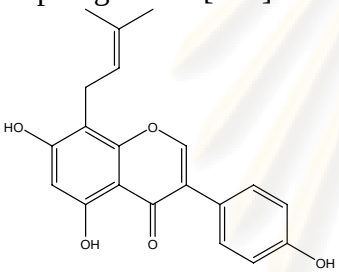	Isoflavone	Stem	Mahabusarakam *et al.*, 2004
Maackiain [**46**] 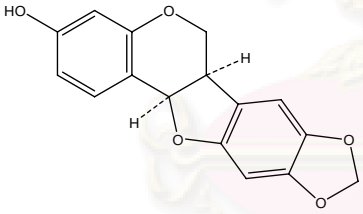	Pterocarpan	Stem	Mahabusarakam *et al.*, 2004
Osajin [**116**] 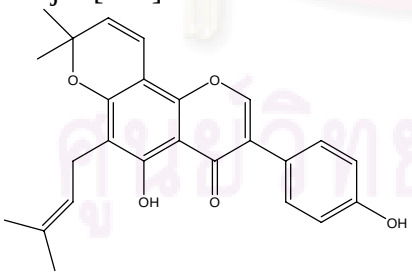	Isoflavone	Whole plant	Rao *et al.*, 2007
Robustic acid [**74**] 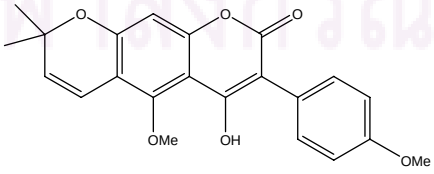	Coumarin	Stem	Rao, Krupadanam and Srimannarayana, 1994

Table 1 (continued)

Plant and compound	Category	Plant part	Reference
Santal [**117**] 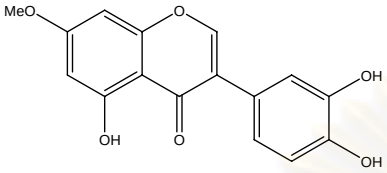	Isoflavone	Stem	Mahabusarakam *et al*., 2004
Scandenal [**118**] 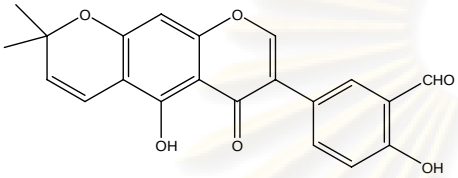	Isoflavone	Stem	Mahabusarakam *et al*., 2004
Scandenin [**119**] 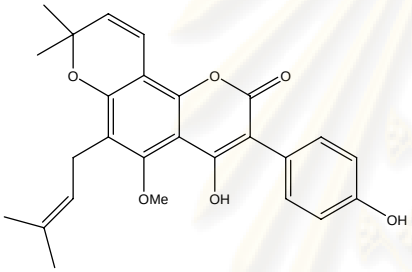	Isoflavone	Stem	Laupattarakasem *et al*., 2004
		Whole plant	Rao *et al*., 2007
Scandenin A [**120**] 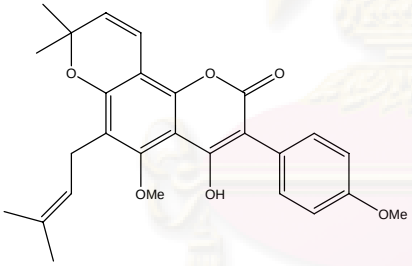	Isoflavone	Whole plant	Rao *et al*., 2007
Scandenin B [**121**] 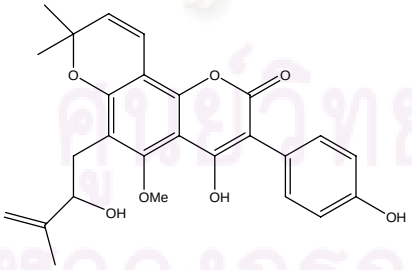	Isoflavone	Whole plant	Rao *et al*., 2007
Scandenone [**122**] 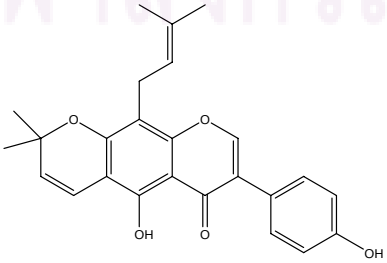	Isoflavone	Whole plant	Rao *et al*., 2007

Table 1 (continued)

Plant and compound	Category	Plant part	Reference
Scanderone [**123**] 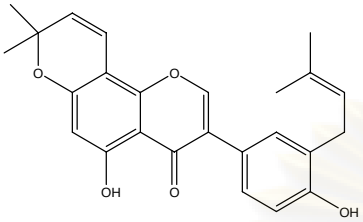	Isoflavone	Stem	Mahabusarakam *et al*., 2004
Scandinone [**124**] 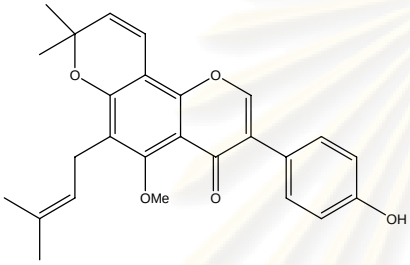	Isoflavone	Stem	Rao *et al*., 1994 ; Sekine *et al*., 1999; Mahabusarakam *et al*., 2004
		Whole plant	Rao *et al*., 2007
Scandione [**125**] 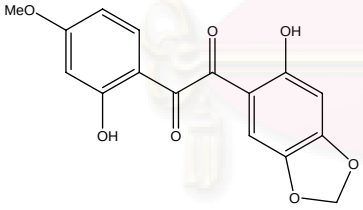	Benzyl derivative	Stem	Mahabusarakam *et al*., 2004
Ulexone A [**126**] 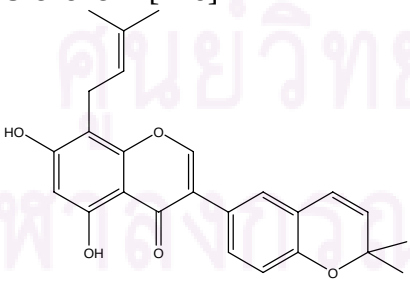	Isoflavone	Stem	Mahabusarakam *et al*., 2004

Table 1 (continued)

Plant and compound	Category	Plant part	Reference
Warangalone [**127**] 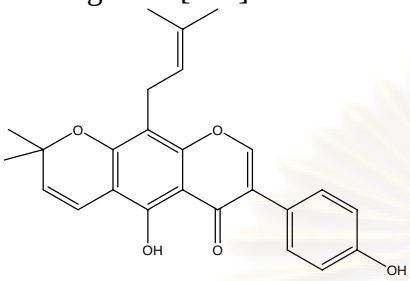	Isoflavone	Stem	Rao *et al*., 1994
Derris trifoliata			
(6*R*,9*R*)-3-Oxo-α-ionyl-*β*-D-glucopyranoside [**128**] 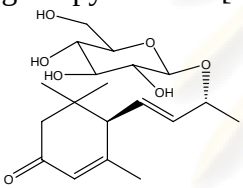	Terpene glycoside	Leaves	Takeda *et al*., 2008
(6*S*,9*R*)-Roseoside [**129**] 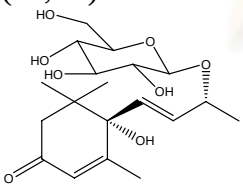	Terpene glycoside	Leaves	Takeda *et al*., 2008
12a-Hydroxyelliptone [**58**] 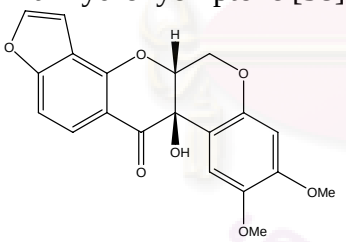	Rotenoid	Stem	Tewtrakul, Cheenpracha and Karalai, 2009
12a-Hydroxyrotenone [**130**] 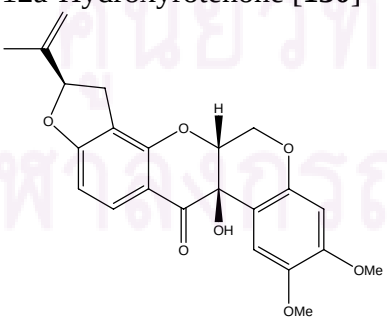	Rotenoid	Stem	Tewtrakul *et al*., 2009

Table 1 (continued)

Plant and compound	Category	Plant part	Reference
2,6-Dimethoxy-*p*-hydroquinone 1-*O*-*β*-D-glucopyranoside [**131**] 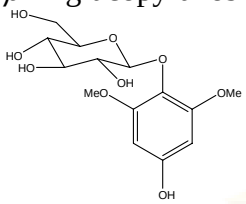	Phenolic glycoside	Leaves	Takeda *et al*., 2008
2-Methyl-3-buten-2-yl *β*-D-glucopyranoside [**132**] 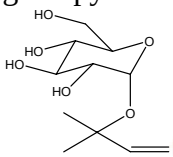	Prenyl Glycoside	Leaves	Takeda *et al*., 2008
6,7-Dimethoxy-4-chromanone [**133**] 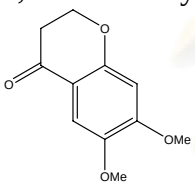	Phenolic compound	Seed	Yenesew *et al*., 2006
6a,12a-Dehydro-*α*-toxicarol [**134**] 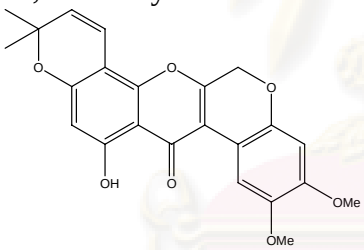	Rotenoid	Stem	Tewtrakul *et al*., 2009
6a,12a-Dehydrodeguelin [**135**] 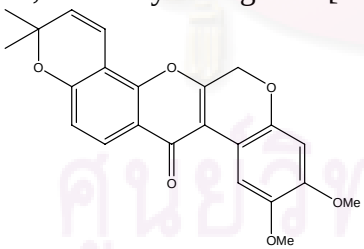	Rotenoid	Stem	Tewtrakul *et al*., 2009
6a,12a-Dehydrorotenone [**136**] 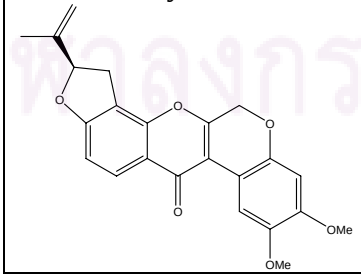	Rotenoid	Stem	Tewtrakul *et al*., 2009

Table 1 (continued)

Plant and compound	Category	Plant part	Reference
6aα,12aα-12a-Hydroxyelliptone [**137**] 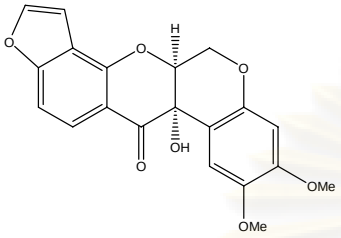	Rotenoid	Stem	Ito *et al*., 2004
7a-*O*-Methyldeguelol [**138**] 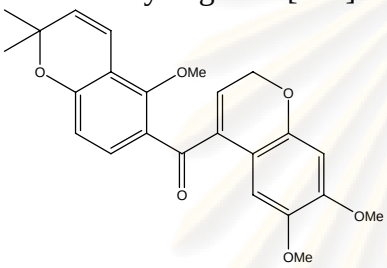	Rotenoid	Root	Yenesew *et al*., 2005
Apocynoside I [**139**] 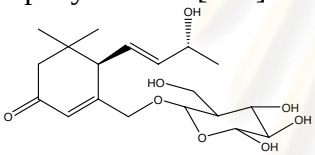	Terpene glycoside	Leaves	Takeda *et al*., 2008
α-Toxicarol [**140**] 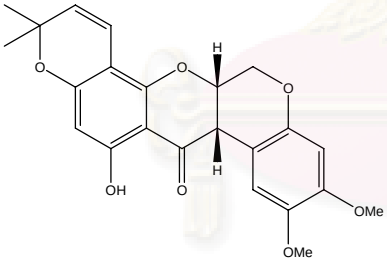	Rotenoid	Root	Yenesew *et al*., 2005
		Stem	Ito *et al*., 2004; Tewtrakul *et al*., 2009
Benzyl-β-D-glucopyranoside [**141**] 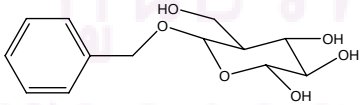	Benzyl glycoside	Leaves	Takeda *et al*., 2008
Betulalbuside A [**142**] 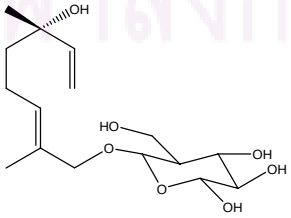	Monoterpene glycoside	Leaves	Takeda *et al*., 2008

Table 1 (continued)

Plant and compound	Category	Plant part	Reference
Citroside A [**143**] 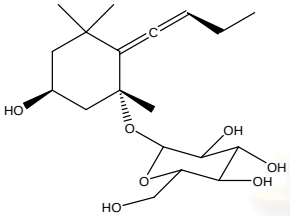	Terpene glycoside	Leaves	Takeda *et al*., 2008
Corchoionoside A [**144**] 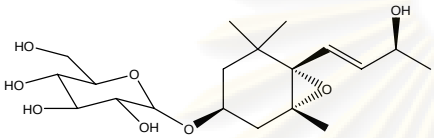	Terpene glycoside	Leaves	Takeda *et al*., 2008
Deguelin [**23**] 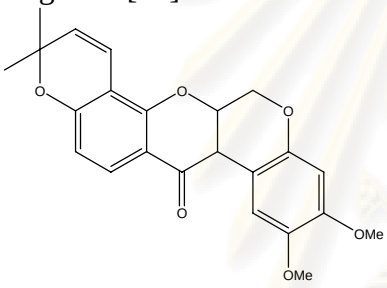	Rotenoid	Root Stem	Yenesew *et al*., 2005 Ito *et al*., 2004; Tewtrakul *et al*., 2009
Dehydrodeguelin [**60**] 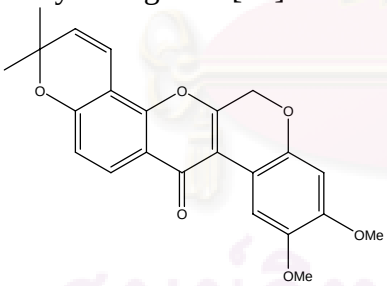	Rotenoid	Seed	Yenesew et al., 2006
Elliptone [**63**] 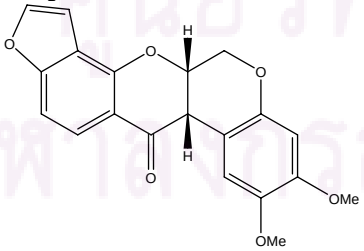	Rotenoid	Stem	Ito *et al*., 2004

Table 1 (continued)

Plant and compound	Category	Plant part	Reference
Inamoside [**145**] 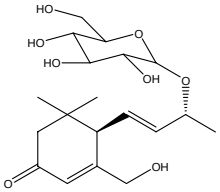	Terpene glycoside	Leaves	Takeda *et al*., 2008
Isotachioside [**146**] 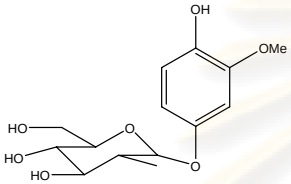	Phenolic glycoside	Leaves	Takeda *et al*., 2008
Kaempferol-3-*O*-α-L-rhamnopyranosyl-(1→6)-β-D-glucopyranoside [**147**] 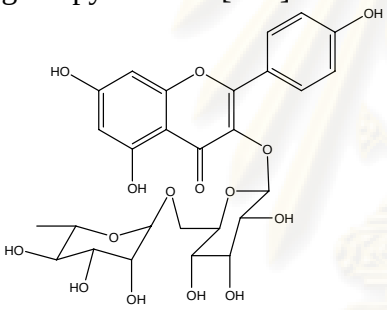	Flavone glycoside	Aerial part	Xu *et al*., 2009
Kaempferol-3-*O*-α-L-rhamnopyranosyl-(1→6)-β-D-glucopyranosyl-(1→3)-β-D-glucopyranoside [**148**] 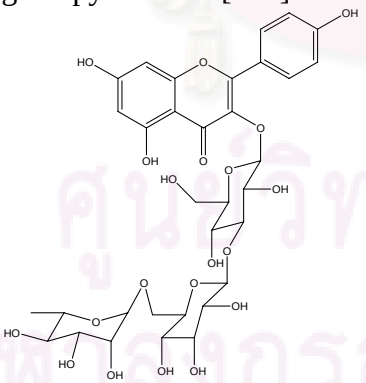	Flavone glycoside	Aerial part	Xu *et al*., 2009
Maltol-β-D-glucopyranoside [**149**] 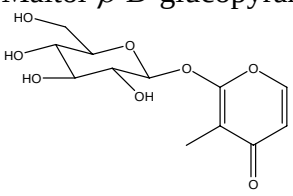	Prenyl glycoside	Leaves	Takeda *et al*., 2008

Table 1 (continued)

Plant and compound	Category	Plant part	Reference
Mauritianin [**150**] 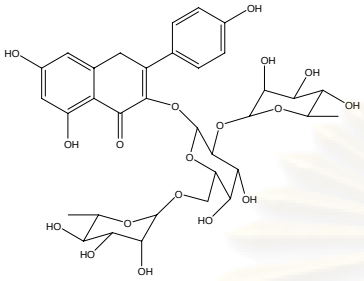	Flavonol glycoside	Leaves	Takeda *et al*., 2008
n-Hexyl-*β*-D-glucopyranoside [**151**] 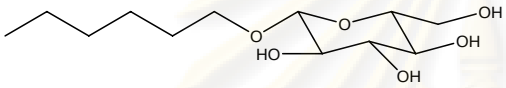	Alkyl glycoside	Leaves	Takeda *et al*., 2008
Quercetin-3-*O*-*α*-L-rhamnopyranosyl-(1→6)-*β*-D-glucopyranosyl-(1→2)-*β*-D-glucopyranoside [**152**] 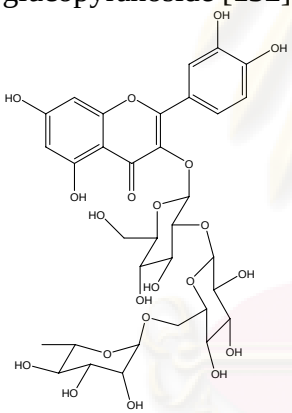	Flavonol glycoside	Aerial part	Xu *et al*., 2009
Quercetin-3-*O*-*α*-L-rhamnopyranosyl-(1→6)-*β*-D-glucopyranosyl-(1→3)-*β*-D-glucopyranoside [**153**] 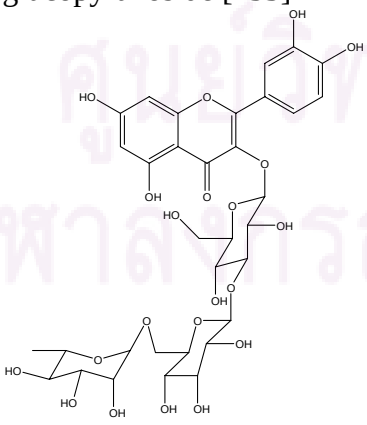	Flavonol glycoside	Aerial part	Xu *et al*., 2009

Table 1 (continued)

Plant and compound	Category	Plant part	Reference
Rotenoloid [**154**] 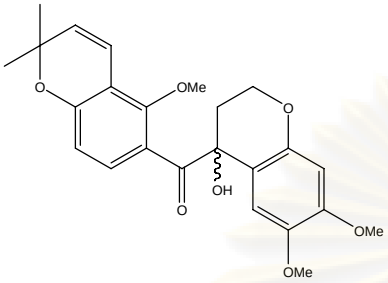	Rotenoid	Seeds	Yenesew *et al*., 2006
Rotenone [**30**] 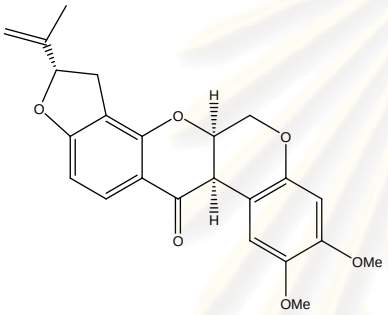	Rotenoid	Root	Yenesew *et al*., 2005
		Seeds	Yenesew *et al*., 2006
		Stem	Ito *et al*., 2004; Tewtrakul *et al*., 2009
Spirohomooxarotenoid [**155**] 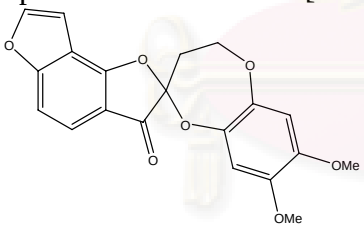	Rotenoid	Seeds	Yenesew *et al*., 2006
Tachioside [**156**] 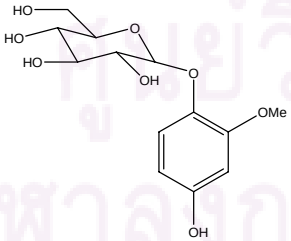	Phenolic glycoside	Leaves	Takeda *et al*., 2008

Table 1 (continued)

Plant and compound	Category	Plant part	Reference
Tephrosin [**64**] 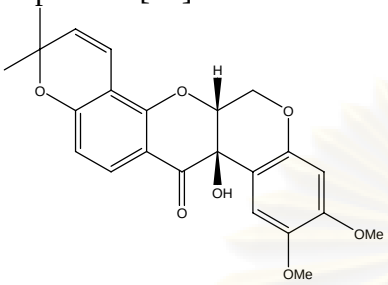	Rotenoid	Seed Stem	Yenesew *et al*., 2006 Ito *et al*., 2004; Tewtrakul *et al*., 2009

2. Chemical constituents of *Carissa* spp.

A number of chemical constituents isolated from the genus *Carissa* can be divided into two groups, terpenes and lignans. In addition, other classes of natural compounds such as cardiac glycosides and miscellaneous substances have been found (Table 2).

Table 2 Distribution of chemical constituents in the genus *Carissa*

Plant and compound	Category	Plant part	Reference
Carissa carandas			
3-*β*-Hydroxy-27-*p*-*E*-coumaroyloxyurs-12-en-28-oic acid [**157**] 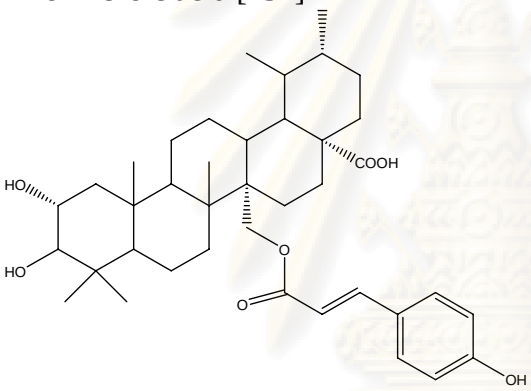	Triterpene	Leaf	Siddiqui *et al*., 2002
β-Sitosterol [**158**] 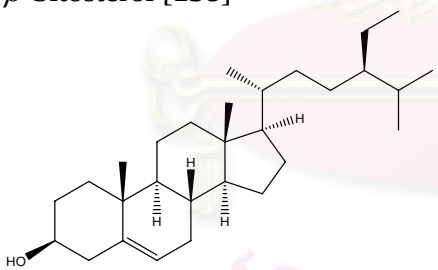	Sterol	Leaf --	Siddiqui *et al*., 2002 Singh and Rastogi, 1972
Carindone [**159**] 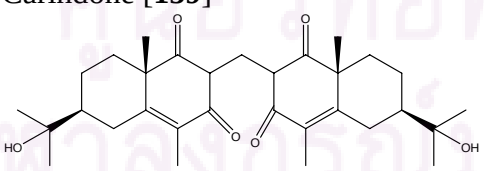	Bisesqui-terpene	-	Singh and Rastogi, 1972

Table 2 (continued)

Plant and compound	Category	Plant part	Reference
Carinol [**160**] 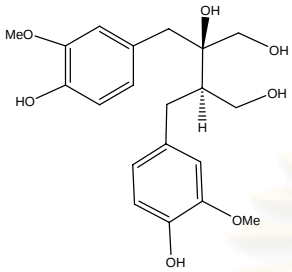	Lignan	Root	Pal, Kulshreshtha and Rastogi, 1975
Carissin [**161**] 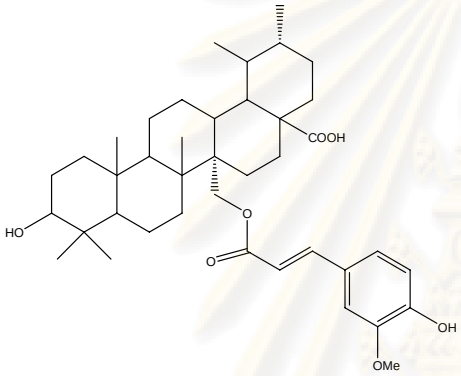	Triterpene	Leaves	Siddiqui *et al.*, 2002
Carissone [**162**] 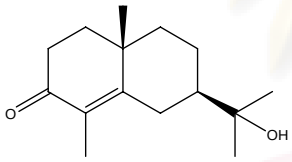	Sesquiterpene	-	Singh and Rastogi, 1972
Lupeol [**163**] 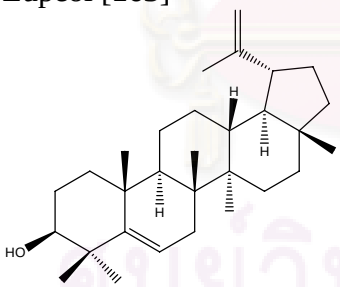	Triterpene	Leaves	Pakrashi, Datta and Ghosh-Dastidar, 1968
Mixture of cardenolides [**164**]	Cardiac glycoside	-	Singh and Rastogi, 1972

Table 2 (continued)

Plant and compound	Category	Plant part	Reference
Oleanolic acid [**165**] 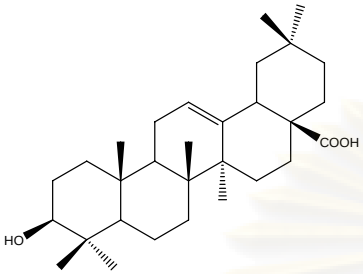	Triterpene	Leaves	Siddiqui *et al.*, 2002
Ursolic acid [**166**] 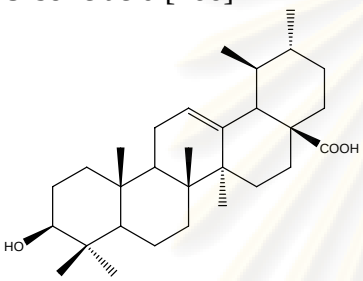	Triterpene	Leaves	Pakrashi *et al.*, 1968; Siddiqui *et al.*, 2002
Carissa spinarum			
β-Sitosterol [**158**] 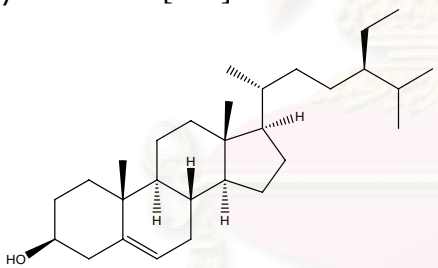	Sterol	Root bark	Pakrashi *et al.*, 1968
Carinol [**160**] 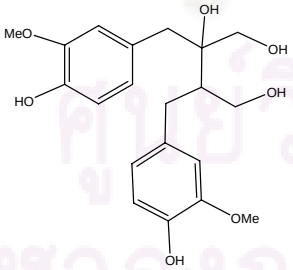	Lignan	Stem	Rao *et al.*, 2005

Table 2 (continued)

Plant and compound	Category	Plant part	Reference
(–)-Carissanol [**167**] 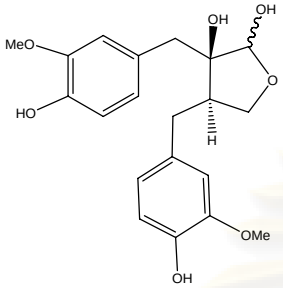	Lignan	Stem	Rao *et al*., 2005
(–)-Nortrachelogenin [**168**] 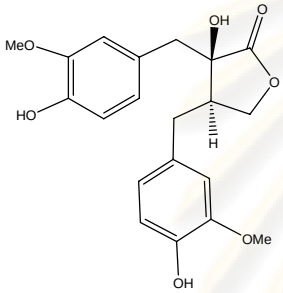	Lignan	Stem	Rao *et al*., 2005
(–)-Olivil [**169**] 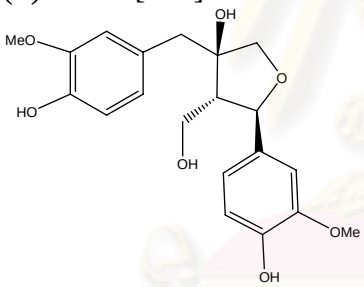	Lignan	Stem	Rao *et al*., 2005
(–)-Secoisolariciresinol [**170**] 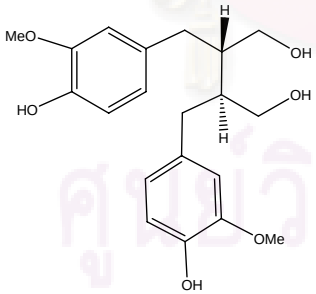	Lignan	Stem	Rao *et al*., 2005
3′-(4′′-methoxyphenyl)-3′-oxo-propionylhexadecanoate [**171**] 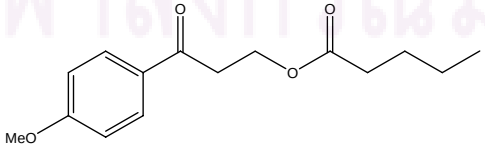	Phenolic compound	Stem	Rao *et al*., 2005

Table 2 (continued)

Plant and compound	Category	Plant part	Reference
Carenone [**172**] 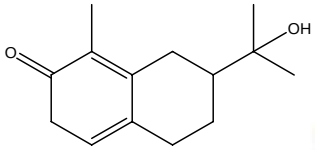	Sesquiterpene	Stem	Rao *et al*., 2005
Coniferaldehyde [**173**] 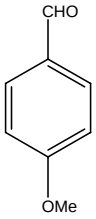	Phenolic compound	Stem	Rao *et al*., 2005
Germacrenone [**174**] 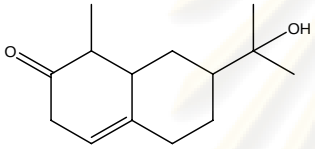	Sesquiterpene	Stem	Rao *et al*., 2005
Lupeol [**163**] 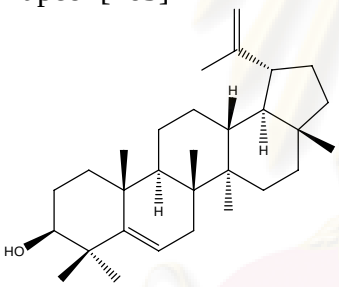	Triterpene	Root bark	Pakrashi *et al*., 1968
Pinoresinol [**175**] 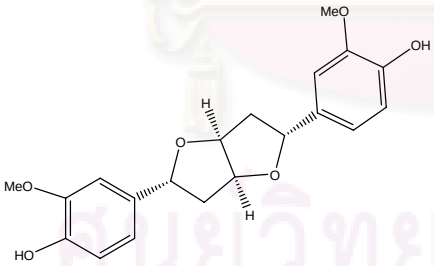	Lignan	Stem	Rao *et al*., 2005

3. Traditional uses of *Derris* species and biological activities of their constituents

Plants of the genus *Derris* (Leguminosae) have been used as fish poisons and insecticides (Thasana *et al*., 2001). They are also widely used in cattle and sheep dips for the control of ticks and other ectoparasites. They are currently employed in horticulture against aphids, caterpillars, sawflies, wasps, raspberry beetles and red spiders (Tewtrakul *et al*., 2009).

D. elliptica Benth and *D. malaccensis* Prain have been known as important sources of pesticidal compounds due to the presence of rotenone [**30**] and its derivatives (Sae-yun *et al*., 2006). Moreover, a number of the rotenoids isolated from *D. malaccensis* showed antibacterial activity against *Helicobacter pylori* (Takashima *et al*., 2002).

Others *Derris* species have also been used traditionally. For example, different parts of *D. indica* (Lam.) Bennet have been used in folk medicine for bronchitis, whooping cough, rheumatic joints and to quench dipsia in diabetes. Flavonoids from the stems and the roots of this plant such as 3,4-methylenedioxy-10-methoxy-7-oxo(2)benzopyrano(4,3-b)benzopyran [**34**], pachycarin [**49**] and pinnatin [**50**] exhibited antimycobacterial activity against *Mycobacterium tuberculosis* H37Ra with minimum inhibitory concentration (MIC) between 6.25 and 200 μg/mL (Koysomboon *et al*., 2006). Chemical constituents of the root extract of *D. indica* such as 3,3′,4′-trihydroxy-4H-furo(2,3-h)chromen-4-one [**32**] and 3′,4′-dihydroxy-4H-furo(2,3-h)chromen-4-one [**33**] displayed moderate intestinal α-glucosidase inhibitory activity as well as free radical scavenging activity, while pongamol [**54**] potently inhibited intestinal α-glucosidase (Rao *et al*., 2009).

The stem of *D. scandens*, locally called “Thao-wan-priang”, is used in Thailand for antidysenteric, diuretic and for relief of muscular pain (Sekine *et al*., 1999). This plant is reported to possess anti-inflammatory, free radical scavenging, antibacterial, antihypertensive, immunomodulatory, anti-HIV properties and α-glucosidase inhibitory activity (Rao *et al*., 2007).

D. trifoliata is known in Thai as Tob-tab-nam. Its stem has been used for its laxative, carminative and expectorant effect. The bark of this plant has been used in the treatment of rheumatism and dysmenorrhea (Tewtrakul *et al*., 2009). The crude methanol extract of its seeds showed potent larvicidal activity against second-instar larvae of *Aedes aegypti* (Tewtrakul *et al*., 2009). Moreover, the ethanol extract of its

leaves given orally at doses of 250 and 500 mg/kg significantly inhibited the acetic acid-induced writhing in mice. The compounds isolated from *D. trifoliata* stems such as 12a-hydroxyelliptone [**9**], deguelin [**23**], 12a-hydroxyrotenone [**130**] and α-toxicarol [**140**] were considered responsible for the NO inhibitory effect (Tewtrakul *et al*., 2009). The rotenoids deguelin [**23**] and α-toxicarol [**140**] have also been reported to possess cancer chemopreventive properties (Ito *et al*., 2004).

4. Traditional uses of *Carissa* species and biological activities of their constituents

Various plants of the genus *Carissa* are used medicinally in India and Asian countries (Achenbach, Waibel and Addae-Mensah, 1983). For example, in India, roots of *C. carandas* are used as a bitter stomachic and an anthelmintic while its leaves are used for remittant fever (Pakrashi *et al*., 1968). In Thailand, its stem and root have been traditionally used as a bitter tonic although the use of its root use should be cautioned due to the presence of cardiac glycosides (Faculty of Pharmaceutical Sciences, Mahidol University, 1995).

Another *Carissa* species that has been used in Indian and Thai folkloric medicine is *C. spinarum*. The stem of this plant is used as a bitter tonic in Thailand whereas its roots are used for purgative action and as an antidote to snake-bite in India (Pakrashi *et al*., 1968; Faculty of Pharmaceutical Sciences, Mahidol University, 1995).

C. edulis (Forssk) Vahl is a thorny shrub widely distributed in Africa. In Ethiopia, its pungent root is used for the treatment of chest complaints, rheumatism, headache, gonorrhoea, syphilis, rabies and as a diuretic. The root wood extract produced a significant increase in urine output at a dose of 50 mg/kg. Urinary electrolyte excretion was also affected by the extract. Chemical substances isolated from this plant include 2-hydroxyacetophenone, soluble phenolics, insoluble proanthocyanidins, lignans predominantly (–)-nortrachelogenin [**168**], (–)-carinol [**160**] and (–)-carissanol [**167**] and sesquiterpenes such as carissone [**162**] (Nedi, Mekonnen and Urga, 2004).

In addition, the root extract of *C. edulis* showed activity against three viruses including herpes simplex virus, Sindbis virus and poliovirus at a concentration of 12 μg/ml (Taylor *et al*., 1996). Moreover, the extract significantly inhibited the formation of plaques in Vero E6 cells infected with 1 wild type or resistant strain of HSV at 50

μg/ml *in vitro* with minimal cell cytotoxicity (CC_{50} = 480 μg/mL). When the extract was examined for *in vivo* efficacy in a murine model using Balb C mice cutaneously infected with wild type or resisitant strains of HSV, the extract at an oral dose of 250 mg/kg significantly delayed the onset of HSV infection by over 50% (Tolo *et al*., 2006).

CHAPTER III

EXPERIMENTAL

1. Source of plant materials

The roots of *Derris malaccensis* Prain were purchased from a drugstore in Bangkok, Thailand in April 2005. Authentication was performed by comparison with a herbarium specimen (BKF No. 14699) at the National Park, Wildlife and Plant Conservation Department, Ministry of Natural Resources and Environment. A voucher specimen (KL-042548) has been deposited at the Department of Pharmacognosy and Pharmaceutical Botany, Faculty of Pharmaceutical Sciences, Chulalongkorn University.

The stems of *Carissa carandas* L. and *Carissa spinarum* L. were collected from the botanical garden of the Faculty of Pharmaceutical Sciences, Chulalongkorn University, Bangkok, Thailand, in October, 2006 and June, 2008, respectively. Authentications were performed by comparison with herbarium specimens at the Museum of Natural Medicine, Faculty of Pharmaceutical Sciences, Chulalongkorn University. Both voucher specimens (RW 102549 for *C. carandas* and RW 062551 for *C. spinarum*) have been on deposit at the Department of Pharmacognosy and Pharmaceutical Botany, Faculty of Pharmaceutical Sciences, Chulalongkorn University.

2. General techniques

2.1 Analytical thin-layer chromatography (TLC)

Technique	:	One dimension, ascending
Adsorbent	:	Silica gel 60 F_{254} (E. Merck) precoated plate
Layer thickness	:	0.2 mm
Distance	:	6 cm
Temperature	:	Laboratory temperature (30-35ºC)
Detection	:	1. Ultraviolet light at wavelengths of 254 and 365 nm.
		2. Anisaldehyde and heating at 105°C for 10 min.

2.2 Preparative thin-layer chromatography (TLC)

Technique	:	One dimension, ascending
Adsorbent	:	Silica gel 60 F_{254} (E. Merck) precoated plate
Layer thickness	:	1 mm
Distance	:	16 cm
Temperature	:	Laboratory temperature (30-35ºC)
Detection	:	Ultraviolet light at wavelengths of 254 and 365 nm.

2.3 Column chromatography

2.3.1 Vacuum liquid column chromatography

Adsorbent	:	Silica gel 60 (No.7734) particle size 0.063-0.200 nm (70-230 mesh ASTM) (E. Merck)
Packing method	:	Dry packing
Sample loading	:	The sample was dissolved in a small amount of organic solvent, mixed with a small quantity of adsorbent, triturated, dried and then placed gently on top of the column.
Detection	:	Fractions were examined by TLC under UV light at the wavelengths of 254 and 365 nm.

2.3.2 Flash column chromatography

2.3.2.1 Normal phase flash column chromatography (Solid phase extraction)

Adsorbent	:	Silica gel particle size 0.055 nm (70 mesh ASTM) (Strata SI-1, Phenomenex)
Packing method	:	Dry packing
Sample loading	:	The sample was dissolved in a small amount of organic solvent, mixed with a small quantity of adsorbent, triturated, dried and then placed gently on top of the column.
Detection	:	Fractions were examined in the same way as described in section 2.2.1

2.3.2.1 Reversed phase flash column chromatography

Column	:	C18 cartridge (40x75 mm, 45 – 75 μm) (VerSaPak)
Flow rate	:	7.35 mL/min
Mobile phase	:	Isocratic 40% methanol (MeOH) in water (H_2O)
Sample preparation	:	The sample was dissolved in a small amount of eluent and filtered through filter paper before injection.
Injection volume	:	10 mL
Pump	:	SciLog (Accu™)
Detector and recorder	:	Tgledyne Isco UA-6 UV/Visible detector
Temperature	:	Room temperature

2.3.3 Normal phase column chromatography

Adsorbent	:	Silica gel 60 (No.9385) particle size 0.040-0.063 nm (70-230 mesh ASTM) (E. Merck)
Packing method	:	Wet packing
Sample loading	:	1. The sample was dissolved in a small amount of organic solvent, mixed with a small quantity of adsorbent, triturated, dried and then placed gently on top of the column. 2. The sample was dissolved in a small amount of eluent and then applied gently on top of the column.
Detection	:	Fractions were examined in the same way as described in section 2.3.1

2.3.4 Gel filtration chromatography

Adsorbent	:	Sephadex LH 20 (Pharmacia)
Packing method	:	Gel filter was suspended in the eluent and left standing to swell for 24 hours prior to use. It was then poured into the column and allowed to set tightly.
Sample loading	:	The sample was dissolved in a small amount of eluent and then applied gently on top of the column.

2.3.5 High pressure liquid chromatography

Column	:	Shim-pack Prep-ODS No. 2025820
Flow rate	:	2 mL/min
Mobile phase	:	1. Isocratic 50% CH_3CN in H_2O

2. Isocratic 60% CH_3CN in H_2O

3. Isocratic 40% MeOH in H_2O

4. Isocratic 14% CH_3CN and 9% MeOH in H_2O

Sample preparation : The sample was dissolved in a small amount of eluent and filtered through Millipore filter paper before injection.

Injection volume : 1 mL

Pump : LC-8A (Shimadzu)

Detector : SPD-10A UV Detector (Shimadzu)

Recorder : C-R6A Chromatopac (Shimadzu)

Temperature : Room temperature

2.4 Spectroscopy

2.4.1 Ultraviolet (UV) absorption spectra

UV (in methanol) spectra were obtained on a Shimadzu UV-160A UV/vis spectrophotometer (Pharmaceutical Research Instrument Center, Faculty of Pharmaceutical Sciences, Chulalongkorn University).

2.4.2 Mass spectra

Mass spectra were recorded on a Micromass LCT spectrometer or a Thermo-Finnigan Polaris Q mass spectrometer (Department of Chemistry, Faculty of Science, Mahidol University) or a Bruker microTOF mass spectrometer (National Center for Genetic Engineering and Biotechnology) or a Micromass Q-TOF Global Tandem mass spectrometer or a Thermo Navigator mass spectrometer (School of Pharmacy, University of London, United Kingdom).

2.4.3 Proton and carbon-13 nuclear magnetic resonance (^{1}H and ^{13}C-NMR) spectra

^{1}H NMR (300 MHz) and ^{13}C NMR (75 MHz) spectra were obtained with a Bruker Avance DPX-300 FT-NMR spectrometer (Faculty of Pharmaceutical Sciences, Chulalongkorn University).

^{1}H NMR (400 MHz) and ^{13}C NMR (100 MHz) spectra were obtained with a Bruker AV-400 NMR spectrometer (School of Pharmacy, University of London, United Kingdom).

^{1}H NMR (500 MHz) and ^{13}C NMR (125 MHz) spectra were obtained with a Bruker AV-500 NMR spectrometer (National Center for Genetic Engineering and Biotechnology or School of Pharmacy, University of London, United Kingdom).

Solvents for NMR spectra were deuterated chloroform ($CDCl_3$), deuterated acetone (acetone-d_6), deuterated methanol (MeOH-d_4) and deuterated pyridine (pyridine-d_5). Chemical shifts were reported in ppm scale using the chemical shift of the solvent as the reference signal.

2.5 Physical properties

2.5.1 Optical rotation

Optical rotations were measured on a Perkin Elmer Polarimeter 341 (Pharmaceutical Research Instrument Center, Faculty of Pharmaceutical Sciences, Chulalongkorn University) or a Perkin Elmer Polarimeter 343 (School of Pharmacy, University of London, United Kingdom), and reported as specific rotations $[\alpha]_D^{20}$, where $[\alpha]_D^{20} = \alpha / L \times C$ (α = observed optical rotation, L = path length in decimeters, C = concentration in g/mL).

2.5.2 Circular dichroism (CD) spectra

CD spectra were recorded on a JASCO J-715 spectropolarimeter (Pharmaceutical Research Instrument Center, Faculty of Pharmaceutical Sciences, Chulalongkorn University).

2.5 Solvents

Organic solvents employed throughout this work were of commercial grade and were redistilled prior to use or were HPLC grade.

3. Extraction and isolation

3.1 Extraction and isolation of compounds from *Derris malaccensis*

3.1.1 Extraction

The dried roots of *Derris malaccensis* (4 kg) were chopped, ground and then macerated with methanol (3x10 L) to give, after removal of the solvent, a methanol extract (200 g, 5% based on dried weight of roots).

3.1.2 Isolation

3.1.2.1 Isolation of compound DM1 (12-deoxo-12α-acetoxyelliptone)

The methanol extract (45 g) was fractionated by vacuum liquid column chromatography using a sintered glass filter column of silica gel (No.7734, 800 g). Elution was performed in a polarity gradient manner with mixtures of hexane and EtOAc (1:0 to 0:1). The eluates were collected 500 ml per fraction and examined by TLC (silica gel, hexane-EtOAc = 7:3) to yield 54 fractions. Fractions with similar chromatographic manner were combined to yield 17 fractions: Dm A (540 mg), Dm B (690 mg), Dm C (2.04 g), Dm D (630 mg), Dm E (1.46 g), Dm F (3.07 g), Dm G (1.75 g), Dm H (3.8 g), Dm I (4.02 g), Dm J (1.85 g), Dm K (4.65 g), Dm L (830 mg), Dm M (330 mg), Dm N (4 g), Dm O (4.76 g), Dm P (1.04 g), Dm Q (4.7 g).

Fraction Dm H (3.8 g) was further separated by flash column chromatography (silica gel 60 No. 9385, 100 g; hexane-EtOAc (1:0 to 0:1) to EtOAc-methanol (1:0 to 0:1)). Forty fractions (50 ml per fraction) were collected and combined based on their chromatographic pattern to give 4 fractions: Dm H1 (780 mg), Dm H2 (260 mg), Dm H3 (200 mg) and Dm H4 (1.8 g).

Fraction Dm H1 (780 mg) was purified on a Sephadex LH 20 column (MeOH) to furnish compound DM1 as a yellowish powder (242.4 mg), namely 12-deoxo-12α-acetoxyelliptone [**14**].

3.1.2.2 Isolation of compounds DM2 (12a-hydroxyelliptone), DM3 (tephrosin), DM4 (dehydroelliptone), DM5 (6-oxo-dehydroelliptone) and DM6 (deguelin)

Fraction Dm L (830 mg) was divided into 8 portions. Each portion was purified by RP18 HPLC (Shimadzu LC-8A, C18, column: Shim-pack Prep-ODS, 20x250 mm, 5 μm) with UV 254 nm detection and eluted with CH_3CN-H_2O = 1:1 (flow rate 2 ml/min) to afford 5 compounds including DM2 (44.5 mg, t_R=80 min), DM3 (236.6 mg, t_R=157.5 min), DM4 (52.1 mg, t_R=216.7 min), DM5 (4.3 mg, t_R=226 min) and DM6 (7.2 mg, t_R=256.3 min). Compounds DM2 - DM6 were subsequently identified as 12a-hydroxyelliptone [**58**], tephrosin [**64**], dehydroelliptone [**176**], 6-oxo-dehydroelliptone [**177**] which is a new rotenoid, and deguelin [**23**], respectively.

3.1.2.3 Isolation of compound DM7 (elliptone)

Fraction Dm N (4 g) was divided into 20 portions. Each portion was purified by RP18 HPLC (Shimadzu LC-8A, C18, column: Shim-pack Prep-ODS, 20x250 mm,

5 μm) with UV 254 nm detection and eluted with MeOH-H_2O = 7.5:2.5 (flow rate 2 ml/min) to yield 6 fractions: Dm N1 (16.1 mg), Dm N2 (35.8 mg), Dm N3 (73.9 mg, t_R=48.8 min), Dm N4 (11.3 mg), Dm N5 (58.4 mg, t_R=57.7 min), Dm N6 (36.5 mg, t_R=79.2 min) and Dm N7 (5.8 mg). Fractions Dm N3 and Dm N6 were later identified as DM2, 12a-hydroxyelliptone [**58**] and DM3, tephrosin [**64**], respectively.

Fraction Dm N5 (58.4 mg) was purified by RP18 HPLC (Shimadzu LC-8A, C18, column: Shim-pack Prep-ODS, 20x250 mm, 5 μm) with UV 254 nm detection and eluted with CH_3CN-H_2O = 3:2 (flow rate 2 ml/min) to give compound DM7 (24.8 mg, t_R=71.8 min) as elliptone [**63**].

3.2 Extraction and isolation of compounds from *Carissa carandas*

3.2.1 Extraction

The dried stems of *Carissa carandas* (2 kg) were chopped, ground and then macerated with methanol (3x10 L) to give, after removal of the solvent, a methanol extract (149.5 g, 7.48% based on dried weight of stems).

3.2.2 Isolation

3.2.2.1 Isolation of compounds CC1 {(6*R*,7*S*,8*S*)-7a-[(*β*-glucopyranosyl) oxy]lyoniresinol}, CC2 {(6*S*,7*R*,8*R*)-7a-[(*β*-glucopyranosyl)oxy]lyoniresinol} and CC3 (carandoside)

The methanol extract (30 g) was divided into 8 portions. Each portion was separated by C18 flash column chromatography (column: *VerSa Pak*, C18 Cartridge (40x75 mm, 45-75μm)) with UV 254 nm detection and isocratic elution MeOH-H_2O = 4:6 (flow rate 7.35 ml/min) to yield 5 fractions: Cc A (19.8 g), Cc B (780 mg), Cc C (790 mg), Cc D (530 mg) and Cc E (3.57 g).

Fraction C (790 mg) was separately isolated on a Sephadex LH 20 column (MeOH) to afford 7 fractions: Cc C1 (50 mg), Cc C2 (110 mg), Cc C3 (230 mg), Cc C4 (80 mg), Cc C5 (130 mg), Cc C6 (70 mg) and Cc C7 (40 mg).

Fraction Cc C2 (110 mg) was further purified by RP18 HPLC (Shimadzu LC-8A, C18, column: Shim-pack Prep-ODS, 20x250 mm, 5 μm) with UV 254 nm detection and eluted with CH_3CN-MeOH-H_2O = 1.4:0.9:7.7 (flow rate 2 ml/min) to give 3 compounds, CS1 (22.9 mg, t_R=85.4 min), CS2 (12 mg, t_R=91.5 min) and CS3 (9.1 mg, t_R=109.7 min). Compounds CS1, CS2 and CS3 were characterized as 6*R*,7*S*,8*S*)-7a-[(*β*-glucopyranosyl)oxy]lyoniresinol [**178**], a new lignan glucoside

named ((6*S*,7*R*,8*R*)-7a-[(*β*-glucopyranosyl)oxy]lyoniresinol) [**179**] and a new sesquiterpene glucoside named carandoside [**180**].

3.2.2.2 Isolation of compound CC4 [(–)-carissanol]

Fraction Cc C5 (130 mg) was divided into 3 portions. Each portion was subjected to RP18 HPLC (Shimadzu LC-8A, C18, column: Shim-pack Prep-ODS, 20x250 mm, 5 μm) with UV 254 nm detection and eluted with MeOH-H_2O = 4:6 (flow rate 2 ml/min) to give 6 fractions: Cc C5A (35 mg), Cc C5B (14 mg), Cc C5C (2 mg), Cc C5D (19 mg), Cc C5E (21 mg) and Cc C5F (28 mg).

Fraction Cc C5D (19 mg) was further chromatographed on a silica gel column (No. 9385), eluted with CH_2Cl_2-MeOH gradient to yield compound CC4 (5.2 mg) which was identified as (–)-carissanol [**167**].

3.2.2.3 Isolation of compound CC5 [(–)-nortrachelogenin]

Fraction Cc D (530 mg) was divided into 6 portions. Each portion was fractionated on a Sephadex LH 20 column (MeOH) to give 7 fractions: Cc D1 (46 mg), Cc D2 (180 mg), Cc D3 (120 mg), Cc D4 (29 mg), Cc D5 (9 mg), Cc D6 (6 mg) and Cc D7 (12 mg).

Fraction Cc D3 (120 mg) was separated into 2 portions which were further purified by RP18 HPLC (Shimadzu LC-8A, C18, column: Shim-pack Prep-ODS, 20x250 mm, 5 μm) with UV 254 nm detection and eluted with MeOH-H_2O = 4:6 (flow rate 2 ml/min) to give 6 fractions: Cc D3A (13 mg), Cc D3B (14 mg), Cc D3C (19 mg), Cc D3D (13 mg), Cc D3E (15 mg) and Cc D3F (11 mg).

Fractions Cc C5E (21 mg) and Cc D3D (13 mg) were combined according to their TLC patterns (silica gel, CH_2Cl_2-MeOH = 9.6:0.4) and later purified on a silica gel column (No. 9385), eluted with CH_2Cl_2-MeOH gradient to afford compound CC5 (25.3 mg). It was identified as (–)-nortrachelogenin [**168**].

3.3 Extraction and isolation of compounds from *Carissa spinarum*

3.3.1 Extraction

The dried stems of *Carissa spinarum* (2 kg) were chopped, ground and then macerated with methanol (3x10 L) to give, after removal of the solvent, a methanol extract (123 g, 6.15% based on dried weight of stems).

3.3.2 Isolation

3.3.2.1 Isolation of compounds CS1 (6-methoxycoumarin) and CS2 [(–)-nortrachelogenin]

The methanol extract (55 g) was divided into 13 portions. Each portion was separated on a C18 flash column [column: *VerSa Pak*, C18 Cartridge (40x75 mm, 45-75μm)] with UV 254 nm detection and eluted with MeOH-H_2O = 4:6 (flow rate 7.35 ml/min) to yield 5 fractions: Cs A (37.8 g), Cs B (2.8 g), Cs C (1.1 g), Cs D (800 mg) and Cs E (9 g).

Fraction Cs A (37.8 g) was divided into 40 portions. Each portion was re-fractionated on a Sephadex LH 20 column (MeOH). The eluates (50 ml per fraction) were examined by reversed phase TLC (C18, MeOH-H_2O = 4:6), and combined according to their TLC pattern to afford 6 fractions: Cs A1 (1.6 g), Cs A2 (11.5 g), Cs A3 (16 g), Cs A4 (2.5 g), Cs A5 (3 g) and Cs A6 (253 mg).

Fraction Cs A3 (16 g) was further chromatographed on a silica gel column (No. 9385), eluted with CH_2Cl_2-MeOH gradient to give 8 fractions: Cs A3A (0.4 mg), Cs A3B (7 mg), Cs A3C (326.2 mg), Cs A3D (396.6 mg), Cs A3E (191.3 mg), Cs A3F (243.1 mg), Cs A3G (2 g) and Cs A3H (4.7 g).

Fraction Cs A3C (326.2 mg) was divided into 16 portions which were purified on preparative TLC (silica gel No. 9385, CH_2Cl_2-MeOH = 9.8:0.2, double development) to give compounds CS1 (15.2 mg) and CS2 (172.5 mg), subsequently identified as scopoletin [**181**] and (–)-nortrachelogenin [**168**], respectively.

3.3.2.2 Isolation of compound CS3 [(–)-carissanol]

Fraction Cs A3D (396.6 mg) was further purified on a silica gel column (No. 9385), eluted with CH_2Cl_2-MeOH gradient to afford compound CS3 (81.4 mg) as (–)-carissanol [**167**].

3.3.2.3 Isolation of compound CS4 [(–)-carinol]

Fraction Cs A3E (191.3 mg) was divided into 8 portions which were then separated on preparative TLC (silica No. 9385, CH_2Cl_2-MeOH 9.6:0.4, triple development) to give compounds CS2 (6 mg), CS3 (33.6 mg) and CS4 (102.8 mg), which were subsequentially identified as (–)-nortrachelogenin [**168**], (–)-carissanol [**167**] and (–)-carinol [**160**], respectively.

3.3.2.4 Isolation of compound CS5 [(+)-cycloolivil]

Fraction Cs A3F (243.1 mg) was purified on a silica gel column (No. 9385), eluted with CH_2Cl_2-MeOH gradient to yield 2 pure compounds, CS4 (37.7 mg) and CS5 (27.7 mg). They were later identified as (–)-carinol [**160**] and (+)-cycloolivil [**182**], respectively.

3.3.2.5 Isolation of compound CS6 [(+)-8-hydroxypinoresinol]

Fraction Cs B (2.8 g) was divided into 4 portions. Each portion was fractionated on a Sephadex LH 20 column (MeOH). The eluates (50 ml per fraction) were examined by reversed phase TLC (C18, MeOH-H_2O = 4:6), and combined according to their TLC pattern to afford 7 fractions: Cs B1 (63.1 mg), Cs B2 (1.07 g), Cs B3 (1.3 g), Cs B4 (96.8 mg), Cs B5 (81.2 mg), Cs B6 (63.4 mg) and Cs B7 (3.2 mg).

Fraction Cs B3 (1.3 g) was splitted into 3 portions. Each portion was re-chromatographed on a solid phase extraction (SPE) column (silica gel, particle size = 0.055 nm, CH_2Cl_2-MeOH gradient). The eluates were collected 50 ml per fraction and examined by TLC (silica gel, CH_2Cl_2-MeOH = 9.6:0.4) to give 8 fractions: Cs B3A (20 mg), Cs B3B (42.8 mg), Cs B3C (319.5 mg), Cs B3D (41.6 mg), Cs B3E (147.8 mg), Cs B3F (53.7 mg), Cs B3G (192.8 mg) and Cs B3H (226.6 mg). Fractions Cs B3E and Cs B3F were identified as the compounds (–)-(carissanol) [**167**] and (–)-carinol [**160**], respectively.

Fraction Cs B3B (42.8 mg) was divided into 2 portions. Each was purified on preparative TLC (silica gel No. 9385, hexane-EtOAc = 1:1, double development) to yield compound CS1 (29.9 mg) as scopoletin [**181**].

Fraction Cs B3C (319.5 mg) was separated into 10 portions. Each portion was further separated on preparative TLC (silica gel No. 9385, CH_2Cl_2-MeOH = 9.6:0.4, triple development) to afford compounds CS2 (222.7 mg) and CS6 (6 mg). These two compounds were subsequently identified as (–)-nortrachelogenin [**168**] and (+)-8-hydroxypinoresinol [**183**], respectively.

3.3.2.6 Isolation of compound CS7 [(–)-olivil]

Fraction Cs B3G (192.8 mg) was divided into 8 portions. Each portion was purified by preparative TLC (silica gel No. 9385, CH_2Cl_2-Acetone-MeOH = 10:1:0.2, quintuple development) to afford compound CS7 (18.1 mg) as (–)-olivil [**169**].

3.3.2.7 Isolation of compound CS8 [(–)-secoisolariciresinol]

Fraction Cs C (1.1 g) was divided into 3 portions. Each portion was fractionated on a Sephadex LH 20 column (MeOH). The eluates (50 ml per fraction) were examined by reversed phase TLC (C18, MeOH-H_2O = 4:6), and combined according to their TLC pattern to afford 7 fractions: Cs C1 (25 mg), Cs C2 (206 mg), Cs C3 (120 mg), Cs C4 (556 mg), Cs C5 (5 mg), Cs C6 (36 mg) and Cs C7 (4 mg).

Fraction Cs C3 (120 mg) was further separated on an SPE column (silica gel, particle size = 0.055 nm, CH_2Cl_2-MeOH gradient). The eluates were collected 50 ml per fraction and examined by TLC (silica gel, CH_2Cl_2-MeOH = 9.6:0.4) to give 6 fractions: Cs C3A (18.1 mg), Cs C3B (8.2 mg), Cs C3C (24.9 mg), Cs C3D (15.2 mg), Cs C3E (11.7 mg) and Cs C3F (39.7 mg).

Fraction Cs C3C (24.9 mg) was purified by preparative TLC (silica gel No. 9385, CH_2Cl_2-MeOH = 9.4:0.6, triple development) to yield compounds CS3 (3.6 mg), CS4 (5.1 mg) and CS8 (2.3 mg), eventually identified as (–)-carissanol [**167**], (–)-carinol [**160**] and (–)-secoisolariciresinol [**170**], respectively.

Fraction Cs C4 (556 mg) was divided into 2 portions. Each portion was re-chromatographed on an SPE column (silica 0.055 nm, CH_2Cl_2-MeOH gradient) to give 5 fractions: Cs C4A (296.7 mg), Cs C4B (98.3 mg), Cs C4C (26 mg), Cs C4D (19 mg) and Cs C4E (40.2 mg).

Fraction Cs C4A (296.7 mg) was divided into 10 portions. Each portion was further purified by preparative TLC (silica gel No. 9385, CH_2Cl_2-MeOH = 9.4:0.6, triple development) to afford compounds CS2 (113.2 mg) and CS3 (39.1 mg) which was identified as (–)-nortrachelogenin [**168**] and (–)-carissanol [**167**], respectively.

Fraction Cs C4B (98.3 mg) was divided into 4 portions. Each portion was re-purified by preparative TLC (silica gel No. 9385, CH_2Cl_2-MeOH = 9.4:0.6, triple development) to afford compound CS4 (67.2 mg) as (–)-carinol [**160**].

3.3.2.8 Isolation of compound CS9 [(+)-pinoresinol]

Fraction Cs D (800 mg) was fractionated by vacuum liquid column chromatography using a sintered glass filter column of silica gel (No. 9385). Elution was performed in a polarity gradient manner with mixtures of CH_2Cl_2 and MeOH (1:0 to 0:1). The eluates were collected 100 ml per fraction and combined according to their chromatographic TLC pattern (CH_2Cl_2-MeOH = 9.4:0.6) to give 13 fractions: Cs D1 (1.3 mg), Cs D2 (1.1 mg), Cs D3 (0.4 mg), Cs D4 (63.2 mg), Cs D5 (69.7 mg), Cs

D6 (16.7 mg), Cs D7 (17.3 mg), Cs D8 (35.8 mg), Cs D9 (11.2 mg), Cs D10 (7.5 mg), Cs D11 (13.2 mg), Cs D12 (132.6 mg) and Cs D13 (375.2 mg).

Fraction Cs D4 (63.2 mg) was divided into 4 portions. Each portion was purified by preparative TLC (silica gel No. 9385, CH_2Cl_2-MeOH = 9.6:0.4, triple development) to afford compounds CS2 (17 mg) and CS9 (9.3 mg) as (–)-nortrachelogenin [**168**] and (+)-pinoresinol [**175**], respectively.

Fraction Cs D5 (69.7 mg) was divided into 4 portions. Each portion was then purified by preparative TLC (silica gel No. 9385, hexane-EtOAc = 3:7, triple development) to give compound CS2 (43.9 mg) as (–)-nortrachelogenin [**168**].

Fraction Cs D8 (35.8 mg) was divided into 2 portions. Each portion was separated using preparative TLC (silica gel No. 9385, CH_2Cl_2-MeOH = 9.6:0.4, triple development) to yield compound CS3 (12.5 mg) which was identified as (–)-carissanol [**167**].

3.3.2.9 Isolation of compound CS10 (carissone)

Fraction Cs E (9 g) was fractionated by vacuum liquid column chromatography using a sintered glass filter column of silica gel (No. 9385). Elution was performed in a polarity gradient manner with mixtures of CH_2Cl_2 and MeOH (1:0 to 0:1). The eluates were collected 300 ml per fraction and combined according to their similar chromatographic TLC pattern (CH_2Cl_2-MeOH = 9.4:0.6) to give 8 fractions: Cs E1 (211.5 mg), Cs E2 (928.2 mg), Cs E3 (1.2 g), Cs E4 (469.4 mg), Cs E5 (229 mg), Cs E6 (765.2 mg), Cs E7 (664.2 mg) and Cs E8 (2.9 g).

Fraction Cs E2 (928.2 mg) was divided into 3 portions. Each portion was re-chromatographed on an SPE column (silica gel 0.055 nm, hexane-CH_2Cl_2-acetone gradient) to afford 8 fractions: Cs E2A (21.4 mg), Cs E2B (98.1 mg), Cs E2C (113.3 mg), Cs E2D (107.9 mg), Cs E2E (125.3 mg), Cs E2F (270.9 mg), Cs E2G (53.6 mg) and Cs E2H (22.2 mg).

Fraction Cs E2F (270.9 mg) was divided into 8 portions. Each portion was purified on preparative TLC (silica gel No. 9385, CH_2Cl_2-MeOH = 9.8:0.2, triple development) to give compound CS10 (76.2 mg) as carissone [**162**].

3.3.2.10 Isolation of compound CS11 (digitoxigenin 3-*O*-*β*-D-digitalopyranoside)

Fraction Cs E3 (1.2 g) was fractionated on a Sephadex LH 20 column [$CHCl_3$-MeOH gradient (1:0 to 0:1)]. The eluates (50 ml per fraction) were examined by TLC

(silica gel No. 9385, CH_2Cl_2-MeOH = 9.6:0.4), and combined according to their TLC pattern to give 9 fractions: Cs E3A (76.2 mg), Cs E3B (96.5 mg), Cs E3C (512.6 mg), Cs E3D (211.5 mg), Cs E3E (128.4 mg), Cs E3F (23.8 mg), Cs E3G (45.7 mg), Cs E3H (93.6 mg) and Cs E3I (20.6 mg).

Fraction Cs E3D (211.5 mg) was further separated on SPE column (silica 0.055 nm, hexane-EtOAc gradient) to obtain compound CS11 (6.8 mg) later identified as digitoxigenin 3-*O*-*β*-D-digitalopyranoside [**184**].

3.3.2.11 Isolation of Compound CS12 (Evomonoside)

Fraction Cs E5 (229 mg) was purified on a Sephadex LH 20 column [CH_2Cl_2-MeOH gradient (1:0 to 0:1)]. The eluates (30 ml per fraction) were examined by TLC (silica gel No. 9385, CH_2Cl_2-MeOH = 9.6:0.4), and combined according to their TLC pattern to yield compound CS12 (12.1 mg) as evomonoside [**185**].

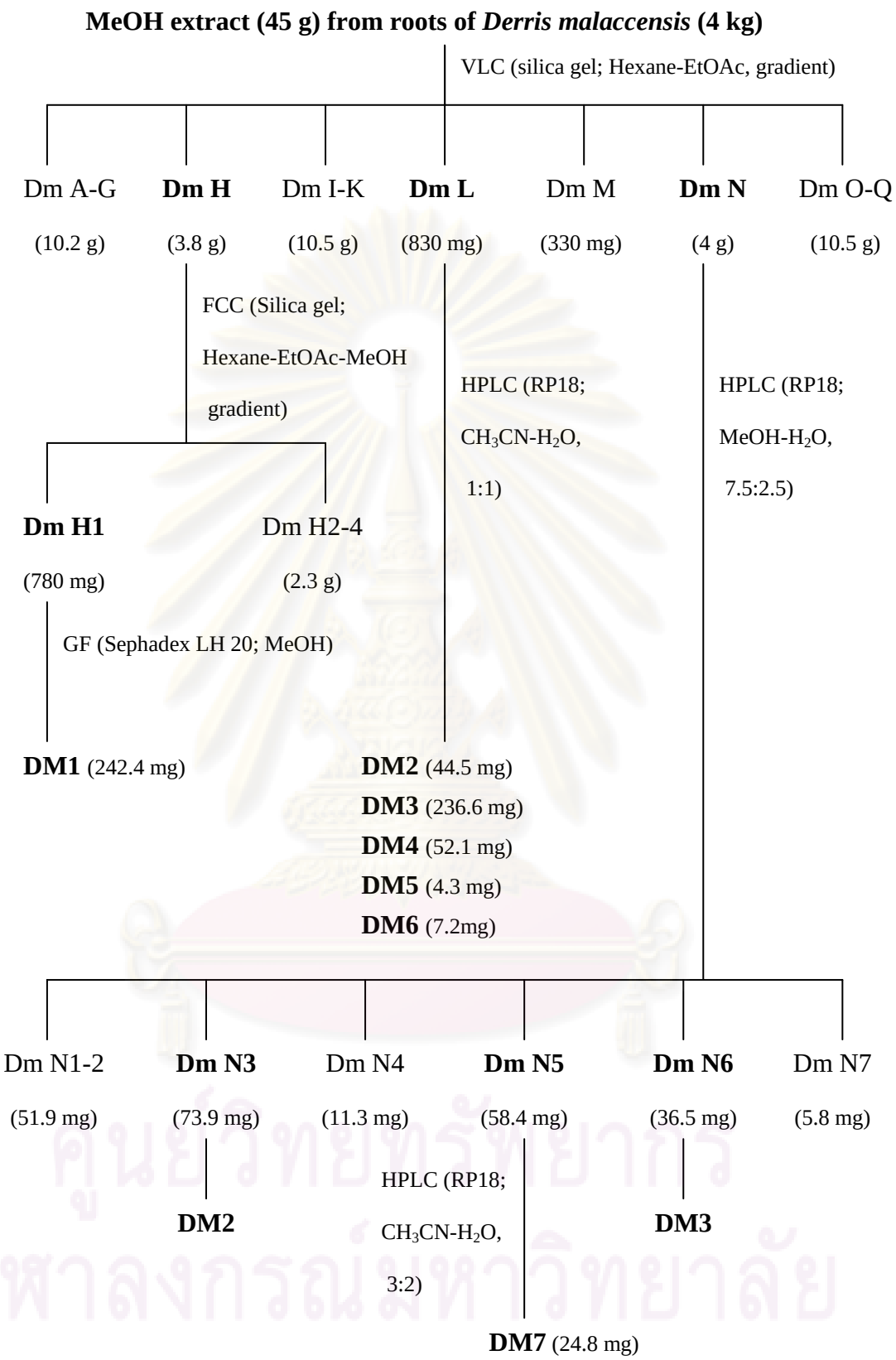

Scheme 1 Separation of the MeOH extract of the roots of *D. malaccensis*

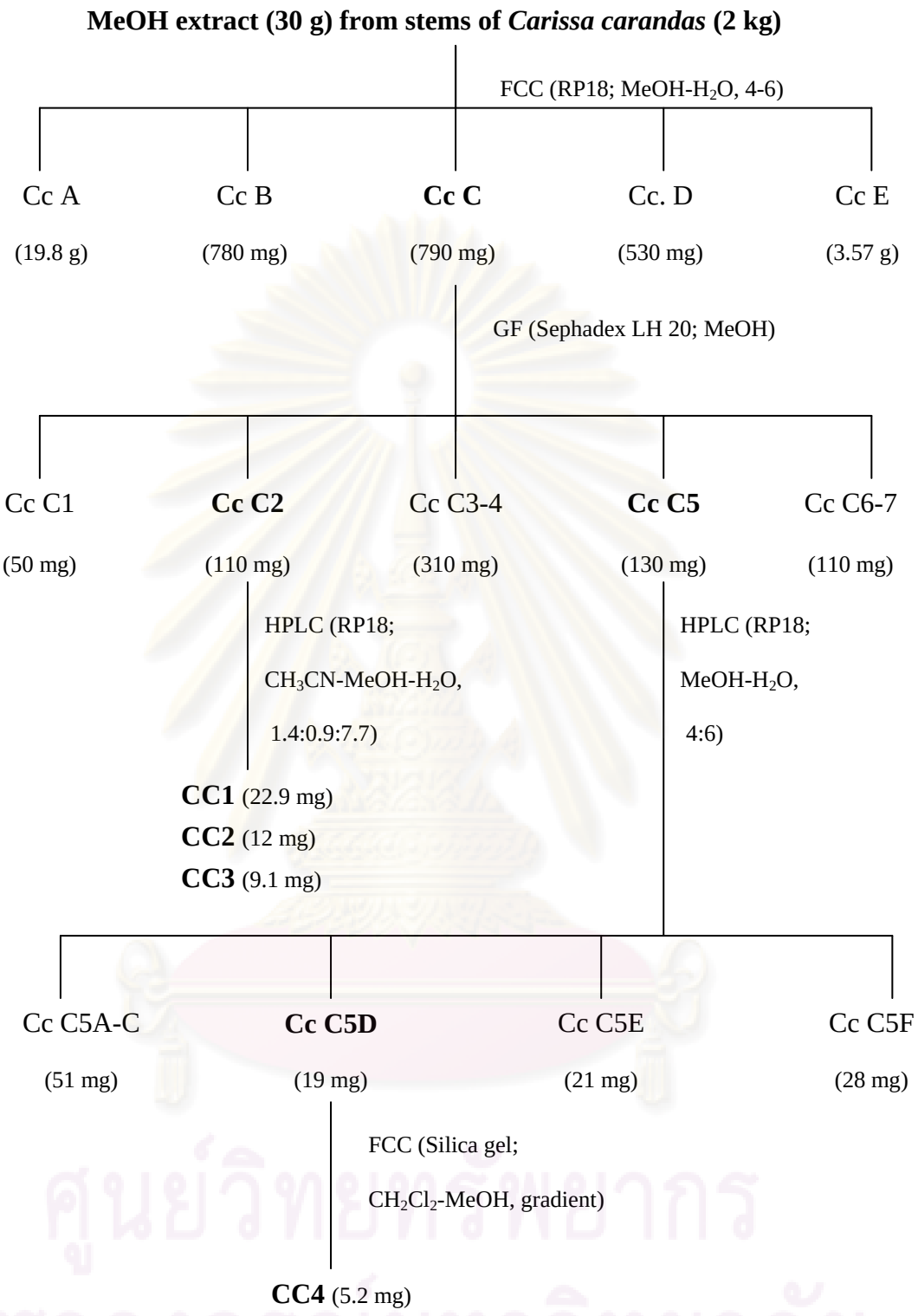

Scheme 2 Separation of the MeOH extract of the stems of *C. carandas*

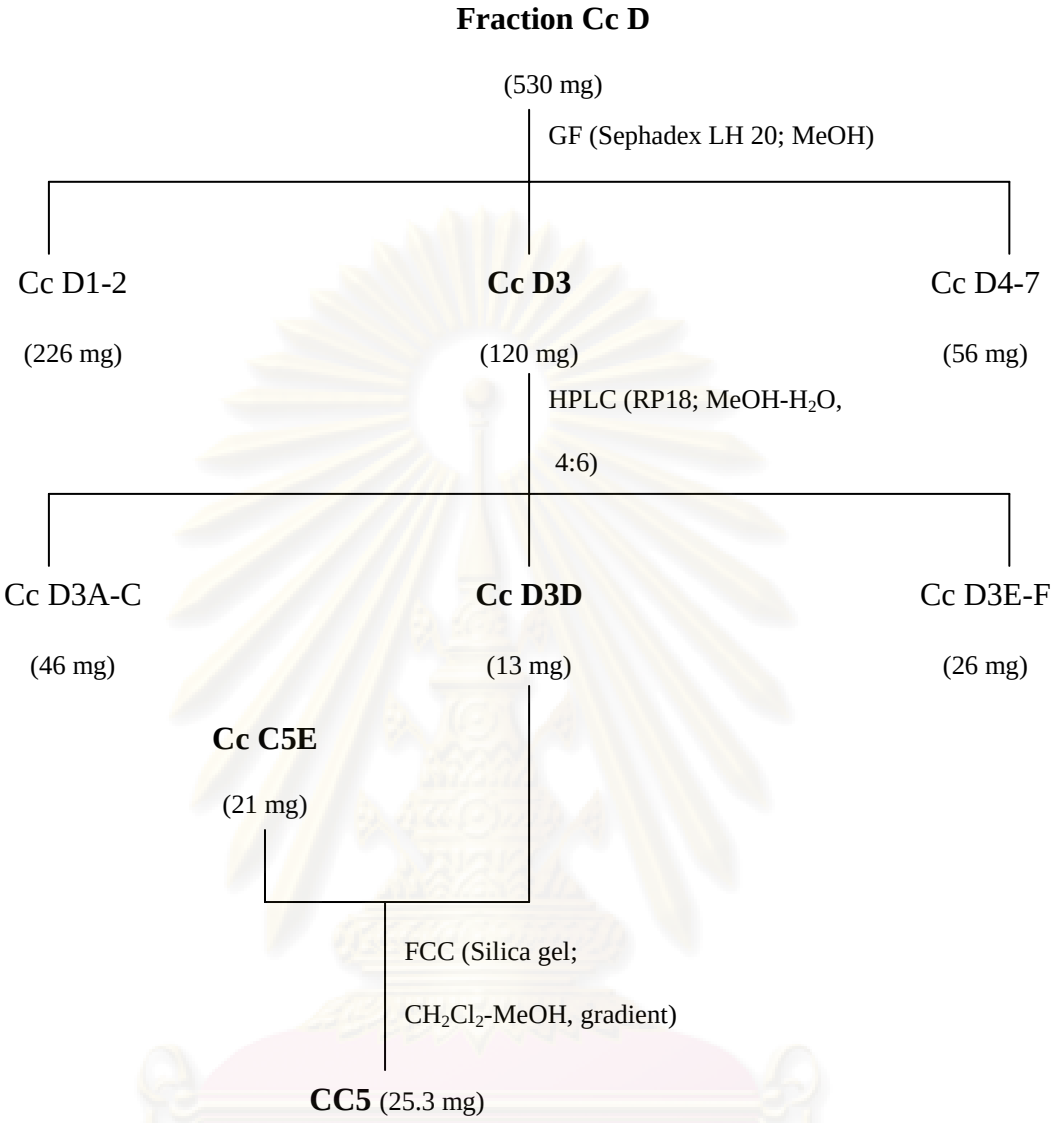

Scheme 3 Separation of fractions Cc C and Cc D from the MeOH extract of the stems of *C. carandas*

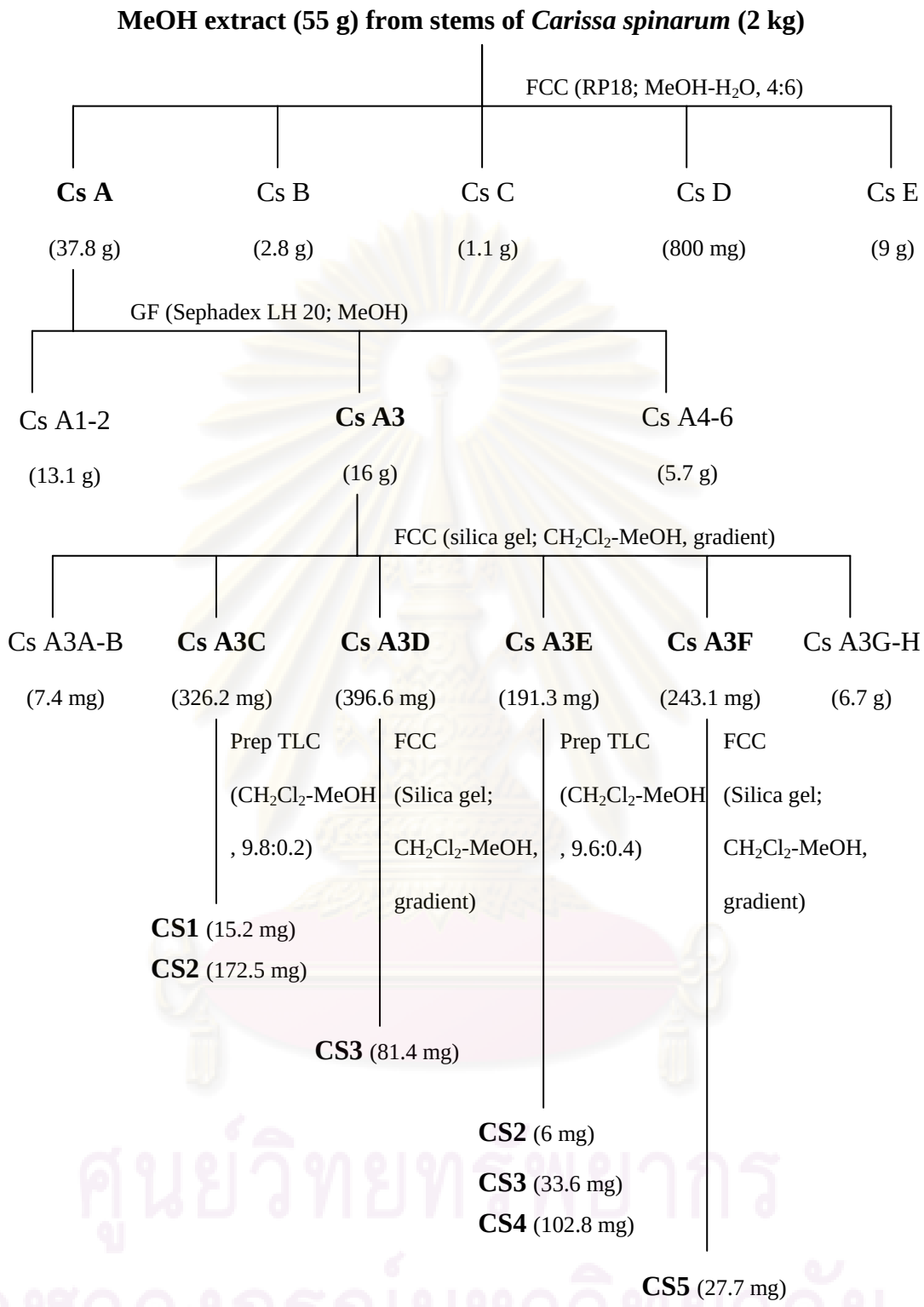

Scheme 4 Separation of fraction Cs A from the MeOH extract of the stems of *C. spinarum*

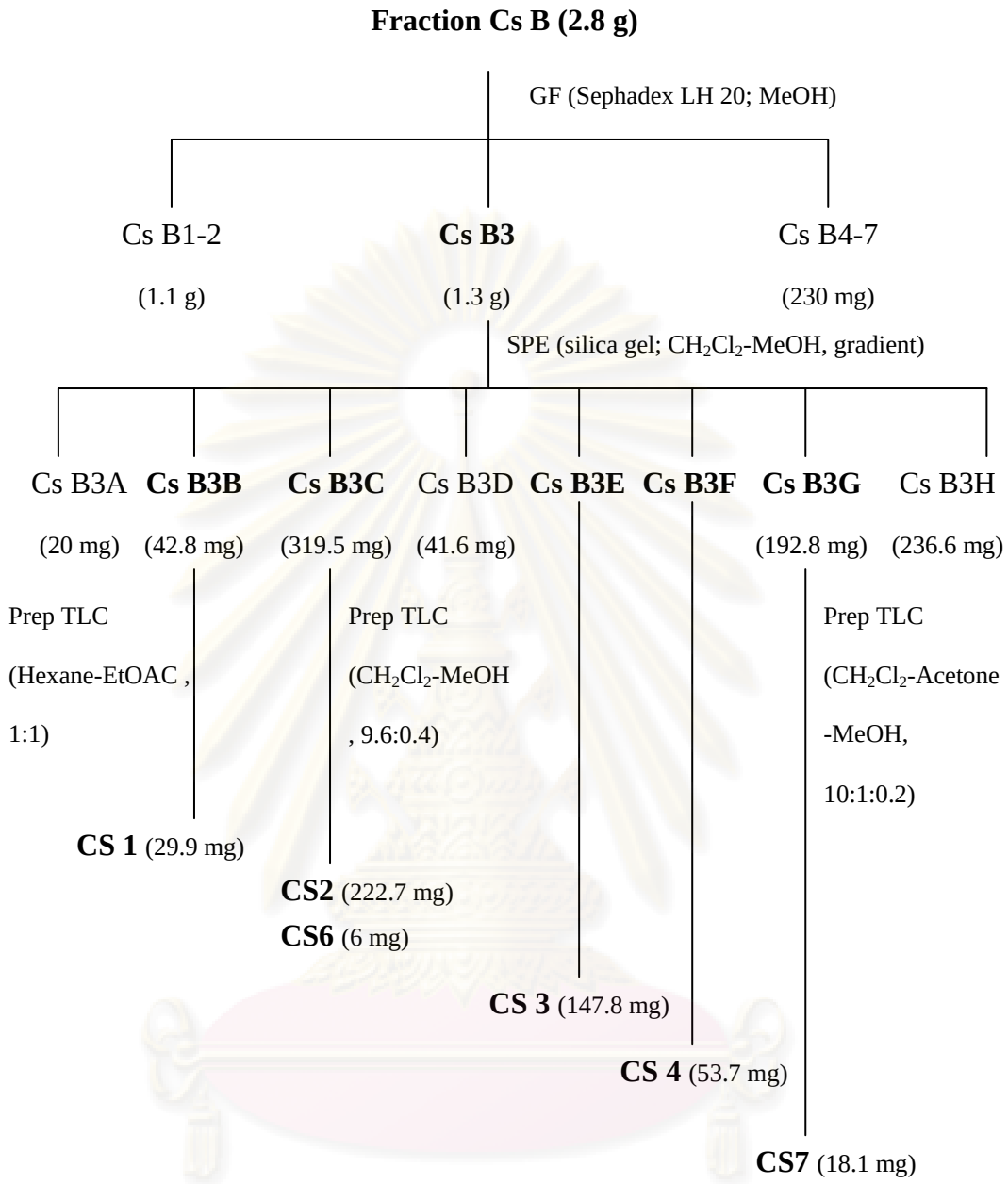

Scheme 5 Separation of fraction Cs B from the MeOH extract of the stems of *C. spinarum*

Fraction Cs C (1.1 g)

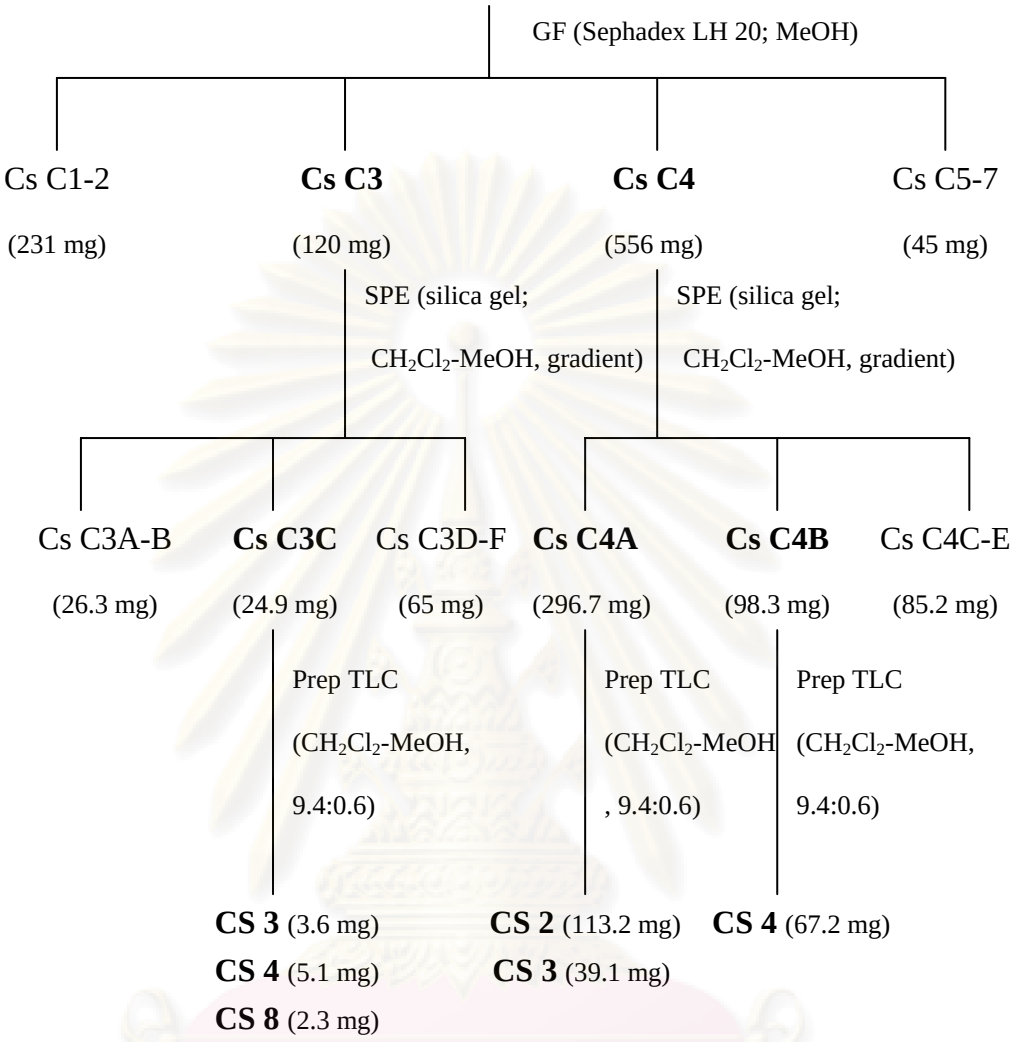

Scheme 6 Separation of fraction Cs C from the MeOH extract of the stems of *C. spinarum*

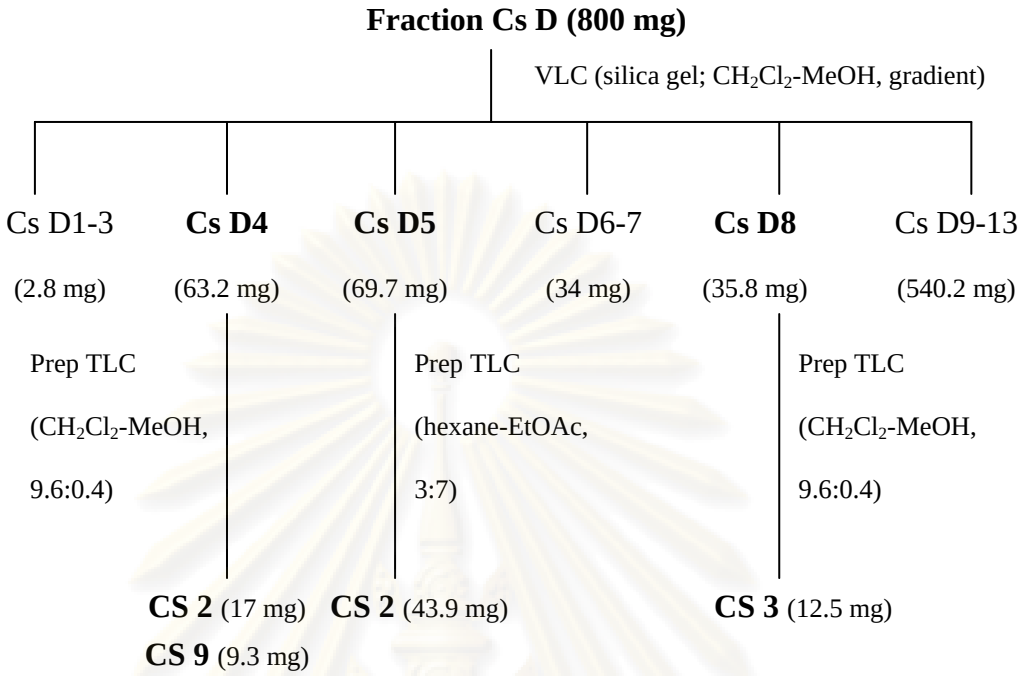

Scheme 7 Separation of fraction Cs D from the MeOH extract of the stems of *C. spinarum*.

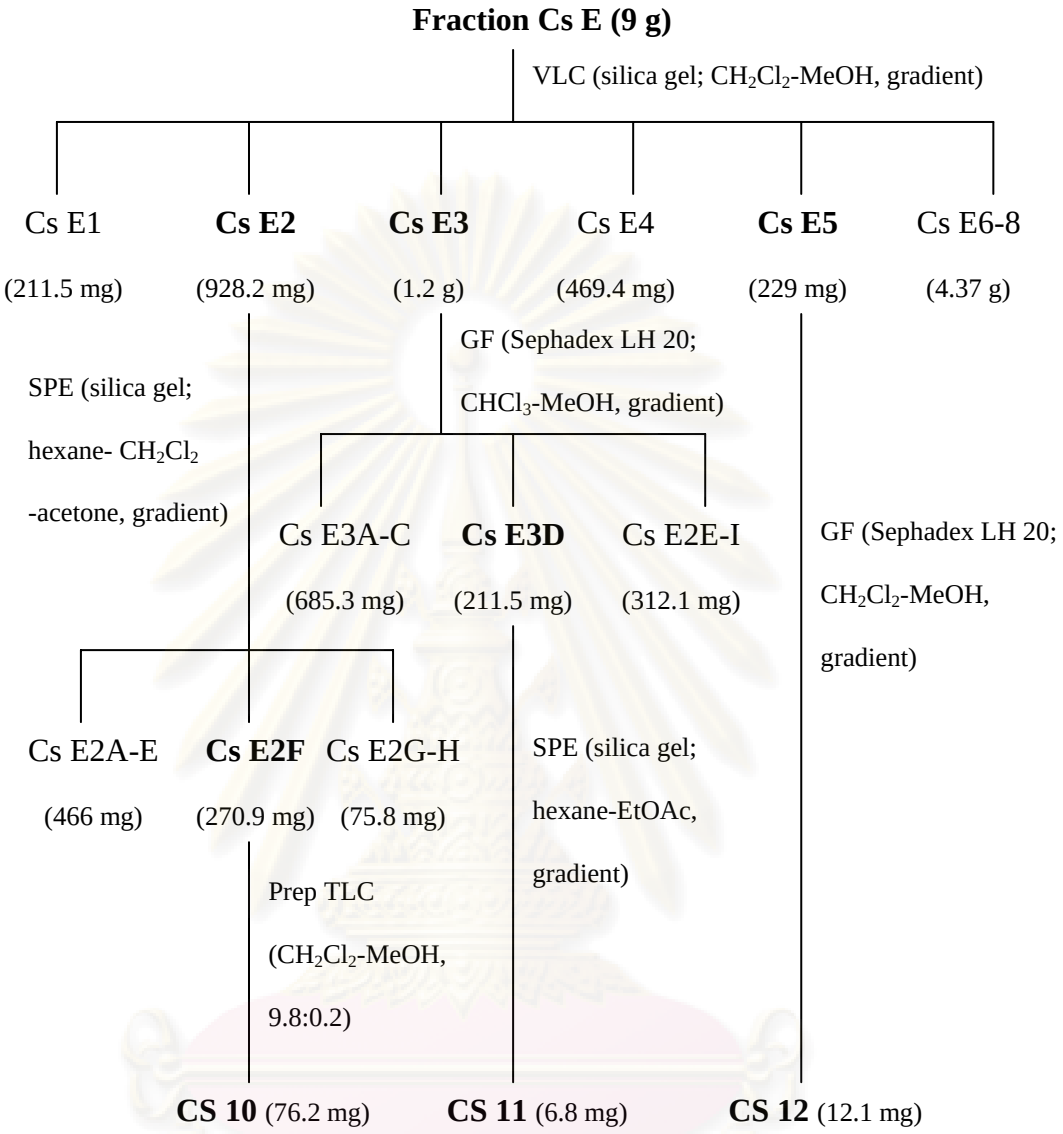

Scheme 8 Separation of fraction Cs E from the MeOH extract of the stems of *C. spinarum*

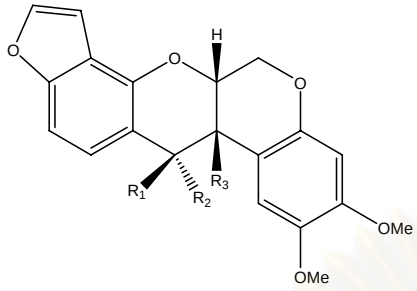

DM1 12-deoxo-12α-acetoxyelliptone [**14**]

R_1 = H, R_2 = OAc, R_3 = H

DM2 12a-hydroxyelliptone [**58**]

R_1, R_2 = O, R_3 = OH

DM7 elliptone [**63**]

R_1, R_2 = O, R_3 = H

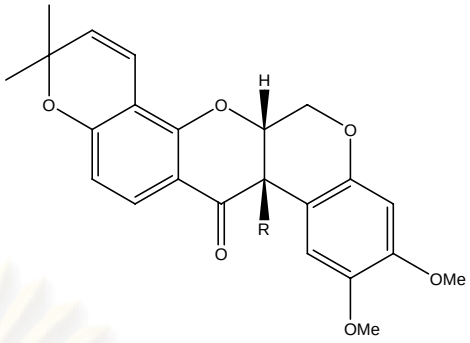

DM3 tephrosin [**64**]

R = OH

DM6 deguelin [**23**]

R = H

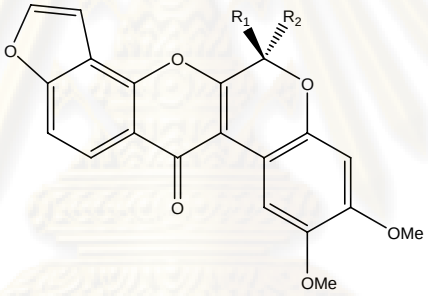

DM4 dehydroelliptone [**176**]

R_1 = R_2 = H

DM5 6-oxo-dehydroelliptone[**177**]

R_1, R_2 = O

Figure 4 Structures of compounds isolated from *D. malaccensis*

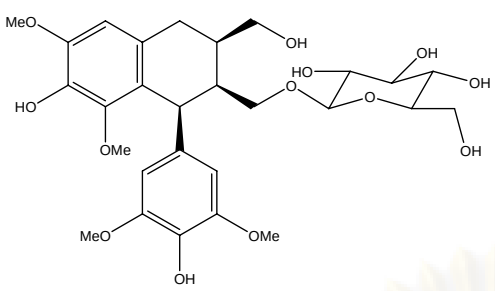

CC1 (6*R*,7*S*,8*S*)-7a-[(*β*-glucopyranosyl)oxy]lyoniresinol [**178**]

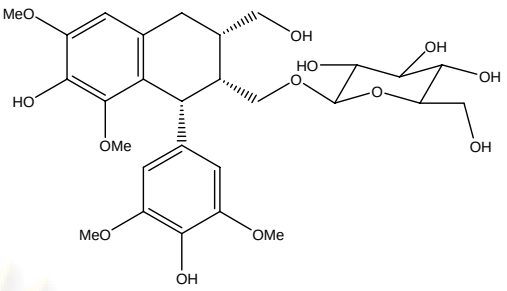

CC2 (6*S*,7*R*,8*R*)-7a-[(*β*-glucopyranosyl)oxy]lyoniresinol [**179**]

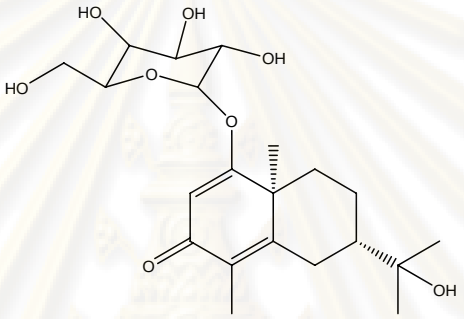

CC3 carandoside [**180**]

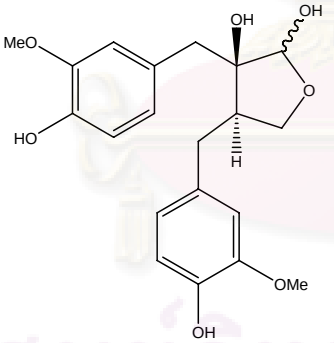

CC4 (–)-carrisanol [**167**]

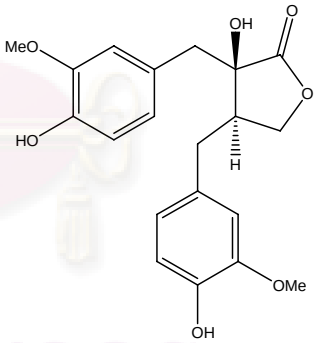

CC5 (–)-nortrachelogenin [**168**]

Figure 5 Structures of compounds isolated from *C. carandas*

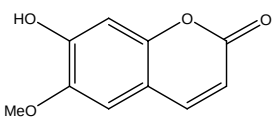

CS1 scopoletin [**181**]

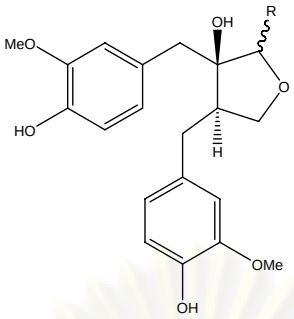

CS2 (–)-nortrachelogenin [**168**]**;** R=O

CS3 (–)-carrisanol [**167**]; R=OH

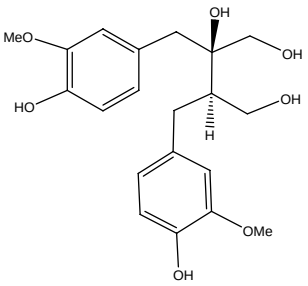

CS4 (–)-carinol [**160**]

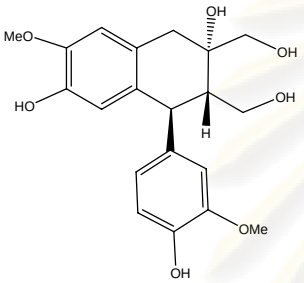

CS5 (+)-cycloolivil [**182**]

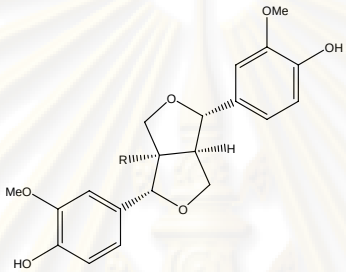

CS6 (+)-8-hydroxypinoresinol [**183**]; R=OH

CS9 (+)-pinoresinol [**175**]; R=H

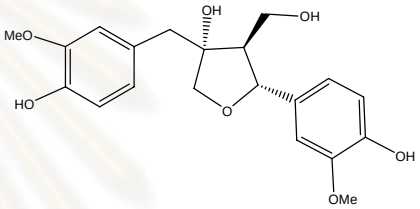

CS7 (–)-olivil [**169**]

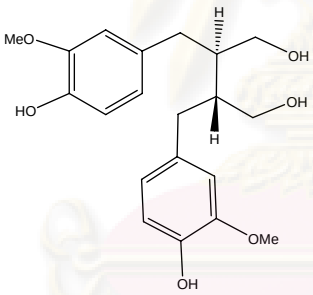

CS8 (–)-secoisolariciresinol [**170**]

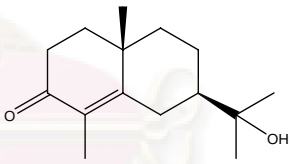

CS10 carissone [**162**]

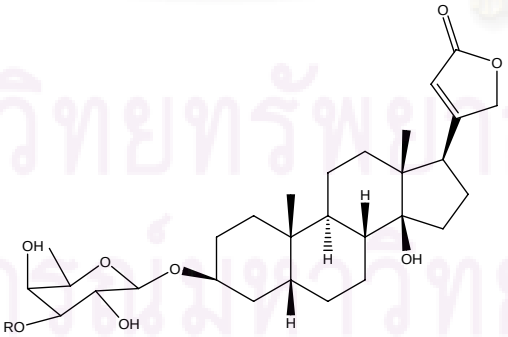

CS11 digitoxigenin 3-*O*-*β*-D-digitalopyranoside [[**184**]; R=Me

CS12 evomonoside [**185**]; R=H

Figure 6 Structures of compounds isolated from *C. spinarum*

4. Physical and Spectra data of isolated compounds

4.1 Compound DM1 (12-Deoxo-12α-acetoxyelliptone)

Compound DM1 was obtained as a yellowish powder, soluble in CH_2Cl_2 (242.4 mg, $6.06x10^{-5}$ % based on dried weight of roots).

ESIMS : $[M+Na]^+$ *m/z* 419.11; Figure 12

$[\alpha]_D^{20}$: −256.4 ° (*c* 0.055; MeOH)

UV : λ_{max} nm (log ε), in methanol; Figure 10
250 (4.38), 253 (4.41), 290 (4.19)

IR : ν_{max} cm^{-1}, KBr disc; Figure 11
3150, 2958, 2860, 1737, 1622, 1602, 1514, 1480, 1221, 1088, 1046

^{1}H NMR : δ ppm, 300 MHz, in $CDCl_3$; Figure 13, Table 3

^{13}C NMR : δ ppm, 75 MHz, in $CDCl_3$; Figure 14, Table 3

4.2 Compound DM2 (12a-Hydroxyelliptone)

Compound DM2 was obtained as a yellowish powder, soluble in CH_2Cl_2 (118.4 mg, $2.96x10^{-5}$ % based on dried weight of roots).

ESIMS : $[M+Na]^+$ *m/z* 391.08; Figure 18

$[\alpha]_D^{20}$: +12.86 ° (*c* 0.07; MeOH)

UV : λ_{max} nm (log ε), in methanol; Figure 16
223 (4.75), 240 (4.66), 280 (4.08)

IR : ν_{max} cm^{-1}, KBr disc; Figure 17
3453, 3124, 2936, 1679, 1614, 1510, 1465, 1217, 1026, 746

^{1}H NMR : δ ppm, 300 MHz, in $CDCl_3$; Figure 19, Table 4

^{13}C NMR : δ ppm, 75 MHz, in $CDCl_3$; Figure 20, Table 4

4.3 Compound DM3 (Tephrosin)

Compound DM3 was obtained as a yellowish powder, soluble in CH_2Cl_2 (273.1 mg, $6.82x10^{-5}$ % based on dried weight of roots).

ESIMS : $[M+Na]^+$ *m/z* 433.33; Figure 24

$[\alpha]_D^{20}$: −31.67 ° (*c* 0.06; MeOH)

UV : λ_{max} nm (log ε), in methanol; Figure 22
236 (4.41), 250 (4.39), 272 (4.46), 300 (4.05)

IR : ν_{max} cm^{-1}, KBr disc; Figure 23
3449, 3016, 2935, 1674, 1598, 1510, 1443, 1218, 1111, 1028, 755

^{1}H NMR : δ ppm, 300 MHz, in $CDCl_3$; Figure 25, Table 5

^{13}C NMR : δ ppm, 75 MHz, in $CDCl_3$; Figure 26, Table 5

4.4 Compound DM4 (Dehydroelliptone)

Compound DM4 was obtained as a yellow powder, soluble in CH_2Cl_2 (52.1 mg, $1.3x10^{-5}$ % based on dried weight of roots).

HRESIMS : $[M+Na]^+$ at *m/z* 373.0701 (calcd for $C_{20}H_{14}O_6Na$ 373.0683)

EIMS : *m/z* (% relative intensity); Figure 30

349 ($[M-H]^-$, 100), 334 (26), 307 (22), 303 (34), 236 (15), 167 (10)

UV : λ_{max} nm (log ε), in methanol; Figure 28

233 (4.54), 270 (4.29), 310 (4.13)

IR : ν_{max} cm^{-1}, KBr disc; Figure 29

3114, 2917, 2849, 1744, 1633, 1508, 1450, 1290, 1157, 763

^{1}H NMR : δ ppm, 300 MHz, in $CDCl_3$; Figure 31, Table 6

^{13}C NMR : δ ppm, 75 MHz, in $CDCl_3$; Figure 32, Table 6

4.5 Compound DM5 (6-Oxo-dehydroelliptone)

Compound DM5 was obtained as a yellow amorphous solid, soluble in CH_2Cl_2 (4.3 mg, $1.08x10^{-6}$ % based on dried weight of roots).

HRESIMS : $[M+H]^+$ at *m/z* 365.0654 (calcd for $C_{20}H_{13}O_7$ 365.0656)

EIMS : *m/z* (% relative intensity); Figure 40

364 (M^+, 100), 349 (18), 321 (43), 293 (19), 278 (16), 194 (12)

UV : λ_{max} nm (log ε), in methanol; Figure 38

226 (3.48), 280 (3.19), 290 (3.22)

IR : ν_{max} cm^{-1}, KBr disc; Figure 39

2922, 2852, 1739, 1645, 1463, 1293

^{1}H NMR : δ ppm, 500 MHz, in $CDCl_3$; Figure 41, Table 7

^{13}C NMR : δ ppm, 125 MHz, in $CDCl_3$; Figure 42, Table 7

4.6 Compound DM6 (Deguelin)

Compound DM6 was obtained as a yellowish powder, soluble in CH_2Cl_2 (7.2 mg, $1.8x10^{-6}$ % based on dried weight of roots).

ESIMS : $[M+H]^+$ *m/z* 395.16; Figure 50

$[\alpha]_D^{20}$: −25.71 ° (*c* 0.04; MeOH)

UV : λ_{max} nm (log ε), in methanol; Figure 48

240 (4.42), 271 (4.44), 320 (4.04)

IR : ν_{max} cm^{-1}, KBr disc; Figure 49

2974, 2932, 1731, 1673, 1598, 1512, 1442, 1214, 1112, 755

^{1}H NMR : δ ppm, 300 MHz, in $CDCl_3$; Figure 51, Table 8

^{13}C NMR : δ ppm, 75 MHz, in $CDCl_3$; Figure 52, Table 8

4.7 Compound DM7 (Elliptone)

Compound DM6 was obtained as a yellowish powder, soluble in CH_2Cl_2 (24.8 mg, $6.2x10^{-6}$ % based on dried weight of roots).

ESIMS : $[M+H]^+$ *m/z* 353.11; Figure 56

$[\alpha]_D^{20}$: −18 ° (*c* 0.05; MeOH)

UV : λ_{max} nm (log ε), in methanol; Figure 54

237 (4.85), 280 (4.21)

IR : ν_{max} cm^{-1}, KBr disc; Figure 55

3016, 2935, 2856, 1676, 1465, 1391, 1214, 1090, 761

^{1}H NMR : δ ppm, 300 MHz, in $CDCl_3$; Figure 57, Table 9

^{13}C NMR : δ ppm, 75 MHz, in $CDCl_3$; Figure 58, Table 9

4.8 Compound CC1 {(6*R*,7*S*,8*S*)-7a-[(*β*-glucopyranosyl)oxy]lyoniresinol}

Compound CC1 was obtained as a yellow amorphous solid, soluble in MeOH (22.9 mg, $1.15x10^{-5}$ % based on dried weight of stems).

ESIMS : $[M+Na]^+$ *m/z* 605.9; Figure 62

$[\alpha]_D^{20}$: +22.7 ° (*c* 0.04; MeOH)

CD : $[\theta]_{214}$ -22594, $[\theta]_{243}$ +15168, $[\theta]_{273}$ +5828, $[\theta]_{287}$ -366; (*c* $3.44x10^{-4}$; MeOH); Figure 63

UV : λ_{max} nm (log ε), in methanol; Figure 60

225 (4.52), 279 (3.83)

IR : ν_{max} cm^{-1}, KBr disc; Figure 61

3368, 2936, 1612, 1515, 1458, 1321, 1216, 1110

^{1}H NMR : δ ppm, 300 MHz, in MeOH-d_4; Figure 64, Table 10

^{13}C NMR : δ ppm, 75 MHz, in MeOH-d_4; Figure 65, Table 10

4.9 Compound CC2 {(6*S*,7*R*,8*R*)-7a-[(*β*-glucopyranosyl)oxy]lyoniresinol}

Compound CC2 was obtained as a yellow amorphous solid, soluble in MeOH (12 mg, $6x10^{-6}$ % based on dried weight of stems).

HRESIMS : $[M+Na]^+$ at *m/z* 605.2216 (calcd for $C_{28}H_{38}NaO_{13}^+$ 605.2210)

ESIMS : $[M+Na]^+$ *m/z* 605.9; Figure 75

$[\alpha]_D^{20}$: –46.9 ° (*c* 0.04; MeOH)

CD : $[\theta]_{220}$ +13687, $[\theta]_{244}$ -16095, $[\theta]_{274}$ -5076, $[\theta]_{286}$ +993; (*c* 3.44x10^{-4}; MeOH); Figure 63

UV : λ_{max} nm (log ε), in methanol; Figure 73
224 (4.32), 278 (3.64)

IR : ν_{max} cm^{-1}, KBr disc; Figure 74
3368, 2937, 1613, 1515, 1458, 1322, 1217, 1111

^{1}H NMR : δ ppm, 300 MHz, in MeOH-d_4; Figure 76, Table 11

^{13}C NMR : δ ppm, 75 MHz, in MeOH-d_4; Figure 77, Table 11

4.10 Compound CC3 (Carandoside)

Compound CC3 was obtained as a yellow amorphous solid, soluble in MeOH (9.1 mg, 4.55x10^{-6} % based on dried weight of stems).

HRESIMS : $[M+H]^+$ at *m/z* 413.2177 (calcd for $C_{21}H_{33}O_8^+$ 413.2175)

ESIMS : $[M+H]^+$ *m/z* 413.1; Figure 86

$[\alpha]_D^{20}$: –93.8 ° (*c* 0.04; MeOH)

UV : λ_{max} nm (log ε), in methanol; Figure 84
218 (3.44), 243 (3.95)

IR : ν_{max} cm^{-1}, KBr disc; Figure 85
3367, 2937, 1603, 1455, 1373, 1202, 1074

^{1}H NMR : δ ppm, 300 MHz, in MeOH-d_4; Figure 87, Table 12

^{13}C NMR : δ ppm, 75 MHz, in MeOH-d_4; Figure 88, Table 12

4.11 Compound CC4 [(–)-Carissanol]

Compound CC4 was obtained as a yellow amorphous solid, soluble in MeOH (5.2 mg, 2.6x10^{-6} % based on dried weight of stems).

ESIMS : $[M+Na]^+$ *m/z* 399.9; Figure 98

$[\alpha]_D^{20}$: –25.9 ° (*c* 0.08; MeOH)

UV : λ_{max} nm (log ε), in methanol; Figure 96
280 (4.23), 300 (4.03)

IR : ν_{max} cm^{-1}, KBr disc; Figure 97
3359, 2922, 1658, 1514, 1427, 1271, 1032

^{1}H NMR : δ ppm, 500 MHz, in acetone-d_6; Figure 99, Table 13

^{13}C NMR : δ ppm, 125 MHz, in acetone-d_6; Figure 100, Table 13

4.12 Compound CC5 [(–)-Nortrachelogenin]

Compound CC5 was obtained as a yellow amorphous solid, soluble in MeOH (25.3 mg, 1.3x10^{-5} % based on dried weight of stems).

ESIMS : $[M+Na]^+$ *m/z* 397.8; Figure 111

$[\alpha]_D^{20}$: -33.63 ° (*c* 0.1; MeOH)

UV : λ_{max} nm (log ε), in methanol; Figure 109
284 (4.29), 300 (3.93)

IR : ν_{max} cm^{-1}, KBr disc; Figure 110
3359, 2922, 1763, 1658, 1514, 1430, 1271, 1032

^{1}H NMR : δ ppm, 300 MHz, in acetone-d_6; Figure 112, Table 14

^{13}C NMR : δ ppm, 75 MHz, in acetone-d_6; Figure 113, Table 14

4.13 Compound CS1 (Scopoletin)

Compound CS1 was obtained as a yellow amorphous solid, soluble in MeOH (45.1 mg, 2.3x10^{-5} % based on dried weight of stems).

ESIMS : $[M+Na]^+$ *m/z* 215.5; Figure 116

UV : λ_{max} nm (log ε), in methanol; Figure 115
300 (4.22), 343 (4.73)

^{1}H NMR : δ ppm, 500 MHz, in MeOH-d_4; Figure 116, Table 15

^{13}C NMR : δ ppm, 125 MHz, in MeOH-d_4; Figure 117, Table 15

4.14 Compound CS2 [(–)-Nortrachelogenin]

Compound CS2 was obtained as a brown amorphous solid, soluble in MeOH (575.3 mg, 2.88 x10^{-4} % based on dried weight of stems). It has physical and spectra data identical with those of compound CC5.

4.15 Compound CS3 [(–)-Carissanol]

Compound CS3 was obtained as a brown amorphous solid, soluble in MeOH (318 mg, 1.59 x10^{-4} % based on dried weight of stems). It has physical and spectra data identical with those of compound CC4.

4.16 Compound CS4 [(–)-Carinol]

Compound CS4 was obtained as a brown amorphous solid, soluble in MeOH (266.5 mg, 1.33x10^{-4} % based on dried weight of stems).

ESIMS : $[M+Na]^+$ *m/z* 401.6; Figure 124

$[\alpha]_D^{20}$: –13.08 ° (*c* 0.13; MeOH)

UV : λ_{max} nm (log ε), in methanol; Figure 123
280 (4.23), 300 (3.92)

^{1}H NMR : δ ppm, 500 MHz, in MeOH-d_4; Figure 125, Table 16

^{13}C NMR : δ ppm, 125 MHz, in MeOH-d_4; Figure 126, Table 16

4.17 Compound CS5 [(+)-Cycloolivil]

Compound CS5 was obtained as a yellow amorphous solid, soluble in MeOH (27.7 mg, 1.39×10^{-5} % based on dried weight of stems).

ESIMS : $[M+Na]^+$ *m/z* 399.6; Figure 135

$[\alpha]_D^{20}$: +29 ° (*c* 0.1; MeOH)

UV : λ_{max} nm (log ε), in methanol; Figure 134
288 (4.22), 300 (3.99)

^{1}H NMR : δ ppm, 400 MHz, in acetone-d_6; Figure 136, Table 17

^{13}C NMR : δ ppm, 100 MHz, in acetone-d_6; Figure 137, Table 17

4.18 Compound CS6 [(+)-8-Hydroxypinoresinol]

Compound CS6 was obtained as a yellow amorphous solid, soluble in MeOH (6 mg, 3×10^{-6} % based on dried weight of stems).

ESIMS : $[M+Na]^+$ *m/z* 397.6; Figure 145

$[\alpha]_D^{20}$: +28.18 ° (*c* 0.11; MeOH)

UV : λ_{max} nm (log ε), in methanol; Figure 144
283 (4.11), 296 (3.80)

^{1}H NMR : δ ppm, 500 MHz, in acetone-d_6; Figure 146, Table 18

^{13}C NMR : δ ppm, 125 MHz, in acetone-d_6; Figure 147, Table 18

4.19 Compound CS7 [(–)-Olivil]

Compound CS7 was obtained as a yellow amorphous solid, soluble in MeOH (18.1 mg, 9.05×10^{-6} % based on dried weight of stems).

ESIMS : $[M+Na]^+$ *m/z* 399.6; Figure 155

$[\alpha]_D^{20}$: –31.82 ° (*c* 0.11; MeOH)

UV : λ_{max} nm (log ε), in methanol; Figure 154
285 (4.17), 298 (3.76)

^{1}H NMR : δ ppm, 400 MHz, in $CDCl_3$; Figure 156, Table 19

^{13}C NMR : δ ppm, 100 MHz, in $CDCl_3$; Figure 157, Table 19

4.20 Compound CS8 [(–)-Secoisolariciresinol]

Compound CS8 was obtained as a yellow amorphous solid, soluble in MeOH (2.3 mg, 1.15×10^{-6} % based on dried weight of stems).

ESIMS : $[M+Na]^+$ *m/z* 385.6; Figure 165

$[\alpha]_D^{20}$: –12 ° (*c* 0.05; MeOH)

UV : λ_{max} nm (log ε), in methanol; Figure 164
280 (4.17), 301 (3.95)

^{1}H NMR : δ ppm, 400 MHz, in MeOH-d_4; Figure 166, Table 20

^{13}C NMR : δ ppm, 100 MHz, in MeOH-d_4; Figure 167, Table 20

4.21 Compound CS9 [(+)-Pinoresinol]

Compound CS9 was obtained as a yellow amorphous solid, soluble in MeOH (9.3 mg, 4.65×10^{-6} % based on dried weight of stems).

ESIMS : $[M+Na]^+$ *m/z* 381.5; Figure 170

$[\alpha]_D^{20}$: +48 ° (*c* 0.1; MeOH)

UV : λ_{max} nm (log ε), in methanol; Figure 169
284 (4.17), 303 (3.98)

^{1}H NMR : δ ppm, 500 MHz, in acetone-d_6; Figure 171, Table 21

^{13}C NMR : δ ppm, 125 MHz, in acetone-d_6; Figure 172, Table 21

4.22 Compound CS10 (Carissone)

Compound CS10 was obtained as a yellow amorphous solid, soluble in MeOH (76.2 mg, 3.81×10^{-5} % based on dried weight of stems).

ESIMS : $[M+Na]^+$ *m/z* 259.6; Figure 179

$[\alpha]_D^{20}$: +113.08 ° (*c* 0.13; MeOH)

UV : λ_{max} nm (log ε), in methanol; Figure 178
270 (3.64), 300 (3.50)

^{1}H NMR : δ ppm, 500 MHz, in $CDCl_3$; Figure 180, Table 22

^{13}C NMR : δ ppm, 125 MHz, in $CDCl_3$; Figure 181, Table 22

4.23 Compound CS11 (Digitoxigenin 3-*O*-*β*-D-digitalopyranoside)

Compound CS11 was obtained as a yellow amorphous solid, soluble in MeOH (6.8 mg, 3.4×10^{-6} % based on dried weight of stems).

ESIMS : $[M+Na]^+$ *m/z* 557.7; Figure 188

$[\alpha]_D^{20}$: –20 ° (*c* 0.055; MeOH)

UV : λ_{max} nm (log ε), in methanol; Figure 187
280 (4.11), 303 (4.29)

^{1}H NMR : δ ppm, 400 MHz, in $CDCl_3$; Figure 189, Table 23

^{13}C NMR : δ ppm, 125 MHz, in $CDCl_3$; Figure 191, Table 23

4.24 Compound CS12 (Evomonoside)

Compound CS12 was obtained as a yellow amorphous solid, soluble in MeOH (12.1 mg, $6.05x10^{-6}$ % based on dried weight of stems).

ESIMS : $[M+Na]^+$ *m/z* 543.9; Figure 201

$[\alpha]_D^{20}$: –18.33 ° (*c* 0.12; MeOH)

UV : λ_{max} nm (log ε), in methanol; Figure 200
280 (3.90), 303 (4.05)

^{1}H NMR : δ ppm, 500 MHz, in $CDCl_3$; Figure 202, Table 24

^{13}C NMR : δ ppm, 125 MHz, in $CDCl_3$; Figure 204, Table 24

5. Determination of free radical scavenging activity (Likhitwitayawuid *et al*., 2006**)**

5.1 TLC screening assay

The samples were loaded as spot on TLC plate and developed with suitable developing solvent. After drying, the TLC plate was sprayed with 0.2% solution of 1,1-diphenyl-2-picrylhydrazyl (DPPH) in methanol. After 30 min, active compounds appeared as yellow spots on the purple background.

5.2 Free radical scavenging activity assay

5.2.1 Preparation of test sample

The test compound (0.5 mg) was dissolved in 1 ml of methanol (or suitable solvent) and diluted with methanol until a suitable range of concentration (mg/mL) was obtained. The concentration was expressed as μM in final concentration. For example, CC1 (MW 376) at 0.5 mg/1mL was equal to 1329 μM (0.5 mg/1mL x 376). For each well, 20 μL of test solution was added to the reaction mixture to furnish the total volume of 200 μL. The final concentration was calculated by the formula below.

$$N_1V_1 = N_2V_2$$

N_1 = Beginning concentration (μM)

V_1 = Beginning volume (μL)

N_2 = Final concentration (μM)

V_2 = Final volume (μL)

Thus, the final concentration of CC1 solution = 1329 μM x 20 μL / 200 μL

= 132.9 μM

5.2.2 Preparation of DPPH solution (100 μM)

DPPH (2 mg) was dissolved in 100 mL of methanol, and the solution was stirred for 30 min.

5.2.3 Measurement of activity

The test sample (20 μl) was added to 180 μl of DPPH solution (100 μM) in 96-well plate. The solution mixture was incubated at 37ºC for 30 min and then the absorbance of each well was measured at 510 nm on a SpectraMax M5 Microplate reader (Pharmaceutical Research Instrument Center, Faculty of Pharmaceutical Sciences, Chulalongkorn University). The DPPH solution (180 μL) mixed with methanol (20 μL) was used as negative control and quercetin was used as a reference compound.

5.2.4 Calculation of percent inhibition of DPPH scavenging activity

The percentage of DPPH reduction was calculated as follows.

$$\% \text{ DPPH reduction} = (A-B) \times 100 / A$$

A = The absorbance of DPPH solution after incubation at 510 nm

B = The absorbance of the reaction mixture after incubation at 510 nm

For IC_{50} evaluation of pure compounds, a graph showing concentration versus % DPPH reduction was plotted. The IC_{50} was calculated from the graph.

6. Determination of Anti-Herpes Simplex Activity

6.1 Viruses and Cells

HSV strains used were HSV-1 (KOS) and HSV-2 (Baylor186). Vero cells (ATCC CCL81) were grown and maintained in Eagle's minimum medium supplemented with 10% fetal bovine serum.

6.2 Plaque Reduction Assay

Anti-HSV activity of the compound was determined by the plaque reduction assay modified from the previously reported method (Chuanasa *et al*., 2008; Lipipun *et al*., 2003). Briefly, in the post-treatment assay, Vero cells, in 96-well tissue culture plate, were infected with 30 plaque forming units of HSV-1 (KOS) or HSV-2 (Baylor186). After 1 hr incubation at room temperature for virus adsorption, the cells were added with overlay media containing various concentrations of the compound. The infected cultures were incubated at 37 °C for 2 days. The infected cells were fixed and stained, and then the number of plaques was counted. The 50% effective concentration (EC_{50}) was determined from the curve relating the plaque number to the concentration of the compound. Acyclovir was used as a positive control. In the inactivation assay, each of 30 plaque forming units of HSV-1 or HSV-2 was mixed with various concentrations of compound and incubated for 1 hour then the mixture was added to Vero cells in 96-well tissue culture plate. After 1 hour incubation for virus adsorption, the overlay media were added. The infected cultures were incubated at 37 °C for 2 days. The infected cells were fixed, stained, and the plaques were counted. The 50% effective concentration (EC_{50}) was determined.

7. Determination of antibacterial activity

In this study, six strains of *Staphylococcus aureus* were used, including ATCC 25943 (*S. aureus* standard strain), SA1199B (*S. aureus* which overexpresses the norA gene encoding the NorA MDR efflux pump), XU212 (*S. aureus* tetracycline resistant strain), RN4220 (*S. aureus* which possesses the MsrA macrolide efflux protein), EMRSA15 and EMRSA16 (*S. aureus* methicillin resistant strains) (Shiu and Gibbons, 2006). Briefly, all strains were cultured on nutrient agar (Oxoid) and incubated for 24 h at 37 °C prior to MIC determination. Control antibiotic, norflorxacin, was obtained from Sigma Chemical Co. Mueller-Hinton broth (MHB; Oxoid) was adjusted to contain 20 and 10 mg/L of Ca^{2+} and Mg^{2+}, respectively. An inoculum density of $5x10^5$ cfu of each bacterial strain was prepared in normal saline (9 g/L) by comparison with a 0.5 MacFarland turbidity standard. All test compounds were dissolved in DMSO before dilution into MHB for use in MIC determinations. The inoculum (125 μL) was added to all wells and the microtitre plate was incubated at 37 °C for 18 h. For MIC determination, 20 μL of a 5 mg/mL methanolic solution of 3-

[4,5-dimethylthiazol-2-yl]-2,5-diphenyltetrazolium bromide (MTT; Sigma) was added to each of the wells and incubated for 20 min. Bacterial growth was indicated by a color change from yellow to dark blue. The MIC was recorded as the lowest concentration at which no growth was observed.

8. Determination of cytotoxic activity

Three cell lines were used in this study including two human cancer cell lines, breast (MCF7) and lung (A549), and one normal human lung fibroblast lines, WI-38 (Gunaratnam *et al*., 2007). Briefly, cells were seeded (4000 cells/wells) into the wells of 96-well plates in DMEM (Dulbecco's modified Eagle medium) and incubated overnight as before to allow the cells to attach. Subsequently, cells were exposed to freshly-made solutions of test compounds at increasing concentrations of 0, 0.1, 1, 5 and 25 μM in quadruplicate and incubated for a further 96 hours. Following this, the cells were fixed with ice cold trichloroacetic acid (TCA) (10%, w/v) for 30 min and stained with 0.4% SRB dissolved in 1% acetic acid for 15 min. All incubations were carried out at room temperature. The IC_{50} value (concentration required to inhibit cell growth by 50%) was determined from the mean absorbance at 540 nm for each compound concentration expressed as a percentage of the absorbance of the control, untreated well.

CHAPTER IV

RESULTS AND DISSCUSSION

Phytochemical investigations of *Derris malaccensis* roots, *Carissa carandas* stems and *Carissa spinarum* stems led to the isolation of twenty-two pure compounds.

The structures of all of the isolates were determined based on their UV, IR, MS and NMR data and further confirmed by comparison with literature values. In addition, the DPPH radical scavenging, anti-HSV, antibacterial and cytotoxic activities of the isolated compounds were evaluated.

1. Structure determination of isolated compounds

1.1 Structure determination of compound DM1

Compound DM1 was obtained as a yellowish powder. The UV spectrum (Figure 7) displayed absorption bands at 250, 253 and 290 nm. The IR spectrum (Figure 8) suggested acetoxy (1737, 1221, 1088, and 1046 cm^{-1}) and aromatic (1602 and 1514 cm^{-1}) groups (Lin, Chen, and Kuo, 1993). Moreover, it showed an $[M+Na]^+$ ion peak at *m/z* 419.11 in the ESI mass spectrum (Figure 9), suggesting the molecular formula $C_{22}H_{20}O_7$.

The ^1H NMR spectrum (Figure 10 and Table 3) exhibited signals for two methoxy groups at δ 3.82 (6H, s), an acetyl group at δ 1.72 (3H, s) and four aromatic protons as a pair of doublets with ortho coupling (δ 7.09 and 7.19 ppm) and two singlets (δ 6.67 and 6.42 ppm). It also exhibited the following signals due to aliphatic protons on carbon atoms bearing oxygen atoms: δ 4.30 and 4.51 (H-6), 4.98 (H-6a), and 6.41 (H-12) ppm. In addition, the characteristic signals of two benzofuranic protons (δ 6.85 and 7.54 ppm) and a one-proton triplet (δ 3.61, H-12a) were observed. The structure of compound DM1 was further supported by the ^{13}C NMR data (Figure 11 and Table 3). Signals for the acetoxy appeared at δ 170.0 and 21.0 ppm. The ^1H and ^{13}C NMR data of compound DM1 were in agreement with previously reported values of 12-deoxo-12α-acetoxyelliptone [**14**] (Lin *et al*., 1993; Thasana *et al*., 2001).

From all of the above data, it was concluded that compound DM1 was 12-deoxo-12α-acetoxyelliptone [**14**]. It was first isolated from the roots of *Derris oblonga* (Lin *et al*., 1993).

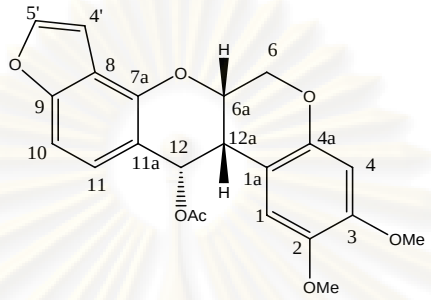

[**14**]

Table 3 NMR spectral data of compound DM1 ($CDCl_3$) compared with 12-deoxo-12α-acetoxyelliptone ($CDCl_3$)

position	Compound DM1		12-deoxo-12α-acetoxyelliptone	
	^1H (mult., *J* in Hz)	^{13}C	^1H (mult., *J* in Hz)	^{13}C
1	6.67 (s)	111.9	6.67 (s)	112.5
1a	-	108.4	-	109.0
2	-	143.3	-	144.0
3	-	148.4	-	149.0
4	6.40 (s)	100.1	6.40 (s)	101.0
4a	-	146.7	-	147.0
6	4.30 (dd, 10.2, 4.8) 4.51 (t, 10.2)	64.3	4.33 (dd, 11.2, 5.3) 4.51 (t, 11.2)	64.5
6a		69.0	4.98 (m)	69.5
7a	4.98 (m)	149.3	-	149.5
8	-	111.2	-	111.5
9	-	156.5	-	157.0
10	-	105.0	7.09 (d, 8.5)	105.5
11	7.09 (d, 8.6)	126.6	7.19 (d, 8.5)	127.0
11a	7.19 (d, 8.6)	116.9	-	117.5
12	-	66.6	6.42 (d, 5.3)	67.0
12a	6.41 (d, 5.1)	36.7	3.67 (t, 5.3)	37.0
4′	3.61 (t, 5.1)	103.8	6.85 (d, 2.4)	104.0
5′	6.85 (d, 1.8)	144.1	7.55 (d, 2.4)	144.5
OMe-2/3	7.54 (d, 1.8)	56.4/55.9	3.83 (s)	57.0/56.0
CH_3-COO	3.82 (s)	20.9	1.73 (s)	21.0
COO	1.72 (s)	169.8	-	170.0
	-			

1.2 Structure determination of compound DM2

Compound DM2 showed UV absorption maxima at 223, 240 and 280 nm (Figure 13), and IR absorptions for chelated carbonyl (1679 cm^{-1}) and hydroxyl groups (3453 cm^{-1}) (Figure 14) (Thasana *et al*., 2001). It has a molecular formula of $C_{20}H_{16}O_7$, as indicated by the molecular ion peak at *m/z* 391.08 in the ESI mass spectrum (Figure 15).

The ^{1}H NMR spectrum (Figure 16 and Table 4) showed four aromatic singlets at δ 6.47 (H-4), 6.53 (H-1), 6.89 (H-4′) and 7.54 (H-5′) ppm, two olefinic proton signals at δ 7.15 (d, *J* = 8.7 Hz) (H-10) and 7.85 (d, *J* = 8.7 Hz) (H-11) ppm which were reminiscent of 4,5-disubstituted benzofuran ring, and two methoxy singlets at δ 3.69 and 3.77 ppm. A pair of nonequivalent methylene proton signals at δ 4.70 (d, *J* = 12.2 Hz, H-6) and 4.53 (d, *J* = 12.2 Hz, H-6) ppm and a methine proton singlet at δ 4.72 ppm (H-6a) are similar to an ABC system of a O-CH_2-CH-O segment. In agreement with the latter assignment, ^{13}C NMR data of compound DM2 showed methylene and methine carbon resonances at C-6 (δ 63.8 ppm) and C-6a (δ 76.7 ppm), respectively. The ^{1}H NMR spectrum of compound DM2 is similar to compound DM1, 12-deoxo-12α-acetoxyelliptone [**14**], except for the absence of proton signals at H-12 and H-12a. The structure of compound DM2 was further supported by the ^{13}C NMR spectrum (Figure 17 and Table 4) which showed a quaternary oxygenated carbon of C-12a at δ 67.7 ppm.

Through comparison of the above spectroscopic data with reported values (Thasana *et al*., 2001), compound DM2 was identified as 12a-hydroxyelliptone [**58**], which was first isolated from the stems of *Derris malaccensis*.

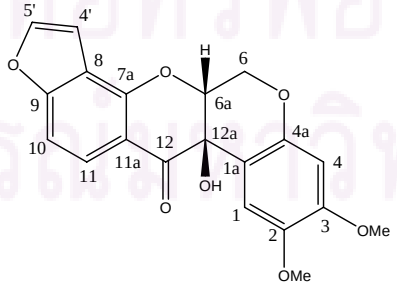

[**58**]

Table 4 NMR spectral data of compound DM2 ($CDCl_3$) compared with 12a-hydroxyelliptone ($CDCl_3$)

position	Compound DM2		12a-hydroxyelliptone	
	^1H (mult., *J* in Hz)	^{13}C	^1H (mult., *J* in Hz)	^{13}C
1	6.53 (s)	109.3	6.56 (s)	109.4
1a	-	108.4	-	108.7
2	-	144.1	-	144.0
3	-	151.2	-	151.2
4	6.47 (s)	101.2	6.45 (s)	101.2
4a	-	148.5	-	148.4
6	4.70 (d, 12.2)	63.8	4.70 (dd, 12.0, 2.3)	64.0
	4.53 (d, 12.2)		4.56 (d, 12.0)	
6a	4.72 (s)	76.7	4.74 (m)	76.8
7a	-	155.8	-	156.0
8	-	112.1	-	112.0
9	-	160.6	-	160.7
10	7.15 (d, 8.7)	107.1	7.17 (dd, 8.6, 1.1)	107.1
11	7.85 (d, 8.7)	123.9	7.87 (d, 8.6)	124.0
11a	-	117.3	-	117.5
12	-	192.2	-	192.1
12a	-	67.7	-	67.9
4′	6.89 (s)	104.8	6.95 (dd, 2.3, 1.1)	104.8
5′	7.54 (s)	145.1	7.56 (d, 2.3)	145.0
OMe-2	3.69/3.77 (s)	56.4/55.9	3.70 (s)	56.4/56.0
OMe-3	3.69/3.77 (s)	56.4/55.9	3.78 (s)	56.4/56.0
OH-12a	-	-	4.53 (s)	-

1.3 Structure determination of compound DM3

Compound DM3 was obtained as a yellowish powder. It showed UV absorptions at 236, 250, 272 and 300 nm (Figure 19), and IR absorptions at 1674 and 3449 cm^{-1} (Figure 20), representing a chelated carbonyl and a hydroxyl group, respectively (Thasana *et al*., 2001). A molecular formula of $C_{23}H_{22}O_7$ was deduced from its $[M+Na]^+$ ion at *m/z* 433.33 in the ESI mass spectrum (Figure 21).

The ^1H NMR spectrum (Figure 22 and Table 5) showed two aromatic singlets at δ 6.46 (H-4) and 6.54 (H-1) ppm, two ortho-coupling aromatic proton signals at δ 6.44 (d, *J* = 8.7 Hz, H-10) and 7.70 (d, *J* = 8.7 Hz, H-11) ppm, and two methoxy signals at δ 3.69 and 3.78 ppm. In addition, a dimethylchromene system is well characterized by two doublets at δ 6.57 (d, *J* = 10.2 Hz, H-4′) and 5.53 (d, *J* = 10.2 Hz, H-5′) ppm for the vinyl protons and signals for two methyl groups at δ 1.35 and 1.42 ppm (Andrei *et al*., 1997). Furthermore, the ^{13}C NMR data of compound DM3 (Figure 23 and Table 5) showed that this compound had a 12a-hydroxyrotenoid skeleton similar to compound DM2, as indicated from a quaternary sp^3 carbon at δ 67.4 ppm (C-12a).

The ^1H and ^{13}C NMR data of compound DM3 were in excellent agreement with previously reported values for tephrosin [**64**] (Luyengi *et al*., 1994).

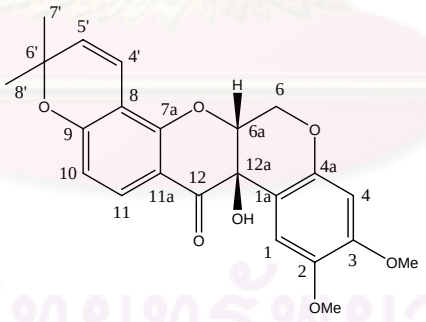

[**64**]

Table 5 NMR spectral data of compound DM3 ($CDCl_3$) compared with tephrosin ($CDCl_3$)

position	Compound DM3		Tephrosin	
	^1H (mult., *J* in Hz)	^{13}C	^1H (mult., *J* in Hz)	^{13}C
1	6.54 (s)	109.3	6.56 (s)	109.3
1a	-	108.5	-	104.0
2	-	143.8	-	144.0
3	-	150.9	-	151.9
4	6.46 (s)	101.0	6.47 (s)	101.0
4a	-	148.2	-	148.2
6	4.44-4.62 (m)	63.9	4.40-4.75 (m)	63.8
6a	4.44-4.62 (m)	76.2	4.40-4.75 (m)	76.2
7a	-	156.4	-	156.3
8	-	109.0	-	104.3
9	-	160.5	-	161.5
10	6.44 (d, 8.7)	111.8	6.45 (d, 8.7)	111.9
11	7.70 (d, 8.7)	128.7	7.72 (d, 8.7)	128.8
11a	-	111.0	-	112.4
12	-	191.1	-	190.1
12a	-	67.5	-	67.5
4′	6.57 (d, 10.2)	115.3	6.59 (d, 10.8)	115.4
5′	5.53 (d, 10.2)	128.4	5.54 (d, 10.8)	128.5
6′	-	77.9	-	78.0
Me-7′/8′	1.35/1.42 (s)	28.3/28.6	1.37/1.44 (s)	28.3/28.5
OMe-2/3	3.69/3.78 (s)	55.8/56.3	3.71/3.80(s)	55.8/56.3

1.4 Structure determination of compound DM4

Compound DM4 possesses the molecular formula $C_{20}H_{14}O_6$, as indicated from its $[M+Na]^+$ ion at *m/z* 373.0701 ($C_{20}H_{14}O_6Na$, calcd. 373.0683) in the HRESI mass spectrum. It showed UV absorption maxima at 223, 270 and 310 nm (Figure 25). IR bands for C=O and C=C functionalities were observed at 1634 and 1450 cm^{-1}, respectively (Figure 26).

The ^1H NMR spectrum of compound DM4 (Figure 28 and Table 6) is similar to that of compound DM2, 12a-hydroxyelliptone [**58**] except for the absence of the proton signal for H-6a. This was supported by the ^{13}C NMR (Figure 29 and Table 6) and DEPT spectra (Figure 30) which represented quaternary carbons at δ 156.1 and 112.5 ppm for C-6a and C-12a, respectively. It was also confirmed by HMBC correlations (Figures 33 and Table 6) of H-6 signal at δ 5.08 (s) to those of C-12a, C-4a and C-6a. In addition, the NOESY correlation (Figure 34) between H-4 and OMe-3 and between H-1 and OMe-2 indicated the methoxy signals at δ 3.85 and 3.95 ppm for OMe-3 and OMe-2, respectively.

Therefore, compound DM4 was identified as dehydroelliptone [**176**]. Although compound DM4 was earlier synthesized (Fukami, Sakata, and Nakajima, 1965) and reportedly detected in *Derris elliptica* (Zeng *et al*., 2002), its isolation and NMR properties were not known. This study is the first report of its isolation from a natural source. Moreover, ^1H and ^{13}C NMR assignments have been obtained for [**176**] for the first time through interpretation of the NOESY and HMBC spectra.

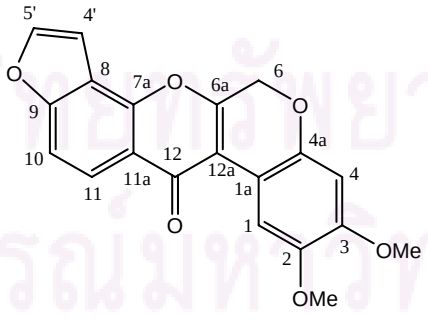

[**176**]

Table 6 NMR spectra data of compound DM4 ($CDCl_3$)

position	Compound DM4		HMBC (correlation with ^1H)
	^1H (mult., *J* in Hz)	^{13}C	
1	8.45 (s)	110.1	-
1a	-	110.4	H-1* and H-4
2	-	144.1	H-1*, H-4 and OMe-2
3	-	149.1	H-1, H-4* and OMe-3
4	6.54 (s)	100.4	-
4a	-	146.4	H-1, H-4* and H-6
6	5.08 (s)	64.8	-
6a	-	156.1	H-6*
7a	-	149.4	H-11
8	-	116.9	H-10, H-4′* and H-5′
9	-	158.0	H-4′ and H-5′
10	7.54 (d, 9.0)	110.4	-
11	8.19 (d, 9.0)	122.2	-
11a	-	120.1	H-10
12	-	174.6	H-11
12a	-	112.5	H-1 and H-6
4′	7.07 (d, 2.0)	104.0	-
5′	7.72 (d, 2.0)	145.9	H-4′*
OMe-2	3.95 (s)	56.3	-
OMe-3	3.85 (s)	55.9	-

*Two-bond coupling

1.5 Structure determination of compound DM5

Compound DM5 was obtained as a yellow amorphous solid. It had the molecular formula $C_{20}H_{12}O_7$, as indicated from its $[M+H]^+$ ion at *m/z* 365.0654 (calcd for $C_{20}H_{13}O_7$, 365.0656) in the HRESI mass spectrum. In the EIMS, two prominent ions, $[M]^+$ and $[M-CH_3]^+$, were found at *m/z* 364 (100%) and 349 (18%). UV absorption maxima at 226, 280 and 290 nm (Figure 35) were indicative of a dehydrorotenoid skeleton, whereas IR bands for a lactone carbonyl and a conjugated ketone were observed at 1739 and 1645 cm^{-1}, respectively (Figure 36).

The ^1H NMR spectrum of compound DM5 (Figure 38 and Table 7) resembled that of compound DM4, showing signals for two methoxy groups at δ 4.01 and 4.08, and six aromatic and olefinic protons at δ 9.06 (s, H-1), 8.28 (d, *J* = 8.9 Hz, H-11), 7.84 (d, *J*=1.4 Hz, H-5′), 7.68 (d, *J*=8.9 Hz, H-10), 7.40 (d, *J*=1.4 Hz, H-4′) and 6.96 (s, H-4). However, it was noted that in compound DM5 each of these protons appeared at a more downfield position than their corresponding protons in compound DM4, and no signals for the C-6 methylene protons were observed for compound DM5. Comparison of the molecular formula of compound DM5 with that of compound DM4 indicated that compound DM5 had one more oxygen atom, but two hydrogen atoms less than compound DM4. These data suggested the presence of a carbonyl functionality for compound DM5, which could be placed only at C-6. In support of this, H-1 of compound DM5 was found to resonate at a very downfield position (δ 9.06 ppm), similar to that of 6-oxo-6a,12a-dehydrodeguelin, a 6-keto dehydrorotenoid previously isolated from *Lonchocarpus utilis* and *L. urucu* (Fang and Casida, 1999). The proposed structure of compound DM5 was further supported by the signals of C-6 appearing as a lactone carbon at δ 156.0 ppm and C-6a at a more upfield position in the ^{13}C NMR spectrum at δ 142.2 ppm. The remaining carbon signals were similar to those of compound DM4. In addition, the ^1H-^1H COSY, HMQC and HMBC correlations (Figures 41-44) were consistent with the proposed structure.

Thus, compound DM5 is a new compound, and has been given the name 6-oxo-dehydroelliptone [**177**].

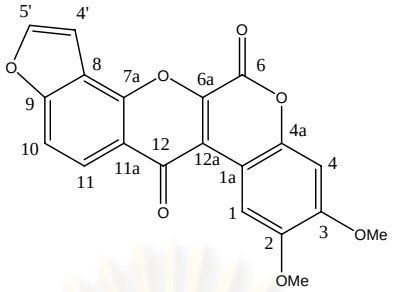

[**177**]

Table 7 NMR spectral data of compound DM5 ($CDCl_3$)

position	Compound DM5		HMBC (correlation with ^1H)
	^1H (mult., *J* in Hz)	^{13}C	
1	9.06 (s)	108.3	-
1a	-	107.9	H-4
2	-	147.1	H-1*, H-4 and OMe-2
3	-	151.5	H-1 and OMe-3
4	6.96 (s)	99.7	-
4a	-	145.5	H-1
6	-	156.0	-
6a	-	142.2	-
7a	-	150.2	H-11
8	-	117.5	H-10, H-4′* and H-5′
9	-	159.1	H-11, H-4′ and H-5′
10	7.68 (d, 8.9)	111.4	-
11	8.28 (d, 8.9)	122.2	-
11a	-	119.7	H-10
12	-	177.1	H-11
12a	-	122.1	H-1
4′	7.40 (d, 1.4)	104.9	H-5′*
5′	7.84 (d, 1.4)	146.4	-
OMe-2	4.08 (s)	56.4	-
OMe-3	4.01 (s)	55.3	-

*Two-bond coupling

1.6 Structure determination of compound DM6

Compound DM6 was obtained as a yellowish powder. The UV spectrum showed absorption maxima at 240, 271, 320 nm (Figure 45). The IR spectrum exhibited absorption bands at 1673 cm^{-1} for C=O and 1442 cm^{-1} for C=C functionalities (Figure 46). The ESI mass spectrum (Figure 50) exhibited the $[M+H]^+$ ion peak at *m/z* 395.16, corresponding to $C_{23}H_{22}O_6$.

The ^1H NMR spectrum (Figure 48 and Table 8) showed two aromatic singlets at δ 6.77 (H-1) and 6.43 (H-4) ppm, two aromatic proton doublets at δ 6.43 (d, *J* = 8.7 Hz, H-10) and 7.73 (d, *J* = 8.7 Hz, H-11) ppm, and two methoxy signals at δ 3.75 and 3.79 ppm. In addition, the presence of 2,2-dimethylpyrano was evident from ^1H NMR by two doublets at δ 6.63 (d, *J* = 10.2 Hz, H-4′) and 5.54 (d, *J* = 10.2 Hz, H-5′) ppm and two methyl singlets at δ 1.37 and 1.43 ppm. The chemical shift value for H-1 at δ 6.77 ppm showed the *cis*-B/C ring junction (δ 6.4-6.8 ppm) for rotenoids (Yenesew, Midiwo, and Waterman, 1998). The ^{13}C NMR (Figure 49) and DEPT (Figure 50) spectra displayed 23 carbon signals, corresponding to one carbonyl, nine quarternary, six sp^2 methines, two sp^3 methines, one sp^3 methylene, two methoxy and two methyl carbons. These ^1H and ^{13}C NMR data were in good agreement with those reported for deguelin [**23**], as shown in Table 8 (Andrei *et al*., 1997). Deguelin [**23**] has been considered as a chemopreventive agent for early stage lung carcinogenesis in a clinical lung cancer chemoprevention trial (Lee *et al*., 2005).

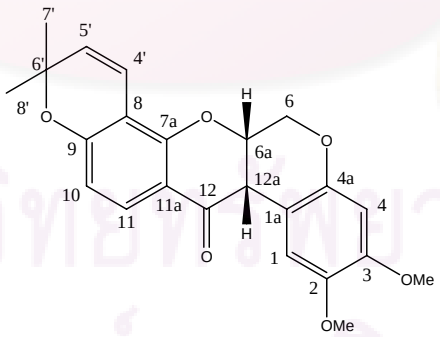

[**64**]

Table 8 NMR spectral data of compound DM6 ($CDCl_3$) compared with deguelin ($CDCl_3$)

position	Compound DM6		Deguelin	
	^1H (mult., *J* in Hz)	^{13}C	^1H (mult., *J* in Hz)	^{13}C
1	6.77 (s)	110.5[a]	6.72 (s)	110.7[a]
1a	-	104.8	-	105.0
2	-	143.9	-	144.1
3	-	149.5	-	149.8
4	6.43 (s)	100.9	6.38 (s)	101.2
4a	-	147.4	-	147.7
6	4.62 (dd, 12.0, 3.0)	66.3	4.56 (dd, 12.4, 3.2)	66.5
	4.17 (d, 12.0)		4.11 (d, 12.4)	
6a	4.90 (t, 3.0)	72.4	4.84 (m)	72.7
7a	-	156.9	-	158.0
8	-	109.1	-	109.4
9	-	160.1	-	160.3
10	6.43 (d, 8.7)	111.5[a]	6.38 (d, 8.8)	111.7[a]
11	7.73 (d, 8.7)	128.6[b]	7.67 (d, 8.8)	128.8[b]
11a	-	112.8	-	113.0
12	-	189.2	-	189.4
12a	3.82 (d, 3.9)	44.4	3.77 (d, 4.0)	44.7
4′	6.63 (d, 10.2)	115.7	6.57 (d, 10.0)	116.0
5′	5.54 (d, 10.2)	128.7[b]	5.48 (d, 10.0)	128.9[b]
6′	-	77.7	-	77.9
7′/8′	1.37/1.43 (s)	55.8/56.3	1.32/1.38 (s)	-
OMe-2/3	3.75/3.79 (s)	28.2/28.5	3.70/3.73 (s)	-

[a,b] interchangeable values in each column

1.7 Structure determination of compound DM7

Compound DM7 was obtained as a yellow amorphous solid. The UV spectrum (Figure 51) showed absorption bands at 237 and 280 nm. The IR spectrum (Figure 52) exhibited C=O stretching at 1676 cm^{-1} and C=C stretching at 1465 cm^{-1}. The ESI mass spectrum (Figure 53) displayed the $[M+H]^+$ at *m/z* 353.11, suggesting the molecular formula $C_{20}H_{16}O_6$.

The ^1H and ^{13}C NMR data (Figure 54 and 55; Table 9) of compound DM7 are similar to those of compound DM4, dehydroelliptone [**179**], except the presence of two methines at δ 5.06 (dd, *J* = 4.2, 3.3 Hz, H-6a) and 4.70 (d, *J* = 4.2 Hz, H-12a) ppm and the upfield carbon signals for C-6a (δ 72.9 ppm) and C-12a (δ 44.7 ppm). The chemical shift value for H-1 at δ 6.75 ppm showed the *cis*-B/C ring junctions (δ 6.4-6.8 ppm) for rotenoids (Yenesew *et al*., 1998). The ^{13}C NMR and DEPT (Figure 56) spectra exhibited 20 carbon signals, including one carbonyl, eight quarternary, six sp^2 methines, two sp^3 methines, one sp^3 methylene and two methoxy carbons. Compound DM7 was identified as elliptone [**63**] by comparison of it NMR data with previously reported values NMR data (Crombie, Kilbee and Whiting, 1975; Birch, Crombie and Crombie, 1985).

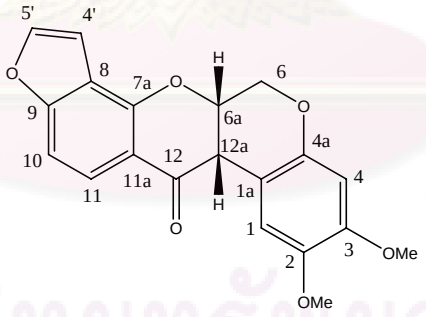

[**63**]

Table 9 NMR spectral data of compound DM7 ($CDCl_3$) compared with elliptone ($CDCl_3$)

position	Compound DM7		Elliptone	
	^1H (mult., *J* in Hz)	^{13}C	^1H (mult., *J* in Hz)	^{13}C
1	6.75 (brs)	110.4	6.77 (brs)	109.1
1a	-	104.5	-	103.0
2	-	143.9	-	141.7
3	-	149.6	-	147.4
4	6.44 (s)	101.0	6.47 (s)	99.6
4a	-	147.5	-	145.2
6	4.22 (d, 12.1)	66.2	4.29 (d, 12.4)	65.1
	4.70 (dd, 12.1, 3.3)		4.74 (dd, 12.1, 3.1)	
6a	5.06 (dd, 4.2, 3.3)	72.9	5.10 (brt, 4.0)	71.8
7a	-	156.0	-	157.6
8	-	113.6	-	111.7
9	-	160.2	-	159.0
10	7.13 (dd, 8.8, 0.9)	106.7	7.16 (dd, 8.8, 0.9)	104.9
11	7.88 (d, 8.8)	124.0	7.90 (d, 8.8)	121.9
11a	-	117.2	-	115.0
12	-	189.9	-	186.6
12a	3.93 (brd, 4.2)	44.7	3.96 (brd, 5.0)	44.0
4′	6.91 (dd, 2.1, 0.6)	104.8	6.94 (dd, 2.3, 0.9)	103.0
5′	7.54 (d, 2.1)	144.9	7.57 (d, 2.1)	142.5
OMe-2/3	3.74/3.77 (s)	55.8/56.3	3.80/3.77 (s)	54.9/55.5

1.8 Structure determination of compound CC1

Compound CC1 was obtained as a yellow amorphous solid. The UV spectrum (Figure 57) showed absorption maxima at 225 and 279 nm. The IR spectrum (Figure 58) exhibited absorption bands at 1612 cm^{-1} (C=C) and 3368 cm^{-1} (hydroxyl). It has a molecular formula of $C_{28}H_{38}O_{23}$ as determined by $[M+Na]^+$ ion at *m/z* 605.9 in the ESI mass spectrum (Figure 59).

The ^1H NMR spectrum (Figure 61; Table 10) revealed three aromatic protons at δ 6.37 (2H, s, H-2′ and H-6′) and 6.51 (1H, s, H-4) ppm, four methoxy groups at δ 3.28 (3H), 3.68 (6H) and 3.78 (3H) ppm and an anomeric proton of a sugar moiety at δ 4.23 ppm. The ^{13}C NMR (Figure 62; Table 10) and DEPT spectra (Figure 63) showed twenty eight carbons including eighteen carbons for basic structure of lignan with four methoxy groups (δ 3.28, 3.68 and 3.78 ppm) and six carbons of glucose at δ 62.8, 71.6, 75.1, 77.9, 78.2 and 104.7 ppm. The coupling constant (7.5 Hz) for anomeric proton at δ 4.23 ppm indicated a *β* configuration of glucose. The location of the glucosidic linkage at C7a was confirmed by HMBC correlation from C-7a to H-1″ (Figure 68). In addition, the assignments of OMe-1 and OMe-3 were confirmed by HMBC correlations from OMe-1 to C-1 and from OMe-3 to C-3. The ROESY cross-peaks (Figure 69) observed for H-6, H-7 and H-8, indicated their relative configurations as *cis*-form. Furthermore, the absolute configuration (6*R*,7*S*,8*S*) was established by the comparison of its CD data (Figure 60) with previously reported values (Sakakibara, Ina, and Yasue, 1974; Ohashi *et al*., 1994).

Based on the above spectroscopic evidence, compound CC1 was determined as (6*R*,7*S*,8*S*)-7a-[(*β*-glucopyranosyl)oxy]lyoniresinol [**178**] (Yang, Chang, and Wu, 2005).

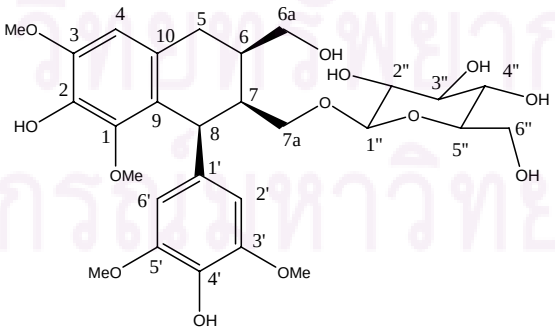

[**178**]

Table 10 NMR spectral data of compound CC1 (MeOH-d_4) compared with (6*R*,7*S*,8*S*)-7a-[(*β*-glucopyranosyl)oxy]lyoniresinol (MeOH-d_4)

position	Compound CC1		(6*R*,7*S*,8*S*)-7a-[(*β*-glucopyranosyl) oxy]lyoniresinol	HMBC (correlation with ^{1}H)
	^{1}H (mult., *J* in Hz)	^{13}C	^{13}C	
1	-	147.5	147.6	OMe-1
2	-	138.9	138.9	H-4
3	-	148.6	148.6	OMe-3
4	6.51 (s)	107.8	107.9	H-5
5	2.62 (d, 7.5)	33.8	33.8	H-4 and H-6a
6	1.65 (m)	40.6	40.6	H-5* and H-8
6a	3.50 (d, 6.0)	66.2	66.2	H-5
7	2.03 (m)	46.6	46.7	H-5 and H-8*
7a	3.39 (dd, 9.6, 3.9) 3.83 (m)	71.5	71.5	H-8 and H-1′′
8	4.36 (d, 6.3)	42.7	42.7	H-2′ and H-6′
9	-	126.4	126.4	H-4, H-5 and H-8*
10	-	130.2	130.2	H-5* and H-8
1′	-	139.3	139.3	H-8*
2′	6.37 (s)	106.9	106.9	H-8
3′	-	148.9	149.0	H-2′* and OMe-3′
4′	-	134.5	134.5	H-2′ and H-6′
5′	-	148.9	149.0	H-6′* and OMe-5′
6′	6.37 (s)	106.9	106.9	H-8
1′′	4.23 (d, 7.5)	104.7	104.8	H-2′′*
2′′	3.19 (m)	75.1	75.2	H-3′′*
3′′	3.32 (m)	78.2	78.2	H-5′′
4′′	3.24 (m)	71.6	71.7	H-3′′*
5′′	3.21 (m)	77.9	77.9	H-6′′*
6′′	3.56 (m) 3.76 (m)	62.8	62.8	-
OMe-1	3.28 (s)	60.2	60.2	-
OMe-3	3.78 (s)	56.6	56.6	-
OMe-3′/5′	3.68 (s)	56.9	56.8	-

*Two-bond coupling

1.9 Structure determination of compound CC2

Compound CC2 was isolated as a yellow amorphous solid. The molecular formula was determined as $C_{28}H_{38}O_{13}$ from $[M+Na]^+$ at *m/z* 605.2216 in the HRESI mass spectrum. The UV (Figure 70) and mass (Figure 72) spectral data suggested that it had a lignan structure similar to that of compound CC1, (6*R*,7*S*,8*S*)-7a-[(*β*-glucopyranosyl)oxy]lyoniresinol [**178**].

The ^{1}H and ^{13}C NMR data of compound CC2 (Figures 73 and 74; Table 11) closely resembled those of compound CC1, indicating that compound CC2 also contained the lyoniresinol aglycone connected to a glucose moiety through the C-7a to C-1″ ether linkage. Nevertheless, several NMR spectral differences between these two compounds were noticed. The resonances for H-8 at δ 4.19 (d, *J*=6.3 Hz) ppm and H-1″ at δ 4.09 (d, *J*=7.9 Hz) ppm of compound CC2 appeared at more upfield positions than their counterparts in compound CC1, at δ 4.36 and 4.23 ppm (Table 10), respectively. Additionally, in the ^{13}C NMR spectrum of compound CC2 for C-7a (δ 72.0 ppm) was found to absorb at a higher frequency than C-4″ (δ 71.5 ppm) whereas the reverse was true for compound CC1. Despite the above-mentioned spectral differences, compound CC1 and CC2 could not be distinguished by 2D-NMR analysis as both showed similar patterns of HMBC correlations (Figures 78-79). Moreover, the ROESY cross peaks (Figure 80) obtained for H-6, H-7, and H-8 indicated that the relative configurations at C-6, C-7, and C-8 of both compounds were identical. The ^{1}H and ^{13}C NMR assignments of compound CC2 were obtained by analysis of ^{1}H-^{1}H COSY (Figure 76), HMQC (Figure 77) and HMBC (Figures 78-79) spectra.

However, compounds CC1 and CC2 were found to have opposite signs of optical rotation ($[\alpha]_D^{20}$ = –46.9° for compound CC1 vs. +22.7° for compound CC2), suggesting the enantiomeric nature for their aglycones. Conclusive evidence came from the circular dichroism (CD) studies. It is known that for this class of lignans and their glucosides, the sign of the couplets at 287 and 273 nm reflects the orientation of the aryl substituent at C-8 (Sakakibara, Ina, and Yasue, 1974; Ohashi *et al*., 1994). In this study, compound CC2 showed positive and negative peaks at 286 and 274 nm, respectively (Figure 63), indicating the (6*S*,7*R*,8*R*)-absolute configuration.

Hence, compound CC2 was elucidated as a new lignan glucoside, (6*S*,7*R*,8*R*)-7a-[(*β*-glucopyranosyl)-oxy]lyoniresinol [**179**]. It is interesting to note that compounds CC1 and CC2 are diastereomeric glucosides with enantiomeric aglycones.

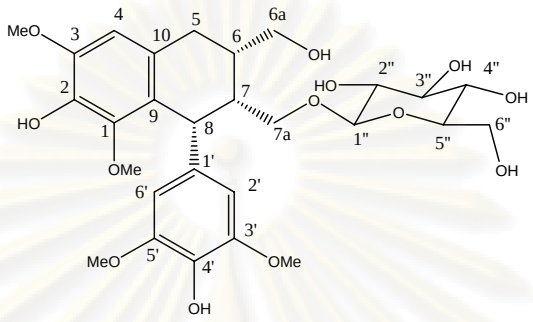

[**179**]

Table 11 NMR spectral data of compound CC2 (MeOH-d_4)

position	Compound CC2		HMBC (correlation with ^{1}H)
	^{1}H (mult., *J* in Hz)	^{13}C	
1	-	147.5	OMe-1
2	-	138.8	H-4
3	-	148.7	OMe-3
4	6.53 (s)	107.8	H-5
5	2.63 (d, 7.5)	33.8	H-4 and H-6a
6	1.65 (m)	41.2	H-5*, H-6a*and H-8
6a	3.58 (d, 4.8)	66.2	H-5
7	2.09 (m)	46.5	H-5 and H-8*
7a	3.54 (m)	72.0	H-8 and H-1′′
	3.88 (m)		
8	4.19 (d, 6.3)	43.2	H-2′ and H-6′
9	-	126.2	H-4, H-5 and H-8*
10	-	130.2	H-5* and H-8
1′	-	139.4	H-8*
2′	6.37 (s)	107.1	H-8
3′	-	149.0	2′* and OMe -3′
4′	-	134.6	2′ and 6′
5′	-	149.0	6′* and OMe-5′
6′	6.37 (s)	107.1	H-8
1′′	4.09 (d, 7.5)	104.2	H-2′′*
2′′	3.17 (m)	75.0	H-3′′*
3′′	3.27 (m)	77.8	H-5′′
4′′	3.27 (m)	71.5	H-3′′*
5′′	3.12 (m)	78.1	H-6′′*
6′′	3.60 (m)	62.7	-
	3.80 (m)		
OMe-1	3.29 (s)	60.1	-
OMe-3	3.81 (s)	56.6	-
OMe-3′/5′	3.71 (s)	56.9	-

*Two-bond coupling

1.10 Structure determination of compound CC3

Compound CC3 was obtained as a yellow amorphous solid. The quasi-molecular ion $[M+H]^+$ at *m/z* 413.2177 in the HRESI mass spectrum indicated a molecular formula of $C_{21}H_{32}O_8$, and the IR absorptions (Figure 82) at 3368 and 1650 cm^{-1} suggested the presence of OH groups and a conjugated C=O functionality, respectively.

The ^{13}C NMR (Figure 85 and Table 12) and DEPT (Figure 86) spectra revealed the presence of a glucose moiety, as indicated by the resonances at δ 100.1 (C-1′), 73.6 (C-2′), 77.4 and 77.0 (C-3′) and C-5′), 70.0 (C-4′), and 61.2 (C-6′). This, together with the molecular formula, suggested that compound CC3 was a glucosidic sesquiterpene. For the aglycone part, the carbon signals observed for four methyl groups at δ 9.7 (C-15), 22.2 (C-14), and 25.4 and 26.7 (C-12 and C-13), two olefinic carbons at δ 127.4 (C-4) and 159.3 (C-5) and a keto-carbonyl group at δ 189.1 (C-3) were reminiscent of carissone (11-hydroxyeudesma-4-en-3-one), an eudesmane-type sesquiterpene previously isolated from this plant (Singh and Rastogi, 1972) and *C. edulis* (Achenbach, Waibel, and Addae-Mensah, 1985). This was also supported by ^1H NMR signals (Figure 84 and Table 12) for methyl groups at δ 1.83 (Me-15), 1.37 (Me-14), and 1.17 and 1.18 (Me-12 and Me-13), which correlated to their corresponding carbons in the HMQC spectrum (Figure 88). However, compound CC3 differed significantly from carissone in that its C-1 and C-2 resonated at much higher frequencies, appearing as an olefinic C-O and a C-H carbon signal at δ 180.3 and 103.3 ppm, respectively. Their assignments were based on the HMBC correlations from Me-14 to C-1, and from H-2 to C-4 (Figures 89-91). This was also in agreement with the γ-effect observed for C-9 (–4.5 ppm) in this compound as compared with its counterpart in carissone (Maatooq *et al*., 1996). The glucose unit should be attached to C-1 of the aglycone, as evidenced by the three-bond coupling between H-1′ and C-1. The appearance of the anomeric proton (H-1′) (in DMSO-d_6) as a doublet (J = 6.9 Hz) at δ 4.72 ppm indicated a *β*-configuration. The relative configuration at C-7 and C-10 was then determined from the NOESY spectrum (Figure 92), which showed cross peaks for the following pairs of H-atoms: H-7/H-8, H-7/H-9, H-8/H-9, H-6/Me-14, and H-6/Me-15.

Based on the above spectroscopic data, compound CC3 was established as a novel compound, 11-hydroxyeudesma-1,4-dien-3-on-1-yl *β*-glucoside and given the

trivial name carandoside [**180**].

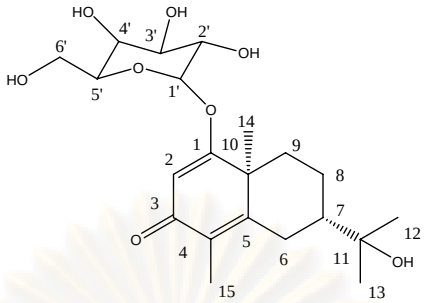

[**180**]

Table 12 NMR spectral data of compound CC3 (MeOH-d_4 and DMSO-d_6)

position	Compound CC3			HMBC (correlation with ^{1}H)
	^{1}H (mult., *J* in Hz) in DMSO-d_6	^{1}H (mult., *J* in Hz) in MeOH-d_4	^{13}C in MeOH-d_4	
1	-	-	180.3	H-1′ and H-14
2	5.64 (s)	5.73 (s)	103.3	-
3	-	-	189.1	H-15
4	-	-	127.4	H-2, H-6 and H-15*
5	-	-	159.3	H-14 and H-15
6	1.97 (brd, 12.9)	2.08 (brd, 12.9)	28.1	-
	2.84 (brd, 12.9)	2.94 (brd, 12.9)		
7	1.25 (m)	1.27 (m)	51.7	H-6* and H-9
8	1.47 (m)	1.54 (m)	22.3	H-6
	1.68 (m)	1.73 (m)		
9	1.21 (m)	1.24 (m)	36.8	H-14
	2.16 (brd, 12.6)	2.26 (brd, 13.2)		
10	-	-	43.3	H-2 and H-6
11	-	-	71.9	-
12/13	1.10/1.11 (s)	1.17/1.18 (s)	25.4/26.7	H-7
14	1.32 (s)	1.37 (s)	22.2	-
15	1.77 (s)	1.83 (s)	9.7	-
1′	4.72 (d, 6.9)	[a])	100.1	-
2′	3.35 (m)	3.32 (m)	73.6	-
3′	3.35 (m)	3.32 (m)	77.0/77.4	2′*, 4′* and 5′
4′	3.35 (m)	3.32 (m)	70.0	-
5′	3.35 (m)	3.32 (m)	77.0/77.4	3′ and 4′*
6′	3.70 (m)	3.73 (m)	61.2	-

*Two-bond coupling

[a]) Hidden under solvent signal

1.11 Structure determination of compound CC4

Compound CC4 was obtained as a yellow amorphous solid. It showed UV absorption maxima at 280 and 300 nm (Figure 93), and IR absorption bands (Figure 94) at 3359 and 1658 cm^{-1} were attributable to hydroxyl and carbonyl group, respectively. It exhibited an $[M+Na]^+$ peak at *m/z* 399.9 in the ESI mass spectrum (Figure 95).

Compound CC4 appeared to be a mixture of two epimeric diarylbutanes with hemiacetal structure. By comparison of its ^1H, ^{13}C NMR and optical rotation properties with previously reported data (Khamlach, Dhal and Brown, 1990), compound CC4 was identified as (–)-carrisanol [**167**]. This compound was earlier isolated from *Carissa edulis* (Achenbach, Waibel and Addae-Mensah, 1983), *C. carandas* and *C. spinarum* (Rao *et al*., 2005). It has also been synthesized (Khamlach, Dhal and Brown, 1990).

The ^1H NMR spectrum of compound CC4 (Figure 96; Table 13) showed two sets of proton signals, for example two methine proton singlets at δ 5.15 and 4.92 ppm, each assignable to H-9′. The ^{13}C NMR spectrum (Figure 97; Table 13) revealed forty carbons suggesting two lignan structures. Each structure was composed of an 18-carbon skeleton with a methoxy group. It also exhibited two sets of carbon signals, for example, C-9 at δ 71.3 and 73.0 ppm and C-7′ at δ 40.1 and 43.8 ppm. The NMR assignments were obtained for structures A and B by examination of ^1H-^1H COSY (Figure 99), HMQC (Figures 100-101) and HMBC spectra (Figures 102-104). In addition, the relative configuration of H-9′ of structure A was assigned as α from the NOESY correlations from H-9′ (δ 5.15 ppm) to H-8 (δ 2.29 ppm) (Figure 105).

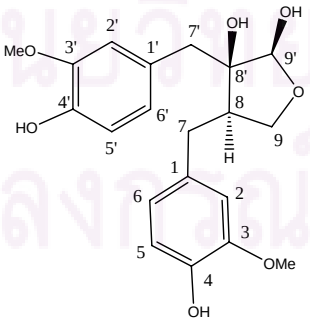

Structure A

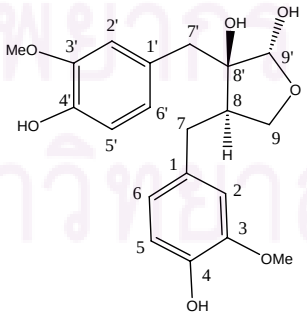

Structure B

[**167**]

Table 13 NMR spectral data of compounds CC4 (acetone-d_6) compared with (−)-carrisanol (acetone-d_6)

position	Compound CS4		(−)-Carrisanol		HMBC (correlation with ^{1}H)
	^{1}H (mult., *J* in Hz)	^{13}C	^{1}H^g (mult., *J* in Hz)	^{13}C^g	
1	-	133.5[a]	-	133.5	H-7*
		133.3[b]		133.2	
2	6.72 (m)[a]	113.0[a]	6.80 (m)	113.0	H-6 and H-7
	6.81 (d, 1.5)[b]	113.1[b]		113.1	
3	-	148.3	-	148.3	OMe-3
4	-	145.7	-	145.7	H-6
5	6.72 (m) [a, b]	115.7[d]	6.80 (m)	115.7	-
6	6.59 (dd, 8.0, 1.5)[a]	121.8	6.80 (m)	121.8	H-2 and H-7
	6.65 (dd, 8.0, 1.5)[b]				
7	2.51 (m)[a, b]	32.3[a]	2.63 (m)	32.8	H-6 and H-9
	2.78 (m)[a, b]	33.3[b]		33.3	
8	2.29 (m)[a]	48.3[a]	2.30 (m)	47.0	H-7*, H-7′, H-9*
	2.60 (m)[b]	47.0[b]		48.3	and H-9′
9	3.57 (t, 8.3)[a]	71.3[a]	3.78 (m)	71.3	H-7 and H-9′
	3.69 (m)[a, b]	73.0[b]		72.9	
	3.87 (t, 8.0)[b]				
1′	-	129.4[a]	-	129.4	H-7′*
		130.2[b]		130.2	
2′	6.91 (brs)[a]	115.1[a]	6.80 (m)	115.1	H-7′
	7.05 (d, 1.5)[b]	115.2[b]		115.4	
3′	-	147.9[a]	-	147.8	OMe-3′
		147.8[b]		147.9	
4′	-	145.9[a]	-	145.9	H-2′
		146.2[b]		146.2	
5′	6.72 (m)[a, b]	115.3[d]	6.80 (m)	115.2	H-6′*[e]
		115.4[b]			
6′	6.72 (m) [a, b]	124.1[a]	6.80 (m)	124.0	H-2′ and H-7′
	6.84 (dd, 8.0, 2.0) [a, b]	124.2[b]		124.2	
7′	2.78 (m)[a, b]	43.8[a]	2.63 (m)	40.1	H-2′and H-9′[f]
	3.00 (d, 13.5)[b]	40.1[b]		43.9	
8′	-	79.6[a]	-	79.6	H-7, H-7′*, H-9
		82.8[b]		82.8	and H-9′*[f]

Table 13 (continued)

position	Compound CS4		(−)-Carrisanol		HMBC (correlation with ^{1}H)
	^{1}H (mult., *J* in Hz)	^{13}C	$^{1}H^{g}$ (mult., *J* in Hz)	$^{13}C^{g}$	
9′	5.15 (s)[a]	101.4[a]	5.15 (d, 3.9)	101.4	H-7′ and H-9
	4.92 (s)[b]	104.4[b]	4.92 (d, 3.9)	104.4	
OMe-3	3.80[c]	56.2[d]	3.82	56.2	-
	3.81[c]	56.3d	3.83	56.3	
OMe-3′	3.82[c]	56.4[d]	3.84		-
	3.83[c]		3.85		
OH-9′	-		5.49		-
			6.15		

*Two-bond coupling
[a,b]NMR signal in structures A and B
[c,d]Interchangeable within the same column
[e]HMBC correlation only in structure B
[f]HMBC correlation only in structure A
[g]NMR signals of reference did not distinguished

1.12 Structure determination of compound CC5

Compound CC5 was obtained as a yellow amorphous solid. It showed UV absorption maxima at 284 and 300 nm (Figure 106) and IR absorption peaks (Figure 107) at 3359 and 1658 cm^{-1} attributable to hydroxyl and carbonyl groups, respectively. Its molecular $[M+Na]^+$ ion at *m/z* 397.8 (Figure 108) was consistent with the molecular formula $C_{20}H_{22}O_7$.

The ^1H NMR spectrum (Figure 109 and Table 14) showed six aromatic protons at δ 6.65 (d, *J* = 7.8, 1.8 Hz, H-6), 6.67 (dd, *J* = 7.9, 1.5 Hz, H-6′), 6.74 (d, *J* = 7.9 Hz, H-5′), 6.75 (d, *J* = 7.8 Hz, H-5), 6.76 (brs, H-2), and 6.81 (d, *J* = 1.5 Hz, H-2′) ppm. The ^{13}C NMR (Figure 110 and Table 14) and DEPT data (Figure 111) revealed carbonyl carbon at δ 178.1 (C-9′) ppm, three methylenes at δ 31.4 (C-7), 41.2 (C-7′), 70.3 (C-9) ppm, one methine at δ 43.7 (C-8) ppm and one quarternary carbinol carbon at δ 76.4 (C-8′) ppm.

Compound CC5 was identified as (–)-nortrachelogenin [**168**] by analysis of the above spectral data and confirmed by comparison with previously published data (Achenbach *et al*., 1983; Lin, Fang and Cheng, 1999). This compound was first isolated from *Trachelospermum asiaticum* (Achenbach *et al*., 1983).

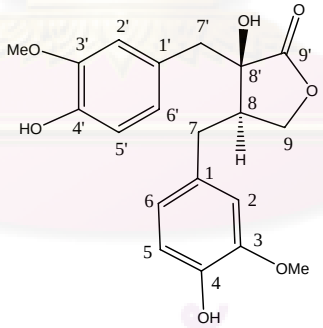

[**168**]

Table 14 NMR spectral data of compounds CC5 (acetone-d_6) compared with (–)-nortrachelogenin (^{1}H in acetone-d_6 and ^{13}C in $CDCl_3$)

position	Compound CC5		(–)-Nortrachelogenin	
	^{1}H (mult., *J* in Hz)	^{13}C	^{1}H (mult., *J* in Hz)	^{13}C
1	-	131.0	-	130.2
2	6.76 (brs)	112.7	6.79 (d, 2.0)	111.4
3	-	147.5	-	146.5
4	-	145.4	-	144.3
5	6.75 (d, 7.8)	115.1	6.76 (d, 8.0)	114.3
6	6.65 (dd, 7.8, 1.8)	121.5	6.66 (dd, 8.0, 2.0)	121.4
7	2.57 (d, 9.5)	31.4	2.55 (m)[b]	31.6
	2.83 (d, 9.5)		2.86 (m)[b]	
8	2.51 (m)	43.7	2.55 (m)[b]	43.9
9	3.98 (d, 7.8)	70.3	3.97 (dd, 14.0, 8.0)	70.1
	3.98 (d, 7.8)		4.02 (dd, 14.0, 8.0)	
1′	-	127.3	-	126.0
2′	6.81 (d, 1.5)	114.3	6.83 (d, 2.0)	112.6
3′	-	146.0	-	145.0
4′	-	147.8	-	146.5
5′	6.74 (d, 7.9)	115.3	6.77 (d, 8.0)	114.5
6′	6.67 (dd, 7.9, 1.5)	123.4	6.66 (dd, 8.0, 2.0)	123.1
7′	2.93 (d, 13.6)	41.2	2.95 (d, 13.5)	42.1
	3.13 (d, 13.6)		3.15 (d, 13.5)	
8′	-	76.4	-	76.4
9′	-	178.1	-	178.4
O-Me	3.77 (s)	55.7[a]	3.79 (s)	-
O-Me′	3.81 (s)	55.7[a]	3.82 (s)	-
Ar-OH	7.44 (brs)	-	7.44 (brs)	-
Ar-OH′	-	-	7.52 (brs)	-
OH-8′	5.13 (brs)	-	5.16 (brs)	-

[a]Interchangeable within the same column

[b] Different signal superimposed

1.13 Structure determination of compound CS1

Compound CS1 was obtained as a yellow amorphous solid. The ESI mass spectrum (Figure 113) exhibited an $[M+Na]^+$ peak at *m/z* 215.5, suggesting the molecular formula $C_{10}H_8O_4$. It had UV absorption maxima at 300 and 343 nm (Figure 112).

The ^1H NMR spectrum of compound CS1 (Figure 114, Table 15) showed the presence of one methoxy (δ 3.88 ppm) group and four sp^2 protons [δ 6.10 (d, *J*=9.3 Hz, H-3), 6.68 (s, H-8), 7.01 (s, H-5) and 7.81 (d, *J* = 9.3 Hz, H-4) ppm]. The ^{13}C NMR spectrum (Figure 115, Table 15) indicated ten carbon signals due to one carbonyl carbon at δ 164.8 (C-2), eight olefinic carbons including four quartenary carbons at δ 111.2 (C-10), 148.5 (C-6), 152.4 (C-9) and 157.0 (C-7) ppm (three of which were attached to an oxygen function) and four methine carbons at δ 104.3 (C-8), 109.4 (C-5), 110.6 (C-3) and 146.5 (C-4) ppm and a methoxy group at δ 56.7 (OMe-6) ppm. These NMR data and its molecular formula indicated this compound is coumarin.

Compound CS1 was identified as scopoletin [**181**] by comparison of its ^1H and ^{13}C NMR data with reported data (Vasconcelos, Silva and Cavaleiro, 1998). Its structure was confirmed by 2D NMR experiments (Figures 120-122). For example, HMBC correlation (Figure 122) from OMe-6 (δ 3.88 ppm) to C-6 (δ 148.5 ppm) indicated that the attachment of methoxy group at C-6.

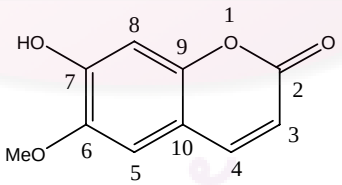

[**181**]

Table 15 NMR spectra data of compound CS1 (^{1}H in MeOH-d_4, ^{13}C in MeOH-d_4 and $CDCl_3$) as compared with scopoletin ($CDCl_3$).

position	Compound CS1			Scopoletin		HMBC (correlation with ^{1}H)
	^{1}H (mult., *J* in Hz)	^{13}C (MeOH-d_4)	^{13}C ($CDCl_3$)	^{1}H (mult., *J* in Hz)	^{13}C	
2	-	164.8	161.6	-	161.5	H-3* and H-4
3	6.10 (d, 9.3)	110.6	113.6	6.28 (d, 9.5)	113.4	-
4	7.81 (d, 9.3)	146.5	143.5	7.60 (d, 9.5)	143.3	H-5
5	7.01 (s)	109.4	107.7	6.85 (s)	107.4	H-4
6	-	148.5	144.2	-	144.0	OMe-6, H-8, H-5*
7	-	157.0	150.5	-	150.2	H-5, H-8*
8	6.68 (s)	104.3	103.4	6.92 (s)	103.2	-
9	-	152.4	149.9	-	150.2	H-5, H-8*
10	-	111.2	111.7	-	111.5	H-3, H-8
OMe-6	3.88 (s)	56.7	56.6	3.96 (s)	56.4	-
OH-7	-	-	-	6.17 (s)	-	-

*Two-bond coupling

1.14 Structure determination of compound CS2

Compound CS2 showed spectroscopic properties (^{1}H, ^{13}C NMR, Mass, UV and IR data) identical with those of compound CC5. Therefore, it was identified as (−)-nortrachelogenin [**168**].

1.15 Structure determination of compound CS3

Compound CS3 had physical and spectra data (^{1}H, ^{13}C NMR, Mass, UV and IR data) as same as compound CC4. Therefore, it was identified as (−)-carrisanol [**167**].

1.16 Structure determination of compound CS4

Compound CS4 was obtained as a brown amorphous solid. The UV spectrum (Figure 120) showed maximum absorption bands at 280 and 300 nm. Its ESI mass spectrum (Figure 121) displayed a molecular ion $[M+Na]^+$ peak at *m/z* 401.6, indicating its molecular formula as $C_{20}H_{26}O_7$.

The ^1H (Figure 122 and Table 16) and ^1H-^1H-COSY (Figure 125) spectra indicated the presence of two sets of aromatic ABX proton systems. They were six aromatic protons observed at δ 6.65 (d, *J* = 8.0 Hz, H-5), 6.67 (dd, *J* = 8.0, 2.0 Hz, H-6), 6.72 (d, *J* = 8.0 Hz, H-5′), 6.77 (dd, *J* = 8.0, 2.0 Hz, H-6′), 6.80 (d, *J* = 1.5 Hz, H-2) and 6.94 (d, *J* = 1.5 Hz, H-2′) ppm. The ^{13}C NMR (Figure 123 and Table 16) and HMQC spectra (Figure 126) showed 20 carbons, analyzed for two methoxyls, four methylenes, seven methines and seven quartenary carbons, and therefore suggested that its structure consists of an 18-carbon skeleton of lignan with two methoxy group substitutions. In addition, ^1H-^1H COSY correlations (Figure 125) from H-7 to H-8 and H-8 to H-9 indicated the connection of C-7, C-8 and C-9. The carbon linkage between C-8 and C-8′ was confirmed by HMBC correlations (Figures 127-130) from C-8′ to H-7′, H-9 and H-9′ and from C-8 to H-7, H-7′, H-9 and H-9′.

Compound CS4 was determined as (–)-carinol [**160**], which was first isolated from *Carissa carandas* (Pal *et al*., 1975). Its spectral data were in good accordance with literature values (Khamlach, Dhal and Brown, 1990).

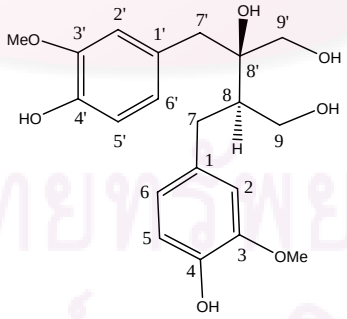

[**160**]

Table 16 NMR spectral data of compound CS4 (MeOH-d_4) compared with (−)-carinol (acetone-d_6)

position	Compound CS4		(-)-Carinol		HMBC
	^{1}H (mult., *J* in Hz)	^{13}C	^{1}H (mult., *J* in Hz)	^{13}C	(correlation with ^{1}H)
1	-	134.0	-	134.0	H-5 and H-7*
2	6.80 (d, 1.5)	113.9	6.85 (d, 1.6)	113.6	H-6 and H-7
3	-	149.0	-	148.2	H-2* and OMe-3
4	-	145.9	-	145.6	H-2 and H-6
5	6.65 (d, 8.0)	115.9	6.74 (d, 8.0)	115.5	-
6	6.67 (dd, 8.0, 2.0)	122.8	6.70 (dd, 8.1, 1.7)	122.5	H-2 and H-7
7	2.54 (dd, 13.5, 11.5)	32.2	2.58 (dd, 13.6, 11.6)	32.0	H-2, H-6, H-8* and H-9
	2.98 (dd, 13.5, 2.5)		3.02 (dd, 13.6, 2.7)		
8	1.92 (m)	50.0	1.97 (m)	49.2	H-7*, H-7′, H-9* and H-9′
9	3.69 (dd, 11.0, 2.5)	60.6	3.74 (dd, 11.1, 2.4)	60.5	H-7
	3.55 (dd, 11.5, 5.5)		3.60 (dd, 11.1, 5.4)		
1′	-	130.0	-	130.0	H-5′ and H-7′*
2′	6.94 (d, 1.5)	115.8	7.00 (d, 1.8)	115.2	H-6′ and H-7′
3′	-	148.7	-	147.8	H-5′ and OMe-3′
4′	-	146.4	-	145.9	H-2′ and H-6′
5′	6.72 (d, 8.0)	116.1	6.74 (d, 8.0)	115.5	-
6′	6.77 (dd, 8.0, 2.0)	124.6	6.81 (dd, 8.0, 1.8)	124.3	H-2′ and H-7′
7′	2.93 (s)	41.8	2.93 (s)	41.5	H-2′, H-6′ and H-9′
8′	-	78.2	-	77.4	H-7′*, H-9 and H-9′*
9′	3.44 (d, 11.3)	65.1	3.44 (d, 11.1)	65.4	H-7′
	3.49 (d, 11.3)		3.50 (d, 11.1)		
OMe-3	3.84 (s)	56.5	3.82 (s)	56.3	-
OMe-3′	3.82 (s)	56.4	3.82 (s)	56.3	-

*Two-bond coupling.

1.17 Structure determination of compound CS5

Compound CS5 was obtained as a yellow amorphous solid. The UV spectrum (Figure 131) showed absorption maxima at 288 and 300 nm. The ESI mass spectrum (Figure 132) exhibited the molecular ion at *m/z* 399.6, corresponding to the molecular formula $C_{20}H_{24}O_7$.

The ^{1}H NMR spectrum (Figure 133 and Table 17) showed six aromatic protons at δ 6.18 (s, H-5′), 6.65 (s, H-2′), 6.66 (dd, *J* = 8.0, 2.0 Hz, H-6), 6.78 (d, *J* = 1.5 Hz, H-2) and 6.78 (d, *J* = 8.0 Hz, H-5) ppm, three methylene protons at δ 2.57 (d, *J* = 16.4 Hz, H-7′), 3.22 (d, *J* = 16.4 Hz, H-7′), 3.58 (2H, dd, *J* = 13.5, 4.3 Hz, H-9 and H-9′), 3.81 (m, H-9′) and 3.85 (m, H-9) ppm and two methine protons at δ 2.30 (m, H-8) and 4.05 (d, *J* = 11.6 Hz, H-7). The ^{13}C NMR (Figure 134 and Table 17) and DEPT (Figure 135) spectra indicated one quarternary at δ 74.1 ppm (C-8′) and two methylene carbons at δ 60.8 (C-9′) and 69.6 (C-9) ppm which were each connected to an oxygen atom. From the molecular formula, compound CS5 appeared to be similar to compound CS4, (–)-carinol [**160**], except that this compound CS5 had two protons less than compound CS4. The ^{1}H and ^{13}C NMR data of compound CS5 were further supported by ^{1}H-^{1}H COSY (Figure 136) and HMQC correlations (Figure 137). The HMBC correlations from C-1′ to H-2′, H-7 and H-7′ were suggestive of a carbon linkage between C-6′ and C-7 (Figures 138-140). Furthermore, the assignments of C-1 and C-1′ were confirmed by HMBC correlations from C-1 to H-7 and C-1′ to H-2′, H-7 and H-7′. It should be noted that the ^{13}C NMR data for C-1 (δ 138.3 ppm) and C-1′ (δ 133.5 ppm) were opposite to those of reference data [C-1 (δ 133.7 ppm) and C-1′ (δ 138.4 ppm)] (Ghogomu-Tih *et al*., 1985).

Upon comparison of the spectral data and specific rotation value in the literature (Ghogomu-Tih *et al*., 1985), the structure of compound CS5 was determined to be (+)-cycloolivil [**182**].

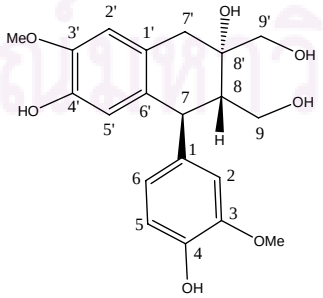

[**182**]

Table 17 NMR spectral data of compound CS5 (acetone-d_6) compared with (+)-cycloolivil (MeOH-d_4)

position	Compound CS5		(+)-cycloolivil		HMBC
	^{1}H (mult., *J* in Hz)	^{13}C	^{1}H (mult., *J* in Hz)	^{13}C	(correlation with ^{1}H)
1	-	138.3	-	133.7	H-7*
2	6.78 (d, 1.5)	113.9	6.68 (d, 1.9)	114.3	H-7
3	-	148.4	-	149.2	H-2*, H-5 and OMe-3
4	-	145.9	-	146.2	H-2 and H-5*
5	6.78 (d, 8.0)	115.7	6.75 (d, 7.8)	117.4	-
6	6.66 (dd, 8.0, 2.0)	123.2	6.66 (dd, 7.8, 1.9)	123.7	-
7	4.05 (d, 11.6)	44.6	4.01 (d, 10.5)	45.0	H-1*, H-1′, H-2 and H-9
8	2.30 (m)	47.5	1.97 (m)	47.9	H-7* and H-7′
9	3.58 (dd, 13.5, 4.3) 3.85 (m)	69.6	3.46 (dd, 12.0, 2.5) 3.77 (dd, 12.0, 4.1)	69.5	-
1′	-	133.5	-	138.4	H-2′*, H-7 and H-7′*
2′	6.65 (s)	112.7	6.20 (s)	113.3	H-7′
3′	-	146.7	-	147.6	H-5′
4′	-	145.2	-	145.5	H-2′
5′	6.18 (s)	116.8	6.61 (s)	116.2	-
6′	6.77 (dd, 8.0, 2.0)	126.5	6.81 (dd, 8.0, 1.8)	126.6	H-5′* and H-7′
7′	2.57 (d, 16.4) 3.22 (d, 16.4)	40.2	2.6 (d, 16.7) 3.21 (d, 16.7)	40.1	H-1′*
8′	-	74.1	-	74.9	H-7′* and H-9′*
9′	3.58 (dd, 13.5, 4.3) 3.81 (m)	60.8	3.76 (d, 11.3) 3.79 (d, 11.3)	61.0	-
OMe-3	3.77 (s)[a]	56.3[b]	3.76 (s)[c]	56.6	-
OMe-3′	3.78 (s)[a]	56.4[b]	3.79 (s)[c]	56.6	-

*Two-bond coupling.
[a, b, c]Interchangeable within the same column.

1.16 Structure determination of compound CS6

Compound CS6 was obtained as a yellow amorphous solid. The UV spectrum (Figure 141) exhibited absorption maxima at 283 and 296 nm. It showed a molecular ion $[M+Na]^+$ peak at *m/z* 397.6 in the ESI mass spectrum (Figure 142), corresponding to $C_{20}H_{22}O_7$.

The ^{1}H NMR spectrum (Figure 143 and Table 18) showed characteristic signals for two ABX systems. The first system was comprised of signals at δ 6.80 (d, *J* = 8.0 Hz, H-5′), 6.90 (dd, *J* = 8.0, 2.0 Hz, H-6′) and 7.08 (d, *J* = 2.0 Hz, H-2′) ppm. The other consisted of singals at δ 6.78 (d, *J* = 8.3 Hz, H-5), 6.88 (dd, *J* = 8.3, 1.7 Hz, H-6) and 7.06 (d, *J* = 1.7 Hz, H-2) ppm. The ^{13}C NMR (Figure 144 and Table 19) and DEPT (Figure 145) spectra also exhibited six aromatic methine carbons at δ 111.1 (C-2′), 112.4 (C-2), 115.2 (C-5), 115.6 (C-5′), 120.1 (C-6′) and 121.2 (C-6) ppm, two oxygenated methylenes at δ 71.9 (C-9′) and 75.9 (C-9) ppm, two oxygenated methines at δ 86.8 (C-7′) and 88.8 (C-7) ppm and two methoxy groups at δ 56.3 ppm. These proton and carbon assignments were established by analysis of ^{1}H-^{1}H COSY (Figure 146) and HMQC (Figure 147) spectra. The presence of tetrahydrofurofuran ring was supported by HMBC correlations (Figures 148-150) from C-7′ to H-2′, H-6′, H-9′ and H-9, and from C-7 to H-2, H-6 and H-9. Moreover, the assignments of C-3 and C-3′ were confirmed by HMBC correlations from C-3 to H-5 and OMe-3 and C-3′ to H-5′ and OMe-3′.

On the basis of the above spectral analysis and comparison of NMR and optical rotation data with literature values (Yeo *et al*., 2004), compound CS6 was determined to be (+)-8-hydroxypinoresinol [**183**].

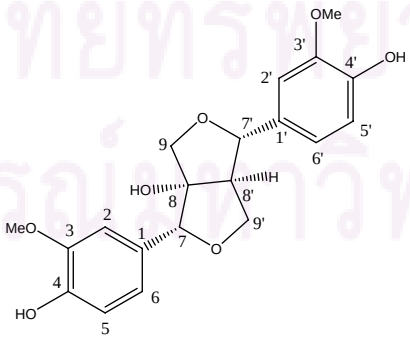

[**183**]

Table 18 NMR spectral data of compound CS6 (acetone-d_6) compared with (+)-8-hydroxypinoresinol (acetone-d_6)

position	Compound CS6		(+)8-hydroxypinoresinol		HMBC
	^{1}H (mult., *J* in Hz)	^{13}C	^{1}H (mult., *J* in Hz)	^{13}C	(correlation with ^{1}H)
1	-	129.4	-	129.3	H-5 and H-7*
2	7.06 (d, 1.7)	112.4	7.05 (d, 1.7)	112.3	H-6 and H-7
3	-	148.3	-	147.9	H-5 and OMe-3
4	-	147.0	-	146.9	H-2 and H-6
5	6.78 (d, 8.3)	115.2	6.76 (d, 8.0)	115.2	-
6	6.88 (dd, 8.3, 1.7)	121.2	6.87 (dd, 8.0, 1.7)	121.1	H-2 and H-7
7	4.67 (s)	88.8	4.66 (s)	88.7	H-2, H-6, H-9 and H-9′
8	-	92.7	-	92.7	H-8′*, H-9* and H-9′
9	3.86 (d, 9.0) 4.04 (d, 9.0)	75.9	3.85 (d, 9.2) 4.03 (d, 9.2)	75.9	H-7 and H-7′
1′	-	134.2	-	134.0	H-5′, H-7′* and H-8′
2′	7.08 (d, 2.0)	111.1	7.07 (d, 1.7)	111.0	H-6′ and H-7′
3′	-	147.9	-	148.3	H-5′ and OMe-3′
4′	-	147.1	-	147.1	H-2′ and H-6′
5′	6.80 (d, 8.0)	115.6	6.78 (d, 8.0)	115.5	-
6′	6.90 (dd, 8.0, 2.0)	120.1	6.89 (dd, 8.0, 1.7)	120.0	H-2′ and H-7′
7′	4.82 (d, 5.0)	86.8	4.81 (d, 5.1)	86.8	H-2′, H-6′, H-9 and H-9′
8′	3.02 (ddd, 8.5, 6.3, 5.0)	62.3	3.01 (ddd, 8.0, 6.2, 5.1)	62.2	H-7′*, H-9 and H-9′*
9′	3.73 (dd, 8.7, 6.3) 4.45 (t, 8.7)	71.9	3.72 (dd, 9.2, 6.2) 4.44 (dd, 9.2, 8.0)	71.8	H-7
OMe-3	3.84 (s)	56.3	3.82 (s)	56.2	-
OMe-3′	3.84 (s)	56.3	3.82 (s)	56.2	-

*Two-bond coupling.

1.17 Structure determination of compound CS7

Compound CS7 was a yellow amorphous solid. The UV spectrum displayed abosorption bands at 285 and 298 nm (Figure 151). Its molecular ion $[M+Na]^+$ at *m/z* 399.6 in ESI mass spectrum (Figure 152) indicated the molecular formula $C_{20}H_{24}O_7$.

The ^1H NMR spectrum (Figure 153 and Table 19) showed six aromatic protons in two characteristic ABX systems. The first system consisted of signals at δ 6.77 (dd, *J* = 10, 1.2 Hz, H-6′), 6.81 (brs, H-2′) and 6.87 (m, H-5′), and the other system consisted of signals at δ 6.87 (m, H-5 and H-6) and 7.01 (brs, H-2) ppm. The presence of two oxygenated methylenes at δ 60.9 (C-9) and 77.4 (C-9′) ppm, a methylene at δ 39.4 (C-7′) ppm, one methine at δ 59.2 (C-8) ppm, an oxygenated methine at δ 83.4 (C-7) ppm and one oxygenated quarternary carbon at δ 81.5 (C-8′) ppm was revealed from the ^{13}C NMR (Figure 154 and Table 19) and DEPT (Figure 155) data. Compound CS7 was identified as (–)-olivil [**169**] by comparison of the ^1H, ^{13}C NMR spectra and optical rotation with those previously published (Yeo *et al*., 2004).

The ^1H and ^{13}C NMR assignments of compound CS7 were confirmed by ^1H-^1H COSY (Figure 156), HMQC (Figure 157) and HMBC experiments (Figures 158-160).

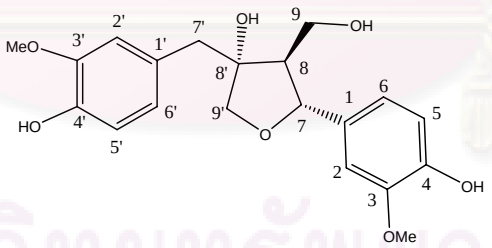

[**169**]

Table 19 NMR spectral data of compound CS7 ($CDCl_3$) compared with (–)-olivil (MeOH-d_4)

position	Compound CS7		(–)-olivil		HMBC (correlation with ^1H)
	^1H (mult., *J* in Hz)	^{13}C	^1H (mult., *J* in Hz)	^{13}C	
1	-	134.0	-	136.2	H-2*, H-5, H-6* and H-8
2	7.01 (brs)	109.0	7.10 (d, 2.0)	112.4	H-7
3	-	147.1	-	149.8	OMe-3
4	-	145.6	-	148.0	H-2 and OH-4*
5	6.87 (m)	114.3	6.68 (brd, 8.0)	116.6	OH-4
6	6.87 (m)	119.7	6.83 (dd, 8.0, 2.0)	121.6	H-2 and H-7
7	4.70 (d, 8.0)	83.4	4.68 (d, 7.3)	86.6	H-8*, H-9 and H-9′
8	2.49 (m)	59.2	2.25 (m)	62.7	H-9*
9	3.83 (dd, 9.6, 4.4)	60.9	3.69 (dd, 11.2, 5.6)	61.6	H-7 and H-8*
	3.95 (d, 9.6)		3.79 (m)		
1′	-	128.4	-	131.2	H-5′ and H-7′*
2′	6.81 (brs)	113.0	6.86 (d, 2.0)	116.1	H-6′ and H-7′
3′	-	146.8	-	144.4	OMe-3′
4′	-	144.9	-	147.0	H-2′, H-6′ and OH-4′*
5′	6.87 (m)	114.7	6.68 (brd, 8.0)	116.5	OH-4′
6′	6.77 (dd, 10.0, 1.2)	123.1	6.68 (brd, 8.0)	124.7	H-2′ and H-7′
7′	2.94 (d, 13.0)	39.4	2.86 (d, 13.9)	41.4	H-9′
	3.06 (d, 13.0)		2.94 (d, 13.9)		
8′	-	81.5	-	83.4	H-9′*
9′	3.67 (brd, 11.5)	77.4	3.56 (brd, 9.0)	78.7	-
	3.95 (m)		3.77 (brd, 9.0)		
OMe-3	3.88 (s)[a]	56.1[c]	3.80 (s)	57.2	-
OMe-3′	3.89 (s)[a]	56.2[c]	3.80 (s)	57.2	-
OH-4	5.64 (s)[b]	-	-	-	-
OH-4′	5.60 (s)[b]	-	-	-	-

*Two-bond coupling.
[a, b, c]Interchangeable within the same column.

1.18 Structure determination of compound CS8

Compound CS8 was obtained as a yellow amorphous solid. The UV spectrum (Figure 161) exhibited absorption maxima at 280 and 301 nm. It showed a $[M+Na]^+$ peak at *m/z* 385.6 in the ESI mass spectrum (Figure 162), suggesting the molecular formula $C_{20}H_{26}O_6$.

The ^1H NMR spectrum (Figure 163 and Table 20) revealed six aromatic protons in two identical ABX systems at δ 6.60 (dd, *J* = 8.0, 1.6 Hz, H-6 and H-6′), 6.65 (d, *J* = 1.6 Hz, H-2 and H-2′) and 6.71 (d, *J* = 8.0 Hz, H-5 and H-5′) ppm, four methylene protons at δ 1.96 (m, H-8 and H-8′), 2.61 (dd, *J* = 13.6, 6.8 Hz, H-7 and H-7′), 2.72 (dd, *J* = 13.6, 6.8 Hz, H-7 and H-7′)and 3.64 (t, *J* = 4.2 Hz, H-9 and H-9′) ppm and one methoxy group at δ 3.79 (s, OMe-3 and OMe-3′) ppm. The ^{13}C NMR (Figure 164 and Table 20) and DEPT spectra (Figure 165) showed only ten carbon signals, corresponding to three aromatic methines, three aromatic quaternary carbons, one oxygenated methylene, one methylene, one methine and one methoxyl. Combining these data with MS data, compound CS8 should be a symmetrical diarylbutane lignan, which has carbon lingkage between C-8 and C-8′.

Compound CS8 was identified as (–)-secoisolariciresinol [**170**]. The ^1H and ^{13}C NMR and optical rotation data of compound CS8 agreed well with those reported for (−)-secoisolariciresinol (Xie *et al*., 2003).

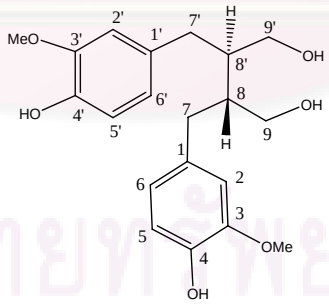

[**170**]

Table 20 NMR spectral data of compound CS8 (MeOH-d_4) as compared with (–)-secoisolariciresinol (MeOH-d_4)

position	Compound CS8		(–)-Secoisolariciresinol	
	^{1}H (mult., *J* in Hz)	^{13}C	^{1}H (mult., *J* in Hz)	^{13}C
1	-	134.0	-	133.9
2	6.65 (d, 1.6)	113.5	6.54 (d, 1.9)	113.4
3	-	148.9	-	148.8
4	-	145.7	-	145.5
5	6.71 (d, 8.0)	115.9	6.61 (d, 8.0)	115.8
6	6.60 (dd, 8.0, 1.6)	122.8	6.49 (dd, 8.0, 1.9)	122.7
7	2.61 (dd, 13.6, 6.8)	36.2	2.50 (dd, 13.8, 7.7)	36.0
	2.72 (dd, 13.6, 6.8)		2.61 (dd, 13.8, 7.0)	
8	1.96 (m)	42.3	1.86 (m)	44.1
9	3.64 (t, 4.2)	62.3	3.54 (m)	62.1
1′	-	134.0	-	133.9
2′	6.65 (d, 1.6)	113.5	6.54 (d, 1.9)	113.4
3′	-	148.9	-	148.8
4′	-	145.7	-	145.5
5′	6.71 (d, 8.0)	115.9	6.61 (d, 8.0)	115.8
6′	6.60 (dd, 8.0, 1.6)	122.8	6.49 (dd, 8, 1.9)	122.7
7′	2.61 (dd, 13.6, 6.8)	36.2	2.50 (dd, 13.8, 7.7)	36.0
	2.72 (dd, 13.6, 6.8)		2.61 (dd, 13.8, 7.0)	
8′	1.96 (m)	42.3	1.86 (m)	44.1
9′	3.64 (t, 4.2)	62.3	3.54 (m)	62.1
OMe-3	3.79 (s)	56.3	3.68 (s)	56.2
OMe-3′	3.79 (s)	56.3	3.68 (s)	56.2

1.19 Structure determination of compound CS9

Compound CS9 was isolated as a yellow amorphous solid. The UV spectrum (Figure 166) showed absorption at 284 and 303 nm. The ESI mass spectrum (Figure 167) showed an $[M+Na]^+$ ion at *m/z* 381.5, suggesting the molecular formula $C_{20}H_{22}O_6$.

Although the molecular formula indicated 20 carbons for compound CS9, there were only 10 carbon signals in the ^{13}C NMR (Figure 169 and Table 21) and DEPT (Figure 170) data, suggesting that compound CS9 was symmetrical in structure. Compound CS9 was identified as (+)-pinoresinol [**175**] by comparing its ^1H and ^{13}C NMR spectral data with reported values (Xie *et al*., 2003).

This compound consists of two phenylpropanoids. Each phenylpropanoid exhibited three aromatic protons in 1,3,4-trisubstituted benzene ring at δ 6.79 (d, *J* = 8.3 Hz, H-5 and H-5′), 6.83 (dd, *J* = 8.3, 2.0 Hz, H-6 and H-6′) and 6.99 (d, *J* = 2.0 Hz, H-2 and H-2′) ppm, a pair of oxygenated methylene proton signals at δ 3.81 (m, H-9 and H-9′) and 4.20 (dd, *J* = 9.0, 6.3 Hz, H-9 and H-9′) ppm, one oxygenated methine proton at δ 4.67 (d, *J* = 4.5 Hz, H-7 and H-7′) ppm, one methine at δ 3.09 (dd, *J* = 6.3, 4.5 Hz, H-8 and H-8′) ppm and one methoxy singlet at δ 3.84 (OMe-3 and OMe-3′) ppm in the ^1H NMR spectrum (Figure 168 and Table 21). The proton and carbon assignments were obtained by analysis of ^1H-^1H COSY (Figure 171), HMQC (Figure 172) and HMBC correlations (Figures 173-174). The presence of tetrahydrofurofuran ring was supported by HMBC correlations from C-7′ to H-2′, H-6′, H-9′ and H-9, and from C-7 to H-2, H-6 and H-9.

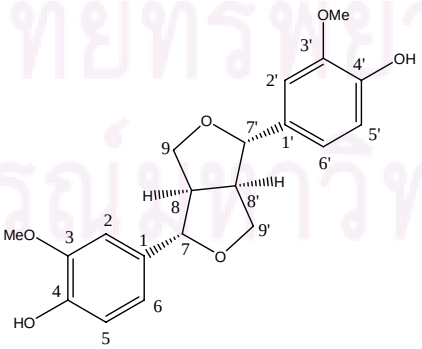

[**175**]

Table 21 NMR spectral data of compound CS9 (acetone-d_6) compared with (+)-pinoresinol (MeOH-d_4)

position	Compound CS9		(+)-Pinoresinol		HMBC
	^{1}H (mult., *J* in Hz)	^{13}C	^{1}H (mult., *J* in Hz)	^{13}C	(correlation with ^{1}H)
1	-	134.3	-	133.8	H-5
2	6.99 (d, 2.0)	110.7	6.93 (d, 1.7)	111.0	H-6 and H-7
3	-	148.4	-	149.1	H-5 and OMe-3
4	-	146.9	-	147.3	H-2 and H-6
5	6.79 (d, 8.3)	115.6	6.75 (d, 8.0)	116.1	-
6	6.83 (dd, 8.3, 2.0)	119.7	6.79 (dd, 8.0, 1.7)	120.1	H-2 and H-7
7	4.67 (d, 4.5)	86.7	4.69 (d, 4.4)	87.5	H-2, H-6 and H-9
8	3.09 (dd, 6.3, 4.5)	55.3	3.12 (m)	55.4	H-7*, H-7′, H-9* and H-9′
9	3.81 (m) 4.20 (dd, 9.0, 6.3)	72.3	3.83 (dd, 8.9, 3.6) 4.21 (dd, 8.9, 6.8)	72.6	H-7
1′	-	134.3	-	133.8	H-5′
2′	6.99 (d, 2.0)	110.7	6.93 (d, 1.7)	111.0	H-6′ and H-7′
3′	-	148.4	-	149.1	H-5′ and OMe-3′
4′	-	146.9	-	147.3	H-2′ and H-6′
5′	6.79 (d, 8.3)	115.6	6.75 (d, 8.0)	116.1	-
6′	6.83 (dd, 8.3, 2.0)	119.7	6.79 (dd, 8.0, 1.7)	120.1	H-2′ and H-7′
7′	4.67 (d, 4.5)	86.7	4.69 (d, 4.4)	87.5	H-2′, H-6′ and H-9′
8′	3.09 (dd, 6.3, 4.5)	55.3	3.12 (m)	55.4	H-7, H-7′*, H-9 and H-9′*
9′	3.81 (m) 4.20 (dd, 9.0, 6.3)	72.3	3.83 (dd, 8.9, 3.6) 4.21 (dd, 8.9, 6.8)	72.6	H-7′
OMe-3	3.84	56.5	3.84	56.4	-
OMe-3′	3.84	56.4	3.84	56.4	-

*Two-bond coupling.

1.20 Structure determination of compound CS10

Compound CS10 was obtained as a yellow amorphous solid. The UV spectrum (Figure 175) showed absorption peaks at 270 and 300 nm. The molecular formula of compound CS10 was determined to be $C_{15}H_{24}O_2$ from the $[M+Na]^+$ ion at *m/z* 259.6 in the ESI mass spectrum (Figure 176).

The ^{1}H NMR spectrum (Figure 177 and Table 22) displayed resonances of five methylenes at δ 1.41 (m, H-7, H-8 and H-9), 1.69 (m, H-8 and H-9), 1.87 (brt, *J* = 13.5 Hz, H-6), 2.35 (dt, *J* = 17.0, 4.0 Hz, H-2), 2.48 (m, H-2) and 2.83 (brd, *J* = 14.5 Hz, H-6) ppm, one methine at δ 1.41 (m, H-7, H-8 and H-9) ppm, and four methyls at δ 1.17 (H-14), 1.21 (H-12 or H-13), 1.22 (H-12 or H-13) and 1.74 (H-15) ppm. The ^{13}C NMR spectrum (Figure 178 and Table 22) showed 15 carbon signals, which were discriminated by DEPT spectra (Figure 179) into five quaternary carbons including one carbonyl, five methylenes, one methine, and four methyls. Three molecular fragments of five methylenes and one methine were assigned by ^{1}H-^{1}H COSY correlation (Figure 180) from H-1 to H-2, H-6 to H-7 and from H-8 to H-9. Its structure was also confirmed by HMQC (Figure 181) and HMBC (Figures 182-183) experiments. The substitutions of two methyl groups at C-4 and C-10 were suggested by HMBC correlations from C-4 to H-6 and H-15 and from C-10 to H-6 and H-14, respectively.

By analysis of above spectroscopic studies and comparison with reported NMR data (Achenbach *et al*., 1985), compound CS10 was identified as carrisone [**162**]. It is the main eudesmane-type sesquiterpene of *Carissa edulis* and has also been found in *C. lanceolata*, *C. carandas* and *C. congesta*. (Achenbach *et al*., 1985).

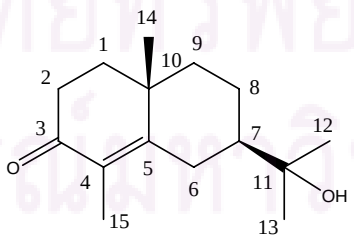

[**162**]

Table 22 NMR spectral data of compound CS10 ($CDCl_3$) and carissone ($CDCl_3$)

Posi-tion	Compound CS10		Carissone		HMBC (correlation with ^1H)
	^1H (mult., *J* in Hz)	^{13}C	^1H (mult., *J* in Hz)	^{13}C	
1	1.69 (m)	37.4	-[e]	37.4	H-2* and H-14
2	2.35 (dt, 17.0, 4.0) 2.48 (m)	33.8	2.39 (ddd, 16.0-17.0, 4.0, 4.0) 2.53 (ddd, 16.0-17.0, 11.0, 7.5)	33.8	-
3	-	199.3	-	199.0	H-2* and H-15
4	-	128.9	-	128.9	H-6 and H-15*
5	-	163.1	-	162.6	H-6*, H-14 and H-15
6	1.87 (brt, 13.5) 2.83 (brd, 14.5)	28.9	1.92 (ddq, 13.0, 13.0, 1.0) 2.87 (ddd, 13.0, 3.0, 3.0)	28.8	-
7	1.41 (m)	49.8	-[e]	49.7	H-6*, H-8*, H-9, H-12 and H-13
8	1.41 (m) 1.69 (m)	22.7	-[e]	22.6	H-6 and H-9*
9	1.41 (m) 1.69 (m)	42.1	-[f]	42.0	H-8* and H-14
10	-	35.9	-	35.9	H-6 and H-14*
11	-	72.5	-	72.4	H-6, H-12 and H-13*
12	1.22[a] (s)	26.8[b]	1.26[c] (s)	26.8[d]	H-13*
13	1.21[a] (s)	27.6[b]	1.27[c] (s)	27.5[d]	H-12*
14	1.17 (s)	22.6	1.21[c] (s)	22.6	-
15	1.74 (s)	11.0	1.79 (d, 1.0)	10.9	-

[a, b, c, d]Interchangeable within the same column.

*Two-bond coupling.

[e]Not observable because of overlapping.

[f]Not reported.

1.21 Structure determination of compound CS11

Compound CS11 was obtained as a yellow amorphous solid. The UV spectrum (Figure 184) showed maximal absorptions at 280 and 303 nm. The molecular formula was determined as $C_{30}H_{46}O_8$ (Figure 185) from its $[M+Na]^+$ peak at *m/z* 557.7 in the ESI mass spectrum.

In the ^1H NMR spectrum (Figure 186 and Table 23), the characteristic methylene protons of H-21 appeared at δ 4.80 (d, *J* = 18.4 Hz) and 4.98 (d, *J* = 18.4 Hz) ppm, and the olefinic proton for a furan ring were observed at δ 5.87 (brs) ppm. The ^{13}C NMR spectrum (Figure 188 and Table 23) and DEPT data (Figure 189) which presented 30 carbons, including an anomeric carbon of a sugar moiety at δ 101.4 ppm, indicated the presence of cardenolide glycoside structure. The configuration of glycosidic linkage was assigned to be *β* due to the value of coupling constant (8.0 Hz) of the anomeric proton (Table 23). The ^1H NMR spectrum also showed the H-17*α* signal at δ 2.80 ppm in pyridine-d_5 (Figure 187), suggesting compound CS11 to be a 17*β*-cardenolide (Yamauchi, Abe, and Wan, 1987). Furthermore, the attachment of sugar unit at C-3 was assigned by the HMBC correlation (Figure 192-194) between C-3 and H-1′. The configuration of the sugar was confirmed by NOESY correlations (Figure 195).

Based on the above spectral evidence and by comparison of its ^{13}C NMR data with previously published values (Cabrera *et al*., 1993), compound CS11 was identified as digitoxigenin 3-*O*-*β*-D-digitalopyranoside [**184**].

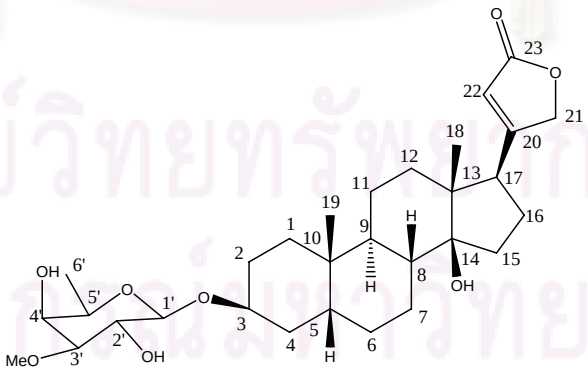

[**184**]

Table 23 NMR spectral data of compound CS11 ($CDCl_3$) and digitoxigenin 3-*O*-*β*-D-digitalopyranoside ($CDCl_3$)

position	Compound CS11		Digitoxigenin 3-*O*-*β*-D-digitalopyranoside	HMBC (correlation with ^1H)
	^1H (mult., *J* in Hz)	^{13}C	^{13}C	
1	1.76 (m)	30.3	30.5	H-19
2	1.76 (m)	27.1[a]	26.8[a]	-
3	4.04 (brs)	74.1	75.0	H-1′
4	1.76 (m)	30.2[b]	30.5	-
5	1.76 (m)	36.7	36.8	H-3
6	1.76 (m)	26.8[a]	27.1[a]	-
7	1.76 (m)	21.3[c]	21.7[b]	-
8	1.76 (m)	42.0	42.0	-
9	1.76 (m)	36.0	36.2	-
10	-	35.4	35.6	H-19*
11	1.76 (m)	21.6[c]	21.9[b]	-
12	1.76 (m)	40.2	40.4	H-17 and H-18
13	-	49.8	50.4	H-17* and H-18*
14	-	85.8	85.8	H-17
15	1.76 (m)	33.3[b]	32.7	-
16	1.76 (m)	26.7[a]	27.4	-
17	2.77 (m)	51.1	51.5	H-18
18	0.87 (s)	16.0	15.8	H-14
19	0.93 (s)	23.9	23.5	-
20	-	174.7	176.4[c]	H-17*, H-21* and H-22*
21	4.80 (d, 18.4) 4.98 (d, 18.4)	73.6	74.6	H-17 and H-22
22	5.87 (brs)	117.9	117.0	H-17 and H-21
23	-	174.7	177.6[c]	H-21 and H-22*
1′	4.25 (d, 8.0)	101.4	102.5	H-2′* and H-5′*
2′	3.65 (dd, 8.0, 10.2)	71.0	70.8	H-3′* and H-4′
3′	3.21 (dd, 10.2, 3.2)	83.0	84.0	H-2′* and OMe-3′
4′	3.86 (m)	68.4	68.1	H-5′* and H-6′
5′	3.56 (d, 6.8)	70.6	70.6	H-6′*
6′	1.35 (d, 6.4)	16.7	16.3	-
OMe-3′	3.52 (s)	57.7	56.6	H-3′

[a, b, c, d]Interchangeable within the same column.

*Two-bond coupling.

1.22 Structure determination of compound CS12

Compound CS12 was obtained as a yellow amorphous solid. The UV spectrum (Figure 197) showed maximal absorptions at 280 and 303 nm. The ESI mass spectrum (Figure 198) showed the $[M+Na]^+$ ion at *m/z* 543.9, analyzed for $C_{29}H_{44}O_8$.

The ^1H and ^{13}C NMR data (Figure 199 and 201; Table 24) of compound CS12 were similar to those of compound CS11, except for the absence of the methoxyl group. From the molecular formula, compound CS12 had two hydrogen atoms and one carbon less than compound CS11. The configuration at the glycosidic linkage was assigned to be β due to the coupling constant of the anomeric proton which was observed to be 8 Hz in $CDCl_3$. The ^1H NMR spectrum in pyridine-d_5 (Figure 200) also showed the H-17α signal at δ 2.81 ppm, suggesting compound CS12 to be a 17β-cardenolide (Yamauchi *et al*., 1987). The HMBC correlation (Figures 205-207) between C-3 and H-1′ indicated that the sugar was linked to the aglycone at C-3. In conclusion, these data indicated that the aglycone part of both compounds CS11 and CS12 were identical and they were different only in the sugar unit. The chemical shift of C-3′ in compound CS12 (δ 72.1 ppm) was lower than that in compound CS11 (δ 83.0 ppm).

Compound CS12 was identified as evomonoside [**185**]. All spectral analysis data were comparable with those published in the literature (Hyun *et al*., 1995).

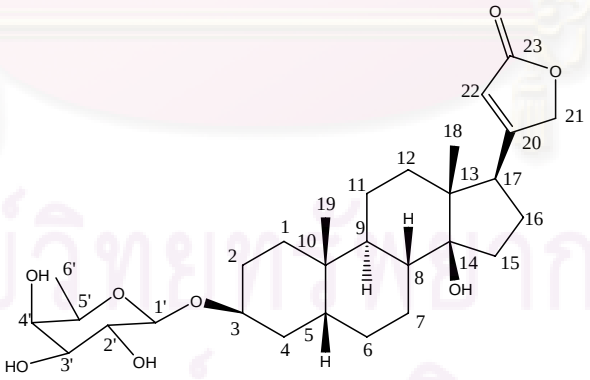

[**185**]

Table 24 NMR spectra data of compound CS12 ($CDCl_3$) as compared with evomonoside (pyridine-d_5).

position	Compound CS12		Evomonoside		HMBC
	^1H (mult., *J* in Hz)	^{13}C	^1H (mult., *J* in Hz)	^{13}C	(correlation with ^1H)
1	1.90 (m)	30.4	-[e]	30.2	H-3 and H-19
2	1.90 (m)	26.8[a]	-[e]	26.9	-
3	4.06 (brs)	74.1	4.16 (brs)	74.1	H-1′
4	1.90 (m)	30.2	-[e]	31.0	-
5	1.90 (m)	36.0	-[e]	37.1	H-3 and H-19
6	1.90 (m)	26.8[a]	-[e]	27.2[a]	-
7	1.90 (m)	21.6[b]	-[e]	21.6[b]	-
8	1.90 (m)	42.0	-[e]	41.9	-
9	1.90 (m)	36.9	-[e]	35.8	H-19
10	-	35.4	-	35.6	H-19*
11	1.90 (m)	21.3[b]	-[e]	22.0[b]	-
12	1.90 (m)	40.2	-[e]	39.9	H-17 and H-18
13	-	49.8	-	50.2	H-17* and H-18*
14	-	85.8	-	84.7	H-18
15	1.90 (m)	33.3	-[e]	33.2	-
16	1.90 (m)	27.1	-[e]	27.3[a]	H-17*
17	2.77 (dd, 9.5, 5.5)	51.1	2.79 (dd, 5.2, 8.8)	51.5	H-18 and H-22
18	0.87 (s)	16.0	0.84 (s)	16.2	-
19	0.94 (s)	23.9	1.01 (s)	24.0	-
20	-	174.7	-	176.0	H-17*, H-21* and H-22*
21	4.80 (dd, 1.5, 18.0) 4.98 (dd, 1.5, 18.5)	73.6	5.01 (dd, 1.5, 18.1) 5.29 (dd, 1.5, 18.1)	73.8	H-17 and H-22
22	5.87 (s)	117.9	6.11 (brs)	117.7	H-17 and H-21
23	-	174.7	-	174.5	H-21 and H-22*
1′	4.61 (d, 8.0)	99.3	5.38 (s)	99.9	H-2′* and H-5′
2′	3.67 (dd, 8.0, 3.5)	69.8	-[e]	77.3	-
3′	4.16 (t, 3.5)	72.1	-[e]	73.0	H-5′
4′	3.60 (d, 3.5)	71.4	-[e]	73.8	H-6′
5′	4.07 (d, 6.5)	70.1	-[e]	70.1	H-6′*
6′	1.25 (d, 6.5)	15.9	1.66 (d, 5.7)	18.7[a,b]	H-5′*

[a, b, c, d]Interchangeable within the same column.

[e]Not report.

*Two-bond coupling.

2. Free Radical Scavenging Activity

In the TLC screening assay, the methanol extracts from the roots of *Derris malaccensis*, from the stems of *Carissa carandas* and *C. spinarum* showed free radical scavenging activity. Pure compounds isolated from *D. malaccensis* and *C. spinarum* were initially tested at 100 μg/mL, whereas those from *C. carandas* were first tested at 50 μg/mL. Compounds causing more than 50% inhibition were further analyzed for their IC_{50} values. Quercetin was used as positive control. The results are summarized in Table 25.

Table 25 Percentage of free radical scavenging activity of pure compounds isolated from *D. malaccensis, C. carandas* and *C. spinarum*

Compounds	% Scavenging activity[a]	IC_{50} (μM)
12-Deoxo-12α-acetoxyelliptone [**14**]	0.36[b]	-
12a-Hydroxyelliptone [**58**]	0.24[b]	-
Tephrosin [**64**]	12.61[b]	-
Dehydroelliptone [**176**]	4.73[b]	-
6-Oxo-dehydroelliptone [**177**]	0.00[b]	-
Deguelin [**23**]	50.54[b]	253.5
Elliptone [**63**]	1.82[b]	-
(6*R*,7*S*,8*S*)-7a-[(β- glucopyranosyl) oxy]lyoniresinol [**178**]	77.74[c]	21.48
(6*S*,7*R*,8*R*)-7a-[(β- glucopyranosyl) oxy]lyoniresinol [**179**]	71.06[c]	42.96
Carandoside [**180**]	52.50[c]	116.50
(–) Carissanol [**167**]	77.5[b]	33.39
(–)-Nortrachelogenin [**168**]	86.25[b]	35.75
Scopoletin [**181**]	6.25[b]	-
(–)-Carinol [**160**]	86.25[b]	20.24
(+)-Cycloolivil [**182**]	75.42[b]	33.21
(+)-8-Hydroxypinoresinol [**183**]	76.67[b]	69.50
(–)-Olivil [**168**]	84.17[b]	18.06

Table 25 (continued)

Compounds	% Scavenging activity[a]	IC_{50} (μM)
(–)-Secoisolariciresinol [**170**]	72.92[b]	26.21
(+)-Pinoresinol [**175**]	75.83[b]	43.36
Carissone [**162**]	8.75[b]	-
Digitoxigenin 3-*O*-*β*-D-digitalopyranoside [**184**]	48.33[b]	-
Evomonoside [**185**]	47.08[b]	-
Quercetin	84.83[c]	4.6

[a]Compound with > 50% inhibition were further analyzed for IC_{50} values.

[b]at 100 μg/mL

[c]at 50 μg/mL

From Table 25, one rotenoid (deguelin [**23**]) and one sesquiterpene glucoside (carandoside [**183**]) showed weak free radical scavenging activity whereas ten lignans including ((6*R*,7*S*,8*S*)-7a-[(*β*-glucopyranosyl)oxy]lyoniresinol [**178**], (6*S*,7*R*,8*R*)-7a-[(*β*-glucopyranosyl)oxy] lyoniresinol [**179**], carissanol [**167**], (–)-nortrachelogenin [**168**], (–)-carinol [**160**], (+)-cycloolivil [**182**]**,** (+)-8-hydroxypinoresinol [**183**], (–)-olivil [**169**], (–)-secoisolariciresinol [**170**] and (+)-pinoresinol [**175**]) showed moderate activity. (–)-Olivil [**169**] exhibited the most potent activity.

Base on the IC_{50} values of (–)-secoisolariciresinol [**170**] and (–)-nortrachelogenin [**168**], it seems that lignans with the butanediol substructure is more effective than the butyrolactone structure. Increasing the number of hydroxyl groups might increase the activity, as seen between (–)-carinol [**160**] and (–)-secoisolariciresinol [**170**]. However, it should be noted that the nature of the hydroxyl groups is far more important than the number of them. This is clearly observed in the cases of (+)-8-hydroxypinoresinol [**183**] and (+)-pinoresinol [**175**]. These results were also supported by previously published data (Eklund *et al*., 2005).

3. Anti-Herpes Simplex Activity

In this study, evaluations of anti-herpes simplex activity of pure compounds and crude extracts were performed using the plaque reduction assay (Lipipun *et al*., 2003; Chuanasa *et al*., 2008). At 25 μg/mL, the MeOH extract from the roots of *D. malaccensis* showed 55% and 100% inhibition for HSV-1 and HSV-2, respectively, in post-treatment assay. The MeOH extracts from the stems of *C. carandas* and *C. spinarum* at 12.5 μg/mL exhibited 100% inhibition for both types of HSV in inactivation-treatment assay.

Pure compounds from *D. malaccensis*, *C. carandas* and *C. spinarum* were tested for this anti-HSV activity at the concentration of not more than 100 μg/mL. Compounds exhibiting more than 50% inhibition, without cytotoxicity to vero cell at 100 μg/mL, were further evaluated for IC_{50} values. Acyclovir was used as positive control. The results are summarized in Table 26.

Table 26 Anti-herpes simplex virus activity of pure compounds isolated from *D. malaccensis, C. carandas* and *C. spinarum*.

Compounds	Anti-herpes simplex virus activity IC_{50} in μg/mL (μM)			
	Post-treatment[a]		Inactivation-treatment[b]	
	HSV-1	HSV-2	HSV-1	HSV-2
12-Deoxo-12α-acetoxyelliptone [**14**]	-	-	-	-
12a-Hydroxyelliptone [**58**]	-	-	-	-
Tephrosin [**64**]	87.5 (213.4)	93.5 (228.0)	43.8 (106.8)	68.8 (167.8)
Dehydroelliptone [**176**]	-	-	-	-
Elliptone [**63**]	62.5 (177.6)	62.5 (177.6)	37.5 (106.5)	46.9 (133.2)
(6*R*,7*S*,8*S*)-7a-[(β-glucopyranosyl)oxy]lyoniresinol [**178**]	-	-	-	-
(6*S*,7*R*,8*R*)-7a-[(β-glucopyranosyl)oxy]lyoniresinol [**179**]	-	-	-	-
Carandoside [**180**]	-	-	-	-

Table 26 (continued)

Compounds	Anti-herpes simplex virus activity IC_{50} in µg/mL (µM)			
	Post-treatment[a]		Inactivation-treatment[b]	
	HSV-1	HSV-2	HSV-1	HSV-2
(–)-Carissanol [**167**]	-	-	-	-
(–)-Nortrachelogenin [**168**]	-	-	-	-
Scopoletin [**181**]	-	-	-	-
(–)-Carinol [**160**]	-	-	-	-
(+)-Cycloolivil [**182**]	-	-	-	-
(+)-8-Hydroxypinoresinol [**183**]	-	-	-	-
(–)-Olivil [**169**]	-	-	-	-
(+)-Pinoresinol [**175**]	-	-	-	-
Carissone [**162**]	-	-	-	-
Digitoxigenin 3-*O*-*β*-D-digitalopyranoside [**184**]	-	-	-	-
Evomonoside [**185**]	-	-	62.5 (120.2)	87.5 (168.3)
Acyclovir	0.50 (2.2)	-[c]	0.63 (2.8)	-[c]

[a] Post-treatment assay: add sample after infected cell with virus
[b] Inactivation-treatment assay: add sample with virus
[c] Not tested

Among the compounds isolated from *D. malaccensis* roots, only tephrosin [**64**] and elliptone [**63**] were active and showed moderate activity against both types of HSV in post- and inactivation-treatment assays. Elliptone [**63**] showed higher activity against HSV-1 and HSV-2 than tephrosin [**64**] in both treatments, suggesting that the presence of furan ring in rotenoid structure is more important for the activity than pyran ring.

The cardiac glycoside evomonoside [**185**] isolated from *C. spinarum* stems displayed moderate activity against both types of HSV but only in inactivation-treatment assay. It should be noted that the structure of evomonoside [**185**] and digitoxigenin 3-*O*-*β*-D-digitalopyranoside [**184**] are similar except for the presence of a hydroxyl group instead of a methoxyl group at C-3′ of sugar unit, but the latter compound had no activity. All compounds obtained from *C. carandas* exhibited no anti-HSV activity. This result contrasts sharply with the preliminary result obtained for the methanol crude extract of this plant. The active compounds might be in other fractions and had not been found in this study.

4. Antibacterial Activity

In this study, the antibacterial activity of each pure compound was determined by minimum inhibitory concentration assay (Shiu and Gibbons, 2006). Five compounds from *D. malaccensis* [12-deoxo-12α-acetoxyelliptone [**14**], 12a-hydroxyelliptone [**58**], tephrosin [**64**], dehydroelliptone [**176**] and elliptone [**63**]) and five compounds from *C. spinarum* ((–)-carissanol [**167**], (–)-nortrachelogenin [**168**], scopoletin [**181**], (–)-carinol [**160**] and carissone [**162**]] were investigated. None of these compounds showed antibacterial activity at the concentration of 128 µg/mL.

5. Cytotoxic Activity

In this study, all the compounds from *D. malaccensis* and *C. spinarum* that were subjected to antibacterial assay were also evaluated for cytotoxicity by sulphorhodamine B method (Gunaratnam *et al*., 2007). The results are summarized in Table 27.

Table 27 IC_{50} of cytotoxic activity of pure compounds isolated from *D. malaccensis* and *C. spinarum*

Compounds	IC_{50} in µg/mL (µM)		
	A549	MCF7	WI-38
12-Deoxo-12α-acetoxyelliptone [**14**][a]	15.14 (38.2)	12.13 (30.6)	>100 (>252.5)
12a-Hydroxyelliptone [**58**][a]	4.60 (12.5)	11.50 (31.3)	86.89 (236.1)
Tephrosin [**64**]	4.00 (9.8)	8.30 (20.2)	36.64 (89.4)
Dehydroelliptone [**176**][a]	>100 (>285.7)	>100 (>285.7)	>100 (>285.7)
Elliptone [**63**][a]	2.55 (7.2)	3.87 (11.0)	>100 (284.1)
(–)-Carissanol [**167**]	11 (29.2)	17.40 (46.2)	6.15 (16.3)
(–)-Nortrachelogenin [**168**]	29.0 (77.5)	88.30 (235.9)	>100 (>267.1)
Scopoletin [**181**][b]	>100 (>520.8)	>100 (>520.8)	>100 (>520.8)
(–)-Carinol [**160**]	<1 (<2.6)	1 (2.6)	<1 (<2.6)
Carissone [**162**]	38.55 (163.3)	62.10 (263.1)	85.11 (360.6)

[a]Cloudy solution

[b]Incompletely soluble

The results observed for elliptone [**63**] and dehydroelliptone [**176**] suggested that the presence of a double bond at C-6a and C-12a is important for cytotoxicity of

this group of rotenoids. Interestingly, elliptone [**63**] possessed selective toxicity against cancerous cells (A549 and MCF7) as compared with the normal one (WI-38).

The most active compound was (–)-carinol [**160**]. This compound displayed stronger activity than (–)carissanol [**167**] and (–)-nortrachelogenin [**168**]. This may suggest that the butanediol structure is more effective than the butyrolactone structure. Moreover, (–)carissanol [**167**] was more potent than (–)-nortrachelogenin [**168**], it might imply that the absence of the hydroxyl group at C-9′ decreases the cytotoxic activity.

.

CHAPTER V

CONCLUSION

In this study, a total of twenty-two natural compounds were isolated from *Derris malaccensis* Prain, *Carissa carandas* L. and *C. spinarum* L. These included three new compounds and nineteen known compounds as summarized in Table 28.

Table 28 Chemical constituents from *Derris malaccensis, Carissa carandas,* and *C. spinarum*.

Plant	Classes of compounds					Total
	Rotenoids	Lignans	Sesquiter-penes	Cardiac glycosides	Coumarin	
Derris malaccensis	7	-	-	-	-	7
Carissa carandas	-	4	1	-	-	5
Carissa spinarum	-	8*	1	2	1	12
Total	7	12	2	2	1	24

*Two lignans were also isolated from *C. carandas*.

From the roots of *Derris malaccensis* Prain, a new rotenoid named 6-oxo-dehydroelliptone [**177**] was isolated along with six known compounds, including 12-deoxo-12α-acetoxyelliptone [**14**], 12a-hydroxyelliptone [**58**], tephrosin [**64**], dehydroelliptone [**176**], deguelin [**23**] and elliptone [**63**]. Chemical examination of the stem of *Carissa carandas* L. led to the isolation of two new compounds, namely, (6*S*,7*R*,8*R*)-7a-[(β-glucopyranosyl)oxy]lyoniresinol [**179**] and carandoside [**180**], along with three known compounds. These known compounds are (6*R*,7*S*,8*S*)-7a-[(β-glucopyranosyl)oxy]lyoniresinol [**178**], (–)-carissanol [**167**] and (–)-nortrachelogenin [**168**]. From the stems of *C. spinarum* L., twelve know compounds were isolated: (–)-carissanol [**167**], (–)-nortrachelogenin [**168**], scopoletin [**181**], (–)-carinol [**160**], (+)-cycloolivil [**182**], (+)-8-hydroxypinoresinol [**183**], (–)-olivil [**169**], (–)-

secoisolariciresinol [**170**], (+)-pinoresinol [**175**], carissone [**162**], digitoxigenin 3-*O*-*β*-D-digitalopyranoside [**184**] and evomonoside [**185**].

All of the isolated compounds were evaluated for their biological activities such as free radical scavenging, anti-herpes simplex virus, antibacterial and cytotoxic activities. These are summarized in Table 29.

Table 29 Biological activities of isolated compounds from *Derris malaccensis*, *Carissa carandas*, and *C. spinarum*.

Activity	Classes of compounds					Total
	Rotenoids	Lignans	Sesquiter-penes	Cardiac glycosides	Coumarin	
Free radical scavenging	1	10	1	-	-	12
Anti-HSV	2	-	-	1	nd	3
Antibacterial	-	-	-	nd	-	-
Cytotoxicity	4	3	1	nd	nd	8

nd not determined

For free radical scavenging activity, deguelin [**23**] and carandoside [**180**] showed weak activity, whereas (6*R*,7*S*,8*S*)-7a-[(*β*-glucopyranosyl)oxy]lyoniresinol [**178**], (6*S*,7*R*,8*R*)-7a-[(*β*-glucopyranosyl)oxy]lyoniresinol [**179**], (–)-carissanol [**167**], (–)-nortrachelogenin [**168**], (–)-carinol [**160**], (+)-cycloolivil [**182**], (+)-8-hydroxypinoresinol [**183**], (–)-olivil [**169**], (-)-secoisolariciresinol [**170**] and (+)-pinoresinol [**175**] showed moderate activity. For anti-herpes simplex virus activity, two compounds, tephrosin [**64**] and elliptone [**63**], exhibited moderate activity against HSV-1 and HSV-2 in post- and inactivation-treatment assays, whereas evomonside [**185**] showed moderate activity against both types of virus but only in inactivation-treatment assay. However, all compounds tested had no antibacterial activity at a concentration of 128 µg/mL. For cytotoxicity test, the most active compound was (–)-carinol [**160**]. Interestingly, elliptone [**63**] was selectively active against cancerous cell lines (A549 and MCF7). 12-Deoxo-12*α*-acetoxyelliptone [**14**], 12a-hydroxyelliptone [**58**], tephrosin [**64**], (–)-carissanol [**167**], (–)-nortrachelogenin [**168**] and carissone [**162**] also showed cytotoxic activity. In contrast, dehydroelliptone [**176**] and scopoletin [**181**] were not cytotoxic at a concentration of 100 µg/mL.

References

Achenbach, H., Waibel, R., and Addae-Mensah, I. 1983. Lignans and other constituents from *Carissa edulis*. Phytochemistry 22: 749-753.

Achenbach, H., Waibel, R., and Addae-Mensah, I. 1985. Sesquiterpenes from *Carissa edulis*. Phytochemistry 24: 2325-2328.

Andrei, C. C., Vieira, P. C., Fernandes, J. B., Silva, M. F. D. G. F. D., and Fo, E. R. 1997. Dimethylchromene rotenoids from *Tephrosia candida*. Phytochemistry 46: 1081-1085.

Birch, N., Crombie, L., and Crombie, W. M. 1985. Rotenoids of *Lonchocarpus salvadorensis*: their effectiveness in protecting seeds against bruchid predation. Phytochemistry 24: 2881-2883.

Cabrera, G. M., Deluca, M. E., Seldes, A. M., Gros, E. G., Oberti, J. C., Crockett, J., and Gross, M. L. 1993. Cardenolide glycosides from the roots of *Mandevilla pentlandiana*. Phytochemistry 32: 1253-1259.

Chibber, S. S., and Sharma, R. P. 1979a. Derrugenin, a new isoflavone from *Derris robusta* seed shells. Phytochemistry 18: 1583-1584.

Chibber, S. S., and Sharma, R. P. 1979b. Robustigenin, a new isoflavone from *Derris robusta* seed shells. Phytochemistry 18: 1082.

Chibber, S. S., and Sharma, R. P. 1980. Derrone, a new pyranoisoflavone from *Derris robusta* seeds. Phytochemistry 19: 1857-1858.

Chibber, S. S., Sharma, R. P., and Dutt, S. K. 1979c. Rubone, a new chalcone from *Derris robusta* seed shells. Phytochemistry 18: 2056.

Chuanasa, T., Phromjai, J., Lipipun V., Likhitwitayawuid, K., Suzuki, M., Pramyothin, P., Hattori, M., and Shiraki, K. 2008. Anti-herpes simplex virus (HSV-1) activity of oxyresveratrol derived from Thai medicinal plant: Mechanism of action and therapeutic efficacy on cutaneous HSV-1 infection in mice. Antiviral Res. 80: 62-70.

Cragg, G. M. and Newman, D. J. 2005. Plants as a source of anti-cancer agents. J. Ethnopharmacol. 100: 72-79.

Crombie, L., Kilbee, G. W., and Whiting, D. A. 1975. Carbon-13 magnetic resonance spectra of natural rotenoids and their relatives. J. Chem. Soc. Perkin Trans. I 15: 1497-1499.

East, A. J., Ollis, W. D., and Wheeler, R. E. 1969. Natural occurrence of 3-aryl-4-hydroxycoumarins. Part I. Phytochemical examination of *Derris robusta* (roxb.) benth. J. Chem. Soc. C. 365-374.

Eklund, P., Langvik, O. K., Warna, J. P., Salmi, T. O., Willfor, S. M., and Sjoholm, R. E. 2005. Chemical studies on antioxidant mechanisms and free radical scavenging properties of lignans. Org. Biomol. Chem. 3: 3336-3347.

Evans, W. C. 2002. Trease and Evans. Pharmacognosy. Fifteenth edition. pp.26, 32. China: W. B. Saunders.

Faculty of Pharmaceutical Sciences, Mahidol University. 1995. Siam medicinal plants: national wisdom. pp. 56-57. Bangkok: Amarin Printing and Publishing.

Fang, N., and Casida, J. E. 1999. Cube resin insecticide: identification and biological activity of 29 rotenoid constituents. J. Agric. Food Chem. 47: 2130-2136.

Fukami, H., Sakata, G., and Nakajima, M. 1965. Total synthesis of (±)-elliptone. Agr. Biol. Chem. 29: 82.

Ghogomu-Tih, R., Bodo, B., Nyasse, B., and Sondengam, B. L. 1985. Isolation and identification of (-)-olivil and (+)-cycloolivil from *Stereospermum kunthianum*. Planta Med. 5: 464.

Gunaratnam, M., Greciano, O., Martins, C., Reszka, A. P., Schultes, C. M., Morjani, H., Riou, J-F., and Neidle, S. 2007. Mechanism of acridine-based telomerase inhibition and telomere shortening. Biochem. Pharmacol. 74: 679-689.

Hooker, J. D. 1882. Flora of British India. Vol. III pp. 630-631. United Kingdom: L. Reeve & Co.

Hyun, J-W., Shin, J-E., Lim, K-H., Sung, M-S., Park, J-W., Yu, J-H., Kim, B-K., Paik, W-H., Kang, S-S., and Park, J-G. 1995. Evomonoside: the cytotoxic cardiac glycoside from *Lepidium apetalum*. Planta Med. 61: 294-295.

Ito, C., Itoigawa, M., Kojima, N., Tan, H. T. –W., Takayasu, J., Tokuda, H., Nishino, H., and Furukawa, H. 2004. Cancer chemopreventive activity of rotenoids from *Derris trifoliata*. Planta Med. 70:8-11.

Khamlach, K., Dhal, R., and Brown, E. 1990. Lignans. 13. Total syntheses of (-)-carinol, (-)-carissanol and (-)-hydroxythujaplicatin methyl ether. Heterocycles 31: 2195-2199.

Khan, M. T. H., Ather, A., Thompson, K. D., and Gambari, R. 2005. Extracts and molecules from medicinal plants against herpes simplex viruses. Antiviral Res. 67: 107-119.

Koysomboon, S., Altena, I. V., Kato, S., and Chantrapromma, K. 2006. Antimycobacterial flavonoids from *Derris indica*. Phytochemistry 67: 1034-1040.

Laupattarakasem, P., Houghton, P. J., and Hoult, J. R. S. 2004. Anti-inflammatory isoflavonoids from the stems of *Derris scandens*. Planta Med. 70: 496-501.

Lee, H-Y., Oh, S-H., Woo, J. K., Kim, W-Y., Van Pelt, C. S., Price, R. E., Cody, D., Tran, H., Pezzuto, J. M., Moriarty, R. M., and Hong, W. K. 2005. Chemopreventive effects of deguelin, a novel akt inhibitor, on tobacco-induced lung tumorigenesis. J. Natl. Cancer Inst. 97: 1695-1699.

Likhitwitayawuid, K., Klongsiriwet, C., Jongbunprasert, V., Sritularak, B., and Wongseripipatana, S. 2006. Flavones with free radical scavenging activity from *Goniothalamus tenuifolius*. Arch. Pharm. Res. 29: 199-202.

Lin, Y-L., Chen, Y-L., and Kuo, Y-H. 1993. A novel 12-deoxorotenone, 12-deoxo-12α-actoxyelliptone, from the roots of *Derris oblonga*. J. Nat. Prod. 56: 1187-1189.

Lin, W-H., Fang, J-M., and Cheng, Y-S. 1999. Lignans from *Taiwania cryptomerioides*. Phytochemistry 50: 653-658.

Lipipun, V., Kurokawa, M., Suttisri, R., Taweechotipatr, P., Pramyothin, P., Hattori, M., and Shiraki, K. 2003. Efficacy of Thaimedicinal plant extracts against herpes simplex virus type 1 infection in vitro and in vivo. Antiviral Res. 60: 175–180.

Lu, H. Y., and Liang, J. Y. 2009a. Novel N-containing rotenoid and seco-rotenoid from the root of *Derris elliptica*. J. Asian Nat. Prod. Res. 11: 58-62.

Lu, H. Y., Liang, J. Y., Yu, P., and Chen, X-Y. 2009b. Rotenoids from the root of *Derris elliptica* (Roxb.) Benth. II. Chin. J. Nat. Med. 7: 24-27.

Lu, H. Y., Liang, J. Y., Yu, P., and Qu, W. 2008a. Isoflavones and their derivatives from the root of *Derris elliptica* (Roxb.) Benth. Chin. J. Nat. Med. 6: 265-267.

Lu, H. Y., Liang, J. Y., Yu, P., Qu, W., and Zhao, L. 2008b. Two new rotenoids from the root of *Derris elliptica*. Chin. Chem. Lett. 19: 1218-1220.

Luyengi, L. Lee, I-S., Mar, W., Fong, H. H. S., Pezzuto, J. M., and Kinghorn, A. D. 1994. Rotenoids and chalcones from *Mundulea sericea* that inhibit phorbol ester-induced ornithine decarboxylase activity. Phytochemistry 36: 1523-1526.

Maatooq, G. T., Stumpf, D. K., Hoffmann, J. J., Hutter, L. K., and Timmermann, B. N. 1996. Antifungal eudesmanoids from *Parthenium argentatum* x *P. tomentosa*. Phytochemistry 41: 519-524.

Mahabusarakam, W., Deachathai, S., Phongpaichit, S., Jansakul, C., and Taylor, W. C. 2004. A benzyl and isoflavone derivatives from *Derris scandens* Benth. Phytochemistry 65: 1185-1191.

Mahidol, C., Prawat, H., Ruchirawat, S., Likhitwitayawuid, K., Lin, L-Z., and Cordell, G. A. 1997. Prenylated flavanones from *Derris reticulata*. Phytochemistry 45: 825-829.

Nascimento, M. C., and Mors, W. B. 1981. Flavonoids of *Derris araripensis*. Phytochemistry 20: 147-152.

Nedi, T., Mekonnen, N., and Urga, K. 2004. Diuretic effect of the crude extracts of *Carissa edulis* in rats. J. Ethnopharmacol. 95: 57-61.

Ohashi, K., Watanabe, H., Okumura, Y., Uji, T., and Kitagawa, I. 1994. Indonesian medicinal plants. XII. Four isomeric lignan-glucosides from the bark of *Aegle marmelos* (Rutaceae). Chem. Pharm. Bull. 42: 1924-1926.

Padua, L. S., Bunyapraphatsara, N., and Lemmens, R. H. M. J. 1999. Plant resourses of South-East Asia. No. 12(1) pp. 241. Indonesia: Prosea foundation.

Pakrashi, S. C., Datta, S., Ghosh-Dastidar, P. P. 1968. Indian medical plants-XVII. Phytochemical examination of *Carissa* spp. Phytochemistry 7: 495-496.

Pal, R., Kulshreshtha, D. K., and Rastogi, R. P. 1975. A new lignan from *Carissa carandas*. Phytochemistry 14: 2302-2303.

Pietta, P-G. 2000. Flavonoids as antioxidants. J. Nat. Prod. 63: 1035-1042.

Rao, M. N., Krupadanam, G. L. D., and Srimannarayana, G. 1994. Four isoflavones and two 3-aryl coumarins from stems of *Derris scandens*. Phytochemistry 37: 267-269.

Rao, R. J., Kumar, U. S., Reddy, S. V., Tiwari, A. K., and Rao, J. M. 2005. Antioxidants and a new germacrane sesquiteroene from *Carissa spinarum*. Nat. Prod. Res. 19: 763-769.

Rao, R. R., Tiwari, A. K., Reddy, P. P., Babu, K. S., Ali, A. Z., Madhusudana, K., and Rao, J. M. 2009. New furanoflavonoids, intestinal α-glucosidase inhibitory and free-radical (DPPH) scavenging, activity from antihyperglycemic root extract of *Derris indica* (Lam.). Bioorg. Med. Chem. 17: 5170-5175.

Rao, S. A., Srinivas, P. V., Tiwari, A. K., Vanka, U. M. S., Rao, R. V. S., Dasari, K. R., and Rao, M. J. 2007. Isolation, characterization and chemobiological quantification of α-glucosidase enzyme inhibitory and free radical scavenging constituents from *Derris scandens* Benth. J. Chromatogr. B 855: 166-172.

Rukachaisirikul, V., Sukpondma, Y., Jansakul, C., and Taylor, W. C. 2002. Isoflavone glycosides from *Derris scandens*. Phytochemistry 60: 827-834.

Sae-Yin, A., Ovatlarnpron, C., Itharat, A., and Wiwattanapatapee, R. 2006. Extraction of rotenone from *Derris elliptica* and *Derris malaccensis* by pressurized liquid extraction compared with maceration. J. Chromatography A. 1125: 172-176.

Sakakibara, J., Ina, H., and Yasue, M. 1974. Studies on the constituents of *Tripetaleia paniculata* Sieb. Et Zucc. IV. On the constituents of the wood. Structure of lyoniside. Yakugaku Zasshi 94: 1377-1383.

Sekine, T., Inagaki, M., Ikegami, F., Fujii, Y., and Ruangrungsi, N. 1999. Six diprenylisoflavones, derrisisoflavones A-F, from *Derris scandens*. Phytochemistry 52: 87-94.

Shiu, W. K. P., and Gibbons, S. 2006. Anti-staphylococcal acylphloroglucinols from *Hypericum beanie*. Phytochemistry 67: 2568-2572.

Siddiqui, B. S., Ghani, U., Ali, S. T., Usmani, S. B., and Begum, S. 2002. Triterpenoidal constituents of the leaves of *Carissa carandas*. Nat. Prod. Res. 17: 153-158.

Singh, B., and Rastogi, R. P. 1972. The structure of carindone. Phytochemistry 11: 1797-1801.

Siripaisarnpipat, S., Kongjinda, V., and Techasakul, S. 2007. Crystal structure of new prenylated chalcone from *Derris malaccensis*. Anal. Sci. 23: x33-x34.

Smitinand, T. 2001. Thai plant names (botanical names-vernacular names) revised edition. pp. 359-360. Bangkok: The Forest Herbarium, Royal Forest Department.

Takashima, J., Chiba, N., Yoneda, K., and Ohsaki, A. 2002. Derrisin, a new rotenoid from *Derris malaccensis* Plain and anti-*Helicobacter pylori* activity of its related constituents. J. Nat. Prod. 65: 611-613.

Takeda, Y., Yano, K., Ayabe, H., Masuda, T., Otsuka, H., Sueyoshi, E., Shinzato, T., and Aramoto, M. 2008. Glycosidic constituents of the leaves of an Okinawan Leguminosae plant, *Derris trifoliata* Lour. J. Nat. Med. 62: 476-478.

Taylor, R. S. L., Hudson, J. B., Manandhar, N. P., and Towers, G. H. N. 1996. Antiviral activities of medicinal plants of southern Nepal. J. Ethnopharmacol. 53: 97-104.

Tewtrakul, S., Cheenpracha, S., and Karalai, C. 2009. Nitric oxide inhibitory principles from *Derris trifoliata* stems. Phytomedicine 16: 568-572.

Thasana, N., Chuankamnerdkarn, M., and Ruchirawat, S. 2001. A new 12a-hydroxyelliptone from the stems of *Derris malaccensis*. Heterocycles 55: 1121-1125.

Tolo, F. M., Rukunga, G. M., Muli, F. W., Njagi, E. N. M., Njue, W., Kumon, K., Mungai, G. M., Muthaura, C. N., Muli, J. M., Keter, L. K., Oishi, E., and Kofi-Tsekpo, M. W. 2006. Anti-viral activity of the extracts of a Kenyan medicinal plant *Carissa edulis* against herpes simplex virus. J. Ethnopharmacol. 104: 92-99.

Valko, M., Rhodes, C. J., Moncol, J., Izakovic, M., and Mazur, M. 2006. Free radicals, metals and antioxidants in oxidative stress-induced cancer. Chem.-Biol. Interact. 160: 1-40.

Vasconcelos, J. M. J., Silva, A. M. S., and Cavaleiro, J. A. S. 1998. Chromones and flavanones from *Artemisia campestris* subsp. *maritima*. Phytochemistry 49: 1421-1424.

Welter, A., and Jadot, J. 1976. 2,5-Dihydroxymethyl 3,4-dihydroxypyrrolidine dans les feuilles de *Derris elliptica*. Phytochemistry 15 :747-749.

Xie, L-H., Akao, T., Hamasaki, K., Deyama, T., and Hattori, M. 2003. Biotransformation of pinoresinol diglucoside to mammalian lignans by human intestinal microflora, and isolation of *Enterococcus faecalis* strain PDG-1 responsible for the transformation of (+)-pinoresinol to (+)-lariciresinol. Chem. Pharm. Bull. 51: 508-515.

Xu, L. -R., Zhou, P., Zhi, Y. -E., Wu, J., and Zhang, S. 2009. Three new flavonol triglycosides from *Derris trifoliata*. J. Asian Nat. Prod. Res. 11: 79-84.

Yamauchi, T., Abe, F., and Wan, A. S. C. 1987. Cardenolide monoglycosides from the leaves of *Cerbera odollam* and *Cerbera manghas* (*Cerbera*. III). Chem. Pharm. Bull. 35: 2744-2749.

Yang, Y-L., Chang, F-R., and Wu, Y-C. 2005. Squadinorlignoside : A novel 7,9′-dinorlignan from the stems of *Annona squanosa*. Helv. Chim. Acta 88: 2731-2737.

Yenesew, A., Kiplagat, J. T., Derese, S., Midiwo, J. O., Kabaru, J. M., Heydenreich, M., and Peter, M. G. 2006. Two unusual rotenoid derivatives, 7a-*O*-methyl-12a-hydroxydeguelol and spiro-13-homo-13-oxoelliptone, from the seeds of *Derris trifoliata*. Phytochemistry 67: 988-991.

Yenesew, A., Midiwo, J. O., and Waterman, P. G. 1998. Rotenoids, isoflavones and chalcones from the stem bark of *Millettia usaramensis* subspecies *usaramensis*. Phytochemistry 47: 295-300.

Yenesew, A., Mushibe, E. K., Induli, M., Derese, S., Midiwo, J. O., Kabaru, J. M., Heydenreich, M., Koch, A., and Peter, M. G. 2005. 7a-*O*-methyldeguelol, a modified rotenoid with an open ring-C, from the roots of *Derris trifoliata*. Phytochemistry 66: 653-657.

Yeo, H., Chin, Y-W., Park, S-Y., and Kim, J. 2004. Lignans of *Rosa multiflora* roots. Arch. Pharm. Res. 27: 287-290.

Zeng, X-N., Coll, J., Zhang, S-X., Liu, X-G., and Camps, F. 2002. Modification of the analytical method for rotenoids in plants. Sepu 20: 144-147.

APPENDIX

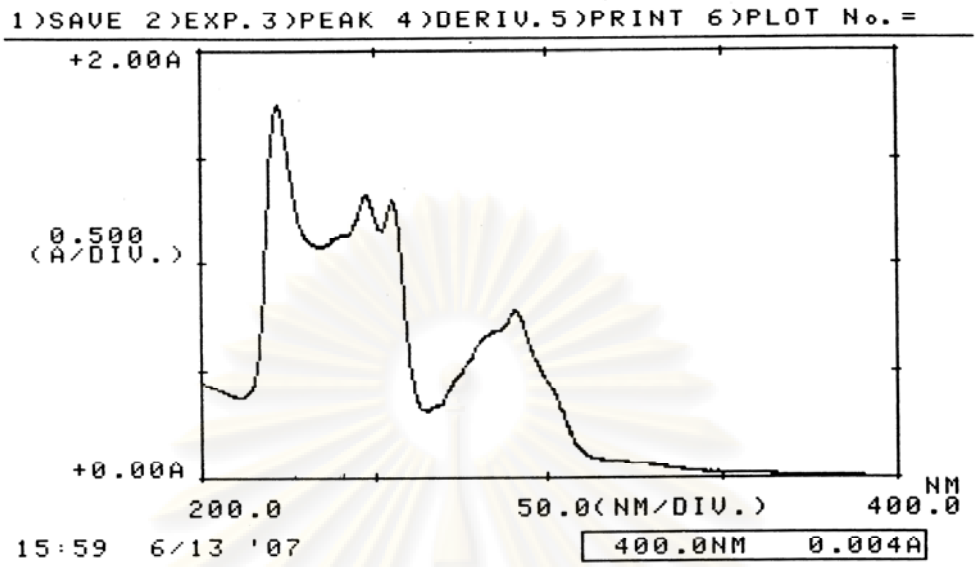

Figure 7 UV spectrum of compound DM1 (methanol)

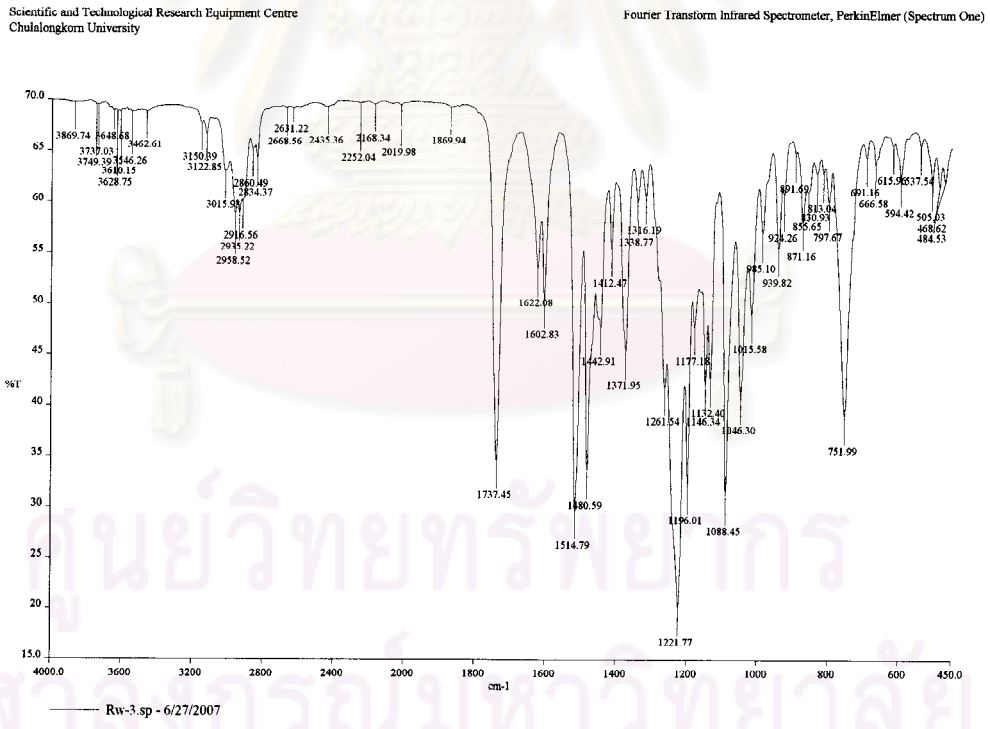

Figure 8 IR spectrum of compound DM1 (KBr disc)

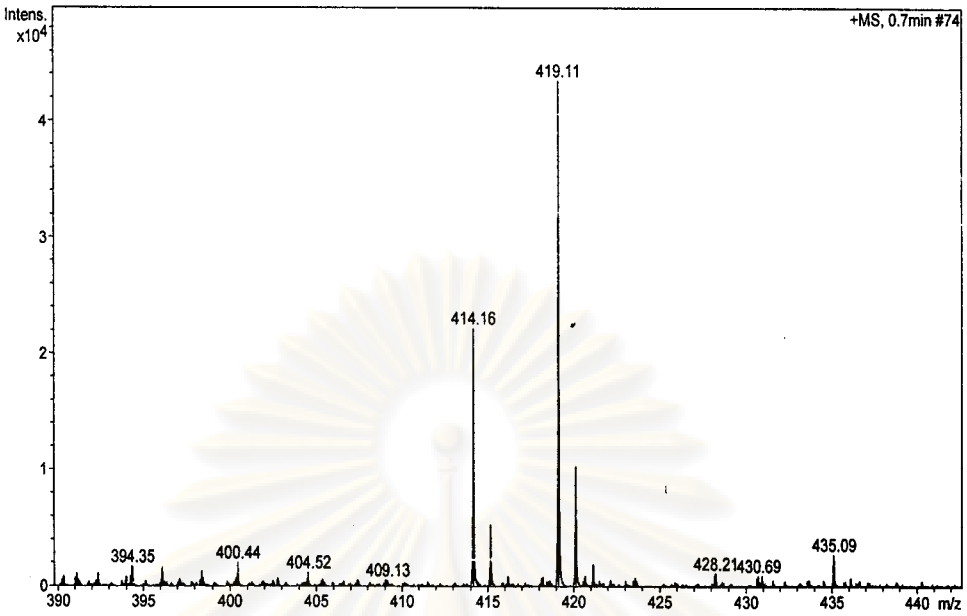

Figure 9 ESI mass spectrum of compound DM1

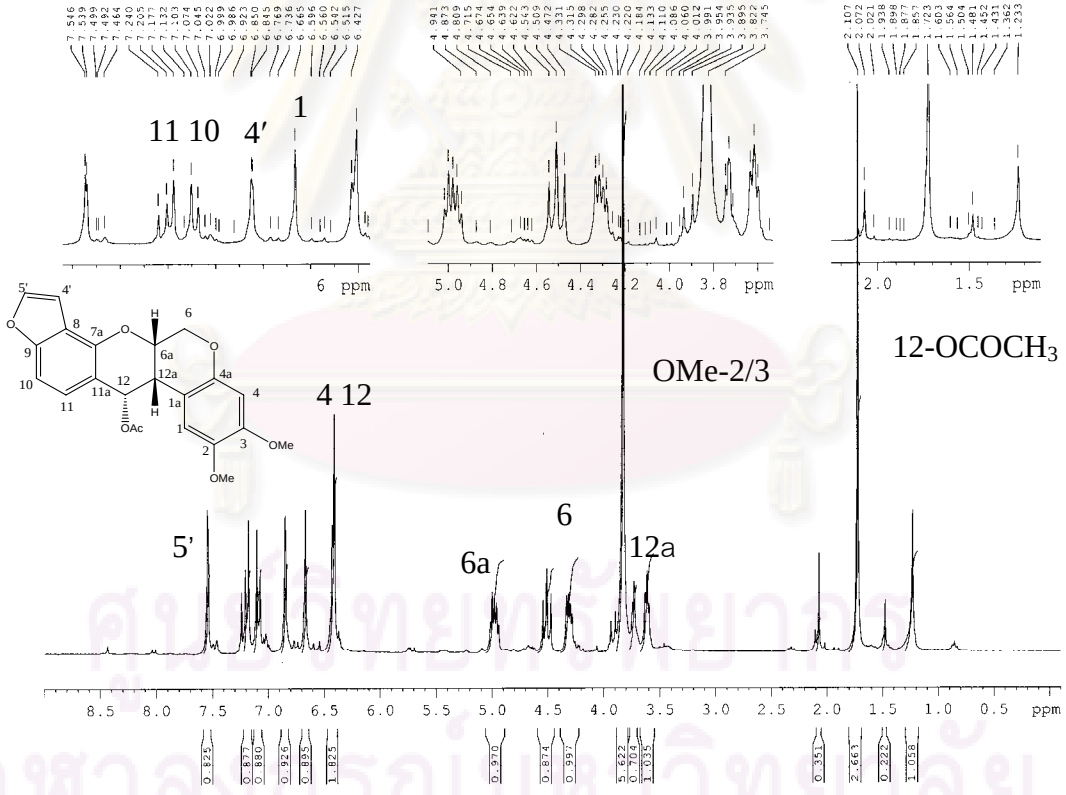

Figure 10 ^{1}H-NMR (300 MHz) spectrum of compound DM1 ($CDCl_3$)

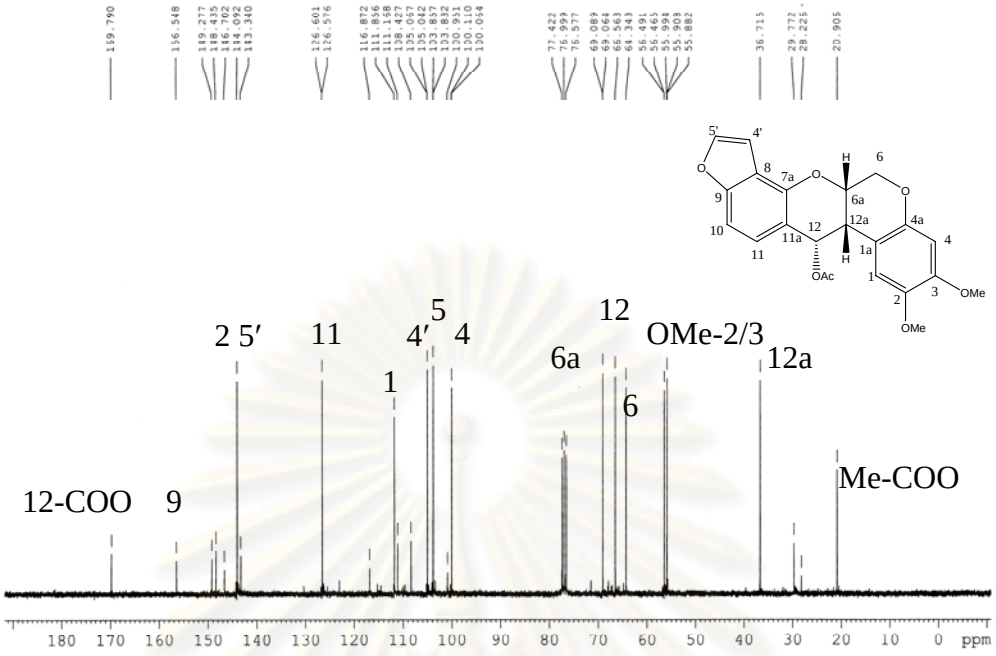

Figure 11 ^{13}C-NMR (75 MHz) spectrum of compound DM1 ($CDCl_3$)

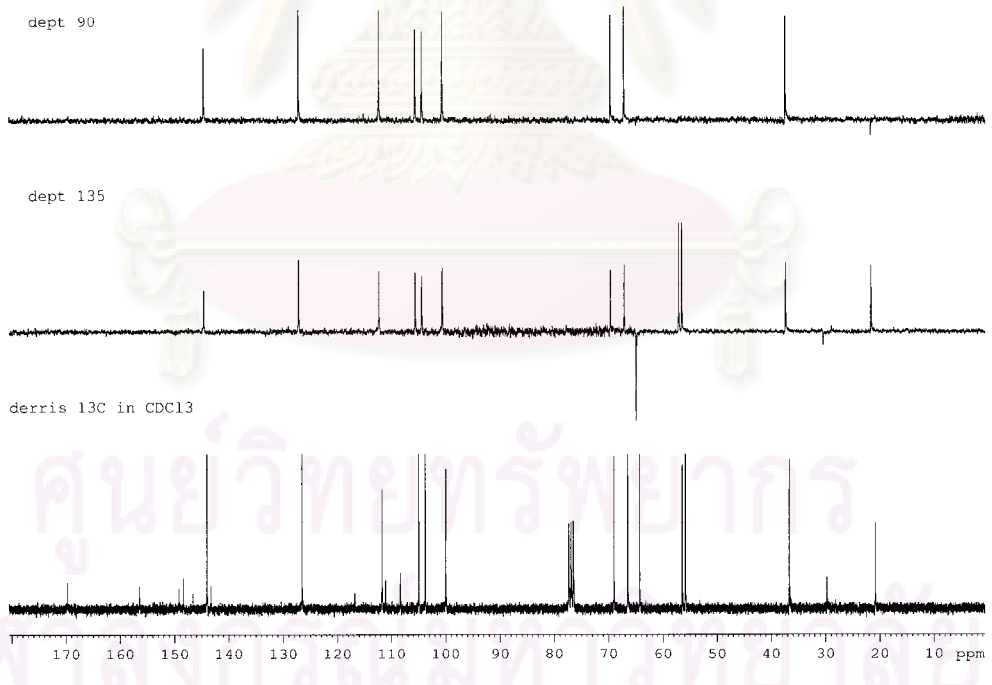

Figure 12 ^{13}C-NMR (75 MHz) and DEPT spectra of compound DM1 ($CDCl_3$)

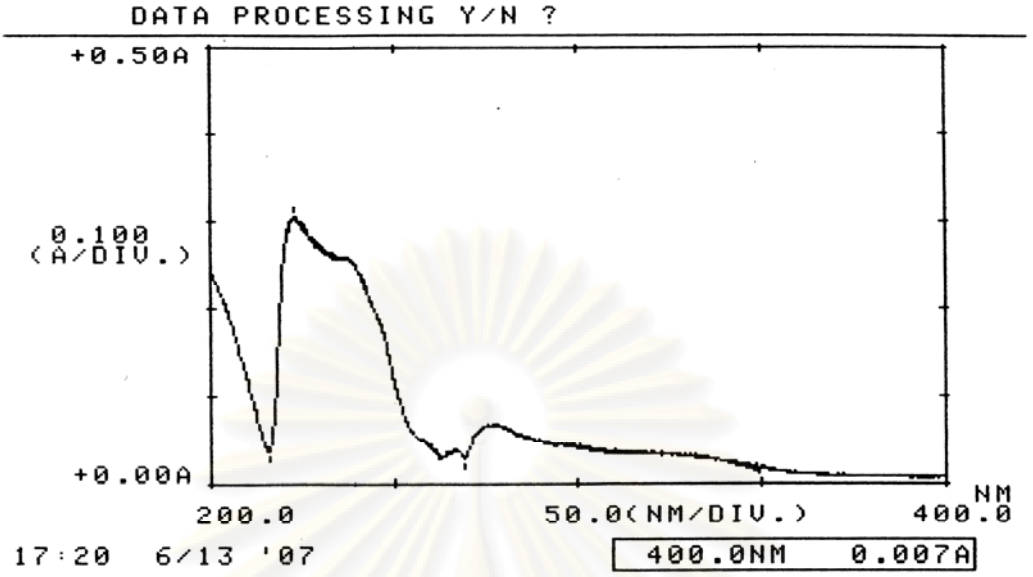

Figure 13 UV spectrum of compound DM2 (methanol)

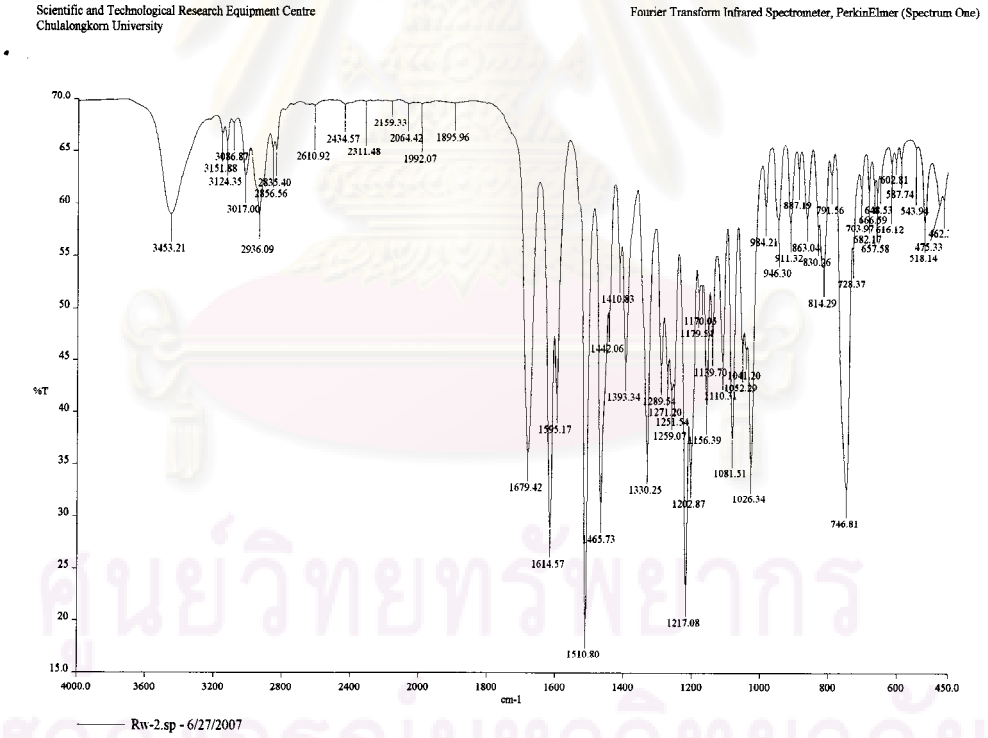

Figure 14 IR spectrum of compound DM2 (KBr disc)

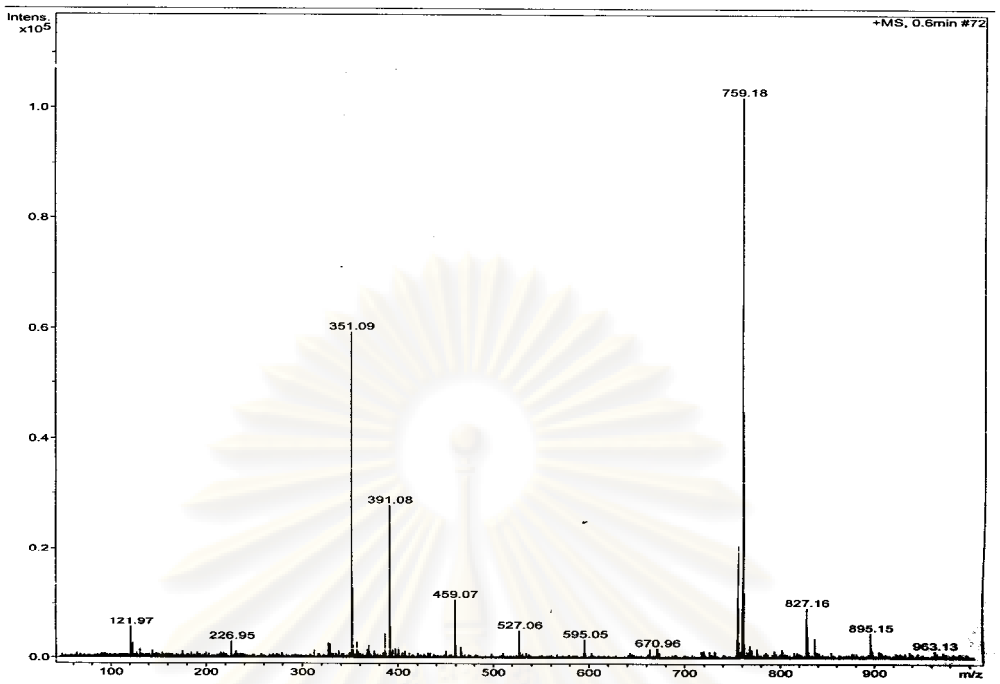

Figure 15 ESI mass spectrum of compound DM2

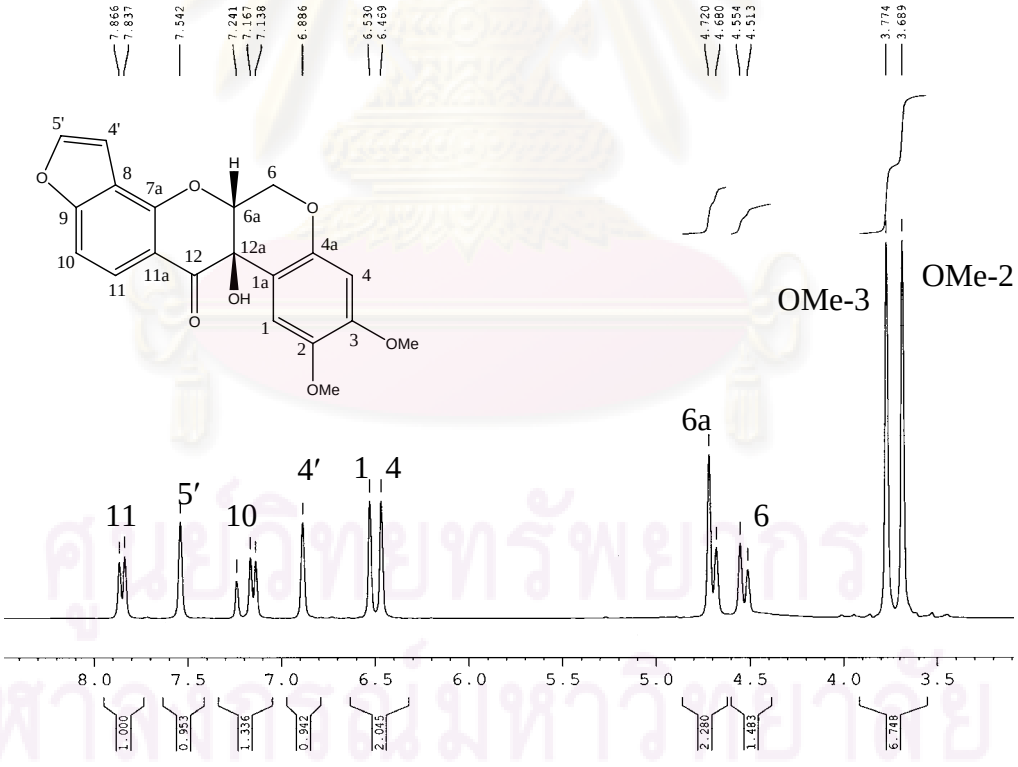

Figure 16 ^{1}H-NMR (300 MHz) spectrum of compound DM2 ($CDCl_3$)

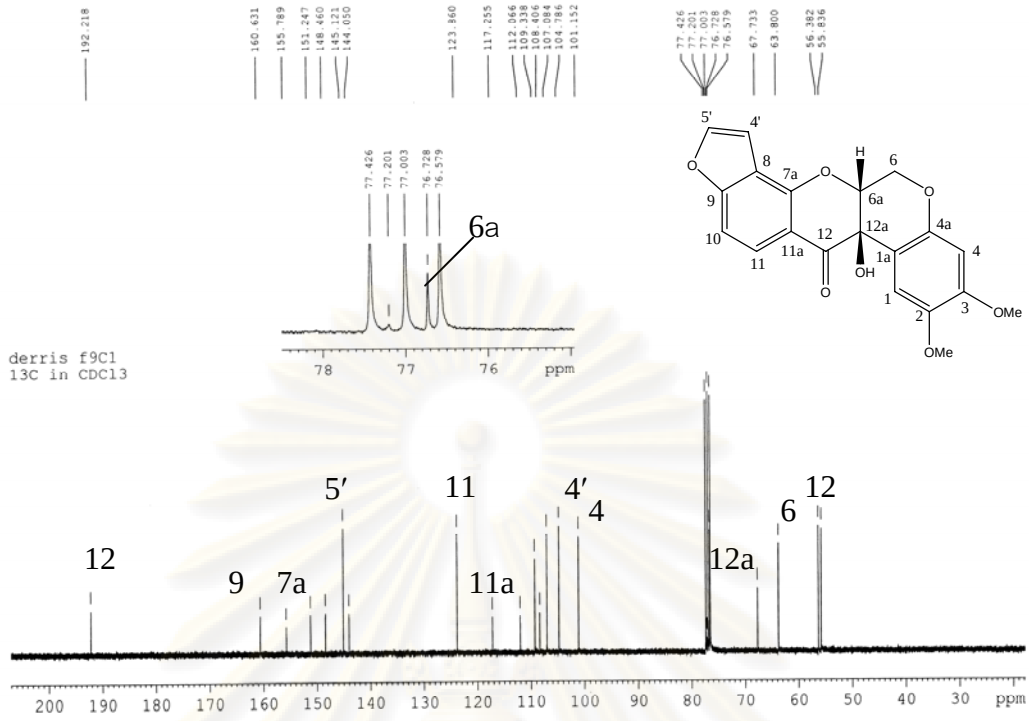

Figure 17 ^{13}C-NMR (75 MHz) spectrum of compound DM2 ($CDCl_3$)

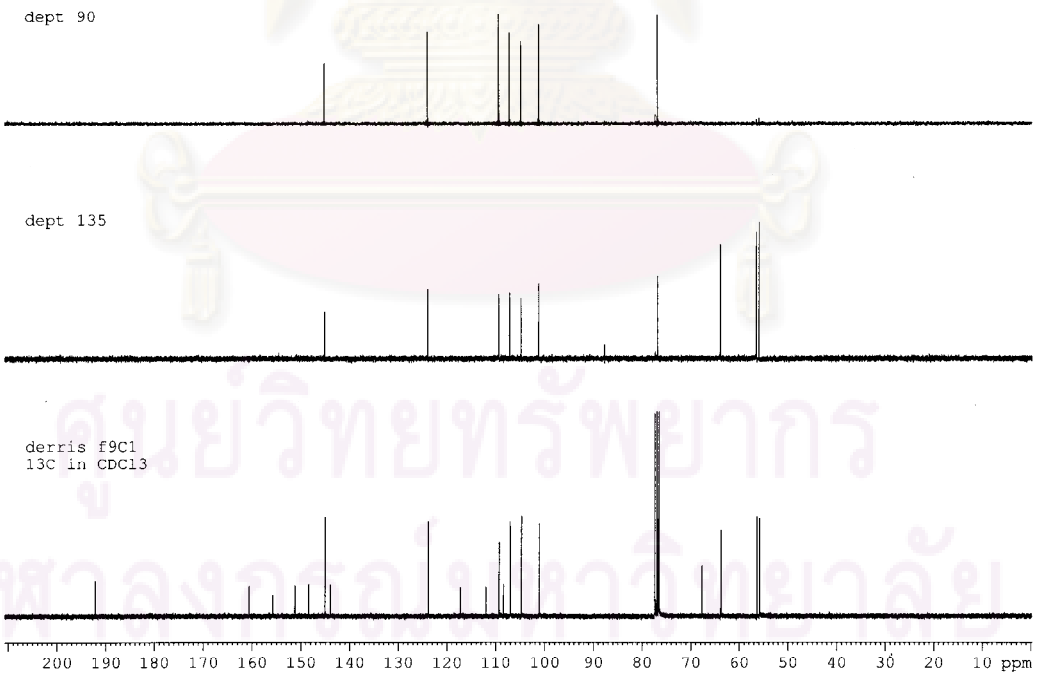

Figure 18 ^{13}C-NMR (75 MHz) and DEPT spectra of compound DM2 ($CDCl_3$)

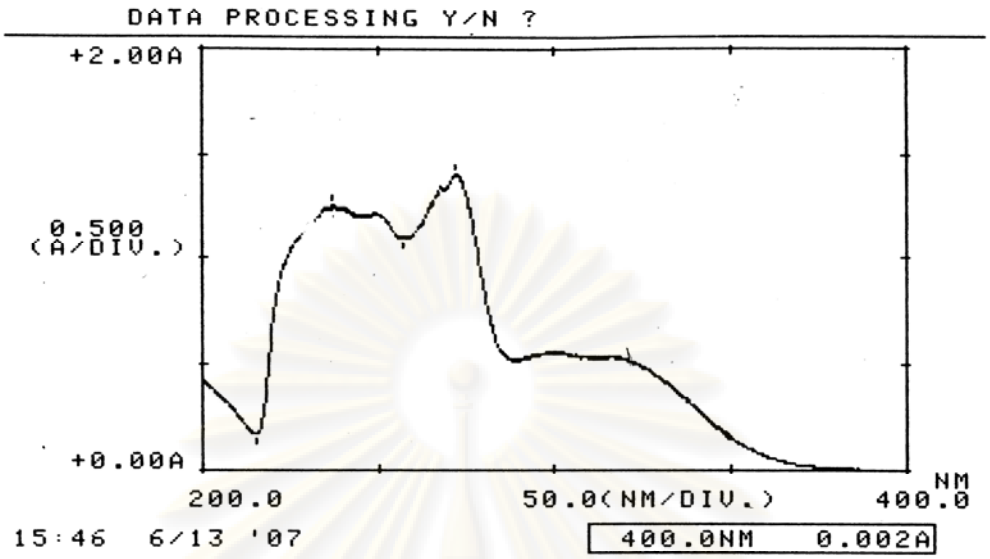

Figure 19 UV spectrum of compound DM3 (methanol)

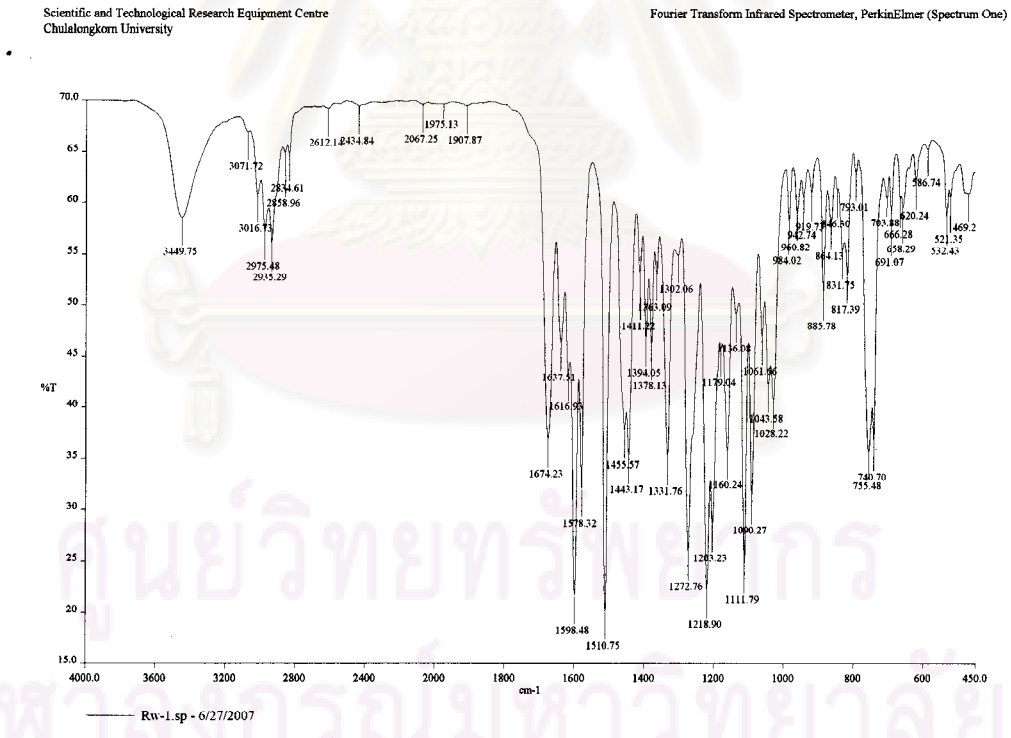

Figure 20 IR spectrum of compound DM3 (KBr disc)

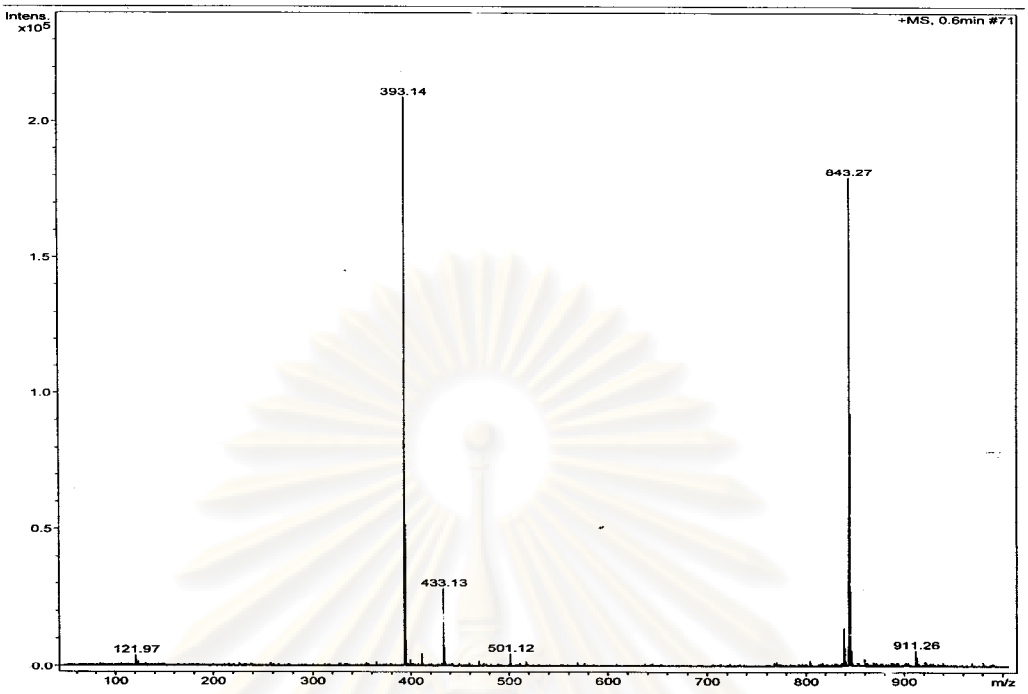

Figure 21 ESI mass spectrum of compound DM3

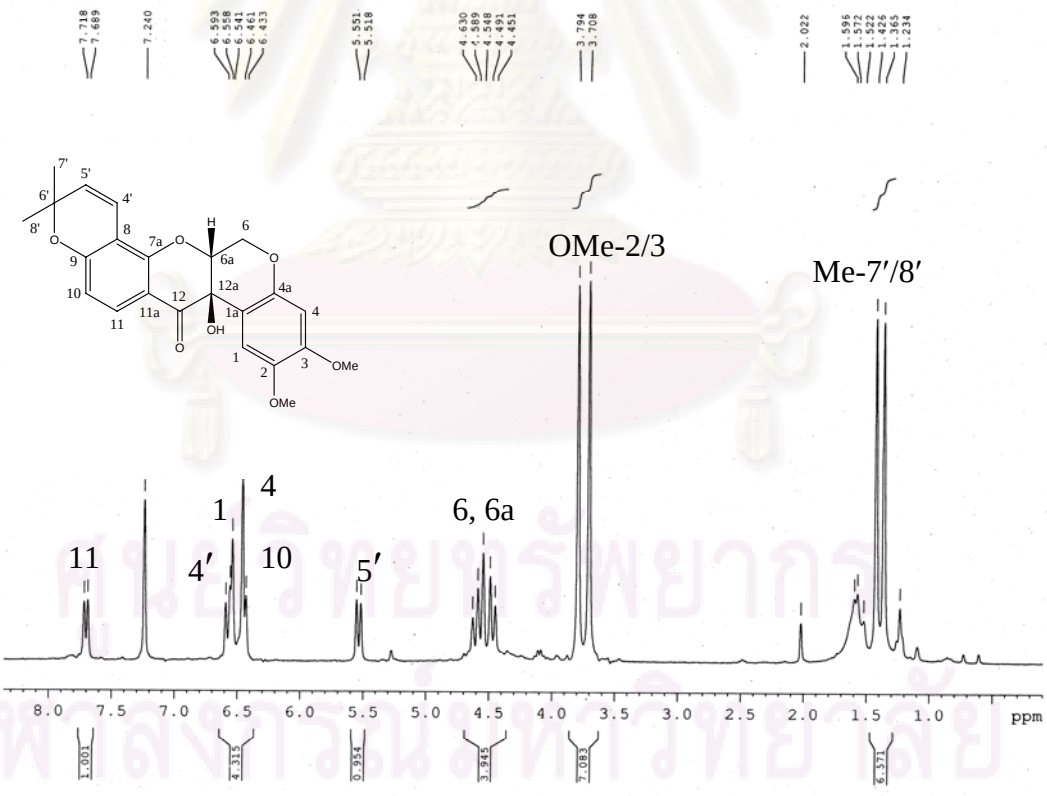

Figure 22 ^{1}H-NMR (300 MHz) spectrum of compound DM3 ($CDCl_3$)

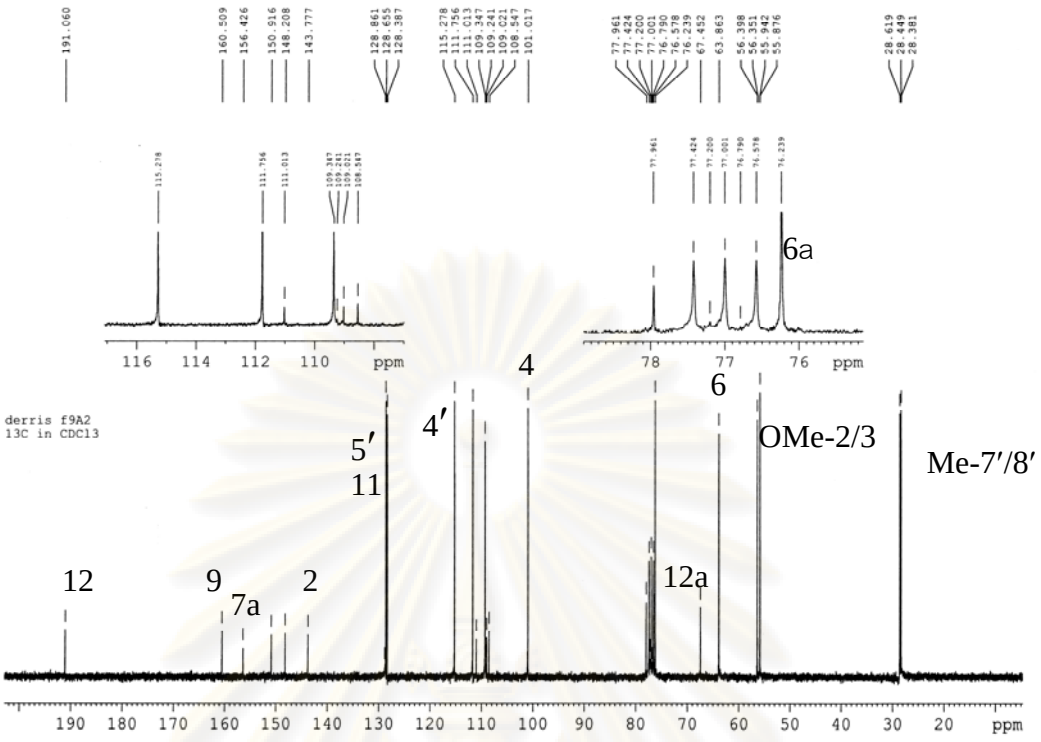

Figure 23 ^{13}C-NMR (75 MHz) spectrum of compound DM3 ($CDCl_3$)

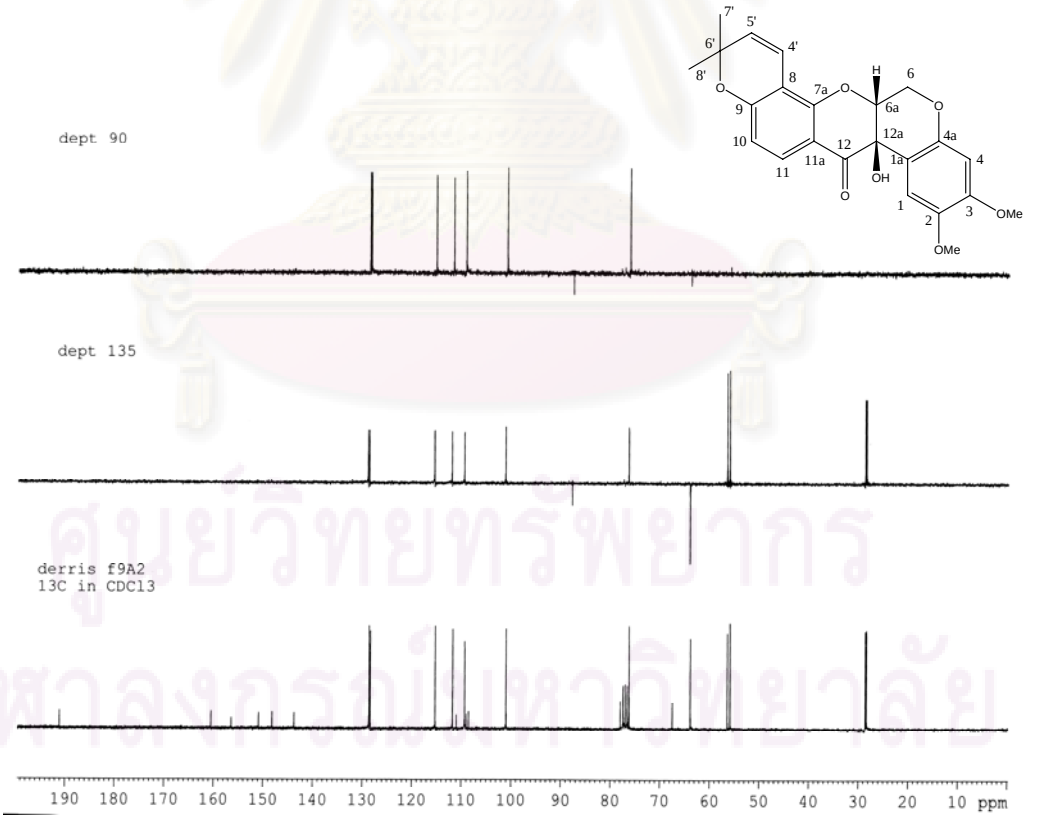

Figure 24 ^{13}C-NMR (75 MHz) and DEPT spectra of compound DM3 ($CDCl_3$)

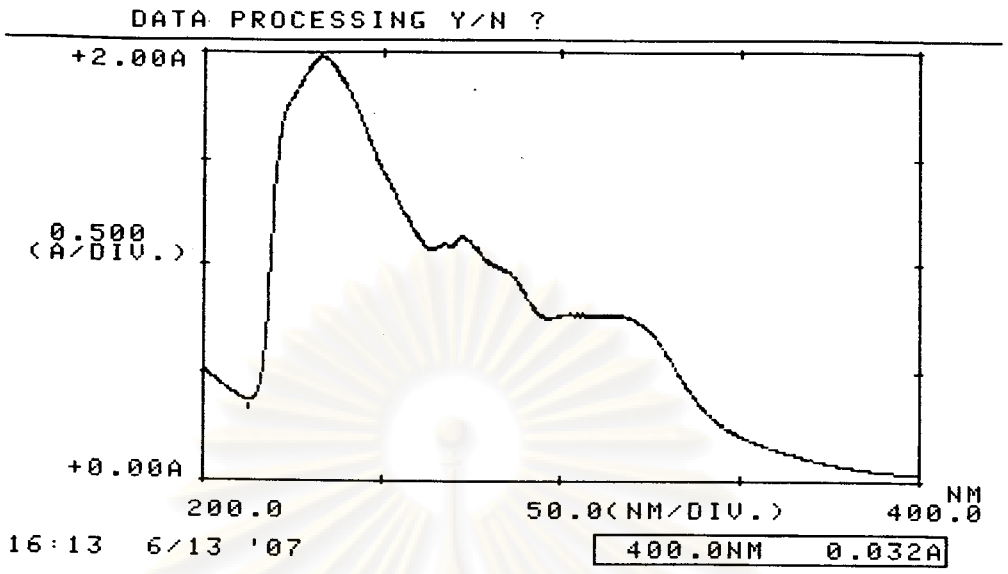

Figure 25 UV spectrum of compound DM4 (methanol)

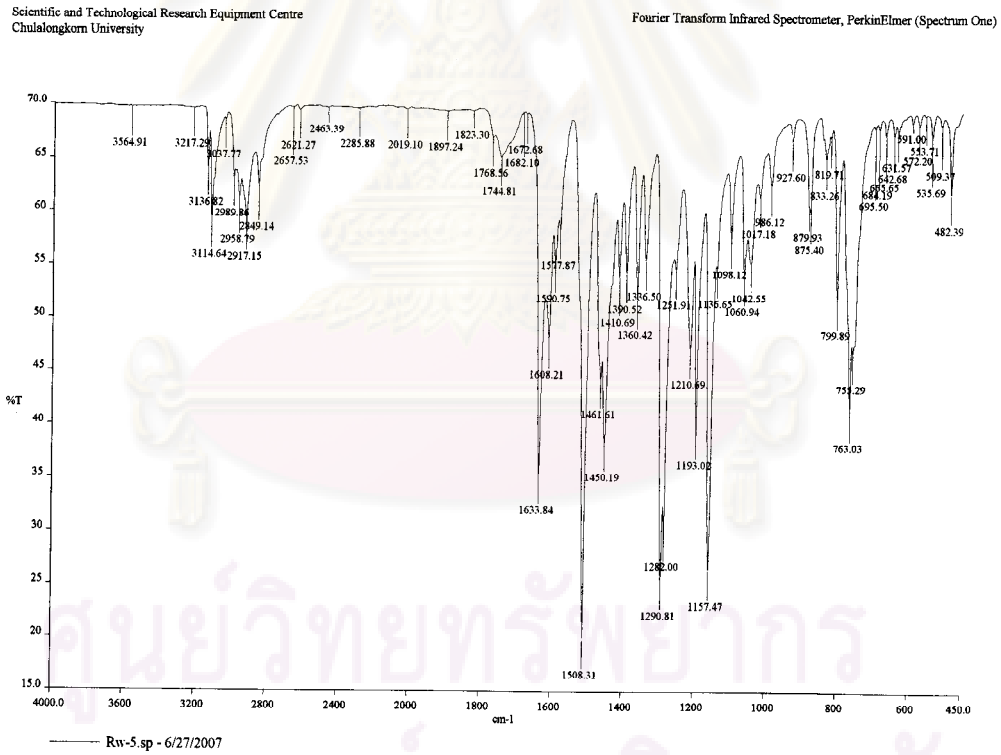

Figure 26 IR spectrum of compound DM4 (KBr disc)

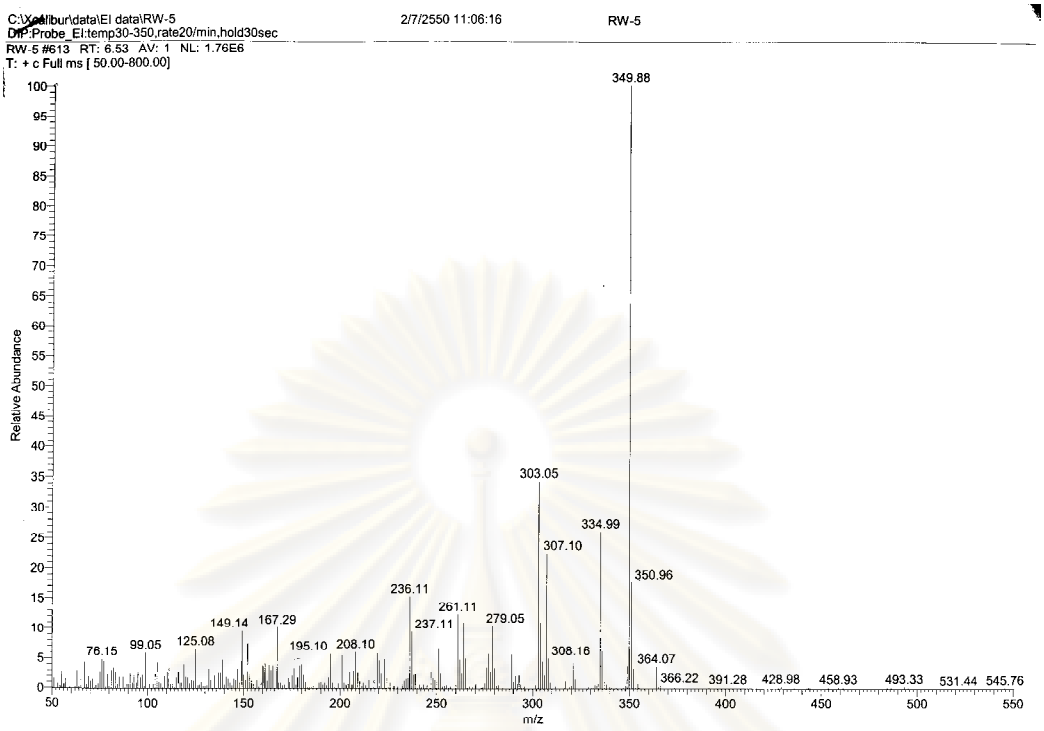

Figure 27 EI mass spectrum of compound DM4

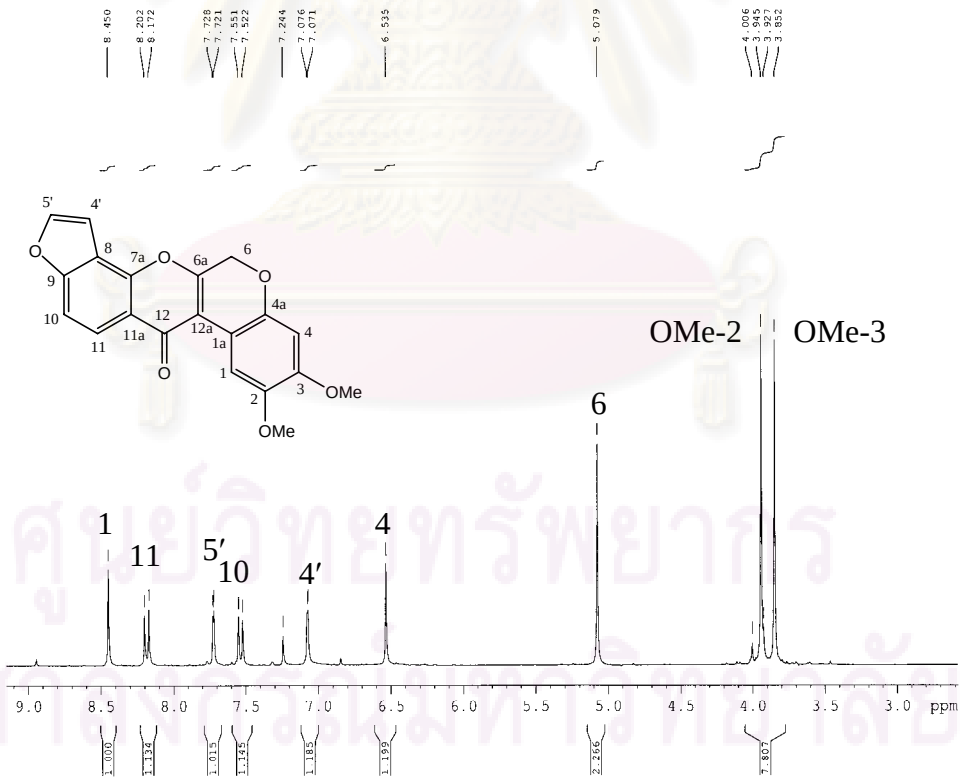

Figure 28 ^{1}H-NMR (300 MHz) spectrum of compound DM4 ($CDCl_3$)

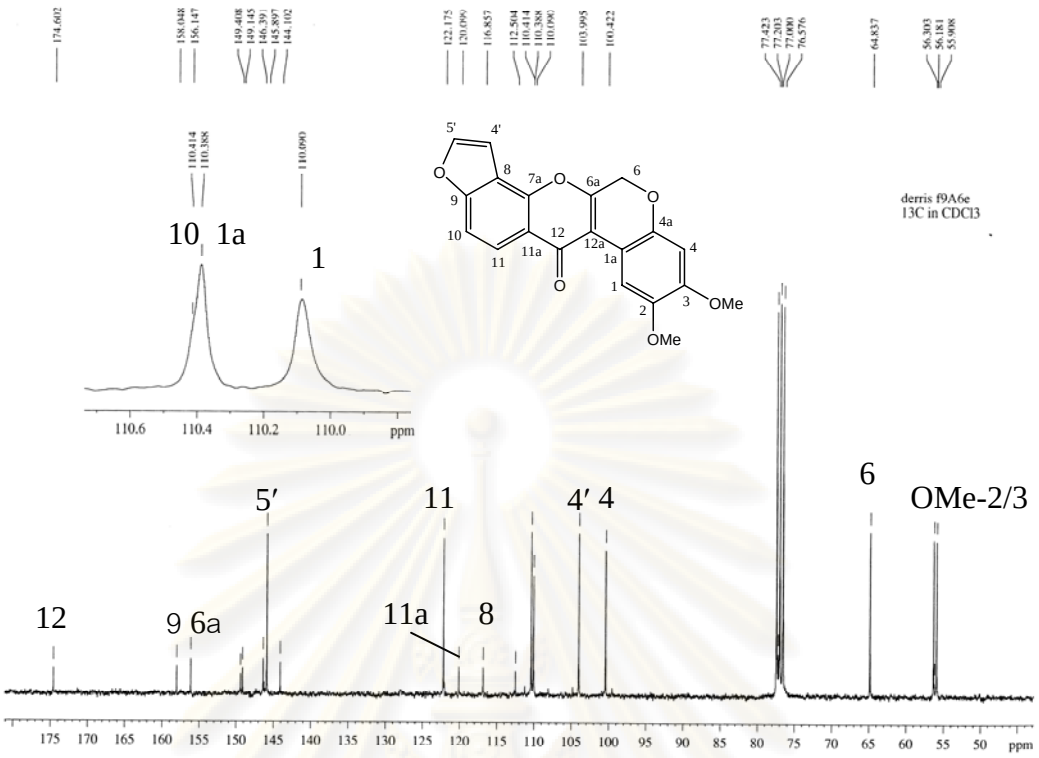

Figure 29 ^{13}C-NMR (75 MHz) spectrum of compound DM4 ($CDCl_3$)

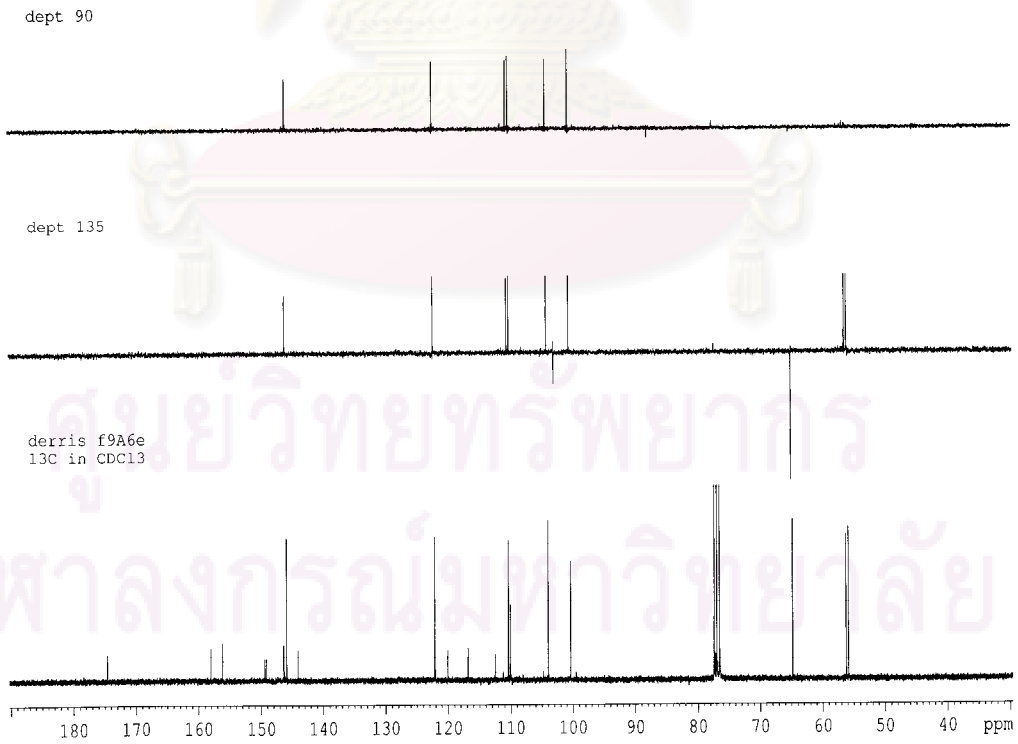

Figure 30 ^{13}C-NMR (75 MHz) and DEPT spectra of compound DM4 ($CDCl_3$)

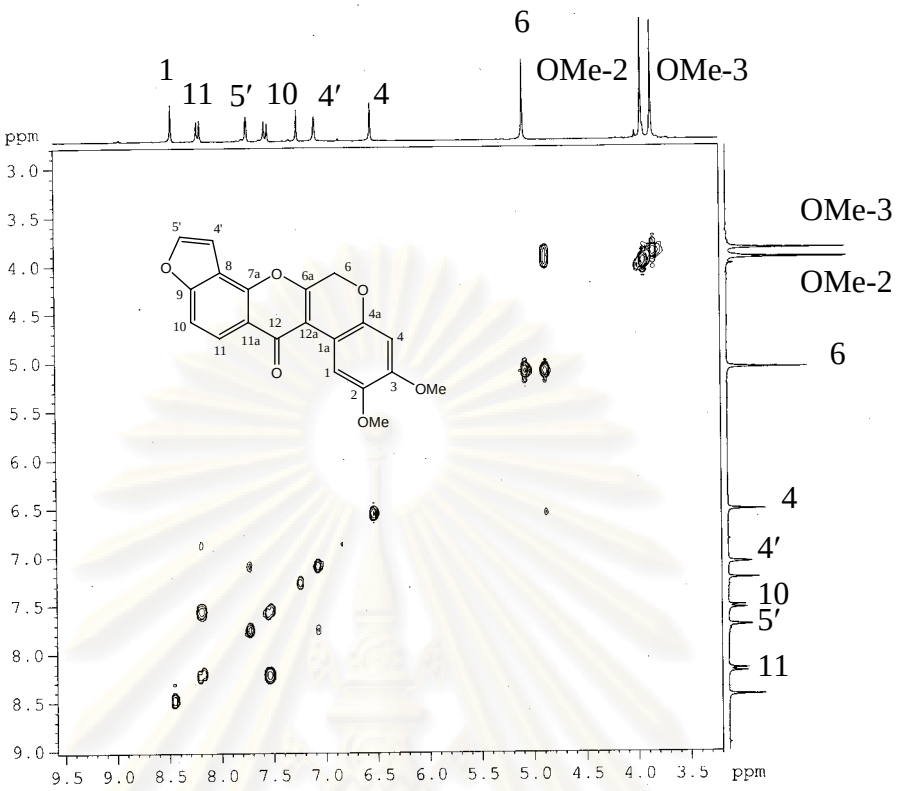

Figure 31 ^{1}H-^{1}H COSY spectrum of compound DM4 ($CDCl_3$)

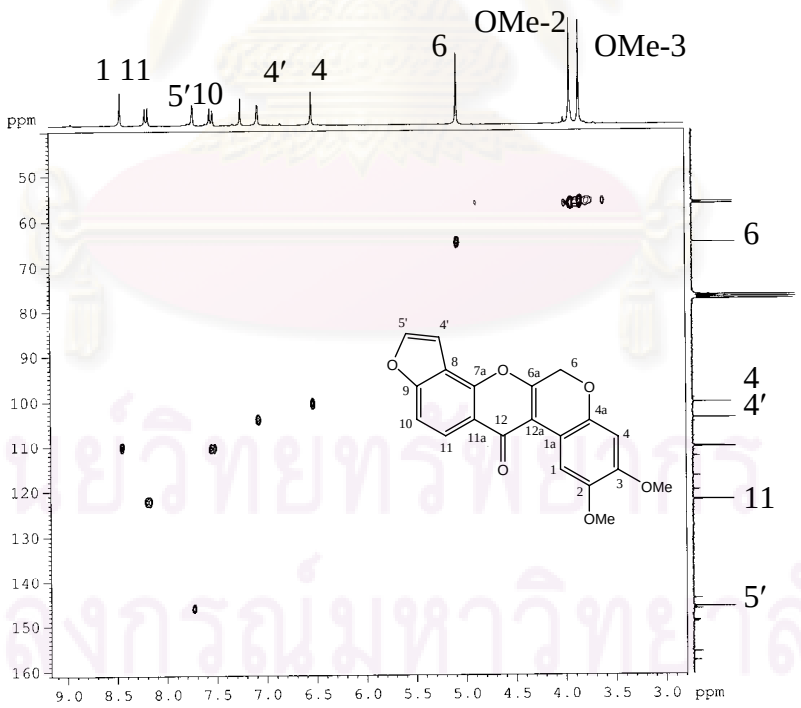

Figure 32 HMQC spectrum of compound DM4 ($CDCl_3$)

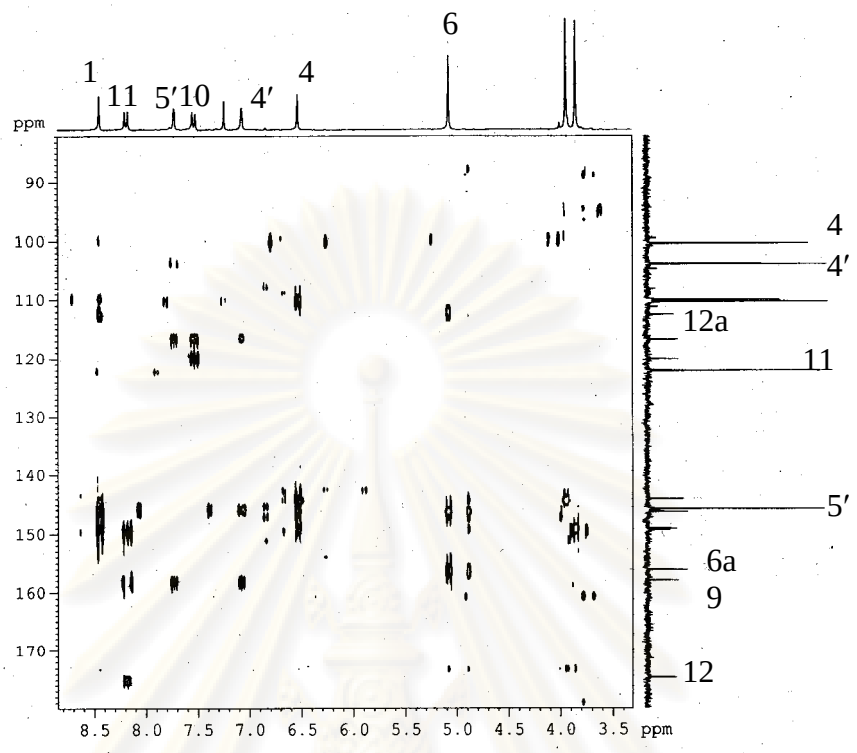

Figure 33 HMBC spectrum of compound DM4 ($CDCl_3$)
[δ_H 3.3-8.8 ppm, δ_C 82-180 ppm]

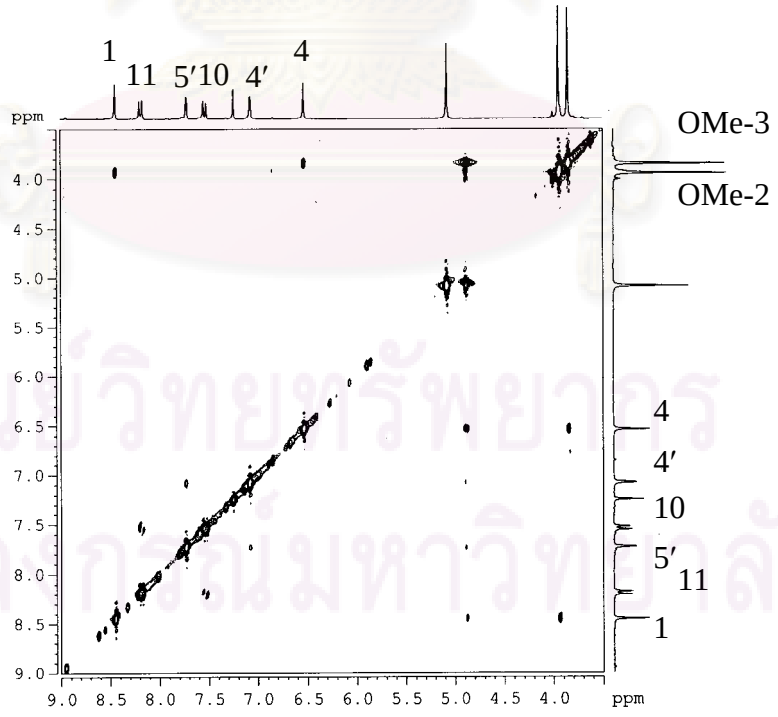

Figure 34 NOESY spectrum of compound DM4 ($CDCl_3$)

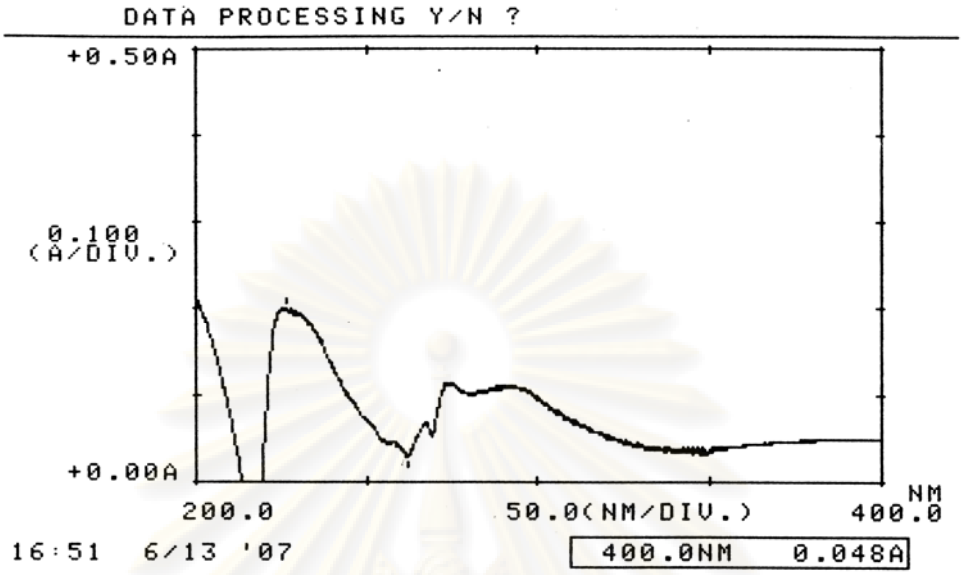

Figure 35 UV spectrum of compound DM5 (methanol)

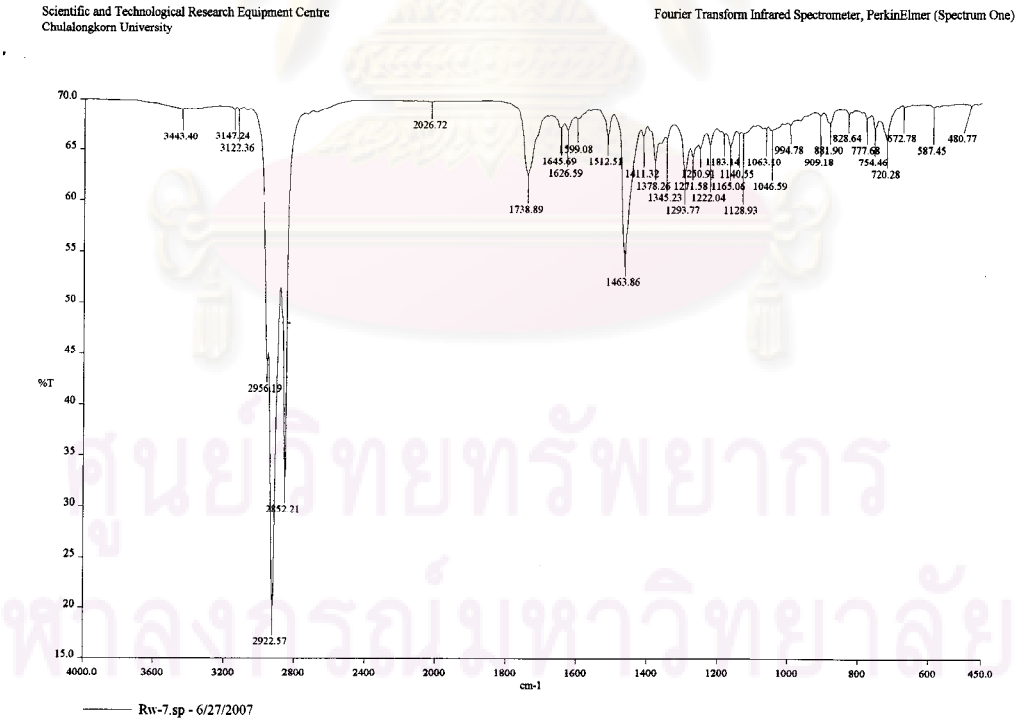

Figure 36 IR spectrum of compound DM5 (KBr disc)

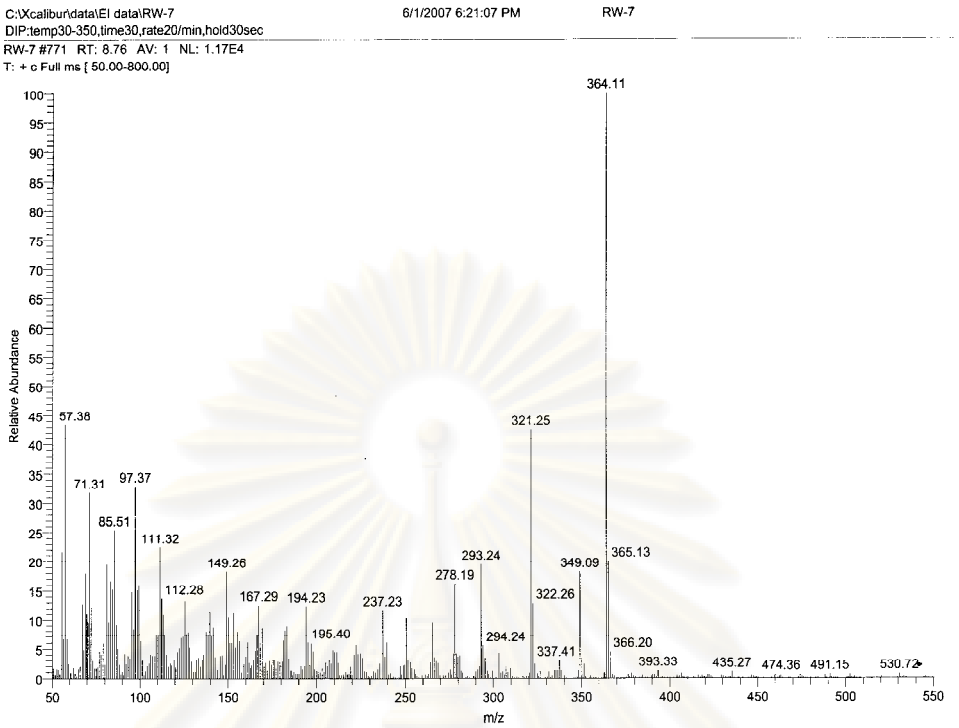

Figure 37 EI mass spectrum of compound DM5

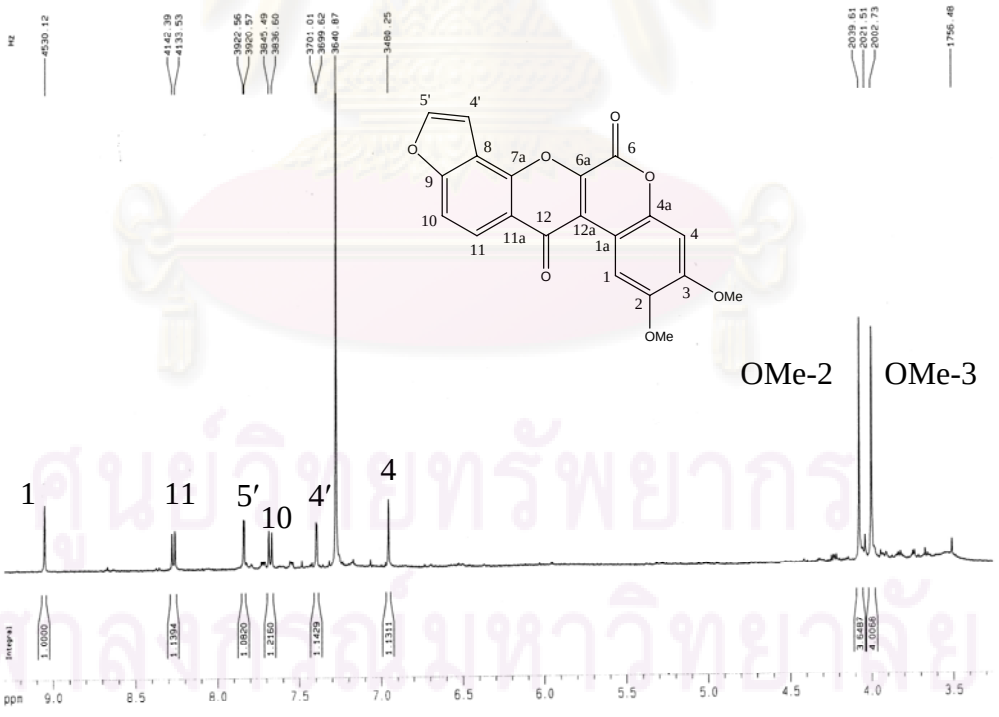

Figure 38 ^{1}H-NMR (500 MHz) spectrum of compound DM5 ($CDCl_3$)

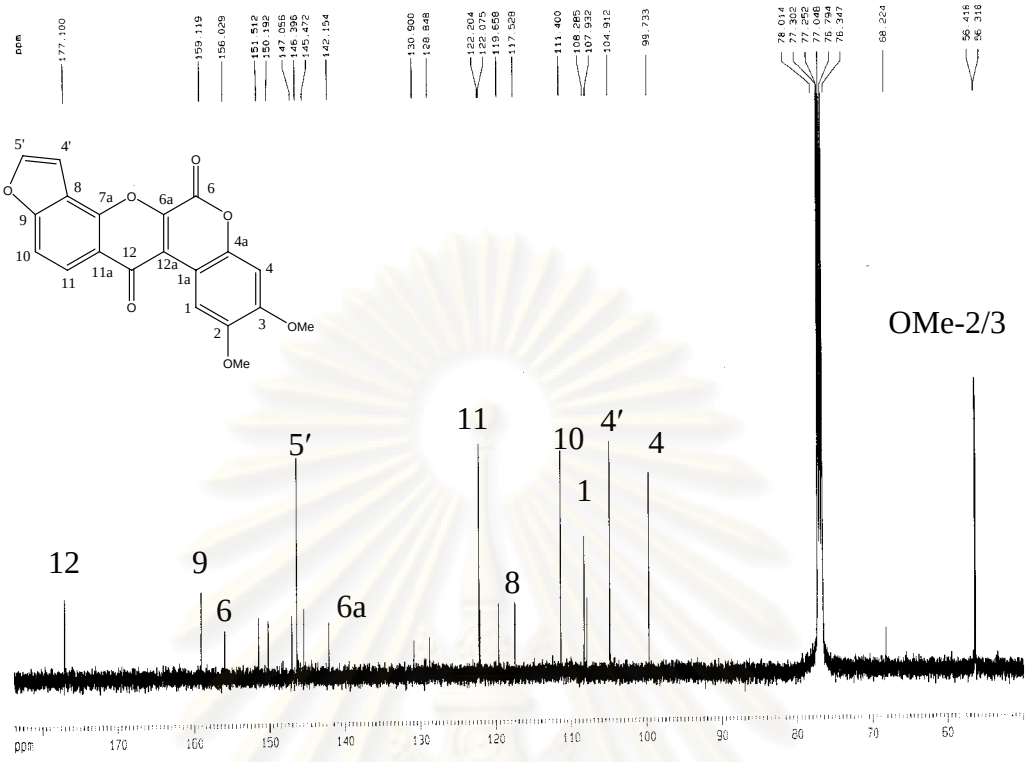

Figure 39 ^{13}C-NMR (125 MHz) spectrum of compound DM5 ($CDCl_3$)

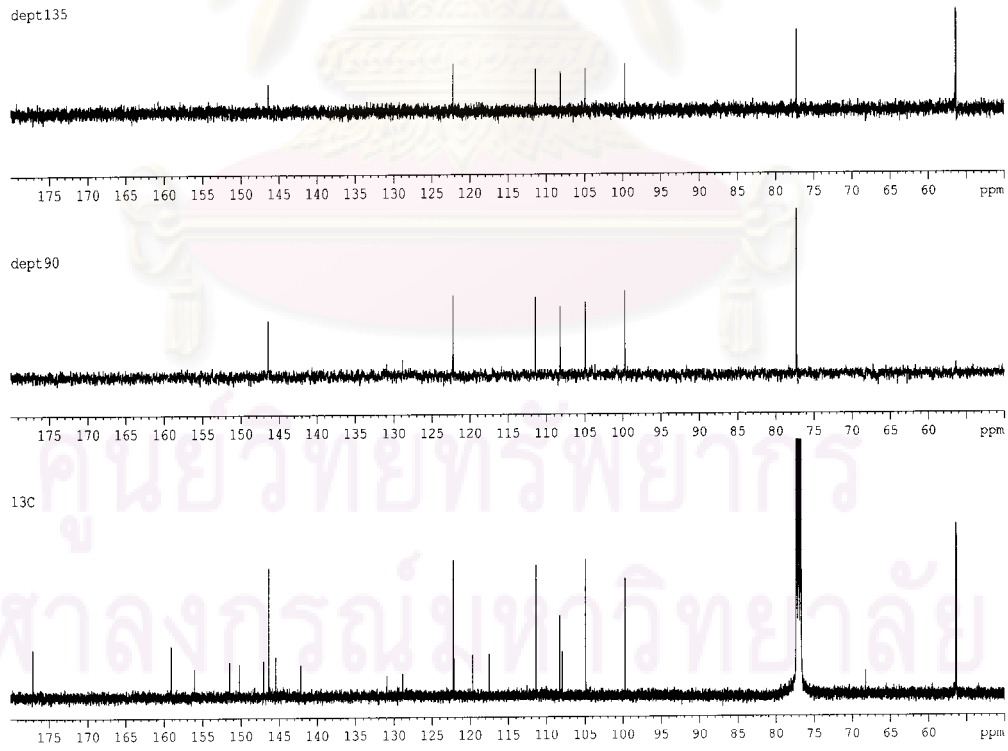

Figure 40 ^{13}C-NMR (125 MHz) and DEPT spectra of compound DM5 ($CDCl_3$)

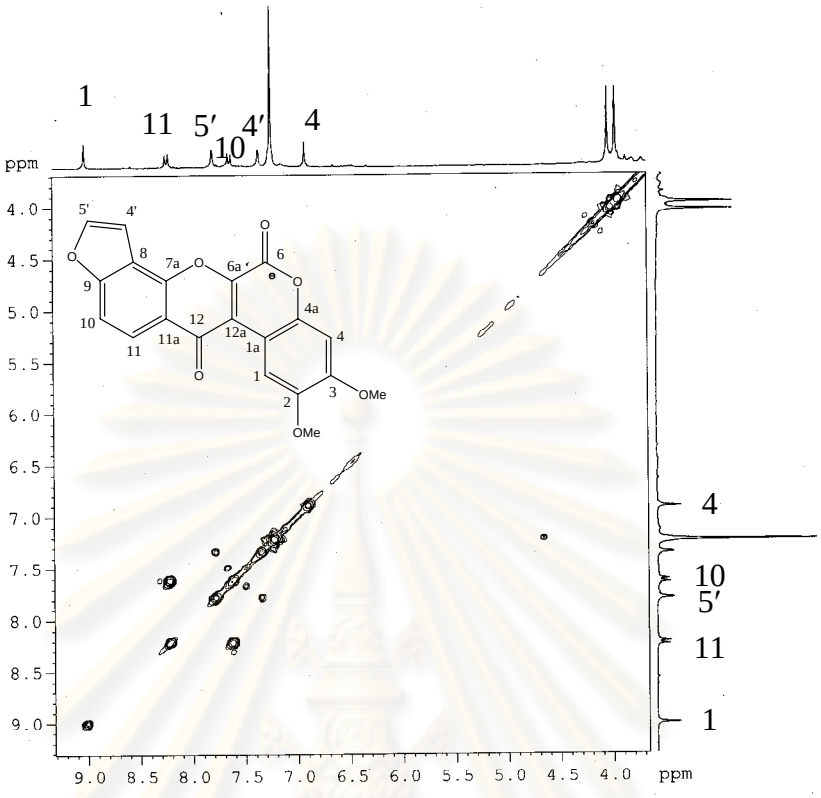

Figure 41 ^{1}H-^{1}H COSY spectrum of compound DM5 ($CDCl_3$)

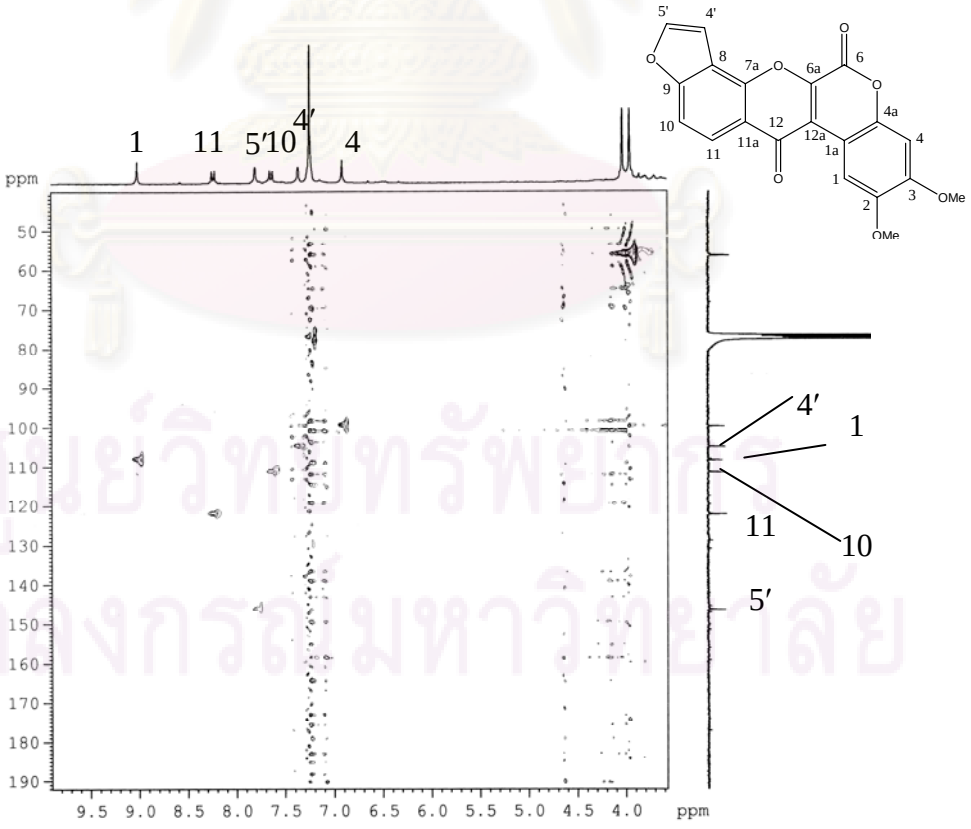

Figure 42 HMQC spectrum of compound DM5 ($CDCl_3$)

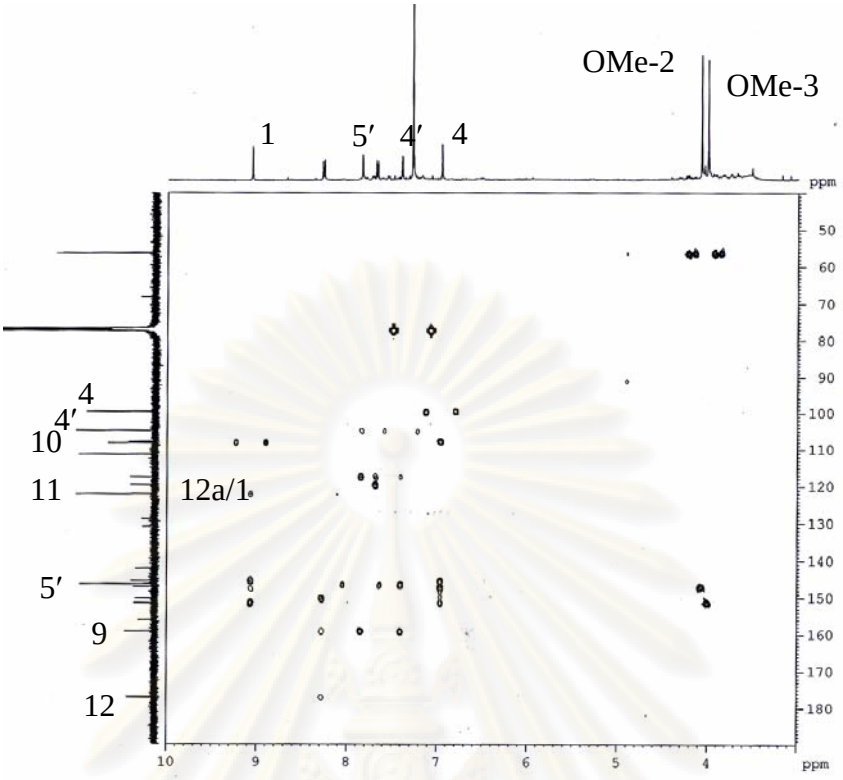

Figure 43 HMBC spectrum of compound DM5 ($CDCl_3$)
[δ_H 3-10 ppm, δ_C 40-190 ppm]

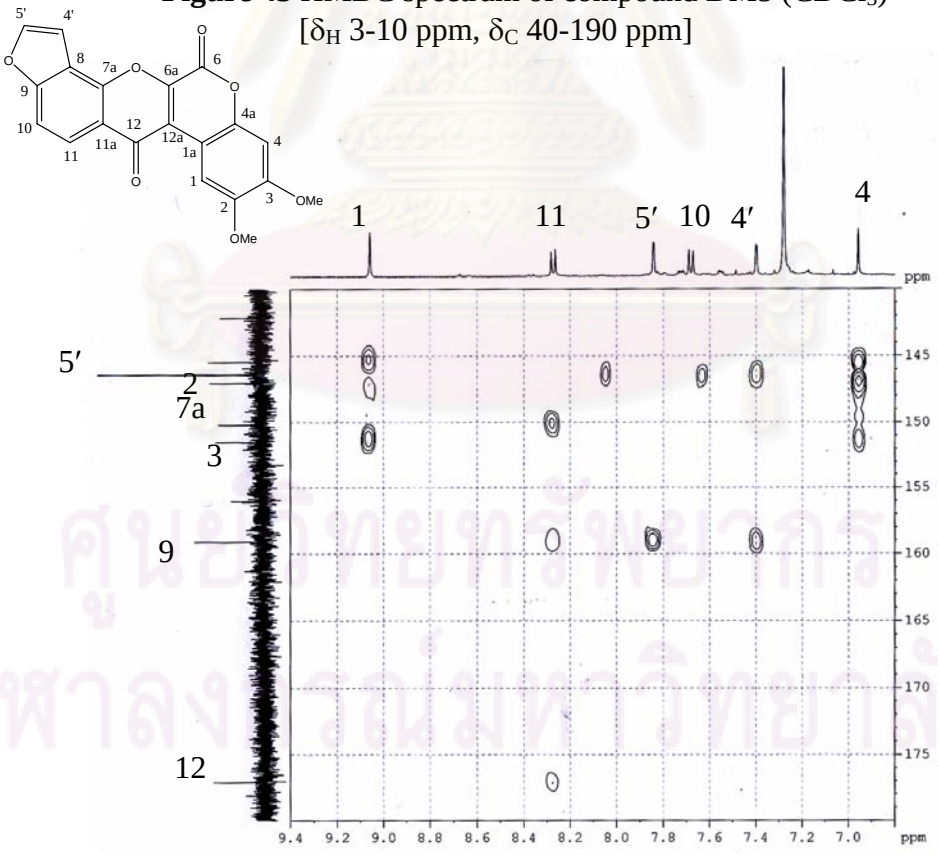

Figure 44 HMBC spectrum of compound DM5 ($CDCl_3$)
[δ_H 6.8-9.4 ppm, δ_C 140-180 ppm]

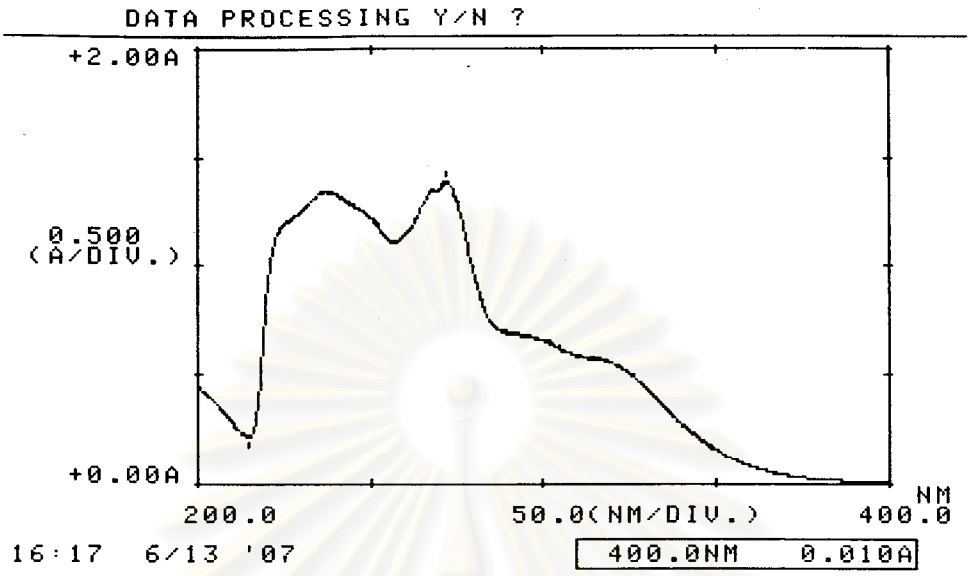

Figure 45 UV spectrum of compound DM6 (methanol)

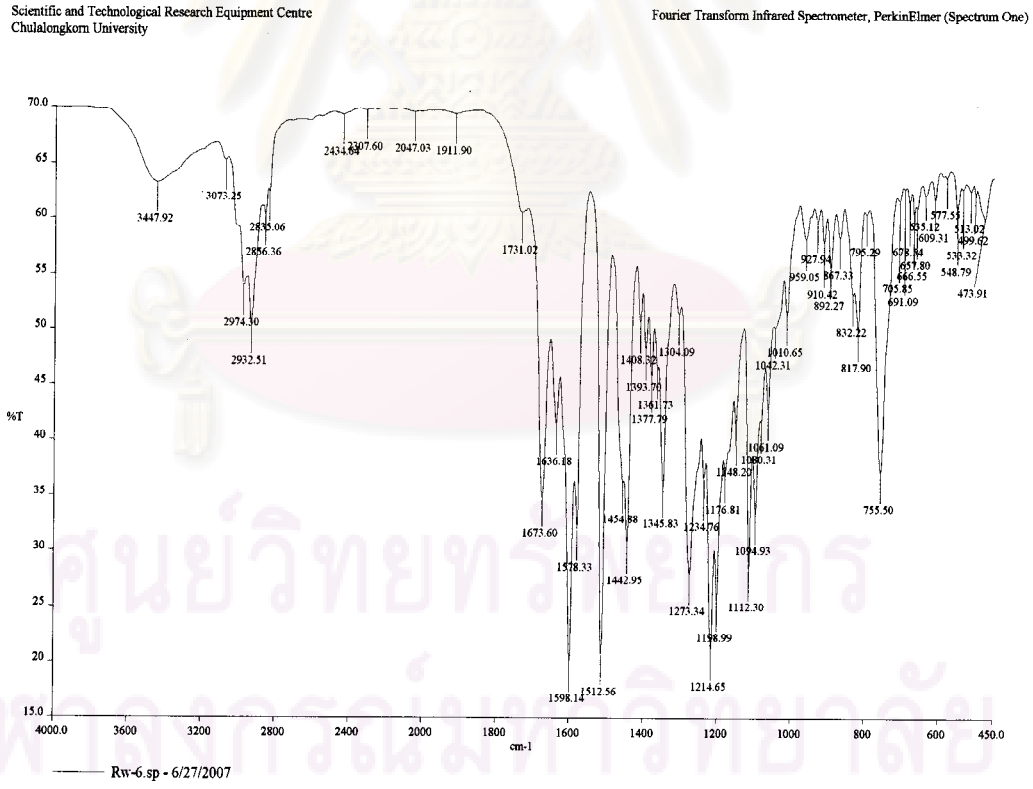

Figure 46 IR spectrum of compound DM6 (KBr disc)

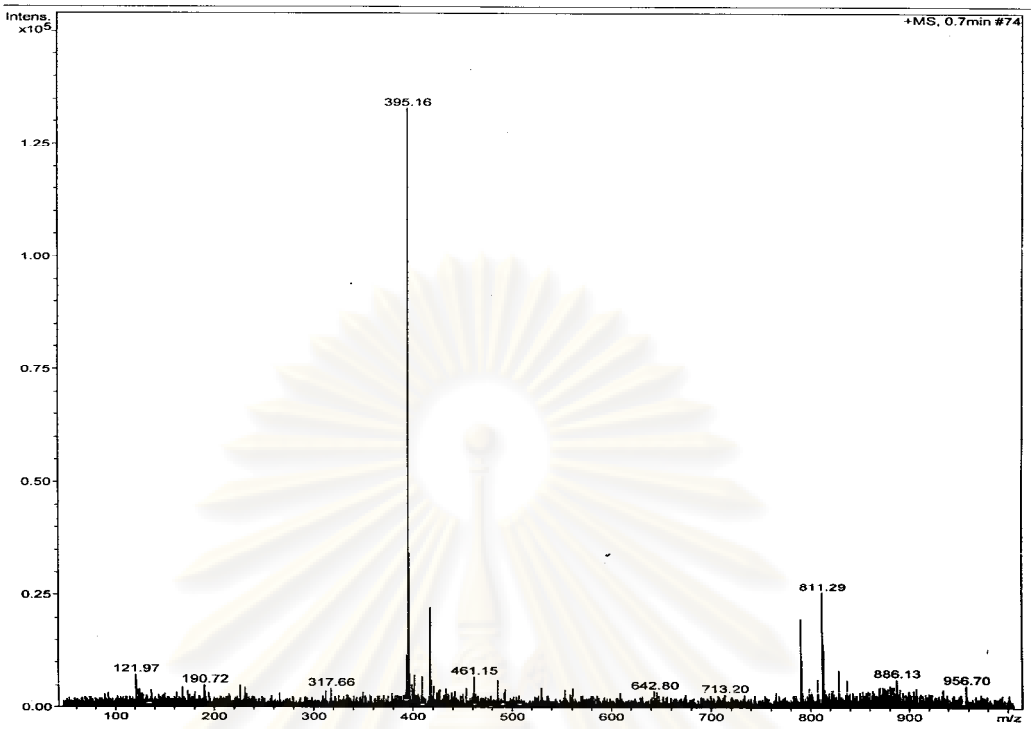

Figure 47 ESI mass spectrum of compound DM6

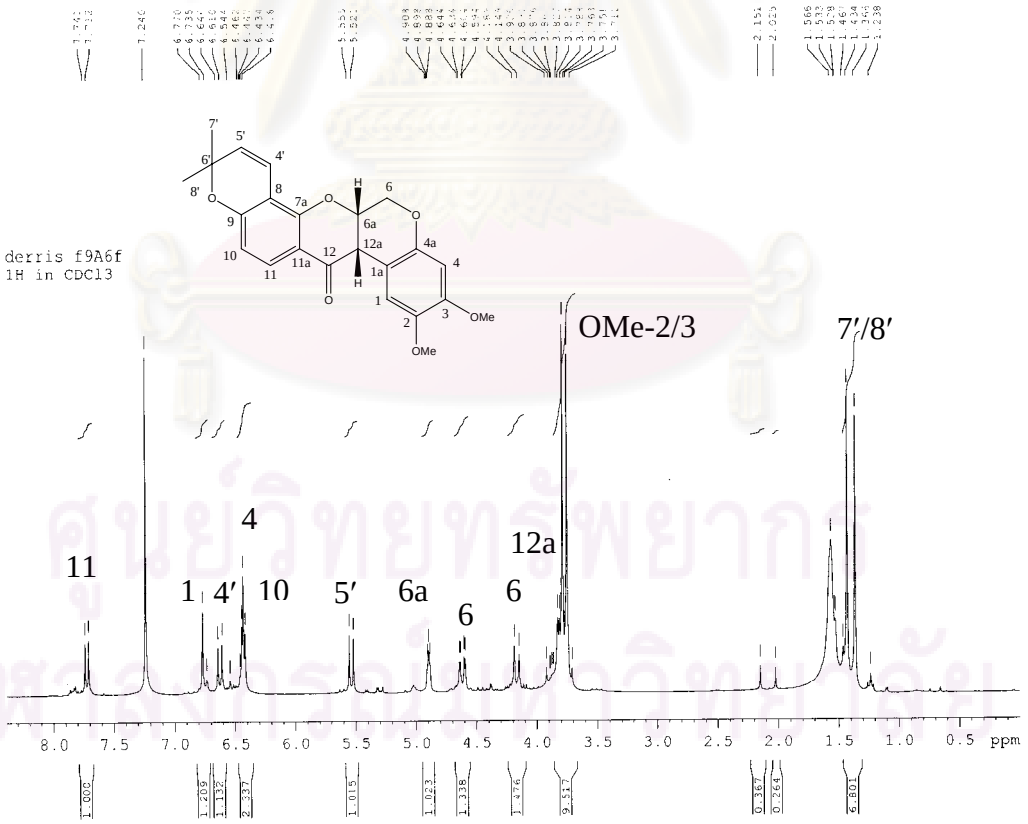

Figure 48 ^{1}H-NMR (300 MHz) spectrum of compound DM6 ($CDCl_3$)

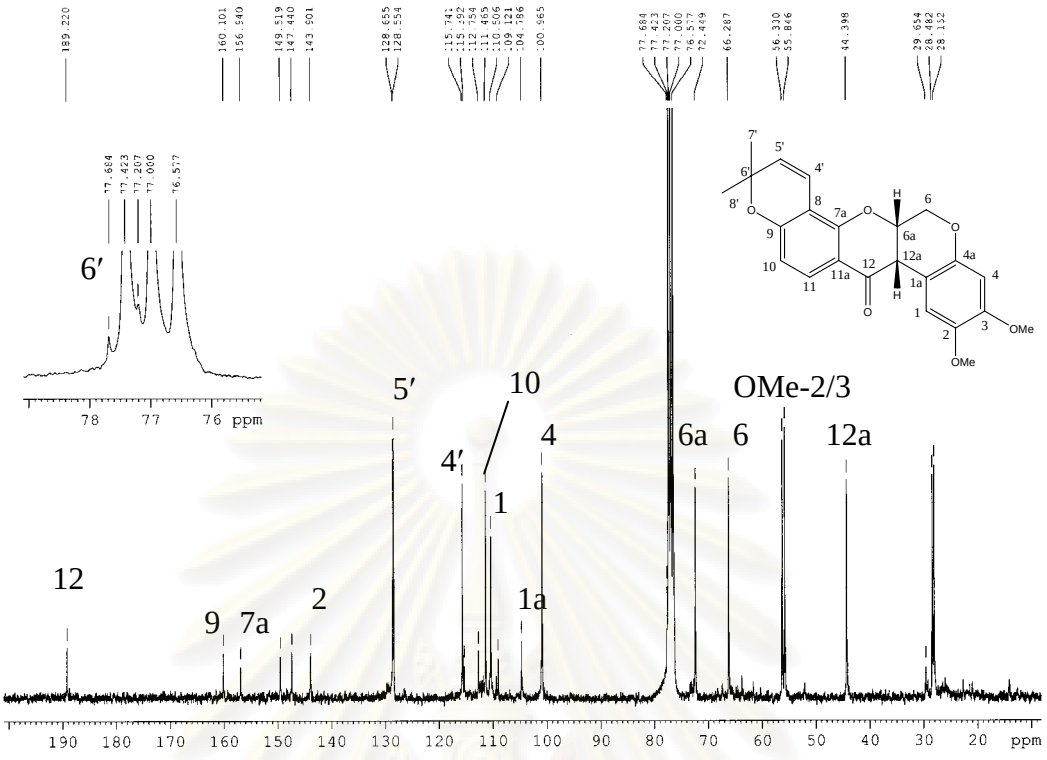

Figure 49 ^{13}C-NMR (75 MHz) spectrum of compound DM6 ($CDCl_3$)

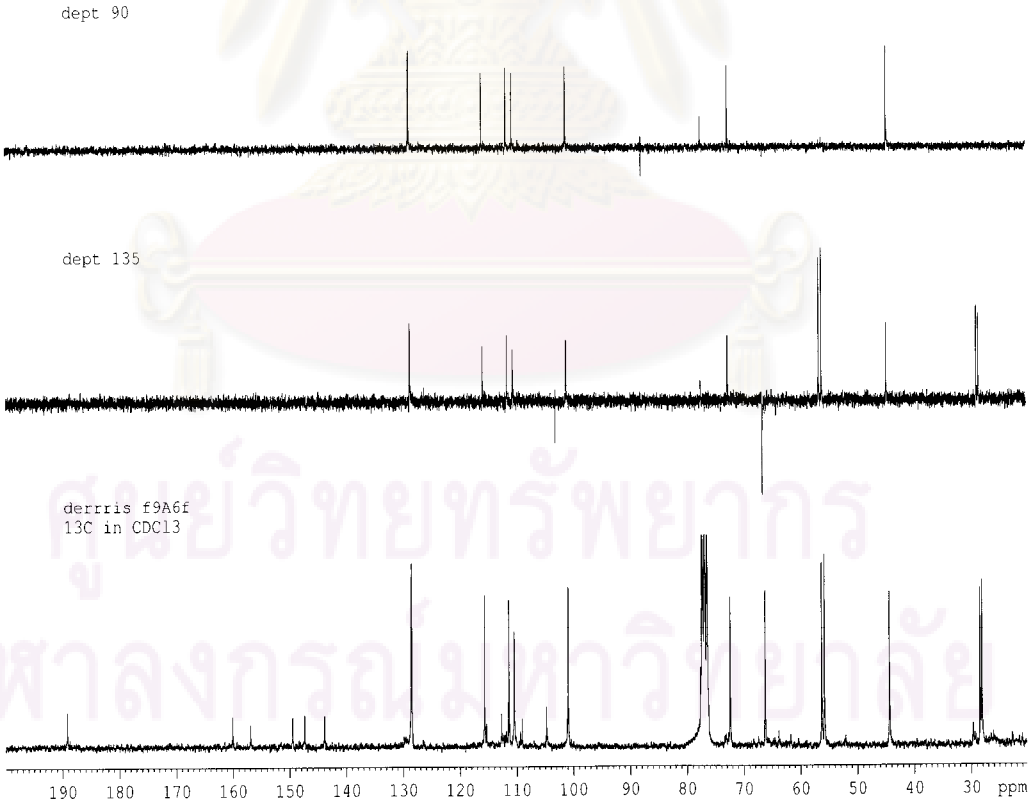

Figure 50 ^{13}C-NMR (75 MHz) and DEPT spectra of compound DM6 ($CDCl_3$)

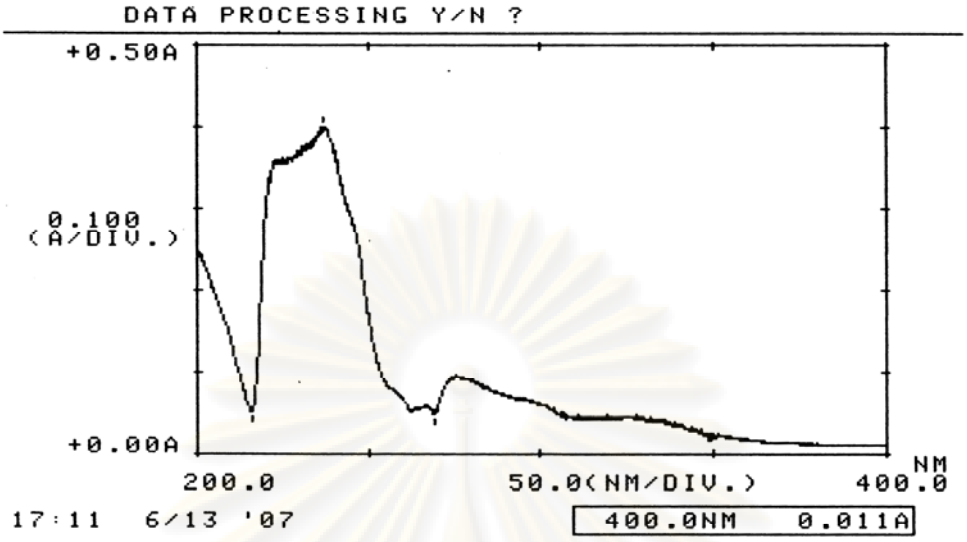

Figure 51 UV spectrum of compound DM7 (methanol)

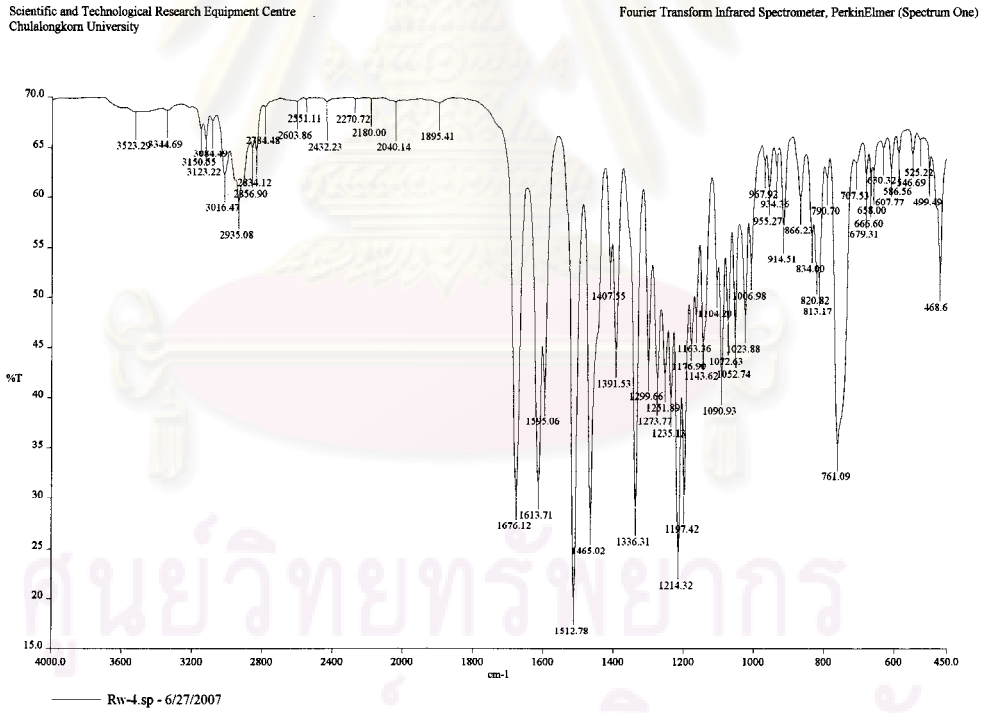

Figure 52 IR spectrum of compound DM7 (KBr disc)

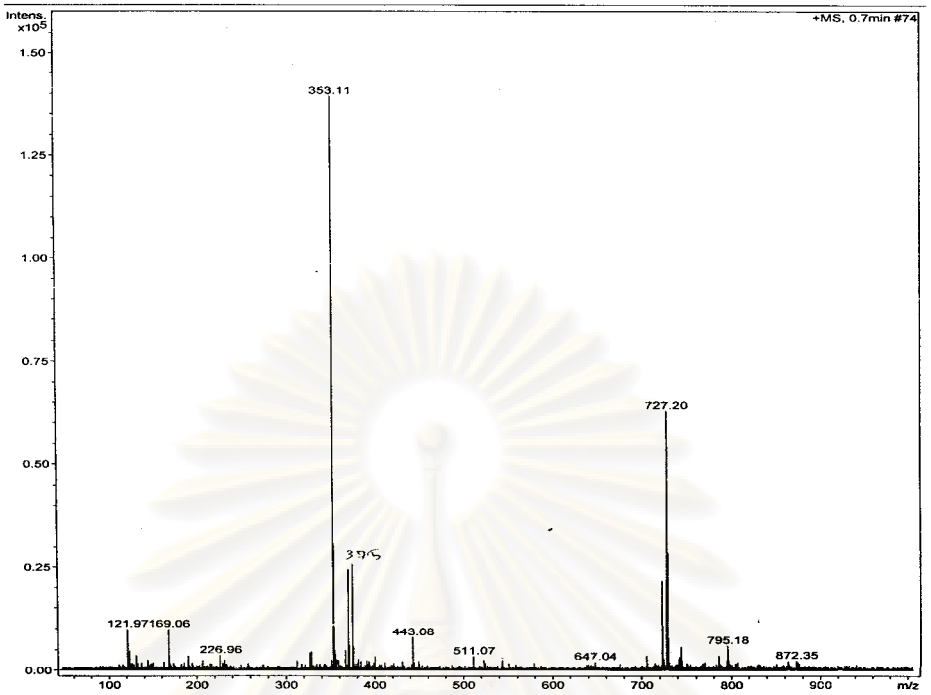

Figure 53 ESI mass spectrum of compound DM7

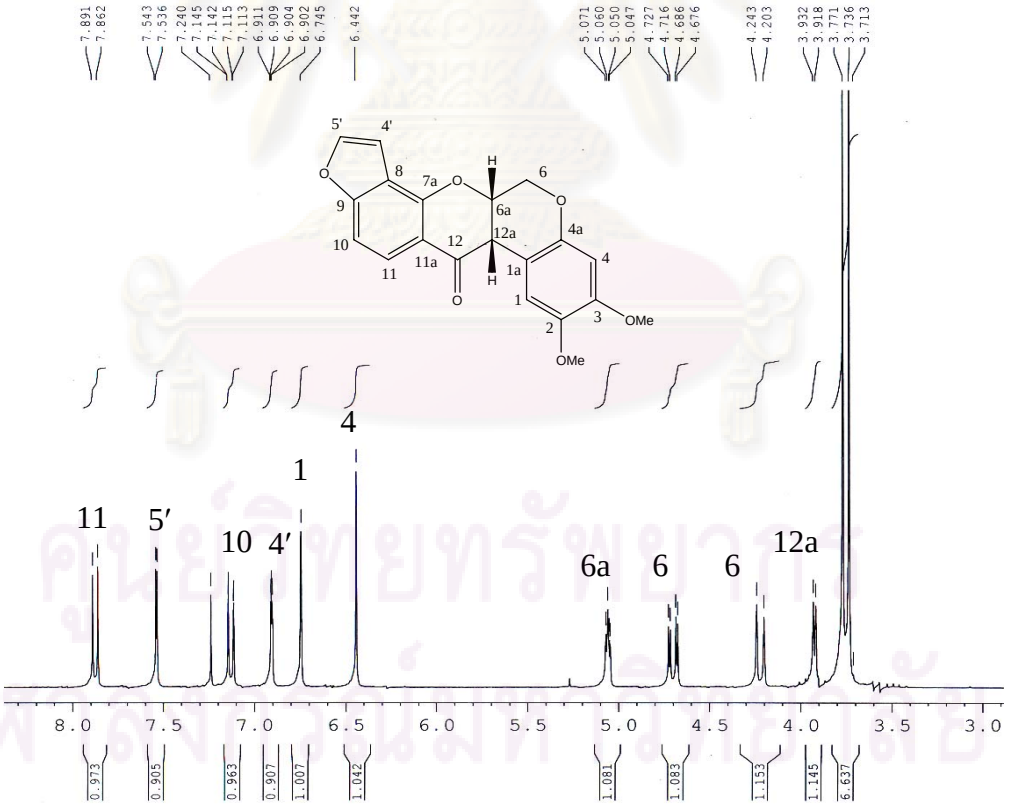

Figure 54 ^{1}H-NMR (300 MHz) spectrum of compound DM7 ($CDCl_3$)

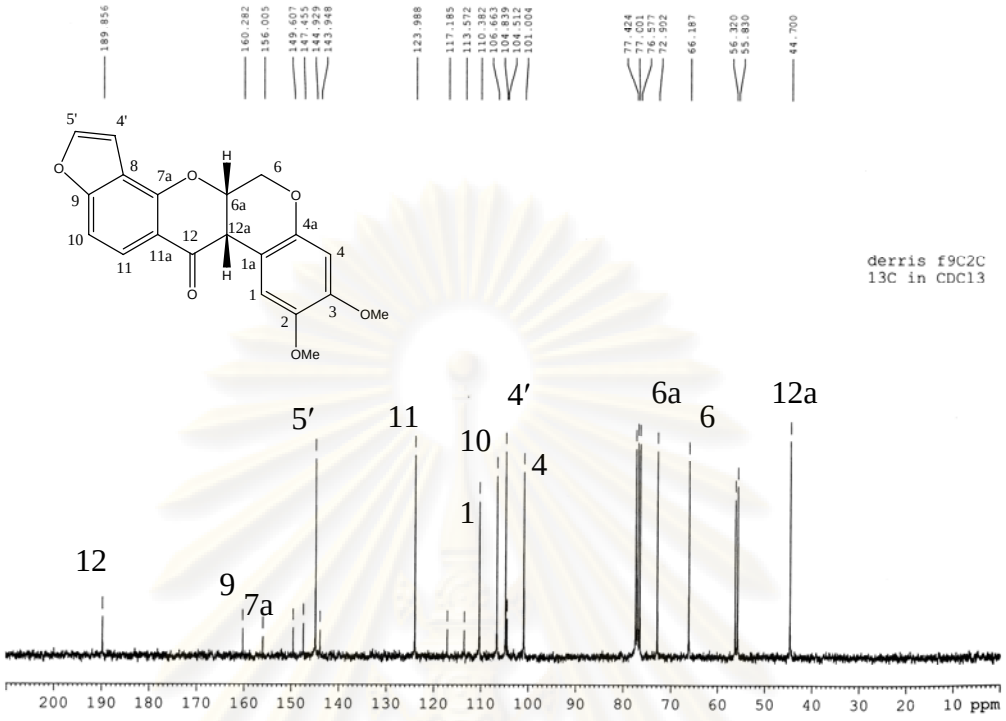

Figure 55 ^{13}C-NMR (75 MHz) spectrum of compound DM7 ($CDCl_3$)

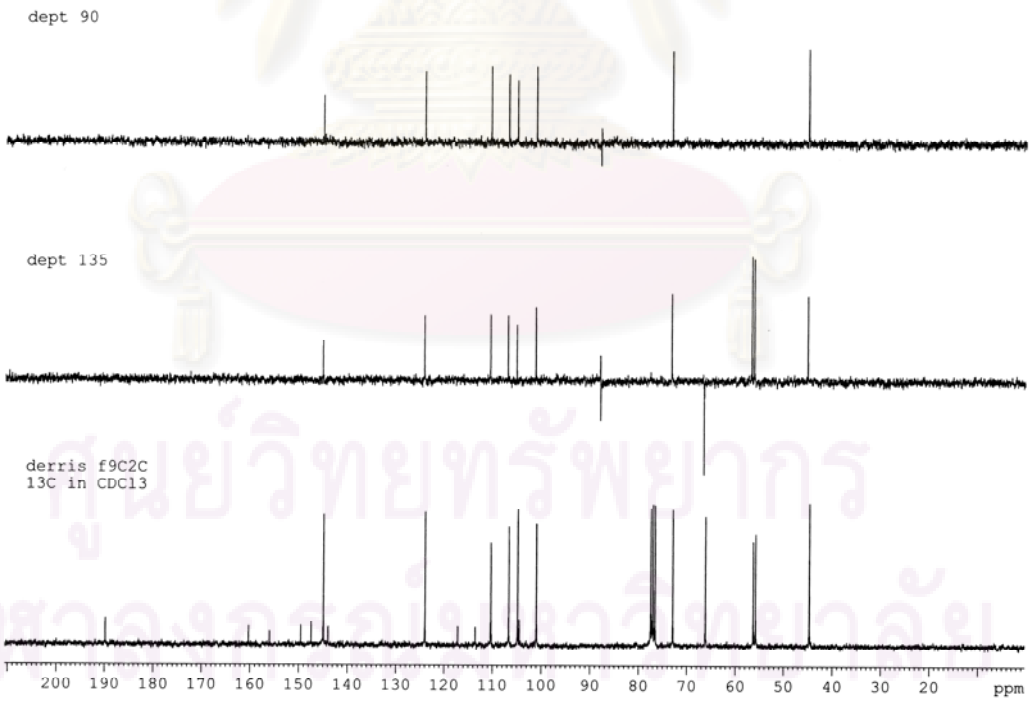

Figure 56 ^{13}C-NMR (75 MHz) and DEPT spectra of compound DM7 ($CDCl_3$)

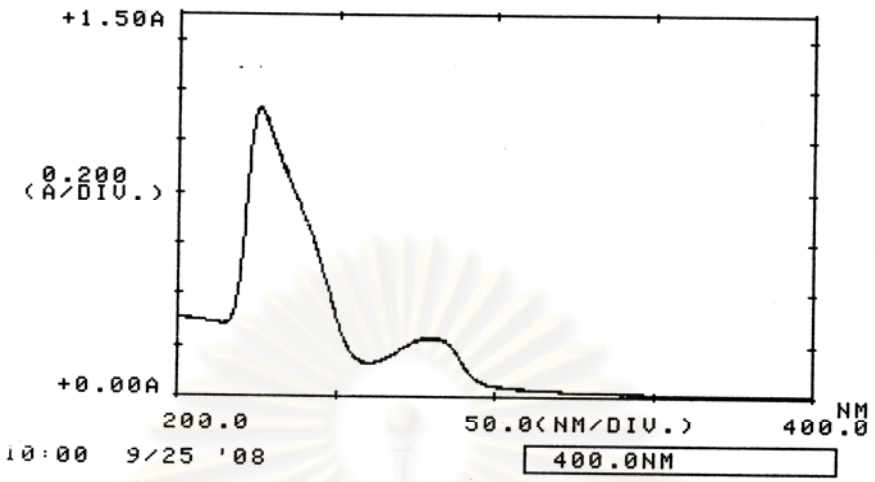

Figure 57 UV spectrum of compound CC1 (methanol)

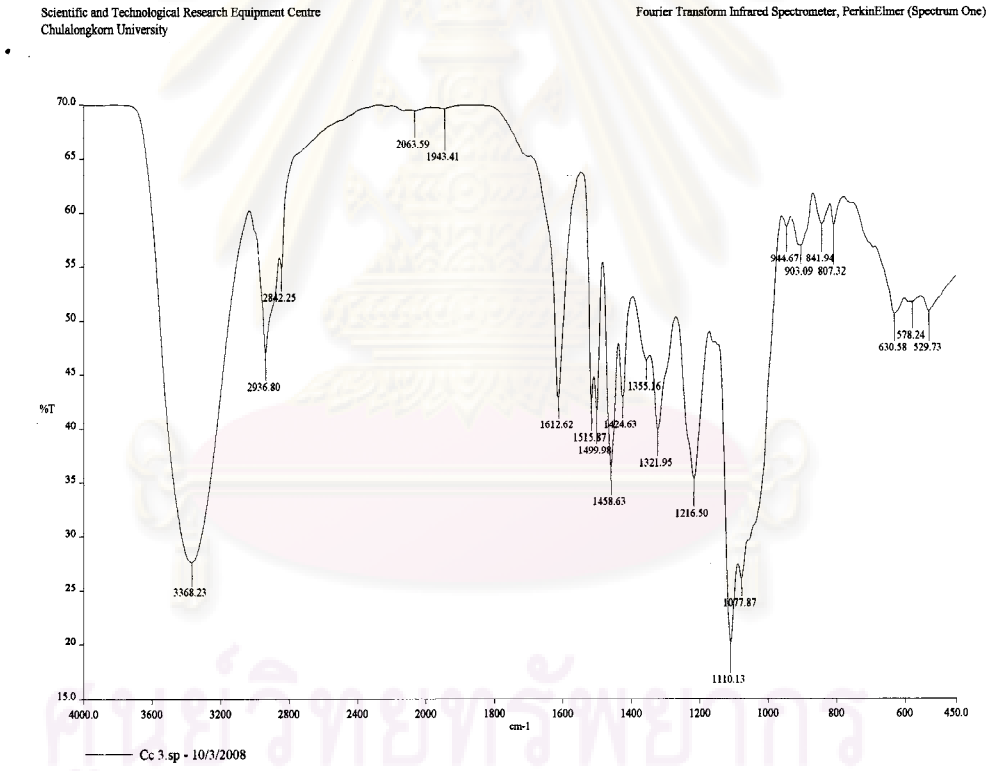

Figure 58 IR spectrum of compound CC1 (KBr disc)

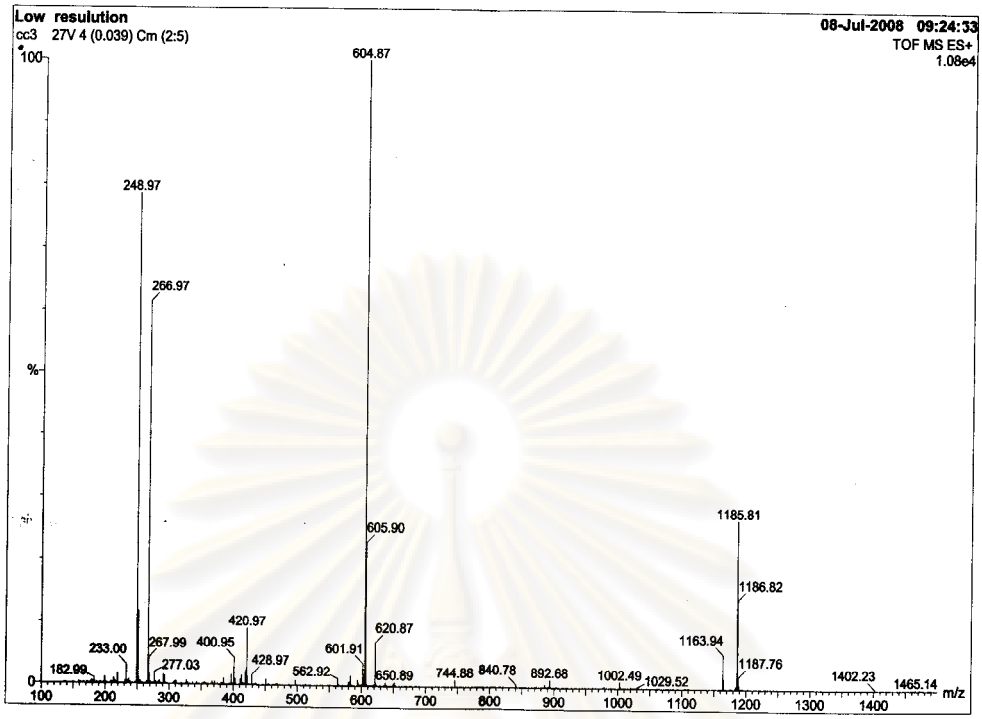

Figure 59 ESI mass spectrum of compound CC1

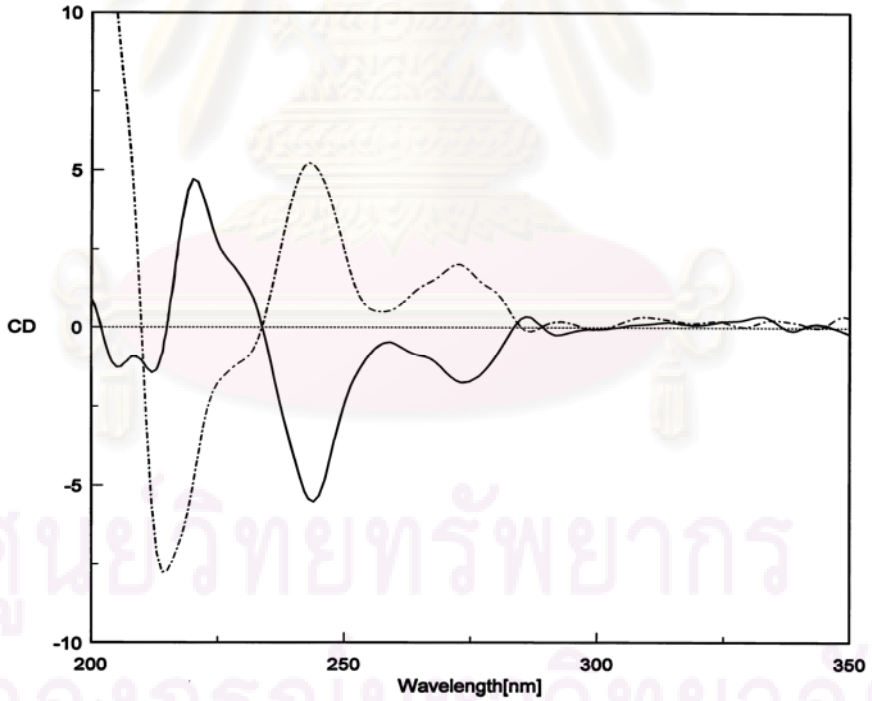

-·-·- , CC1; ——, CC2

Figure 60 CD curves of compounds CC1 and CC2

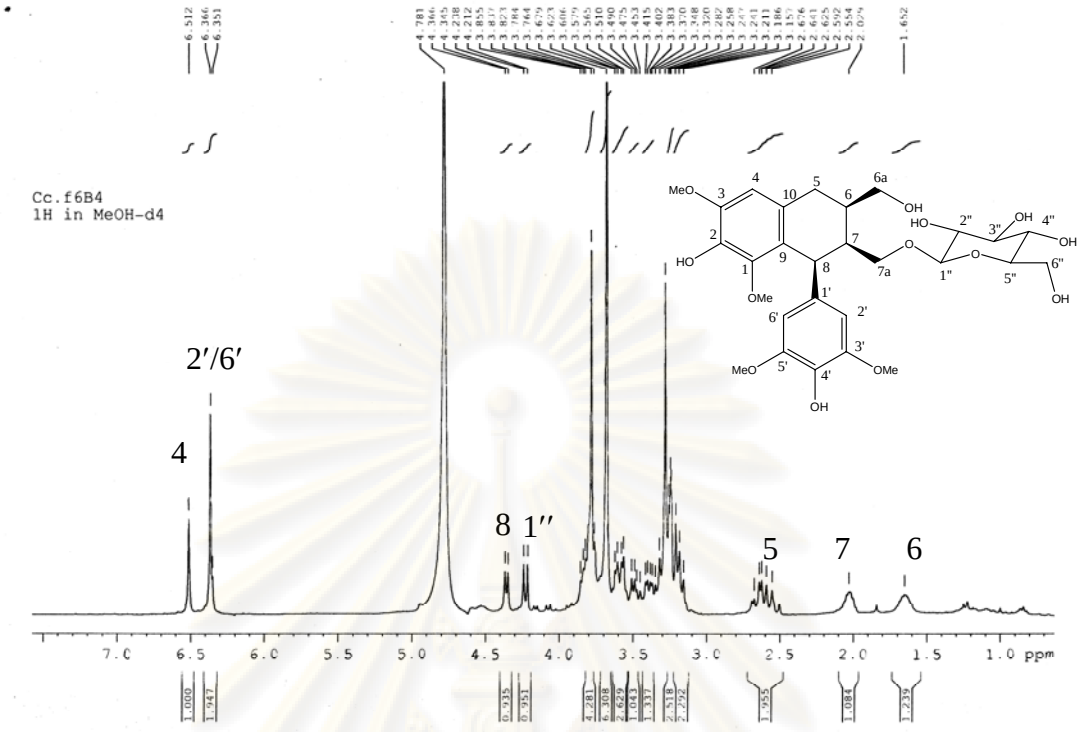

Figure 61 ^{1}H-NMR (300 MHz) spectrum of compound CC1 (MeOH-d_4)

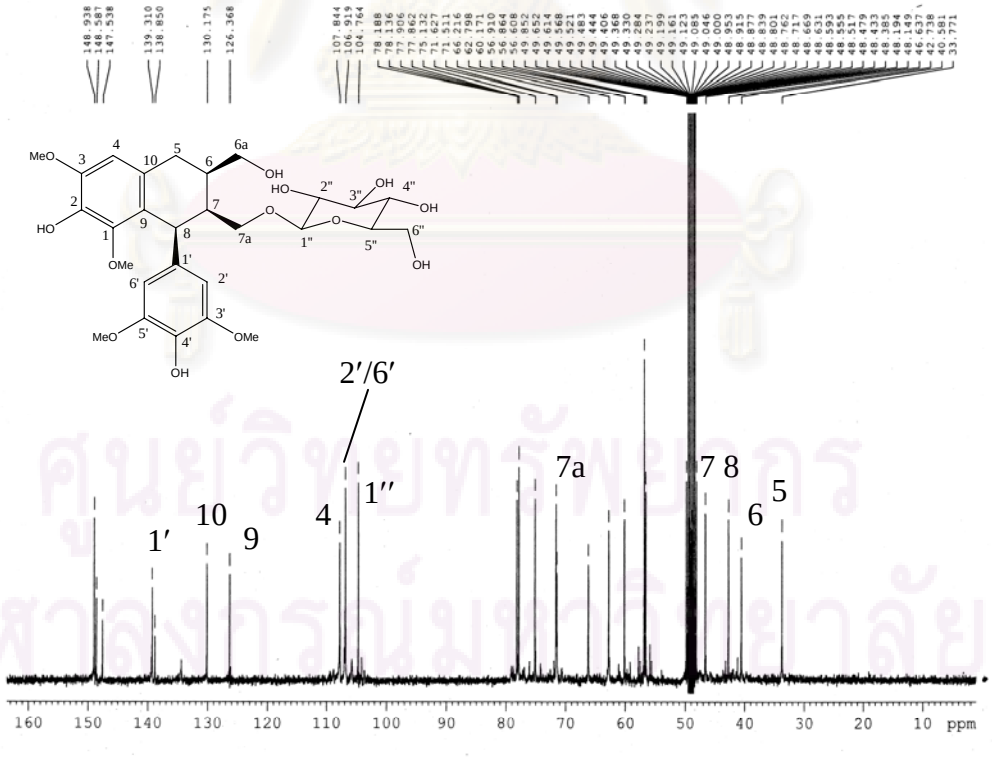

Figure 62 ^{13}C-NMR (75 MHz) spectrum of compound CC1 (MeOH-d_4)

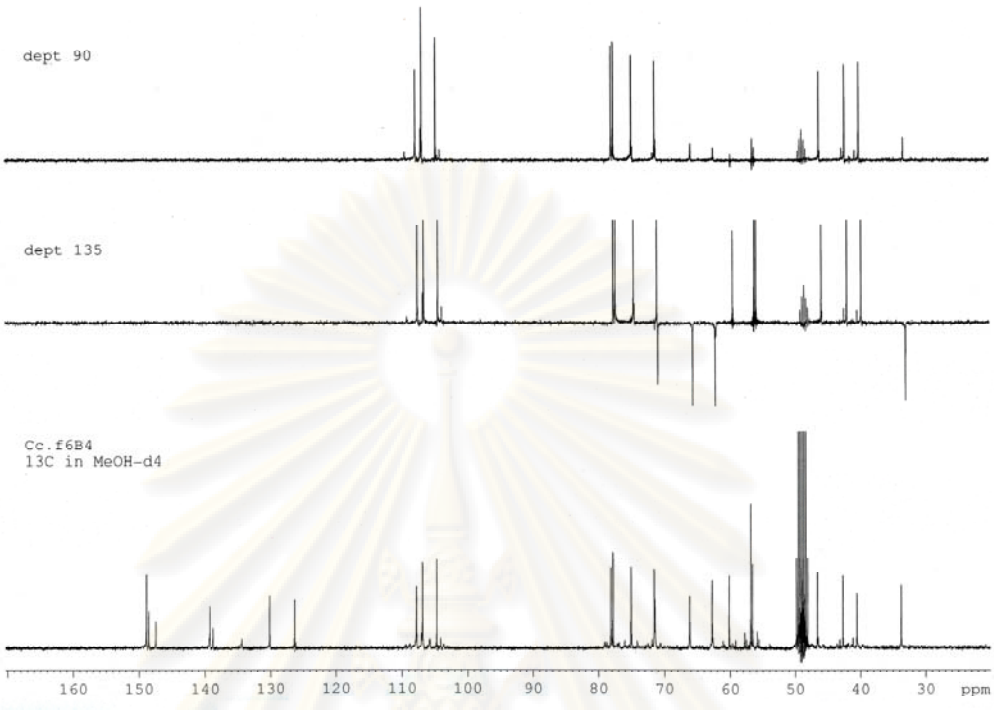

Figure 63 ^{13}C-NMR (75 MHz) and DEPT spectra of compound CC1 (MeOH-d_4)

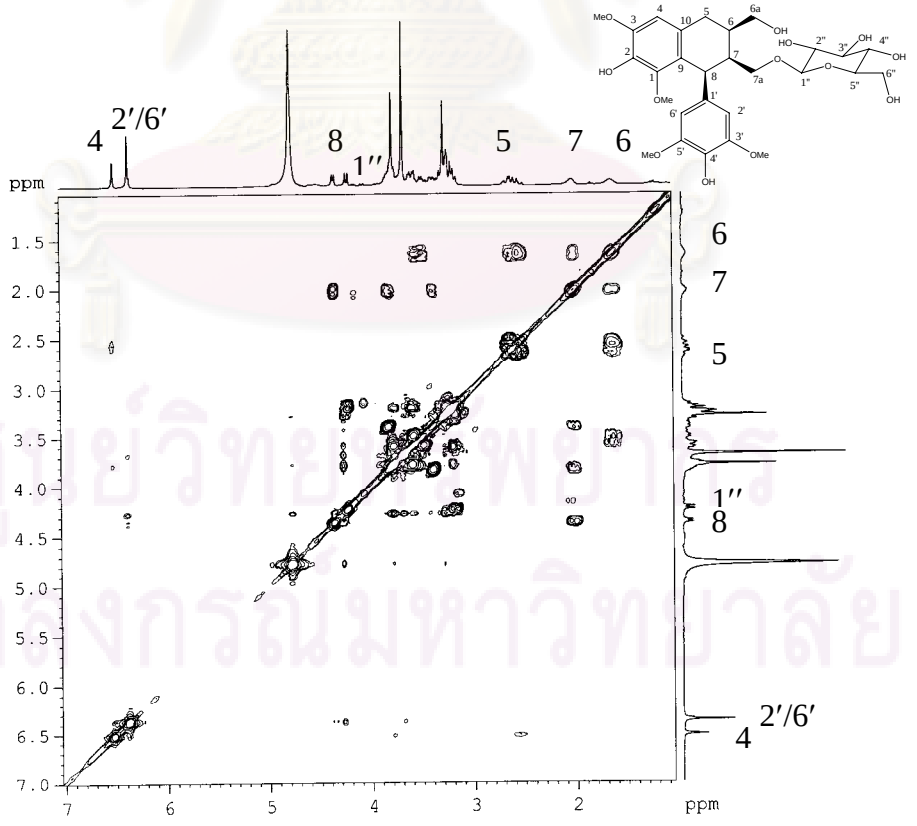

Figure 64 ^{1}H-^{1}H COSY spectrum of compound CC1 (MeOH-d_4)

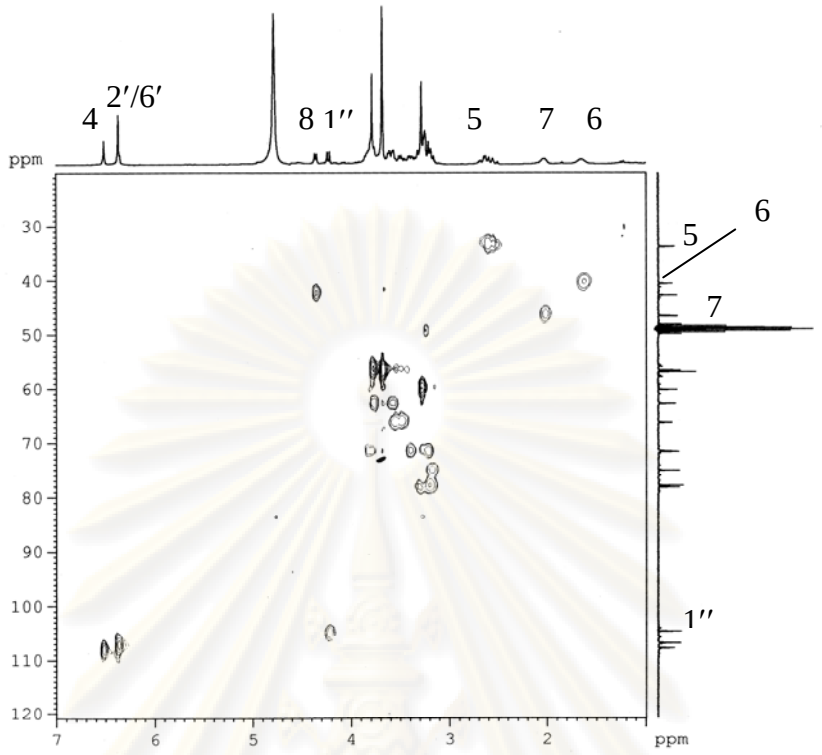

Figure 65 HMQC spectrum of compound CC1 (MeOH-d_4)

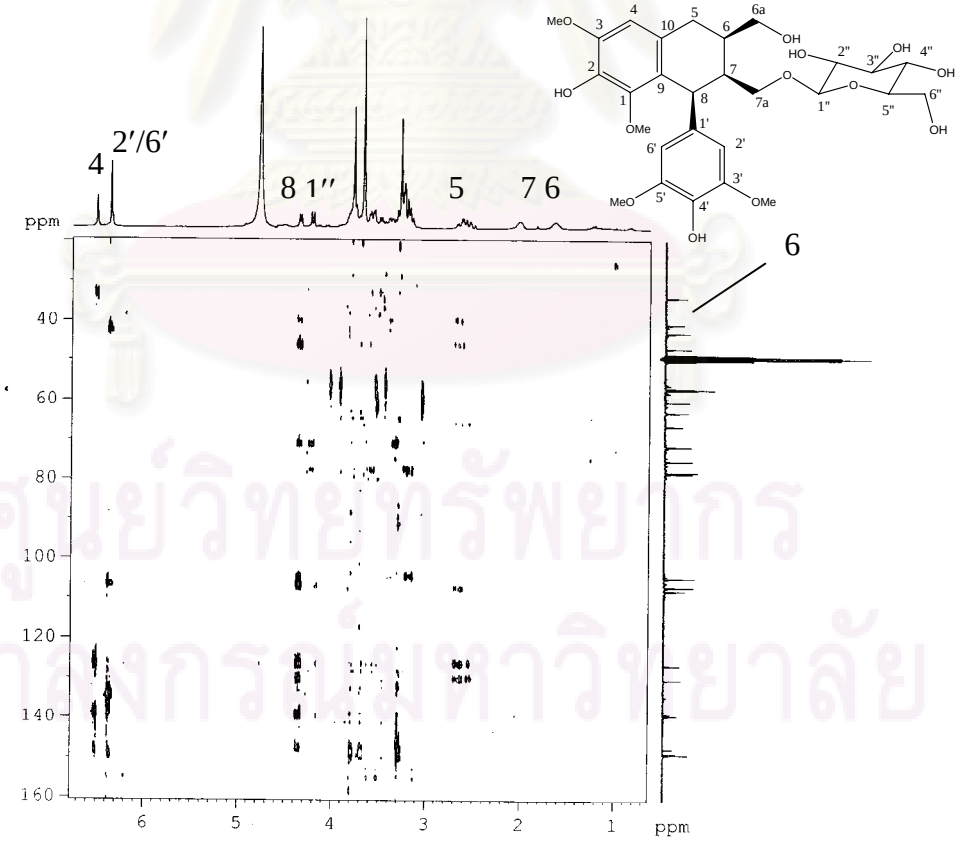

Figure 66 HMBC spectrum of compound CC1 (MeOH-d_4)

[δ_H 0.5-7 ppm, δ_C 30-160 ppm]

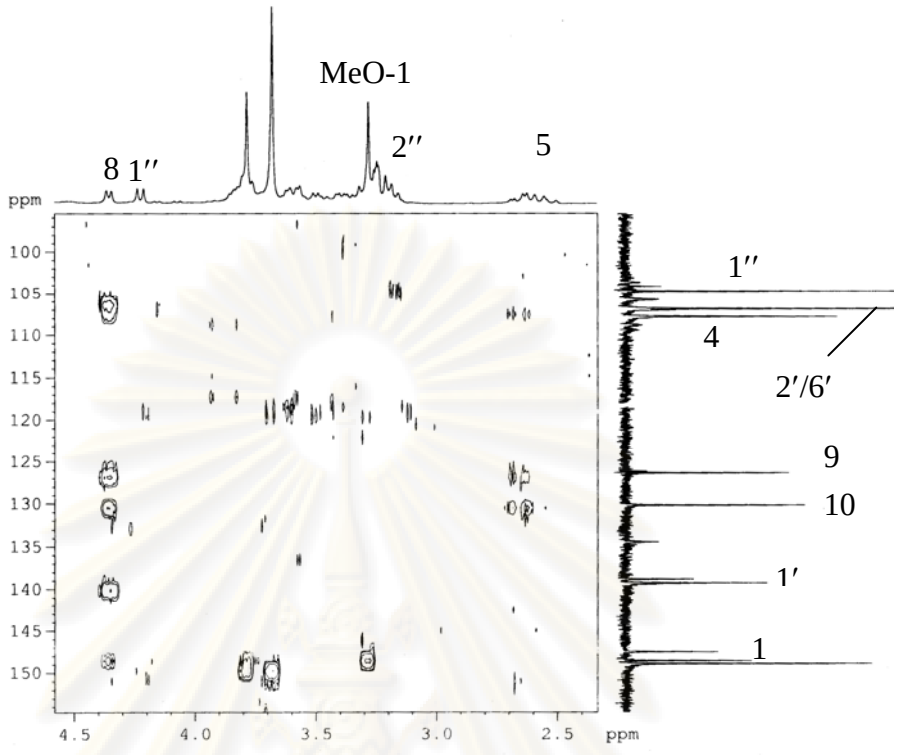

Figure 67 HMBC spectrum of compound CC1 (MeOH-d_4)

[δ_H 2.3-4.6 ppm, δ_C 90-160 ppm]

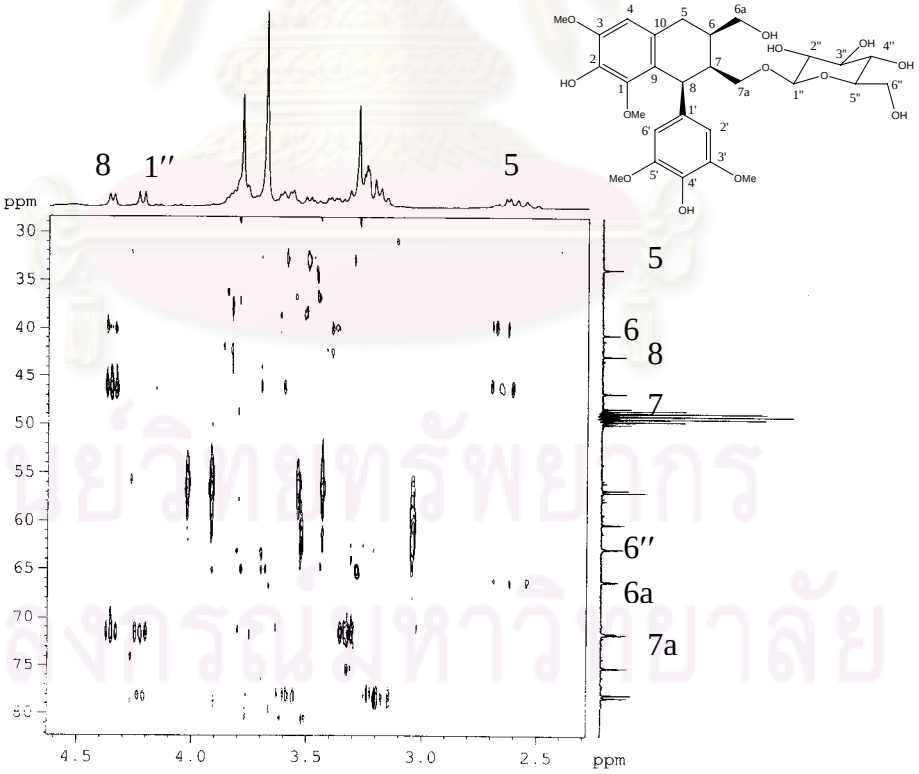

Figure 68 HMBC spectrum of compound CC1 (MeOH-d_4)

[δ_H 2.3-4.6 ppm, δ_C 29-82 ppm]

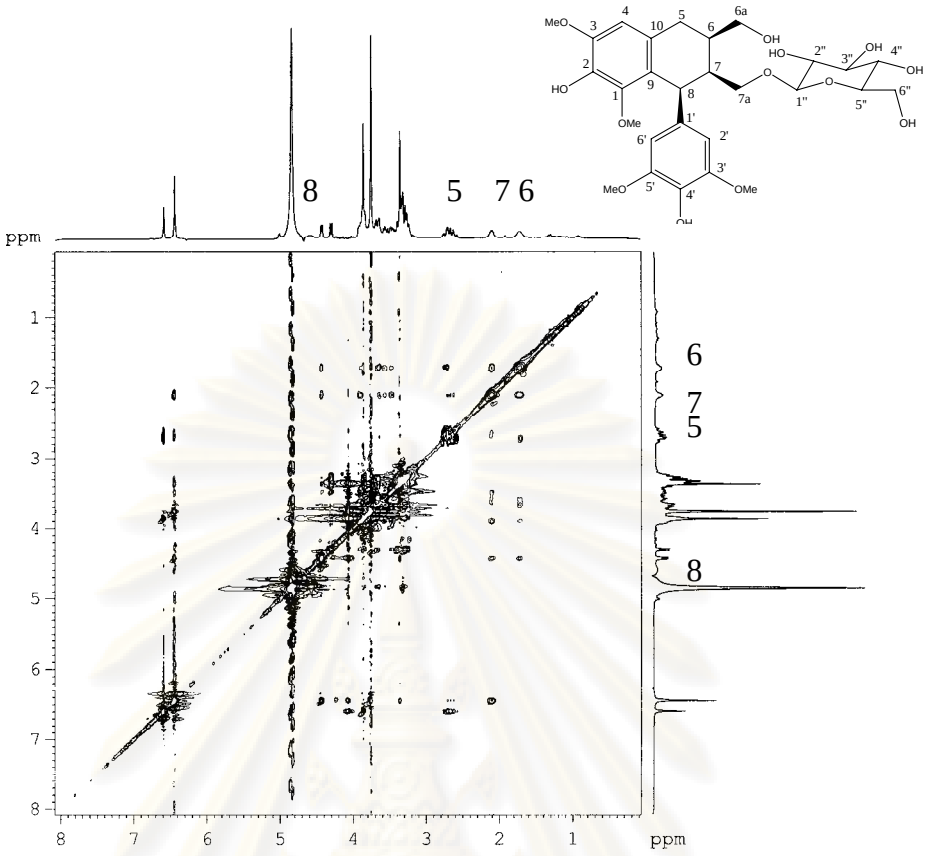

Figure 69 ROESY spectrum of compound CC1 (MeOH-d_4)

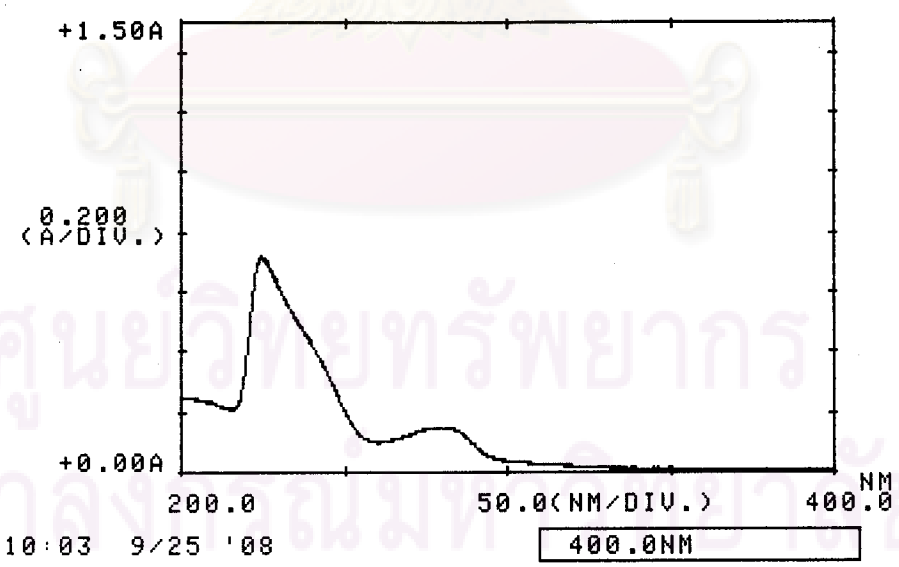

Figure 70 UV spectrum of compound CC2 (methanol)

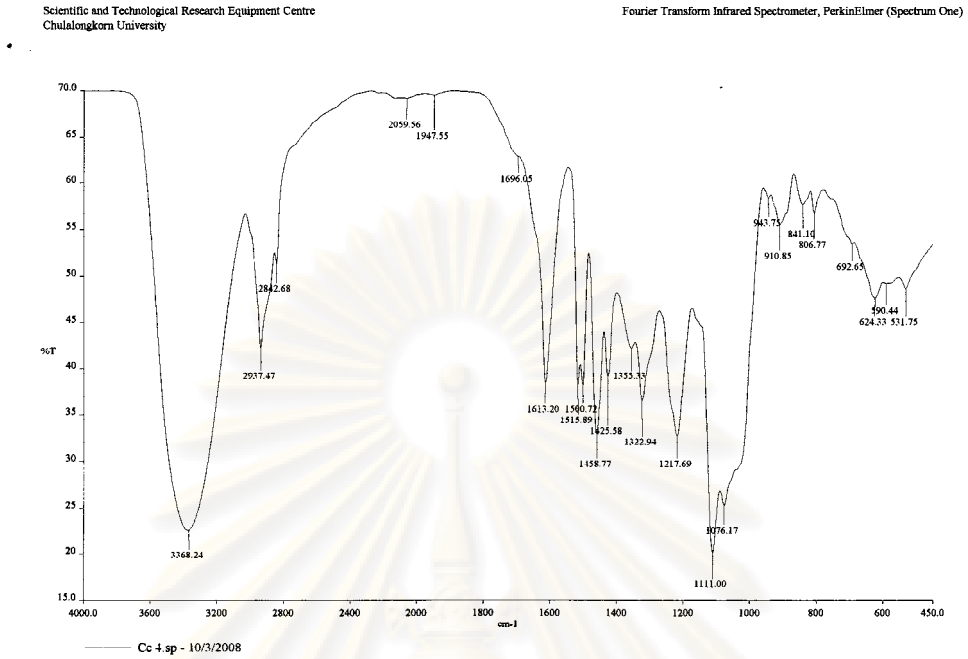

Figure 71 IR spectrum of compound CC2 (KBr disc)

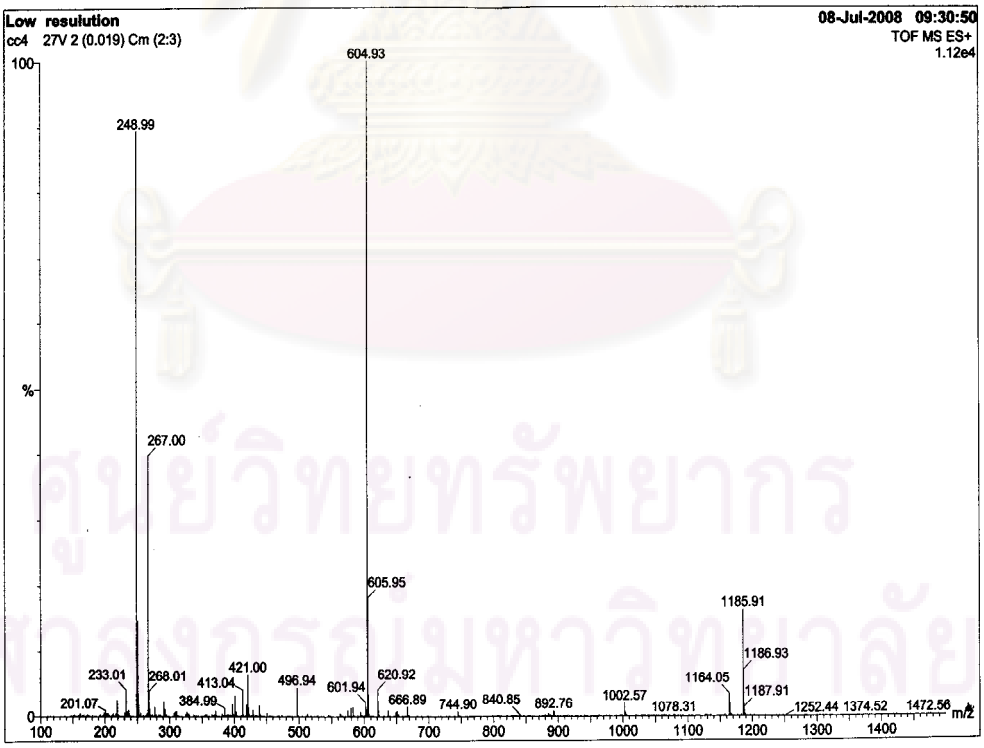

Figure 72 ESI mass spectrum of compound CC2

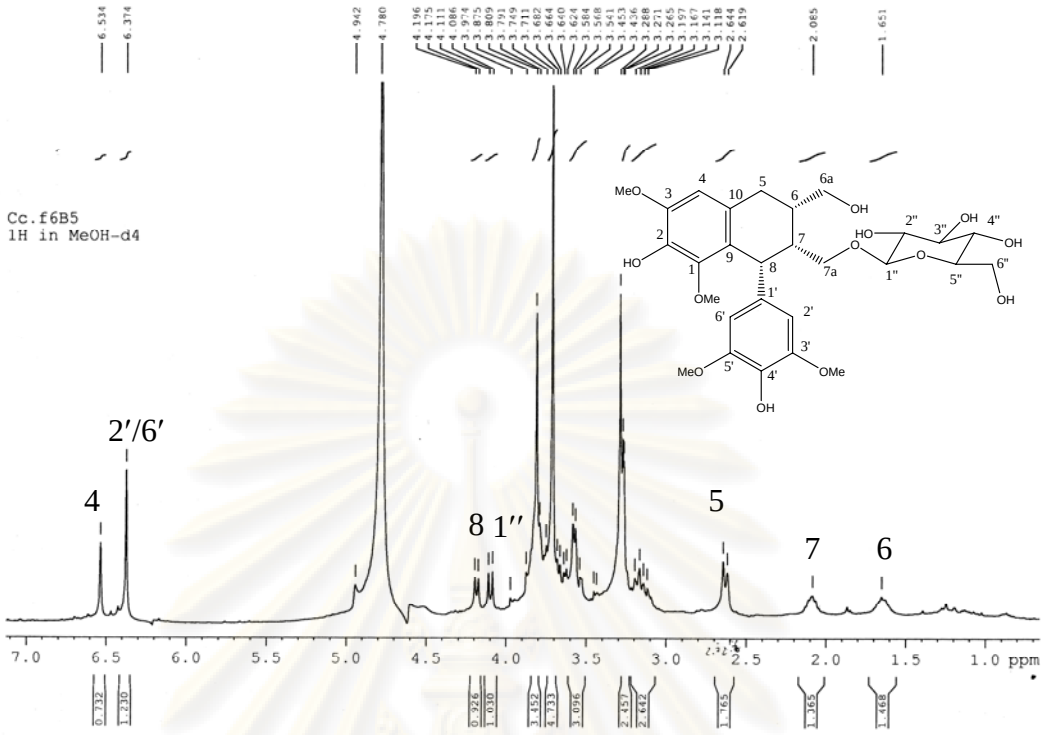

Figure 73 ^{1}H-NMR (300 MHz) spectrum of compound CC2 (MeOH-d_4)

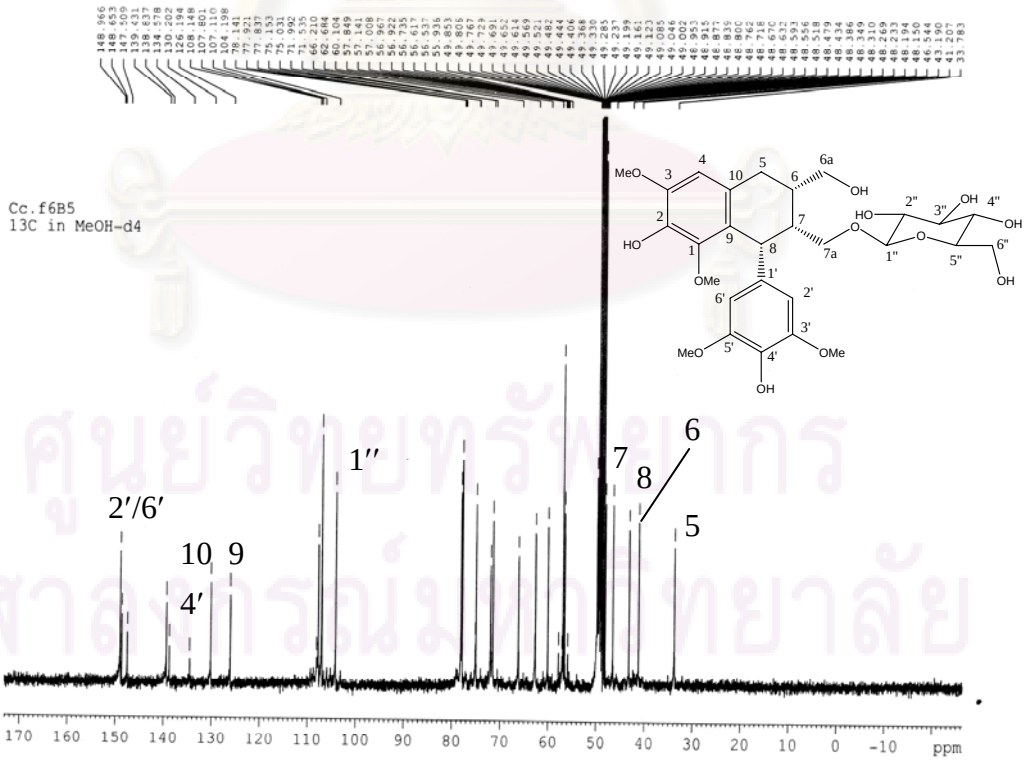

Figure 74 ^{13}C-NMR (75 MHz) spectrum of compound CC2 (MeOH-d_4)

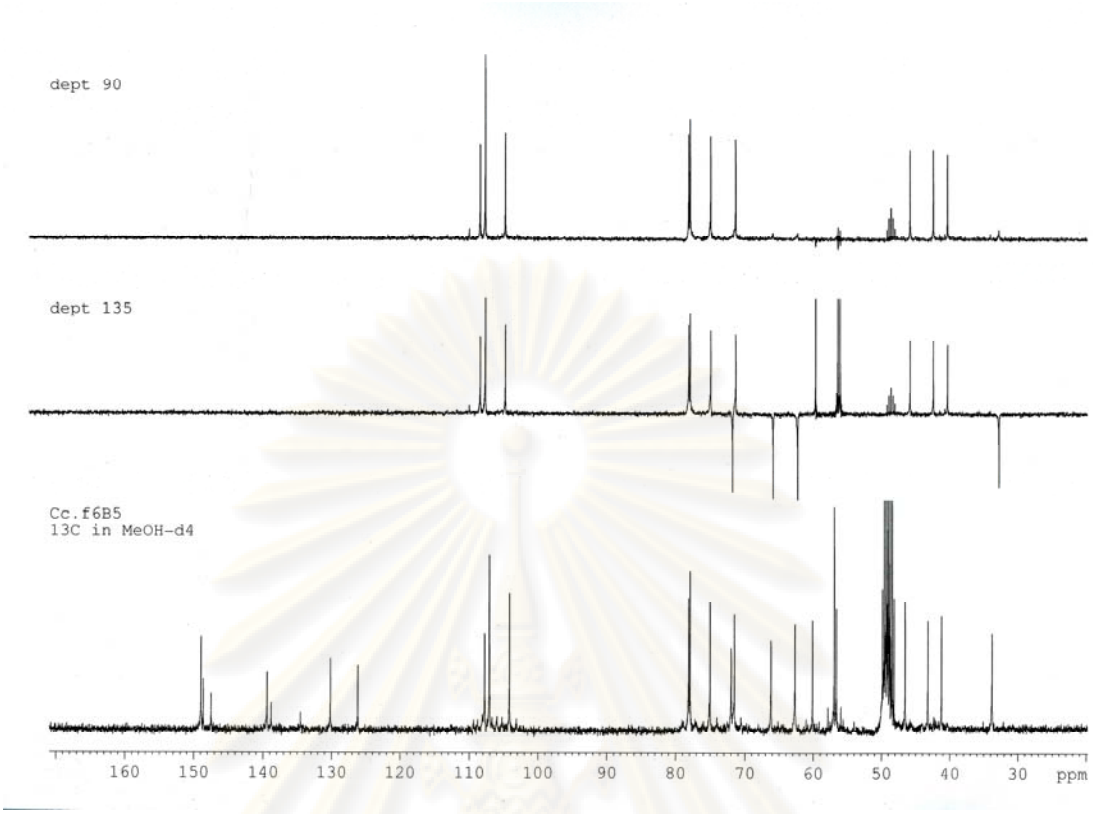

Figure 75 ^{13}C-NMR (75 MHz) and DEPT spectra of compound CC2 (MeOH-d_4)

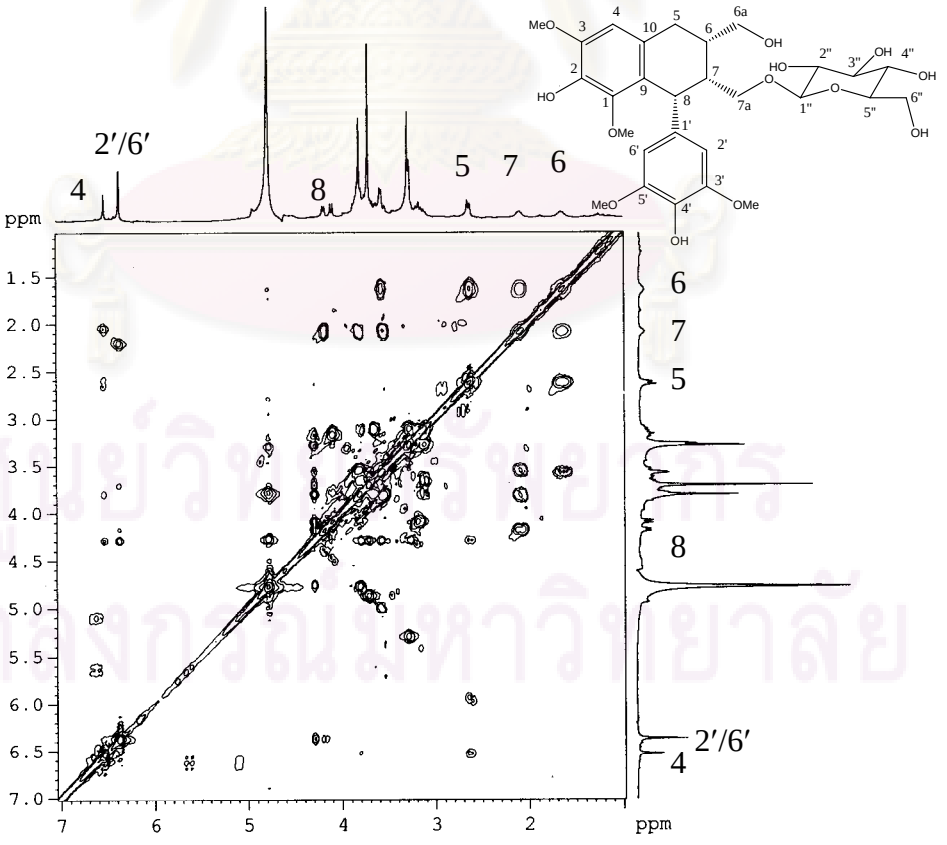

Figure 76 ^{1}H-^{1}H COSY spectrum of compound CC2 (MeOH-d_4)

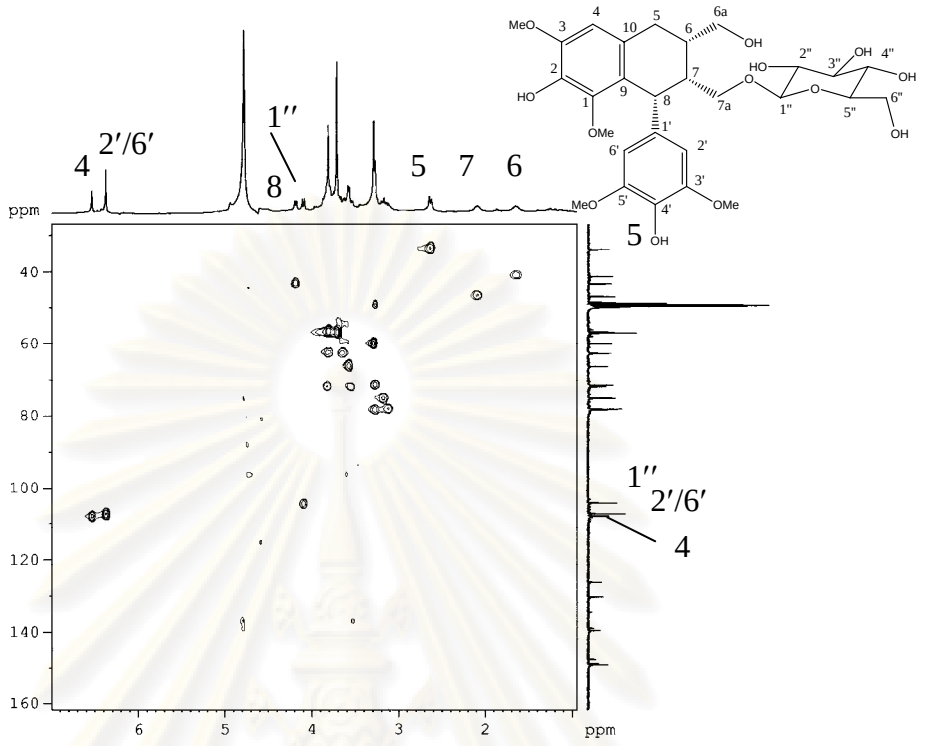

Figure 77 HMQC spectrum of compound CC2 (MeOH-d_4)

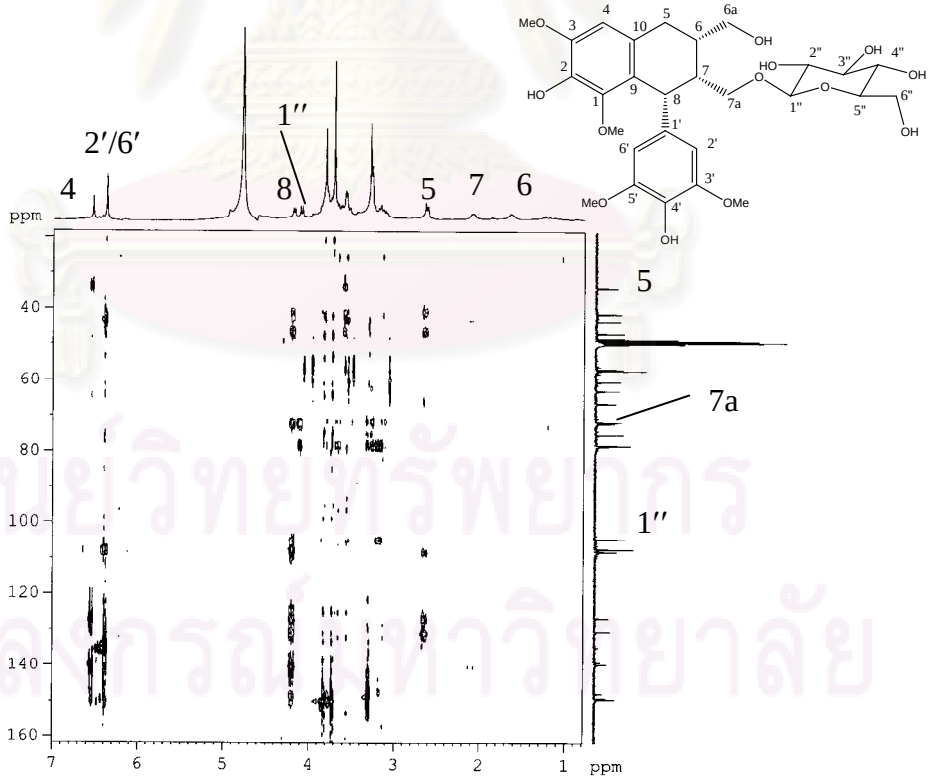

Figure 78 HMBC spectrum of compound CC2 (MeOH-d_4)
[δ_H 0.8-7 ppm, δ_C 30-160 ppm]

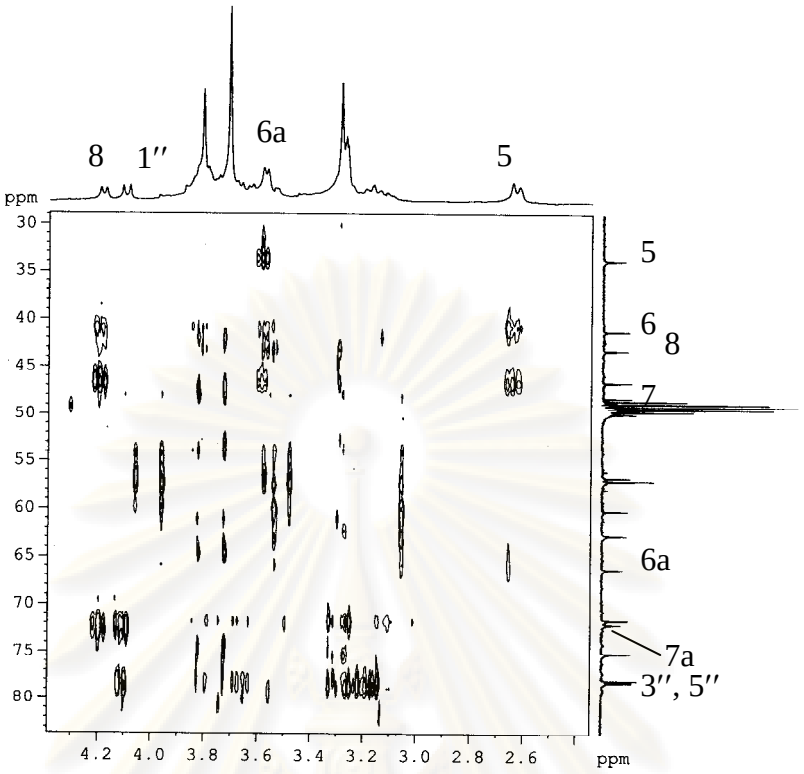

Figure 79 HMBC spectrum of compound CC2 (MeOH-d_4)
[δ_H 2.4-4.4 ppm, δ_C 29-84 ppm]

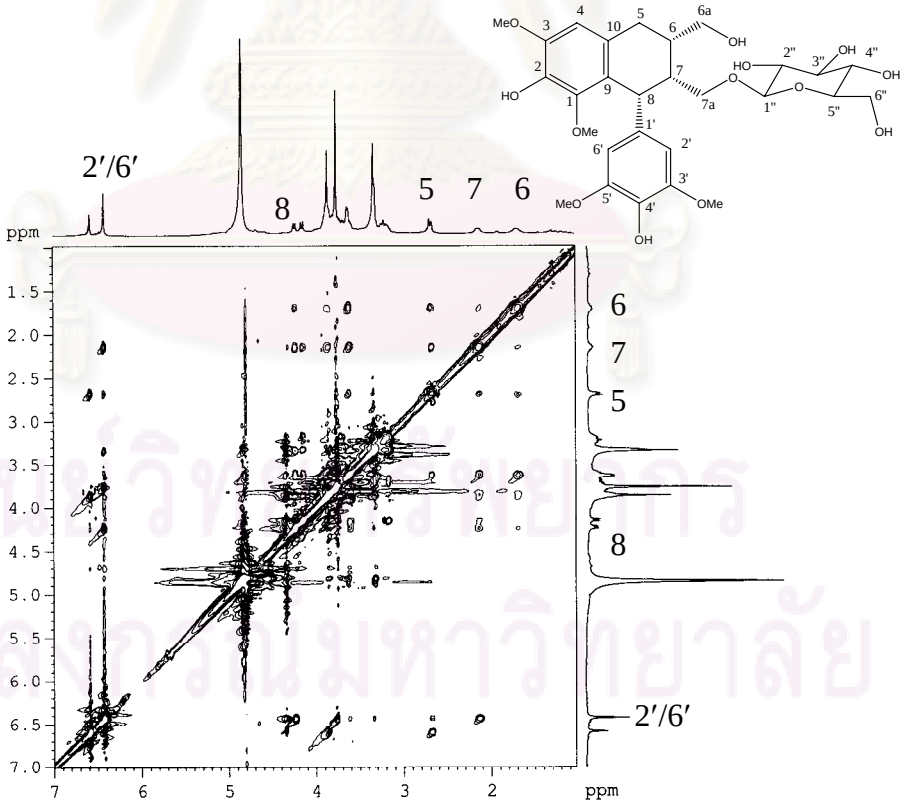

Figure 80 ROESY spectrum of compound CC2 (MeOH-d_4)

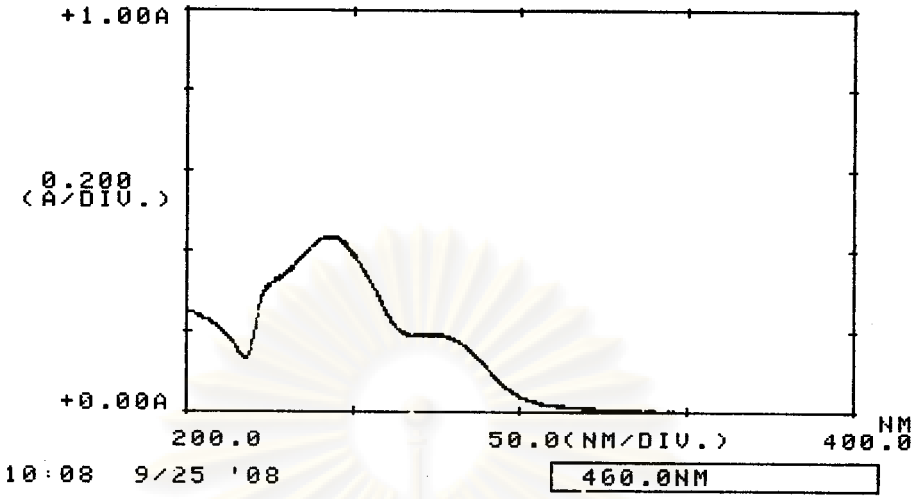

Figure 81 UV spectrum of compound CC3 (methanol)

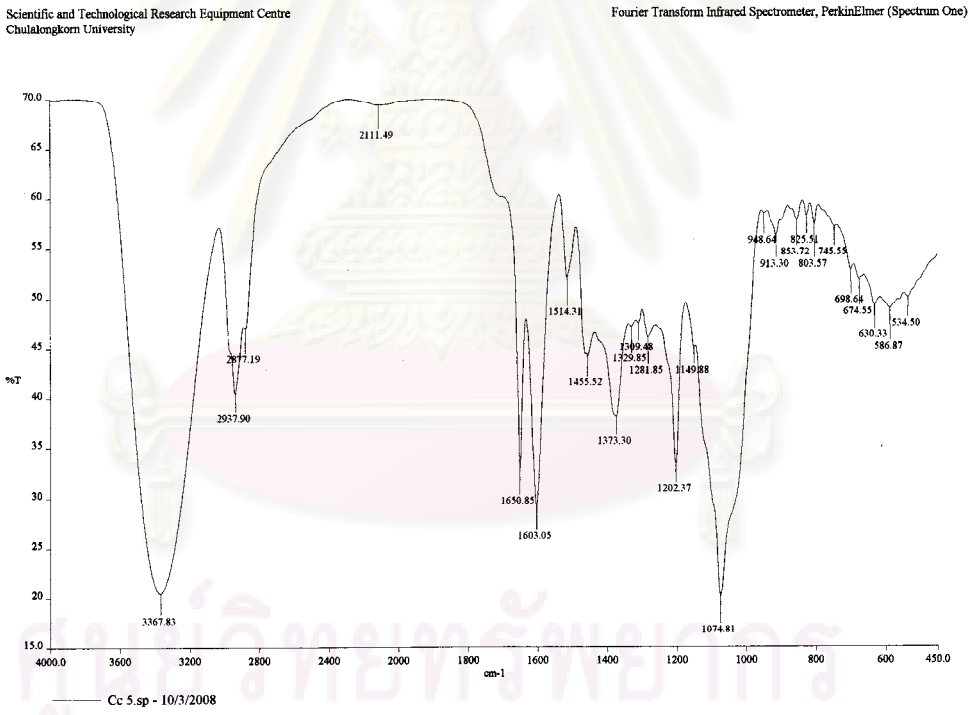

Figure 82 IR spectrum of compound CC3 (KBr disc)

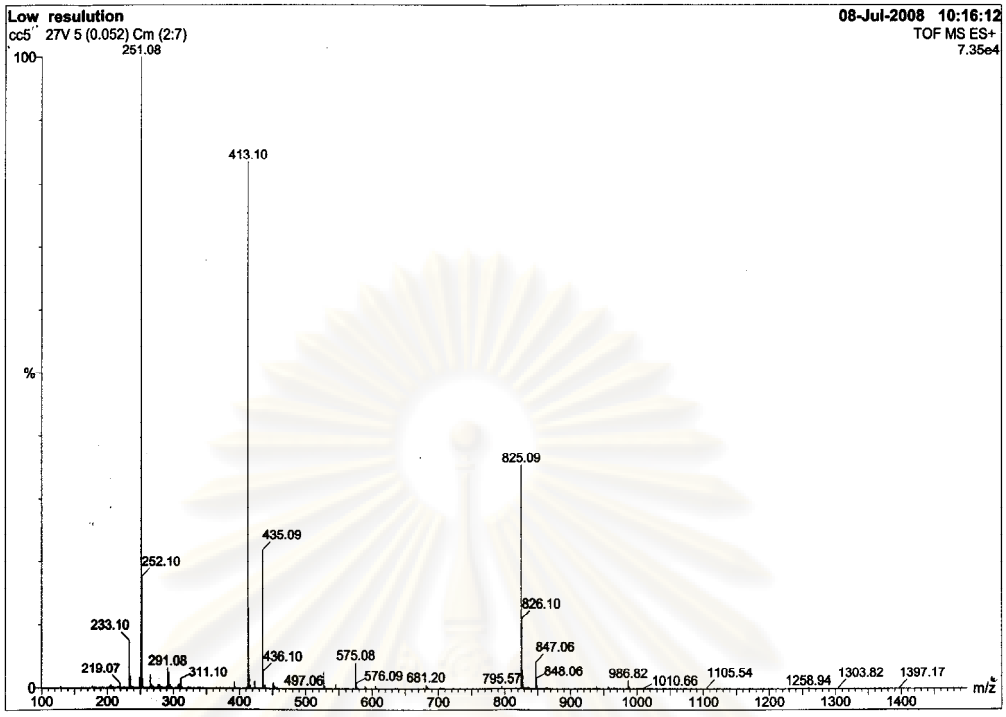

Figure 83 ESI mass spectrum of compound CC3

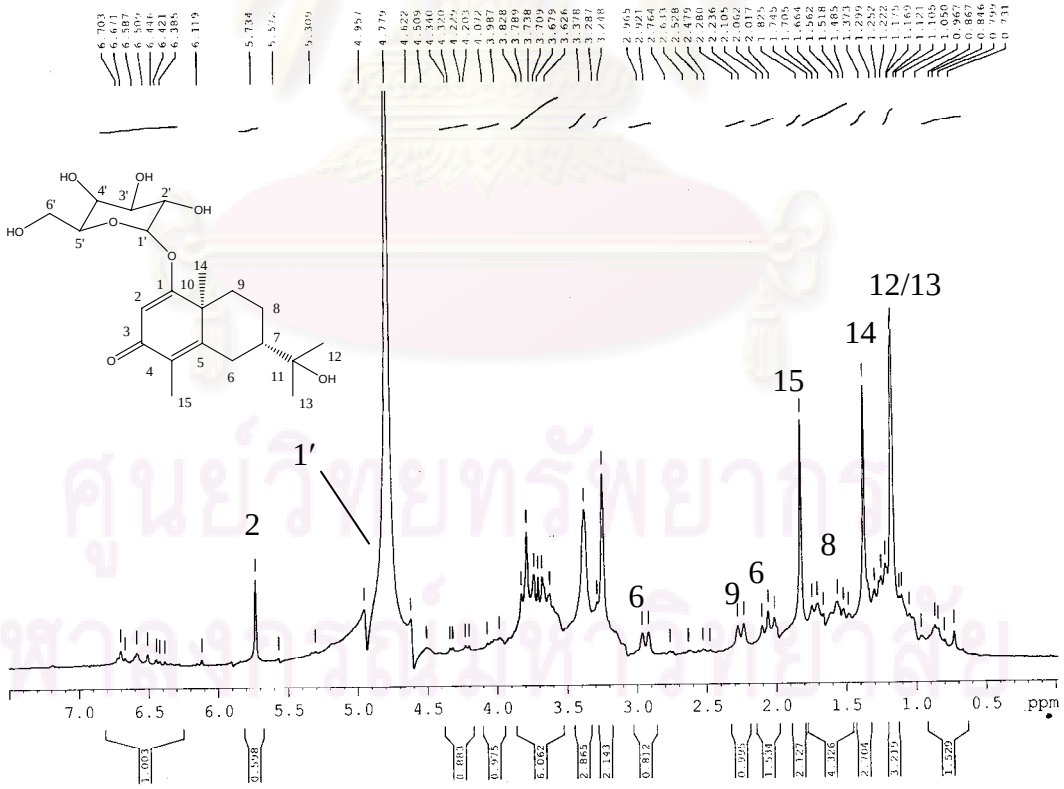

Figure 84 ^{1}H-NMR (300 MHz) spectrum of compound CC3 (MeOH-d_4)

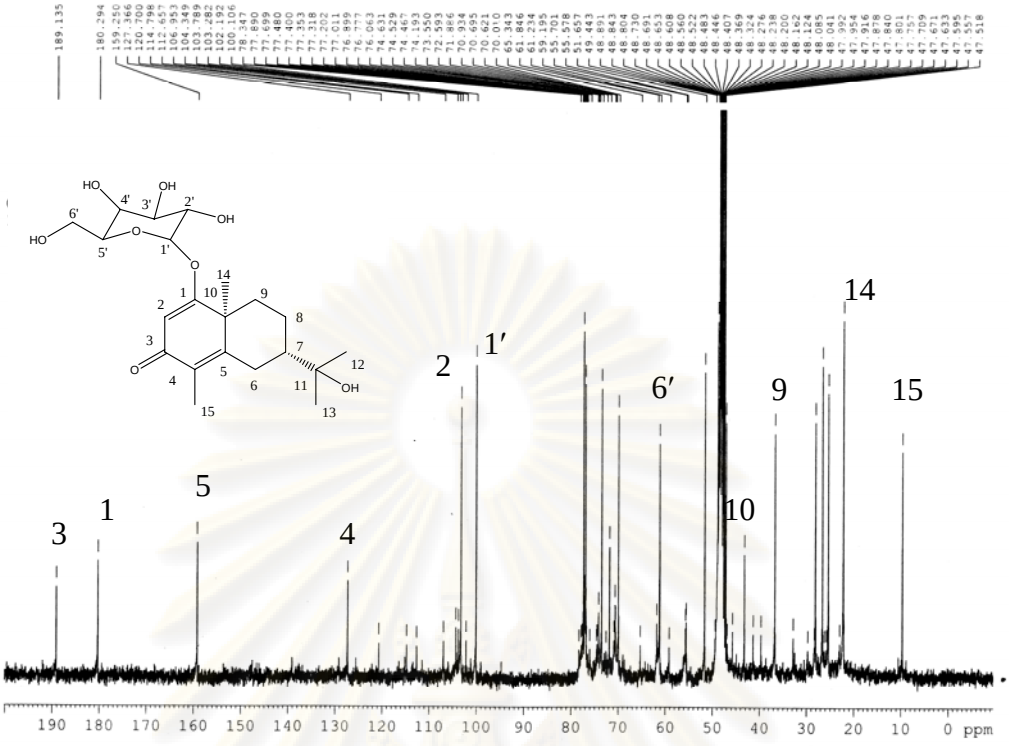

Figure 85 ^{13}C-NMR (75 MHz) spectrum of compound CC3 (MeOH-d_4)

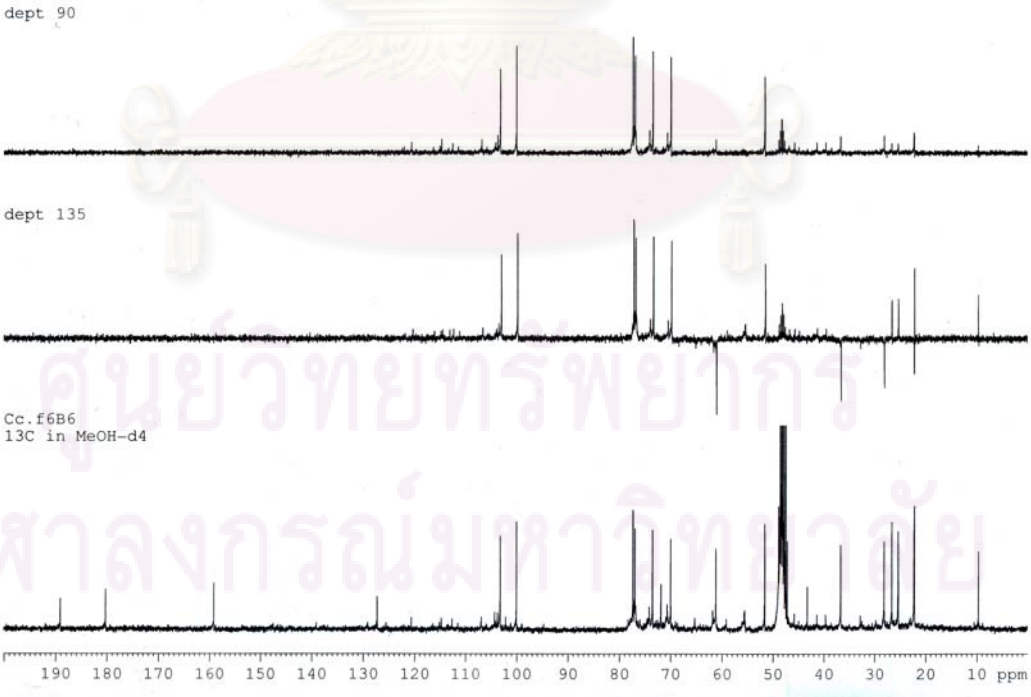

Figure 86 ^{13}C-NMR (75 MHz) and DEPT spectra of compound CC3 (MeOH-d_4)

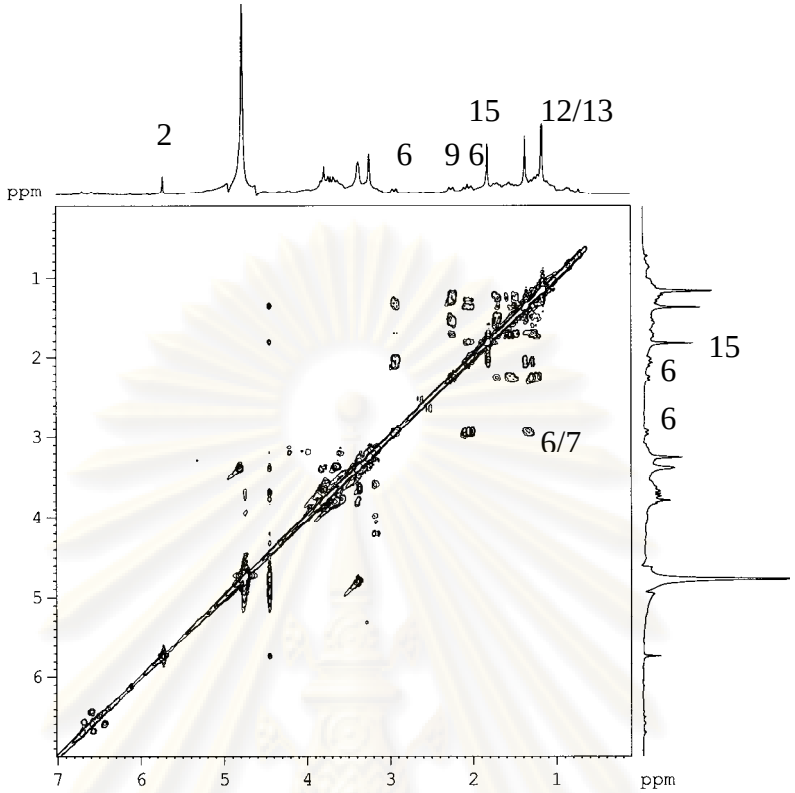

Figure 87 ^{1}H-^{1}H COSY spectrum of compound CC3 (MeOH-d_4)

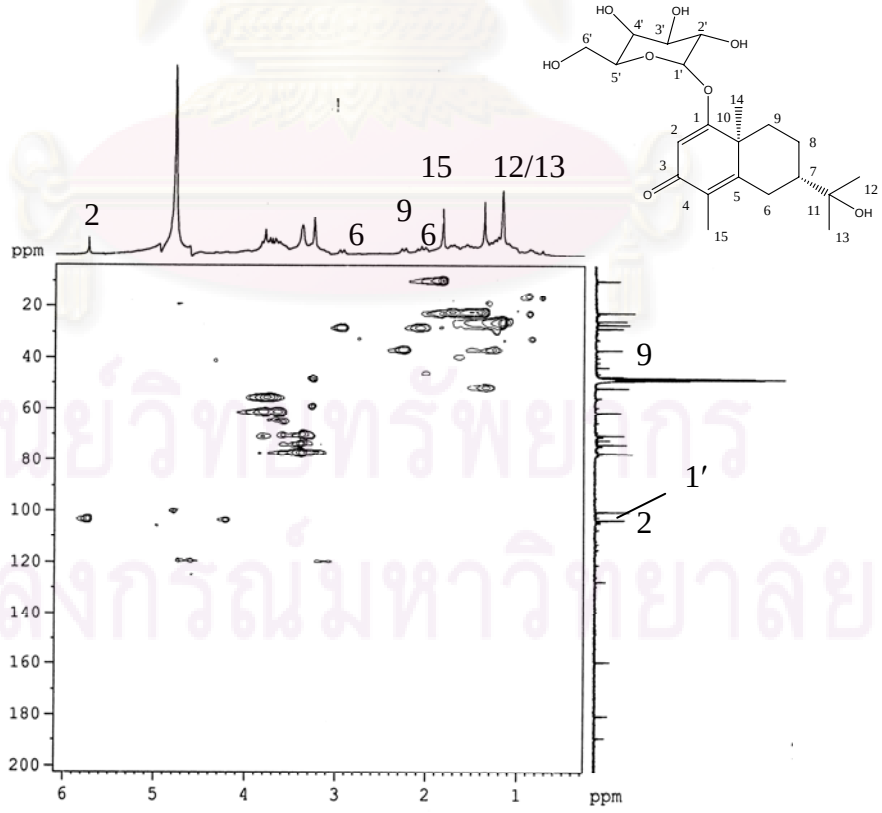

Figure 88 HMQC spectrum of compound CC3 (MeOH-d_4)

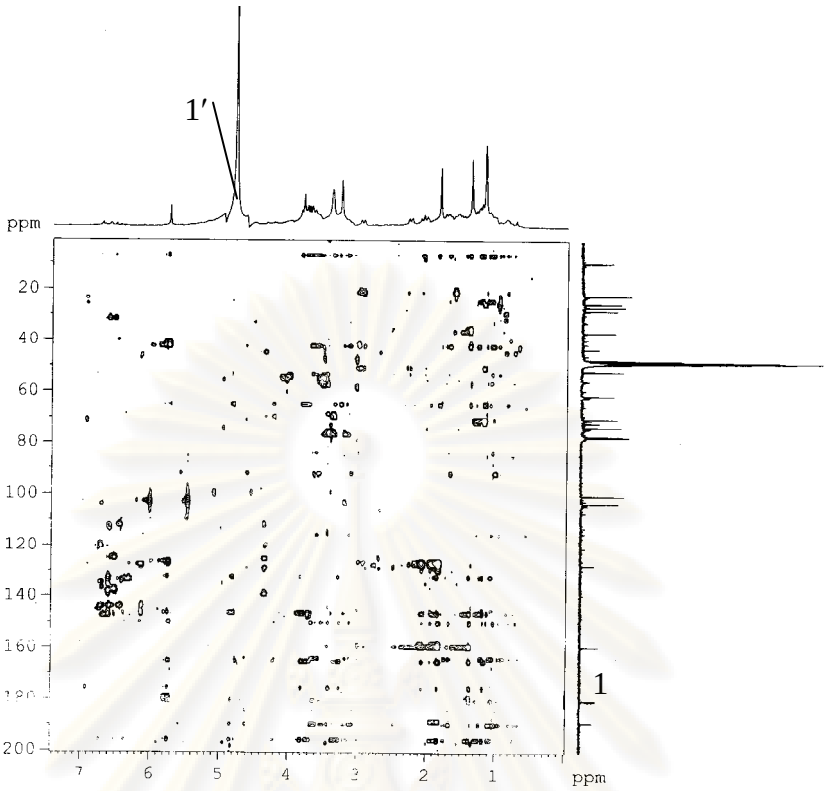

Figure 89 HMBC spectrum of compound CC3 (MeOH-d_4)
[δ_H 0-7.5 ppm, δ_C 10-200 ppm]

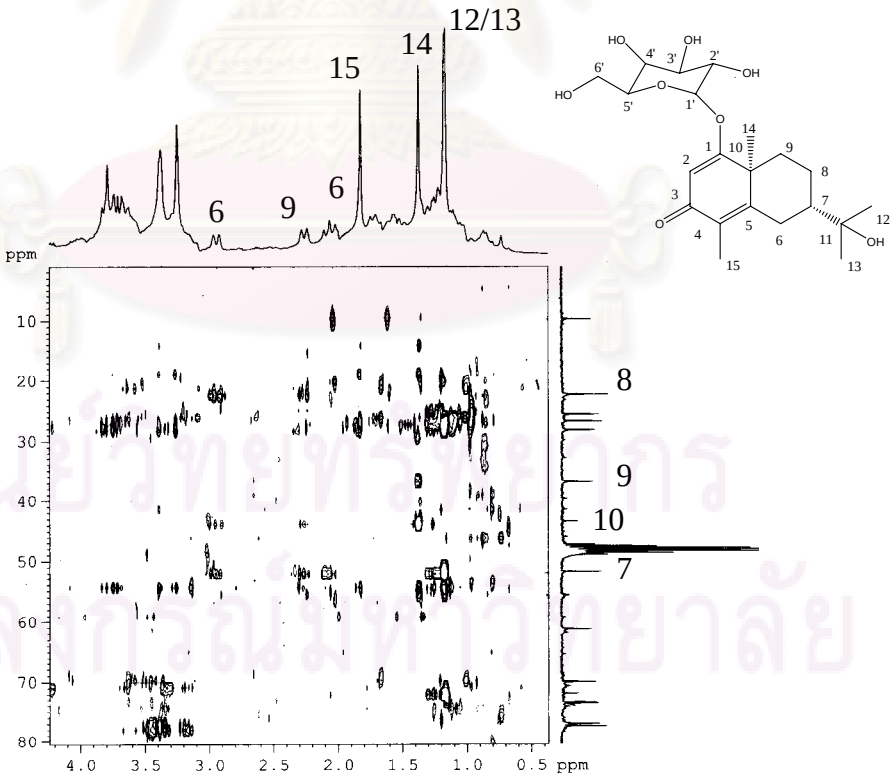

Figure 90 HMBC spectrum of compound CC3 (MeOH-d_4)
[δ_H 0-4.1 ppm, δ_C 0-80 ppm]

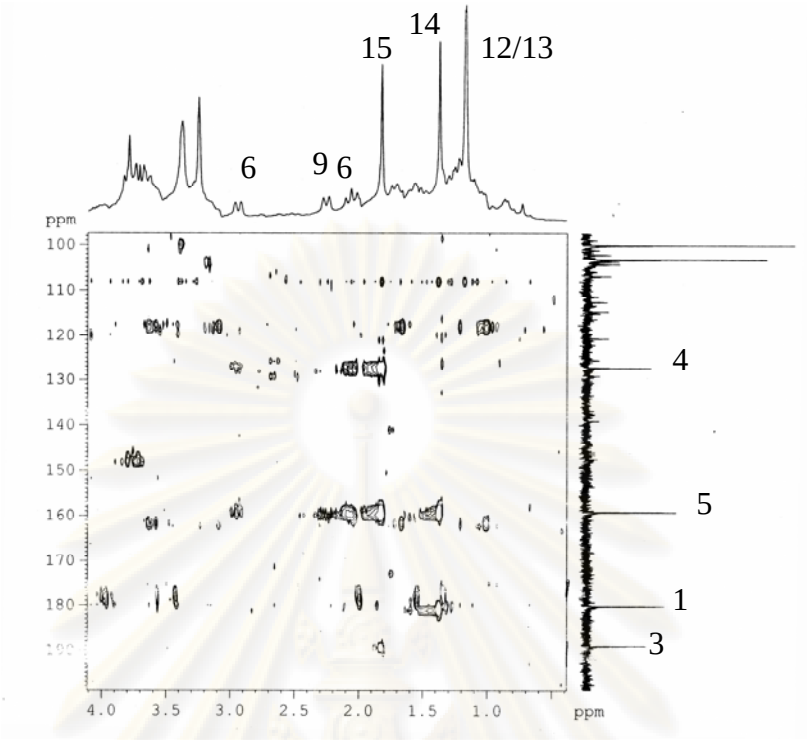

Figure 91 HMBC spectrum of compound CC3 (MeOH-d_4)
[δ_H 0-4.1 ppm, δ_C 98-200 ppm]

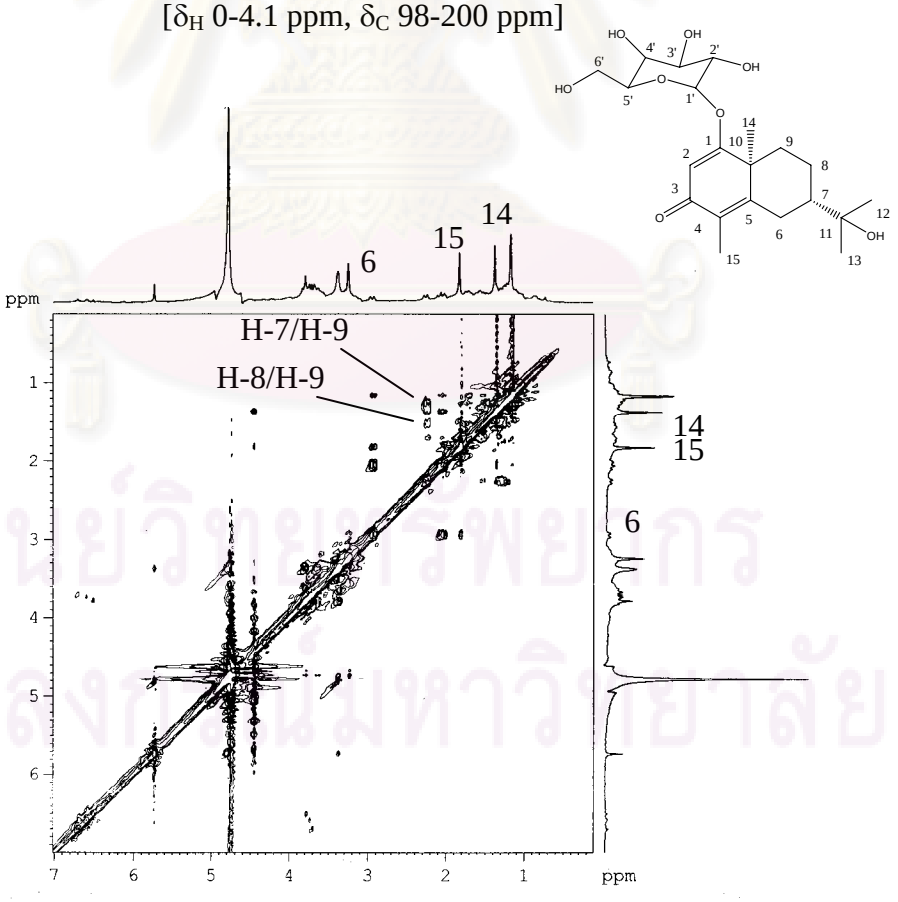

Figure 92 NOESY spectrum of compound CC3 (MeOH-d_4)

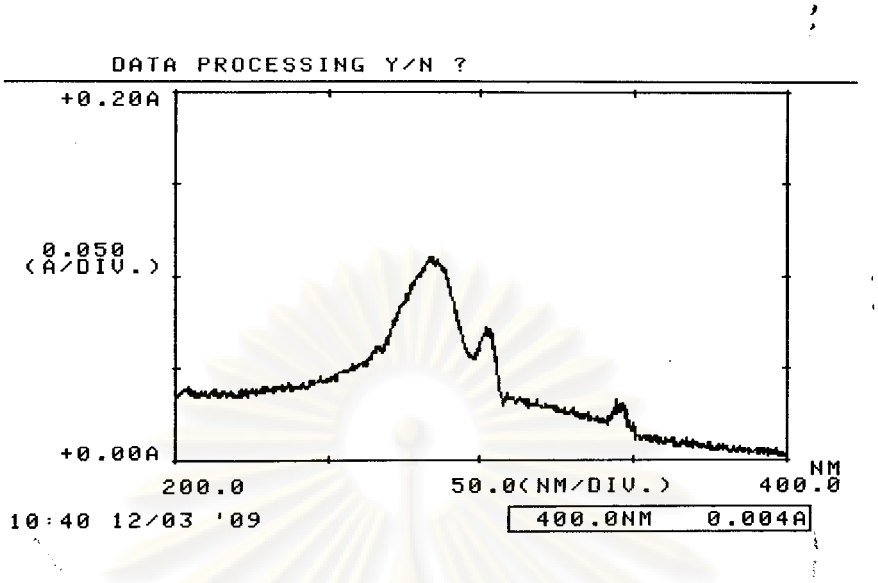

Figure 93 UV spectrum of compound CC4 and CS3 (methanol)

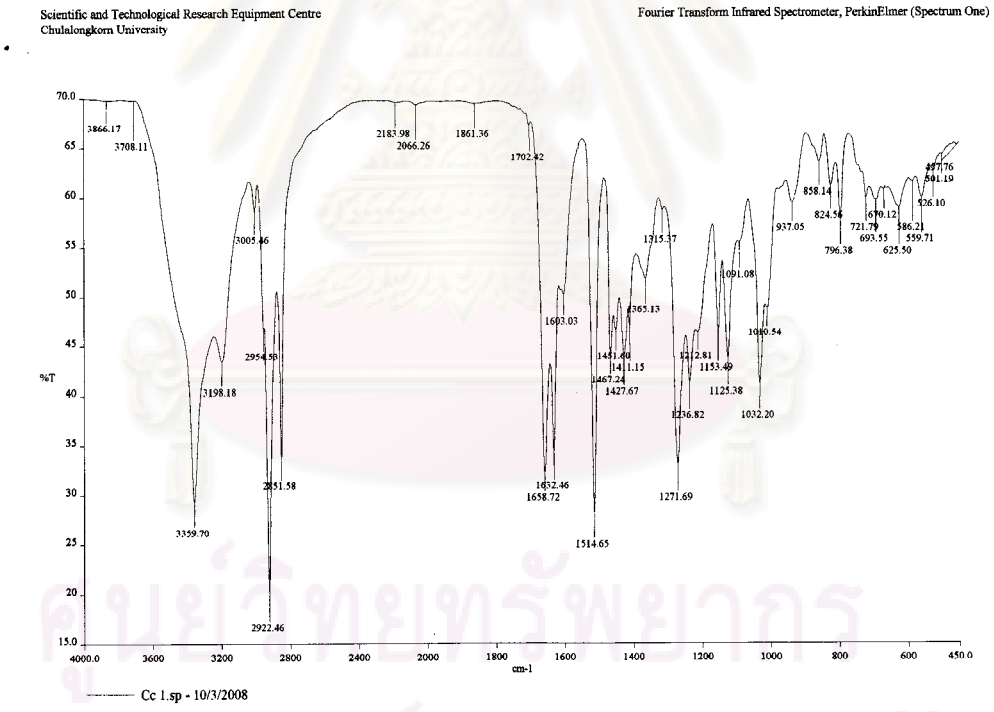

Figure 94 IR spectrum of compound CC4 and CS3 (KBr disc)

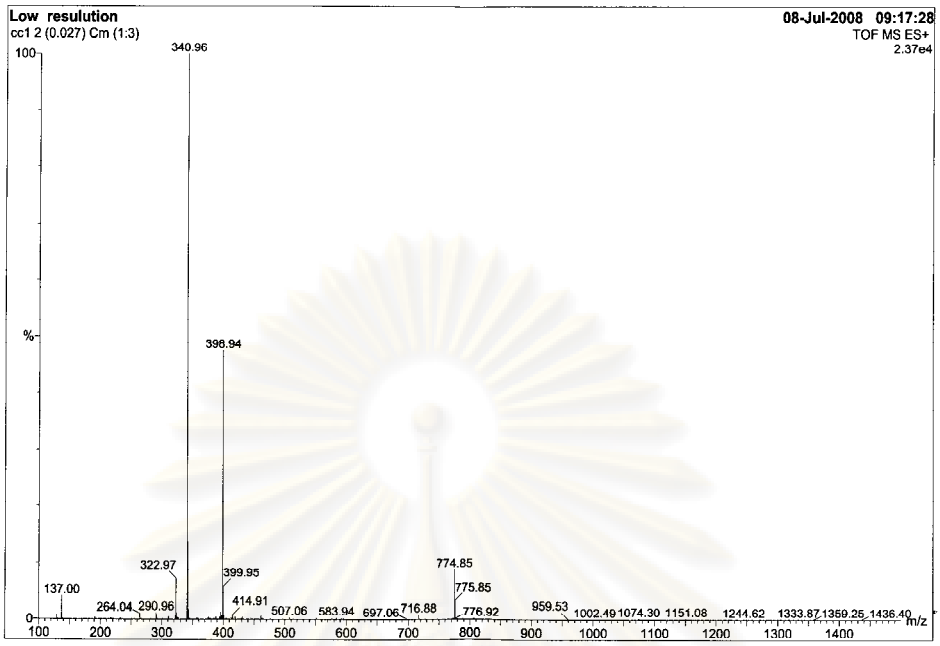

Figure 95 ESI mass spectrum of compound CC4 and CS3

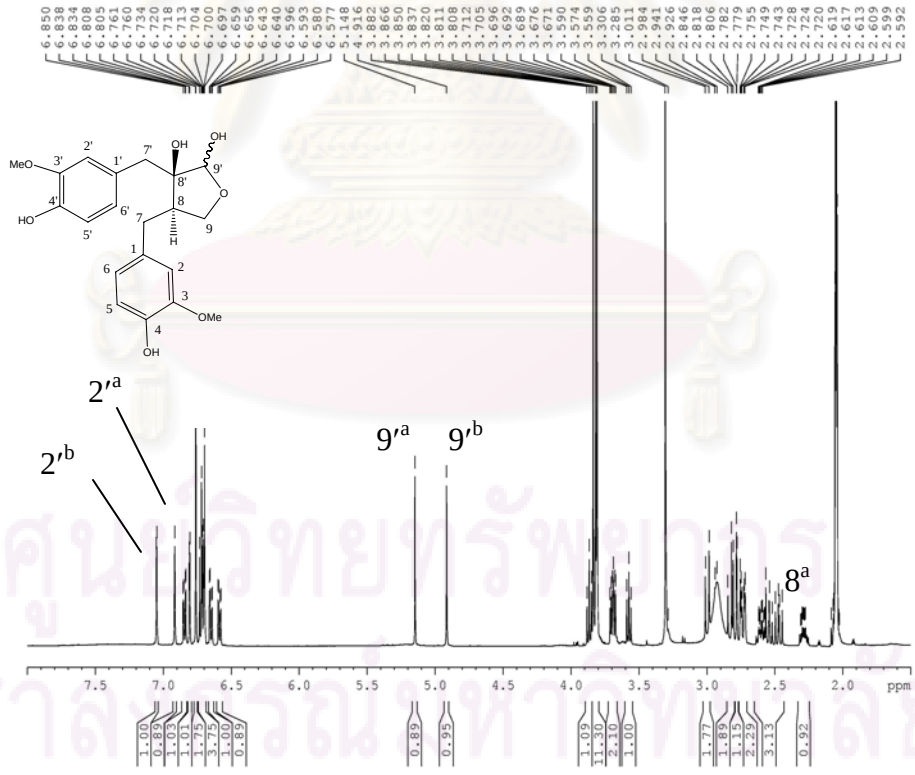

Figure 96 ^{1}H-NMR (500 MHz) spectrum of compound CC4 and CS3 (acetone-d_6)

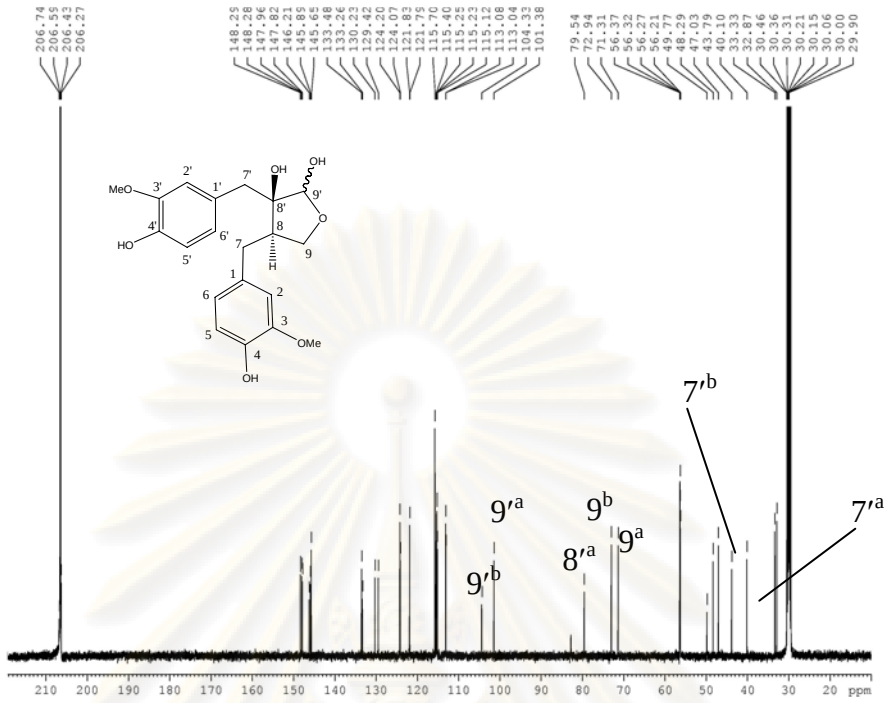

Figure 97 ^{13}C-NMR (125 MHz) spectrum of compound CC4 and CS3 (acetone-d_6)

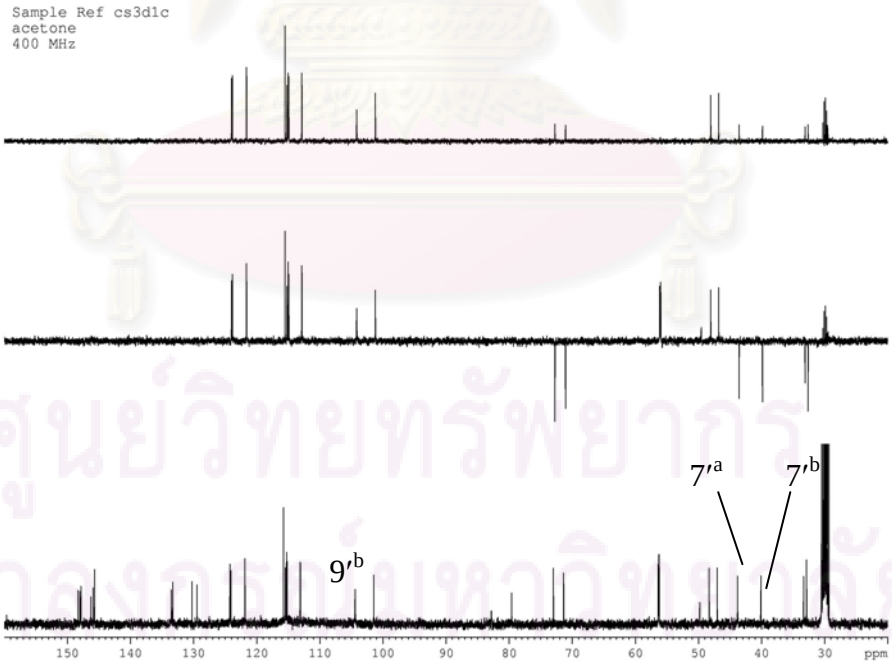

Figure 98 ^{13}C-NMR (125 MHz) and DEPT spectra of compound CC4 and CS3 (acetone-d_6)

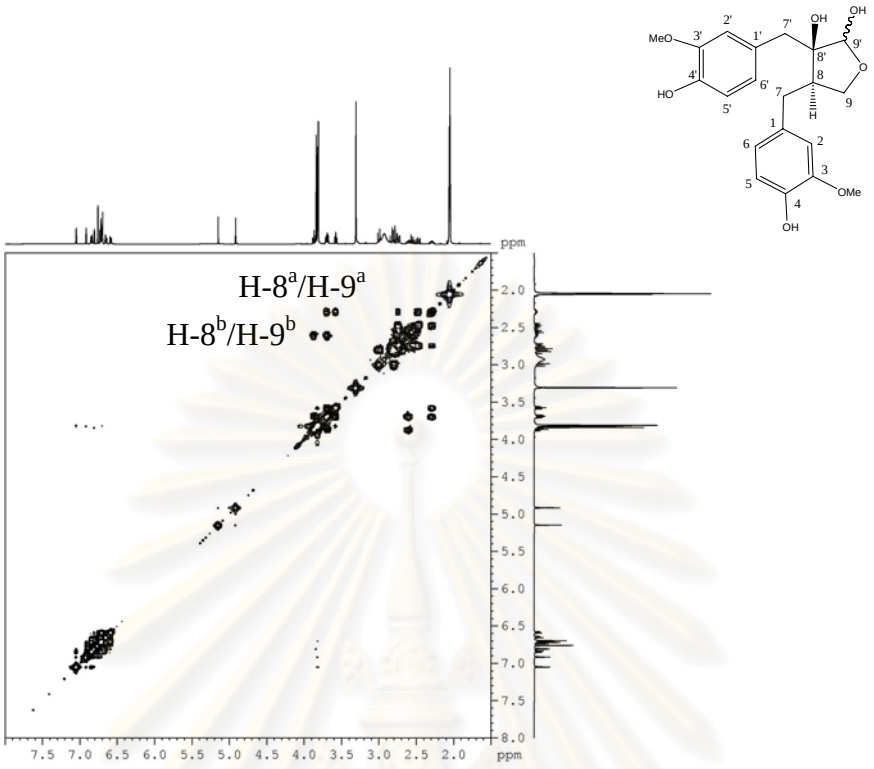

Figure 99 ^{1}H-^{1}H COSY spectrum of compound CC4 and CS3 (acetone-d_6)

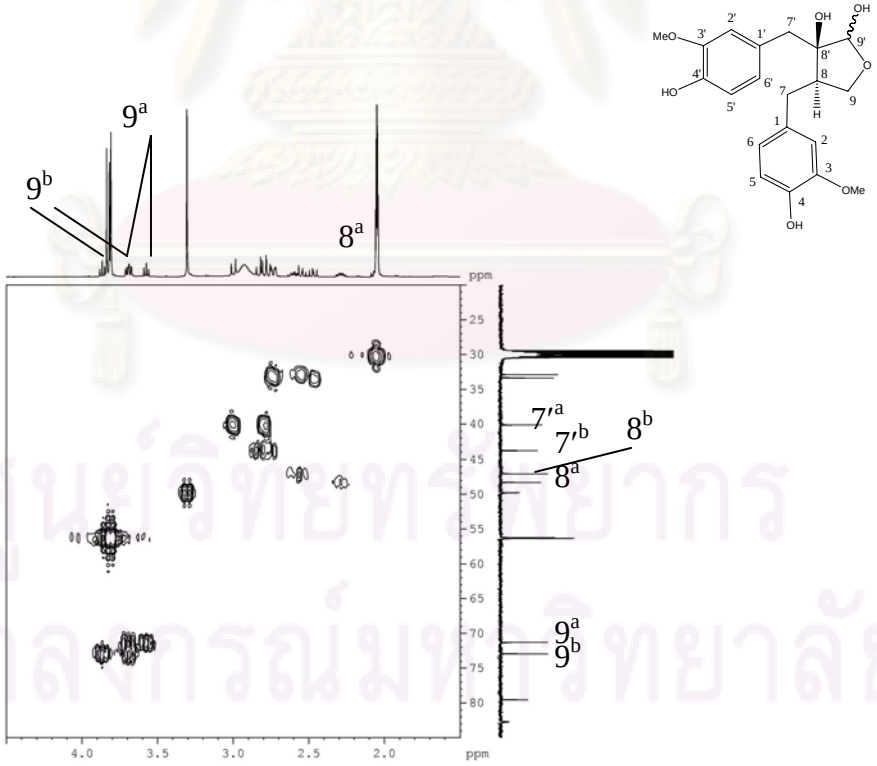

Figure 100 HMQC spectrum of compound CC4 and CS3 (acetone-d_6)
[δ_H 1.5-4.5 ppm, δ_C 20-85 ppm]

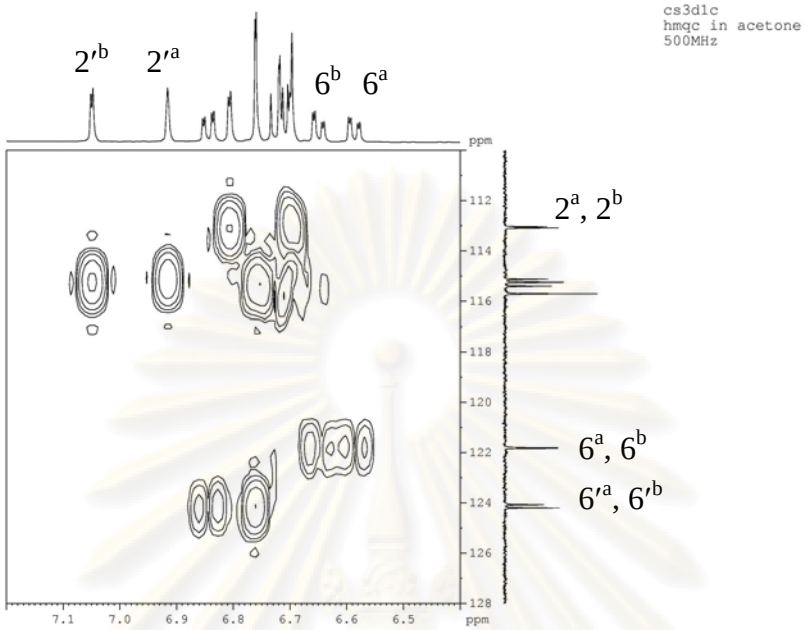

Figure 101 HMQC spectrum of compound CC4 and CS3 (acetone-d_6) [δ_H 6.4-7.2 ppm, δ_C 110-128 ppm]

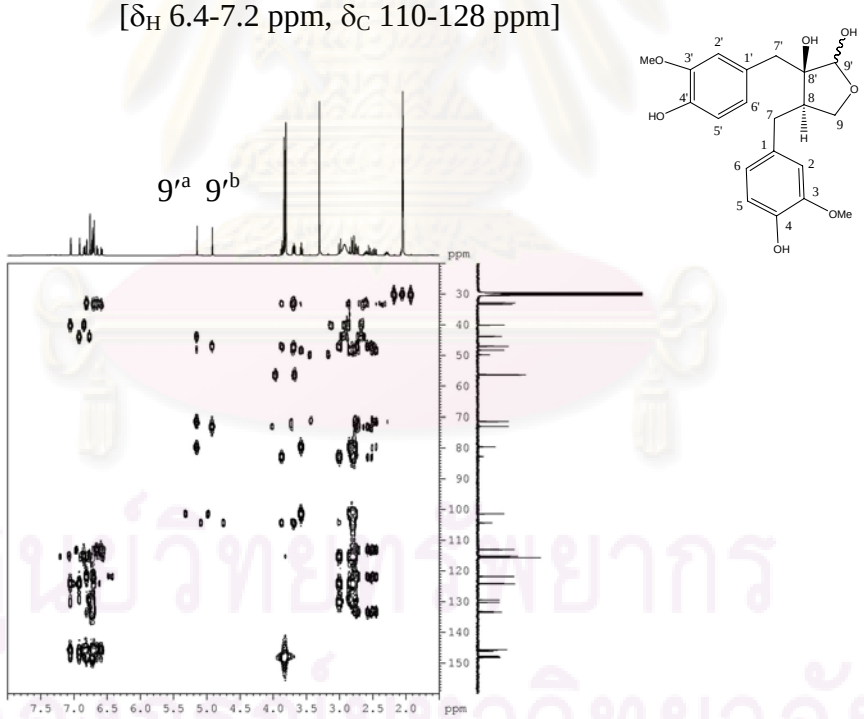

Figure 102 HMBC spectrum of compound CC4 and CS3 (acetone-d_6) [δ_H 1.5-8 ppm, δ_C 20-160 ppm]

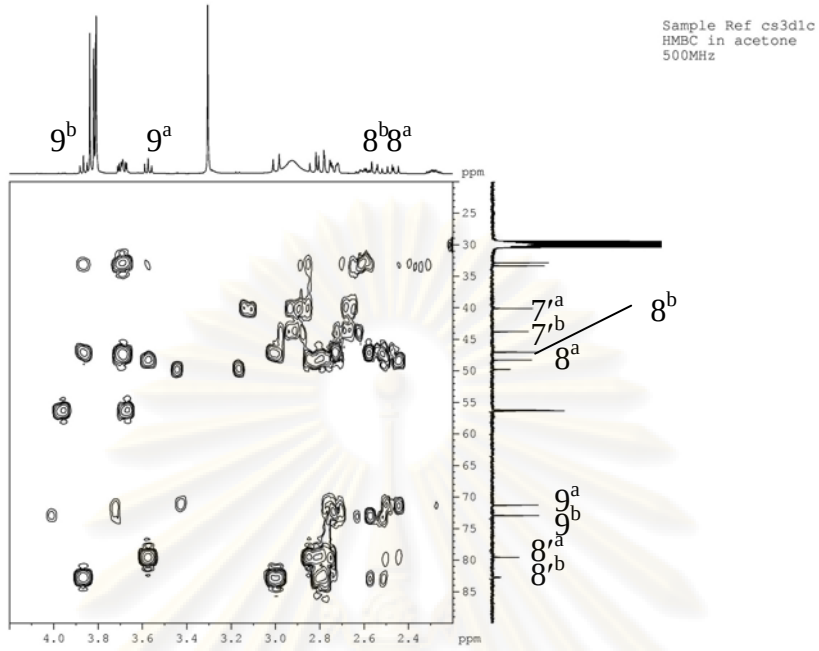

Figure 103 HMBC spectrum of compound CC4 and CS3 (acetone-d_6) [δ_H 2.2-4.2 ppm, δ_C 20-90 ppm]

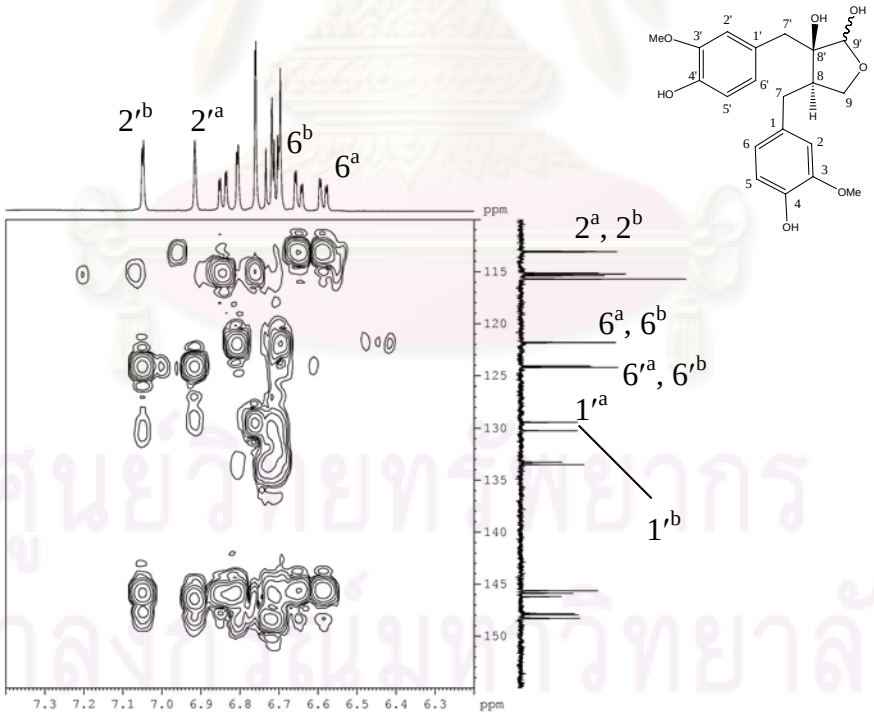

Figure 104 HMBC Spectrum of compound CC4 and CS3 (acetone-d_6) [δ_H 6.2-7.4 ppm, δ_C 114-160 ppm]

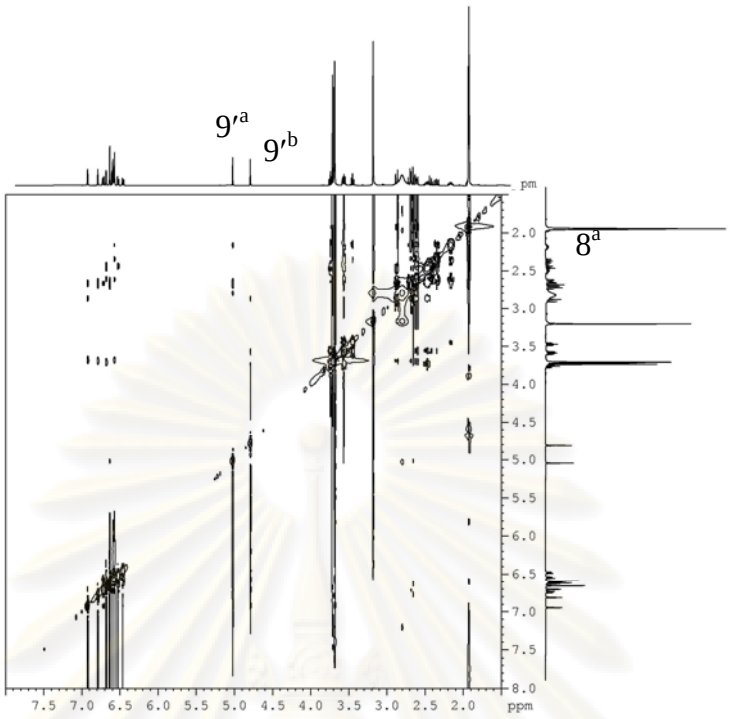

Figure 105 NOESY Spectrum of compound CC4 and CS3 (acetone-d_6)

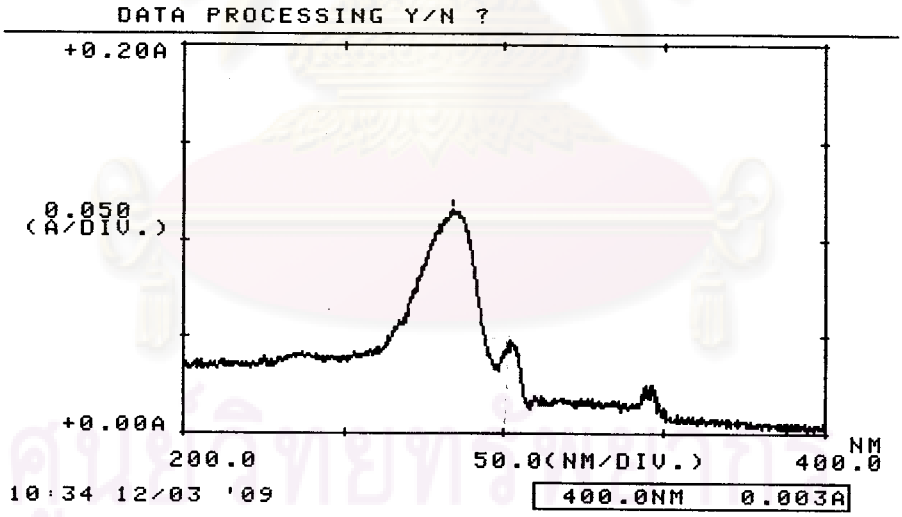

Figure 106 UV spectrum of compound CC5 and CS2 (methanol)

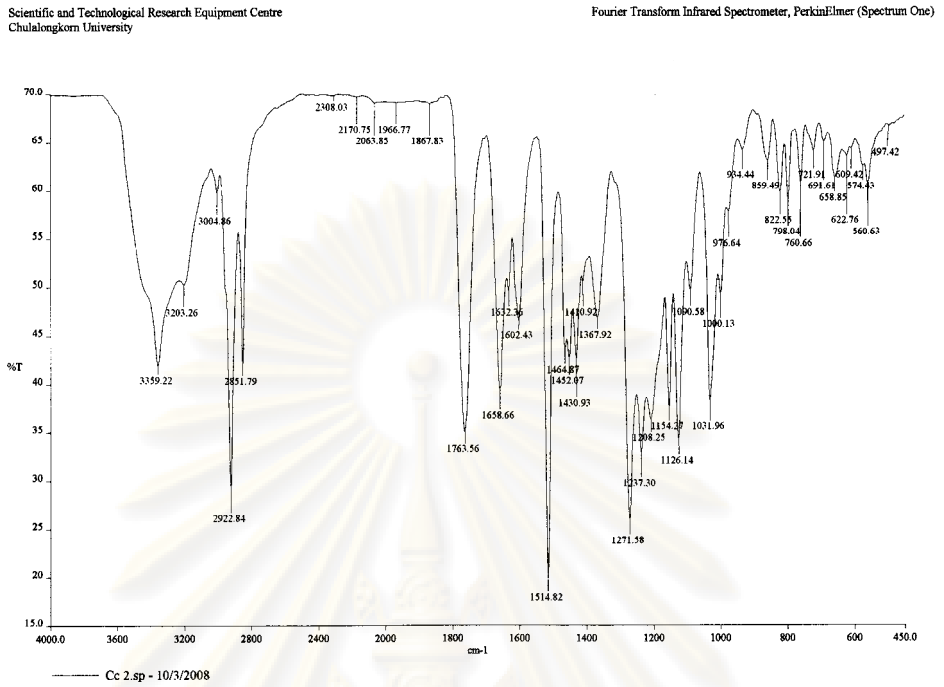

Figure 107 IR spectrum of compound CC5 and CS2 (KBr disc)

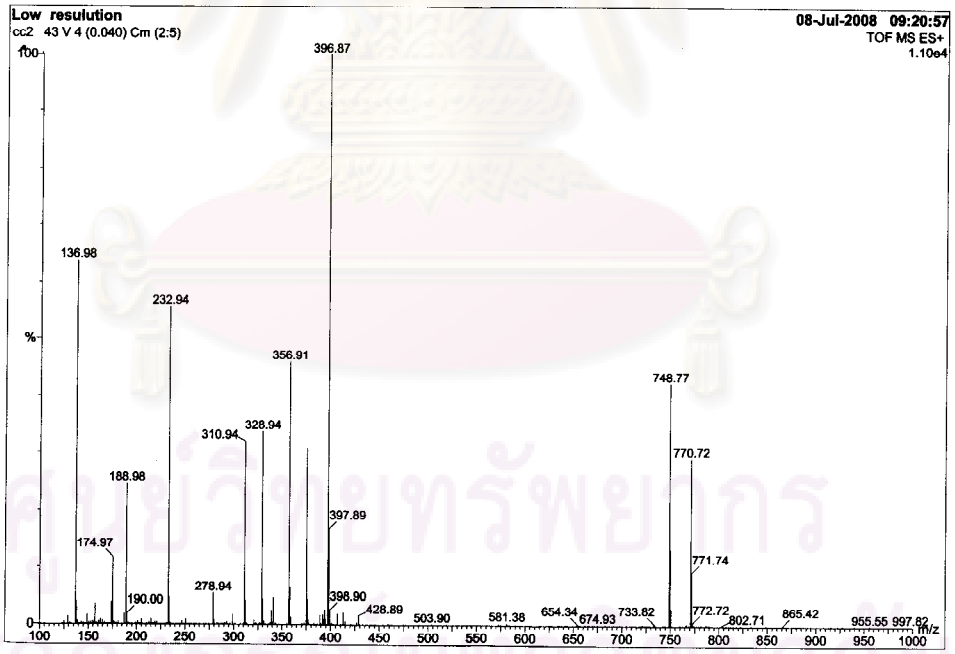

Figure 108 ESI mass spectrum of compound CC5 and CS2

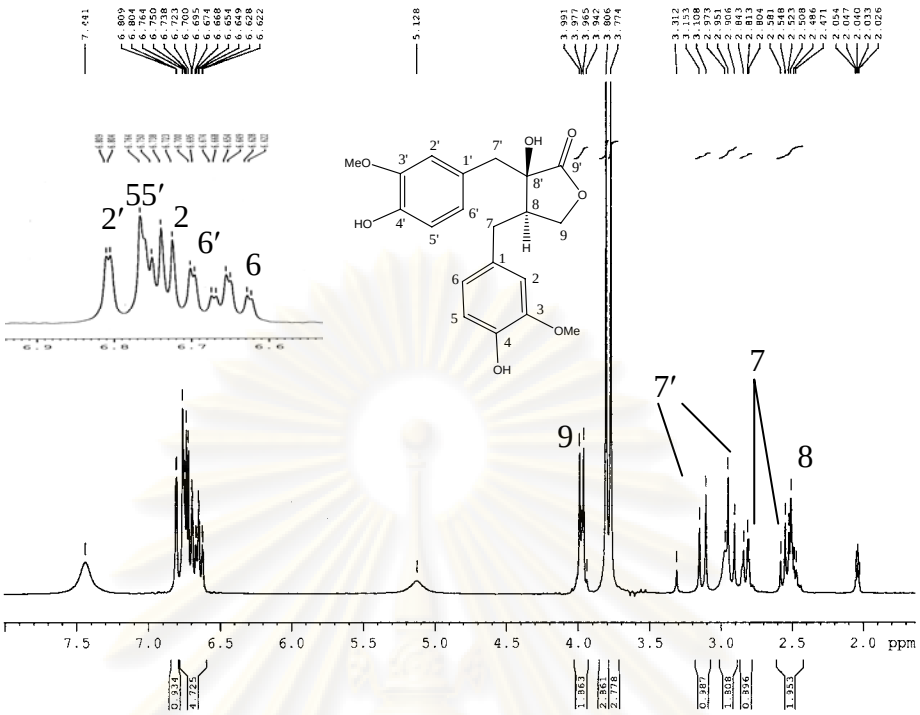

Figure 109 ^{1}H-NMR (300 MHz) spectrum of compound CC5 and CS2 (acetone-d_6)

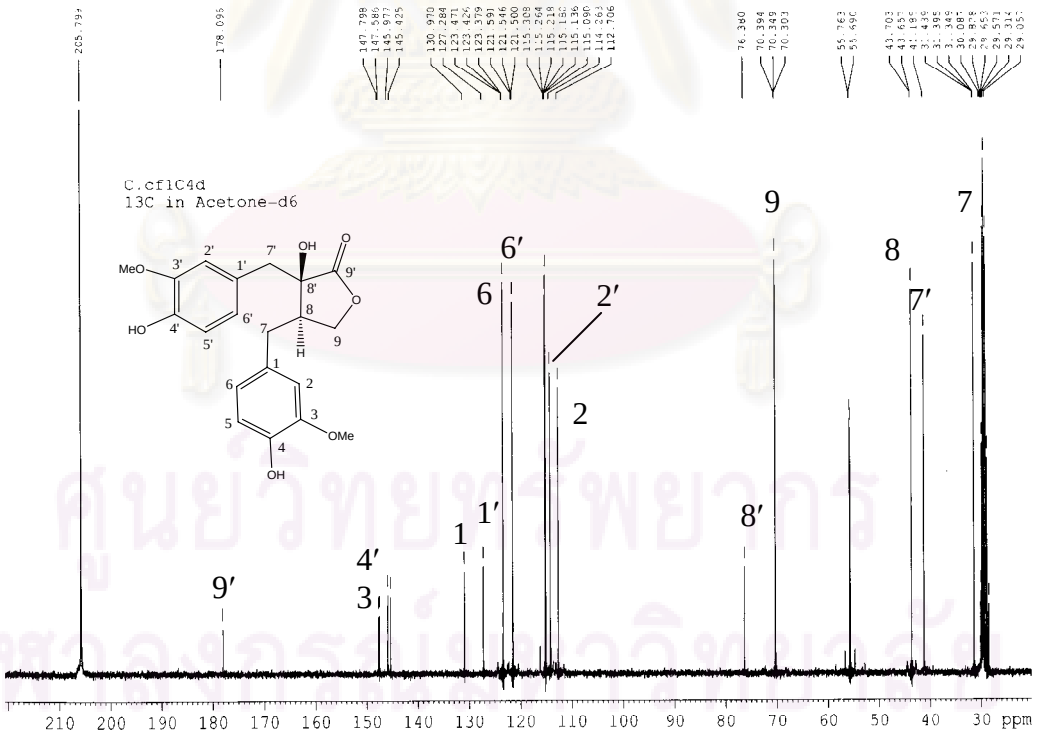

Figure 110 ^{13}C-NMR (75 MHz) spectrum of compound CC5 and CS2 (acetone-d_6)

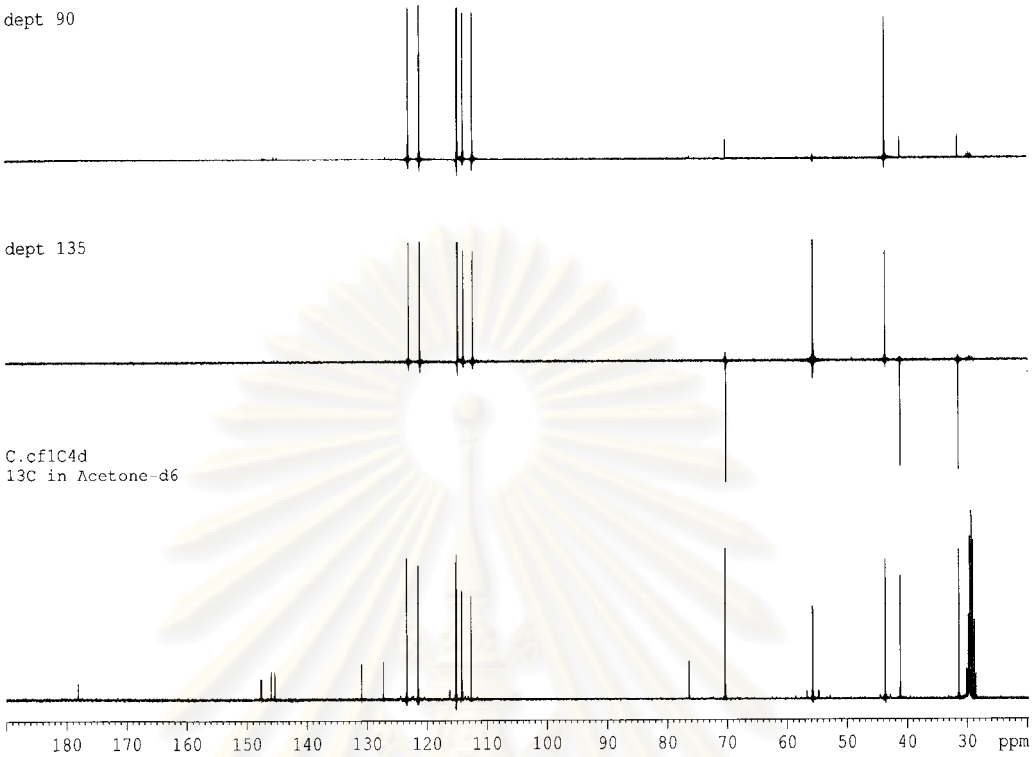

Figure 111 ^{13}C-NMR (75 MHz) and DEPT spectra of compound CC5 and CS2 (acetone-d_6)

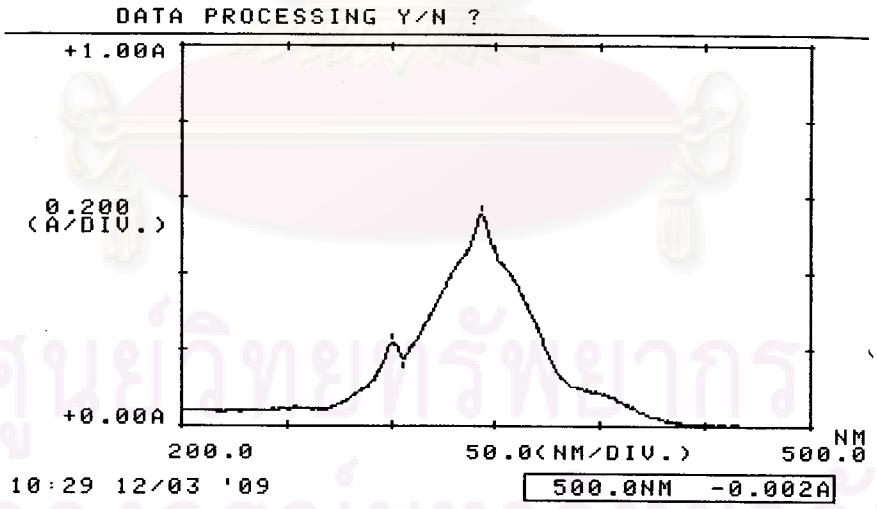

Figure 112 UV spectrum of compound CS1 (methanol)

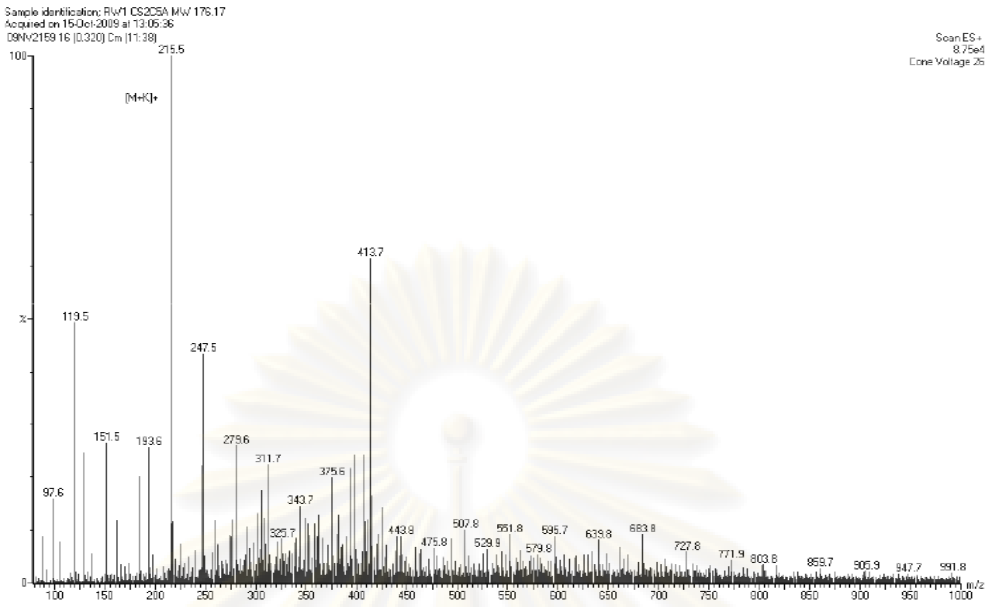

Figure 113 ESI mass spectrum of compound CS1

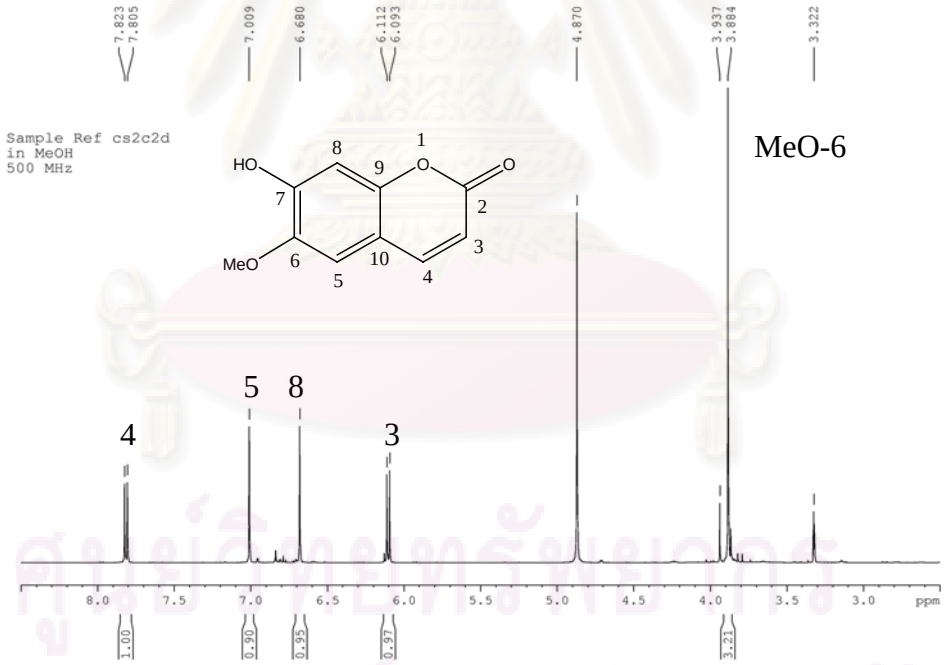

Figure 114 ^{1}H-NMR (500 MHz) spectrum of compound CS1 (MeOH-d_4)

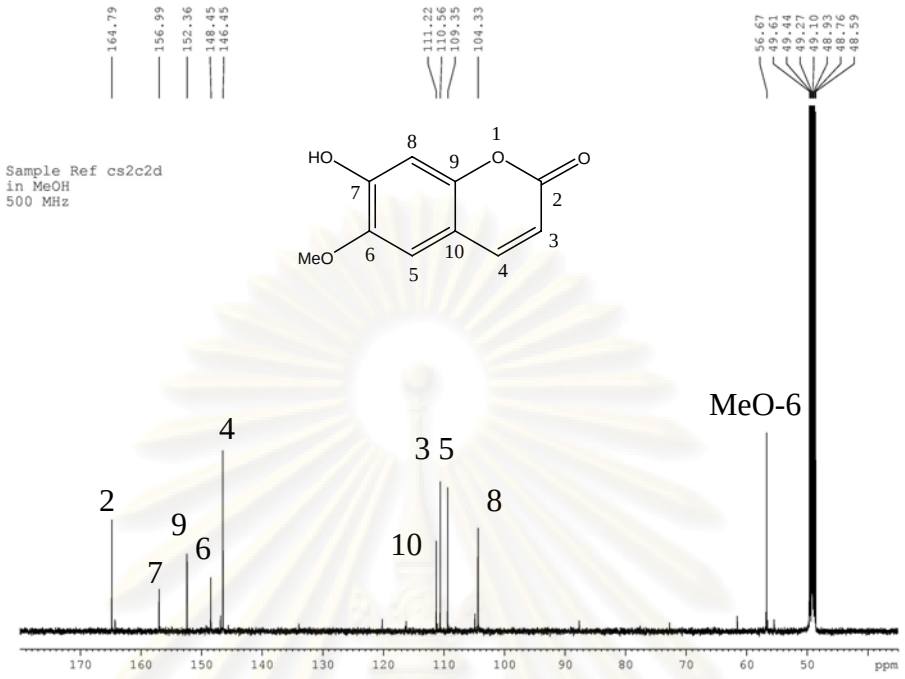

Figure 115 ^{13}C-NMR (125 MHz) spectrum of compound CS1 (MeOH-d_4)

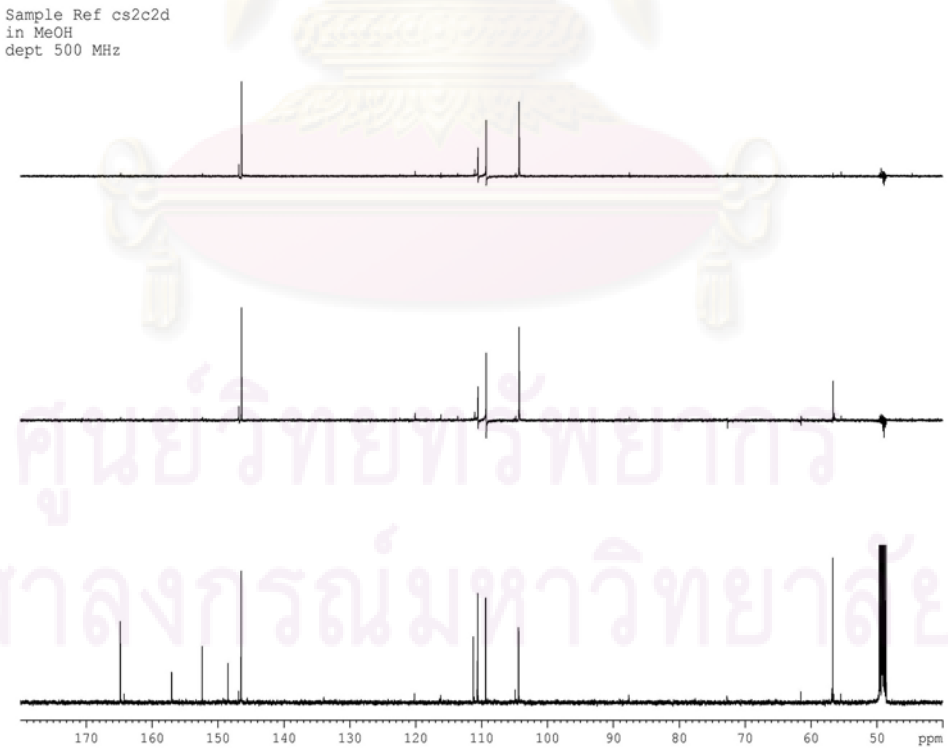

Figure 116 ^{13}C-NMR (125 MHz) and DEPT spectra of compound CS1 (MeOH-d_4)

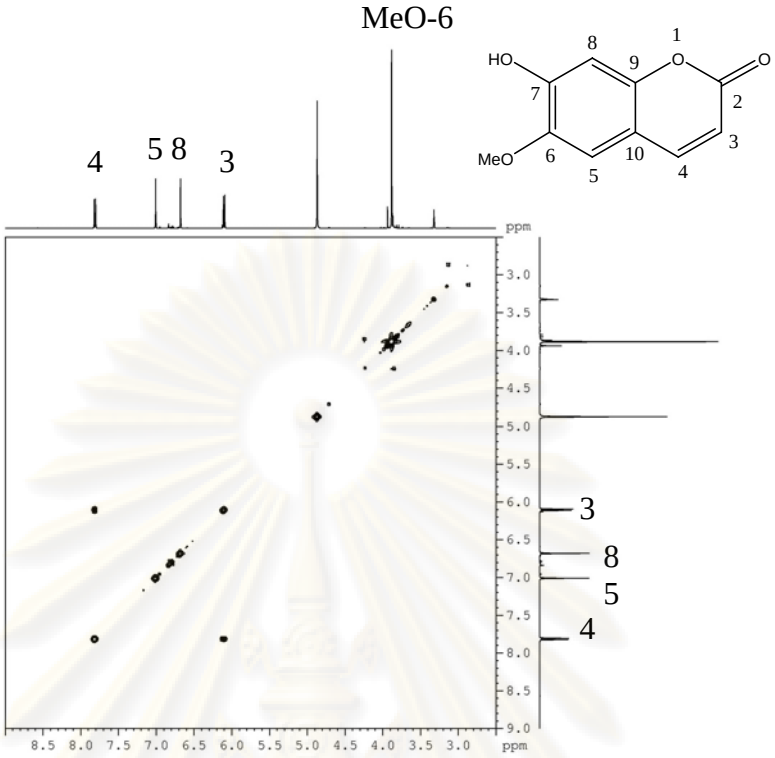

Figure 117 ^{1}H-^{1}H COSY spectrum of compound CS1 (MeOH-d_4)

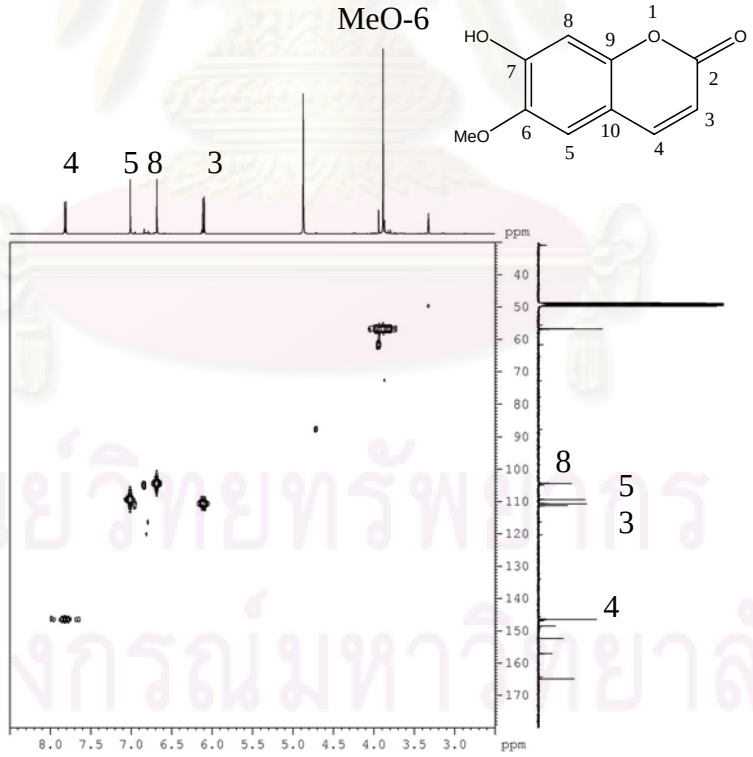

Figure 118 HMQC spectrum of compound CS1 (MeOH-d_4)

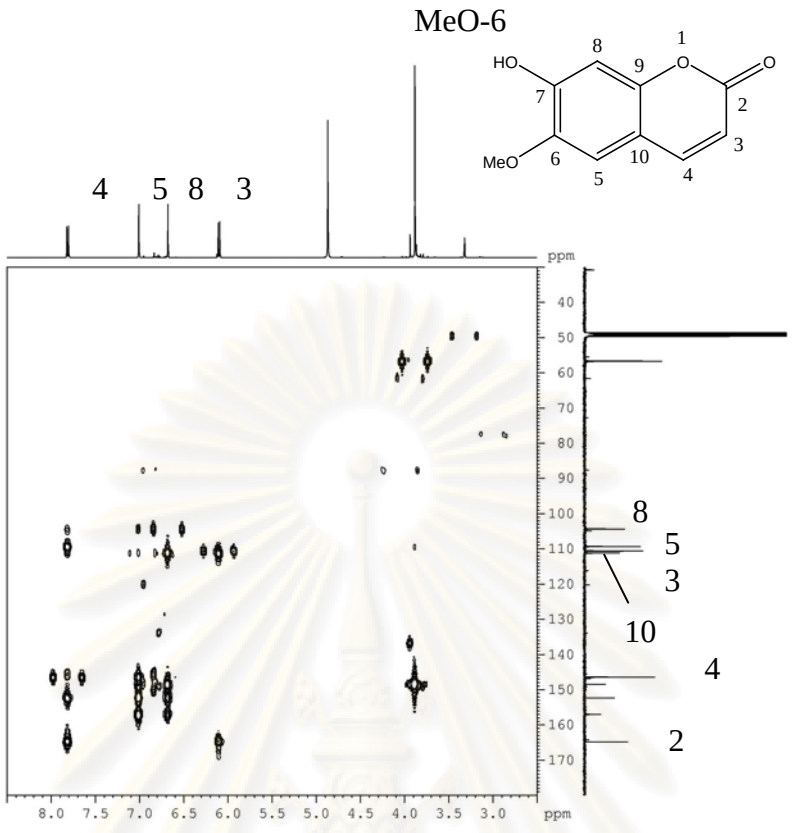

Figure 119 HMBC spectrum of compound CS1 (MeOH-d_4)
[δ_H 2.5-8.5 ppm, δ_C 30-180 ppm]

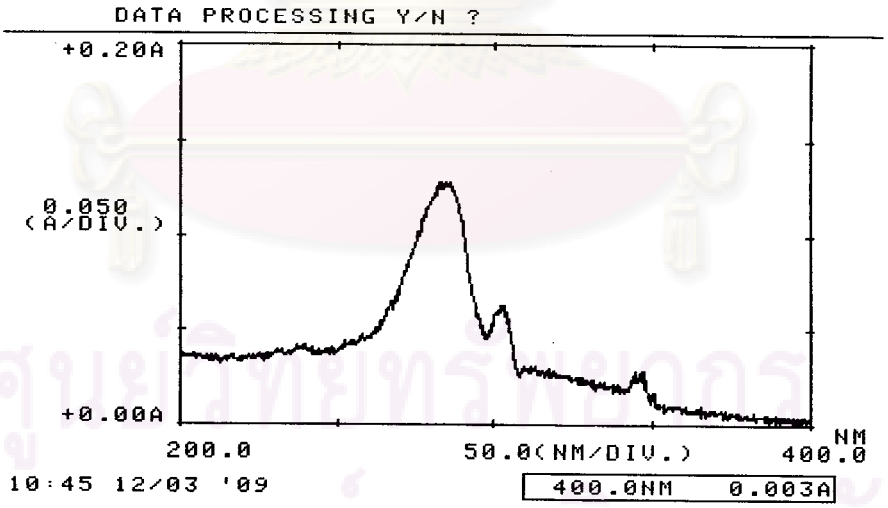

Figure 120 UV spectrum of compound CS4 (methanol)

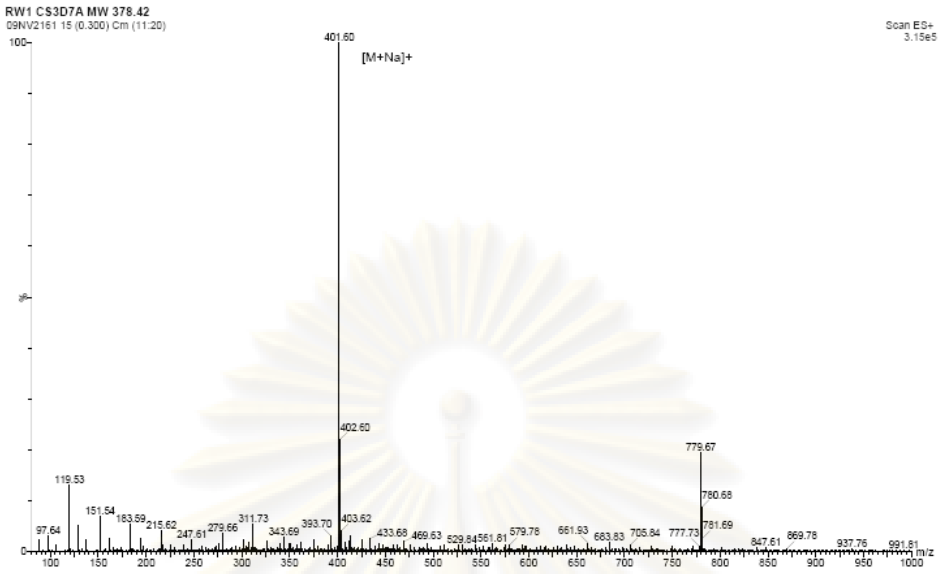

Figure 121 ESI mass spectrum of compound CS4

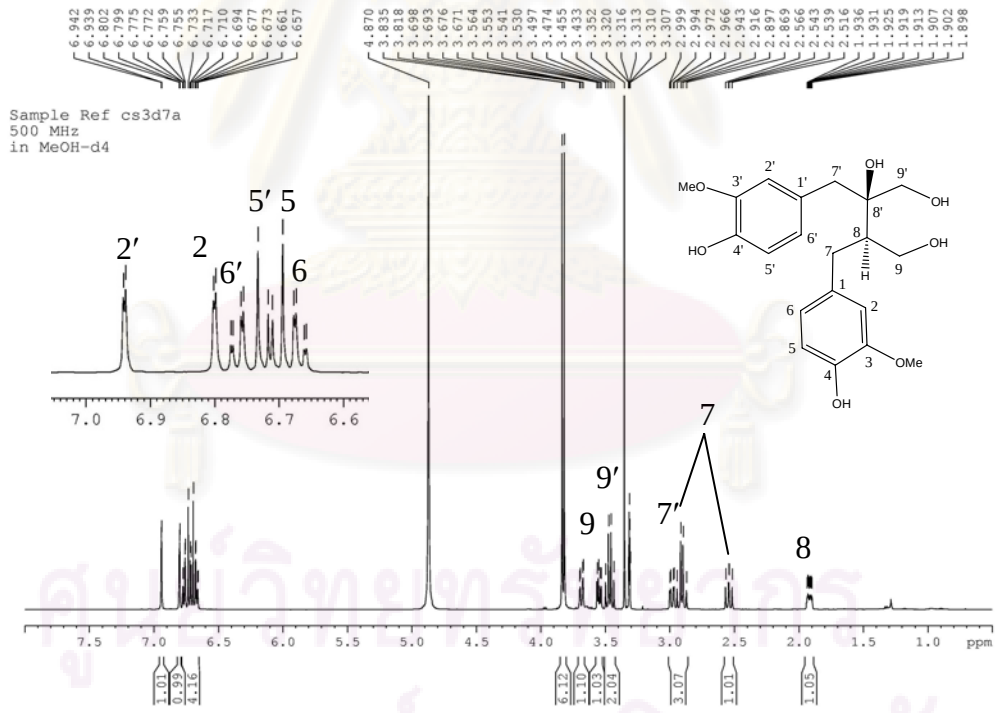

Figure 122 ^{1}H-NMR (500 MHz) spectrum of compound CS4 (MeOH-d_4)

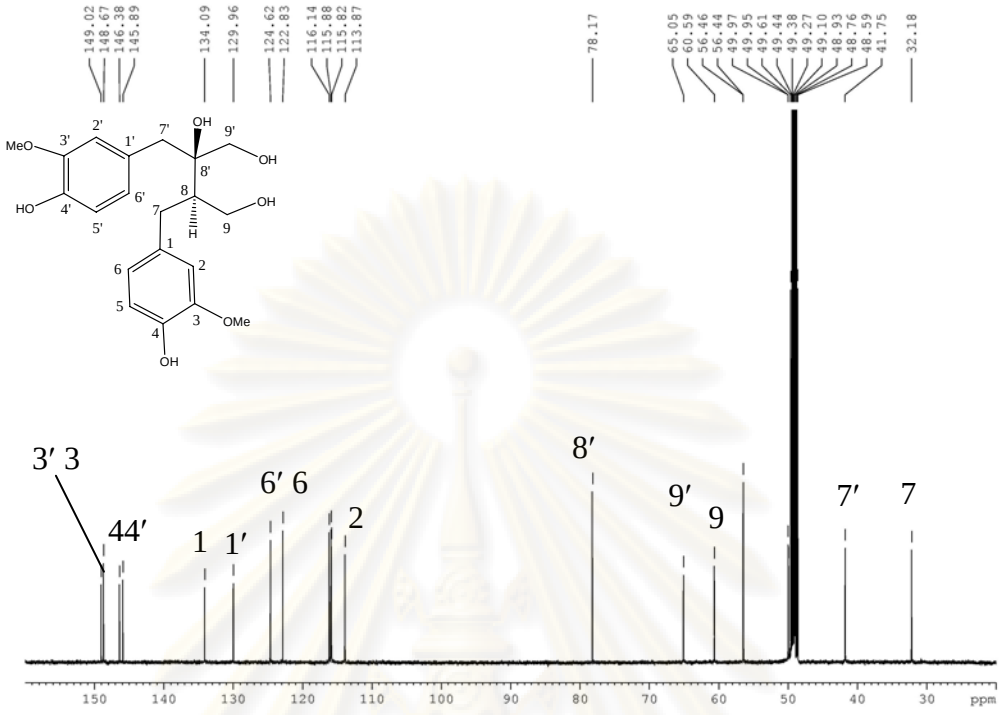

Figure 123 ^{13}C-NMR (125 MHz) spectrum of compound CS4 (MeOH-d_4)

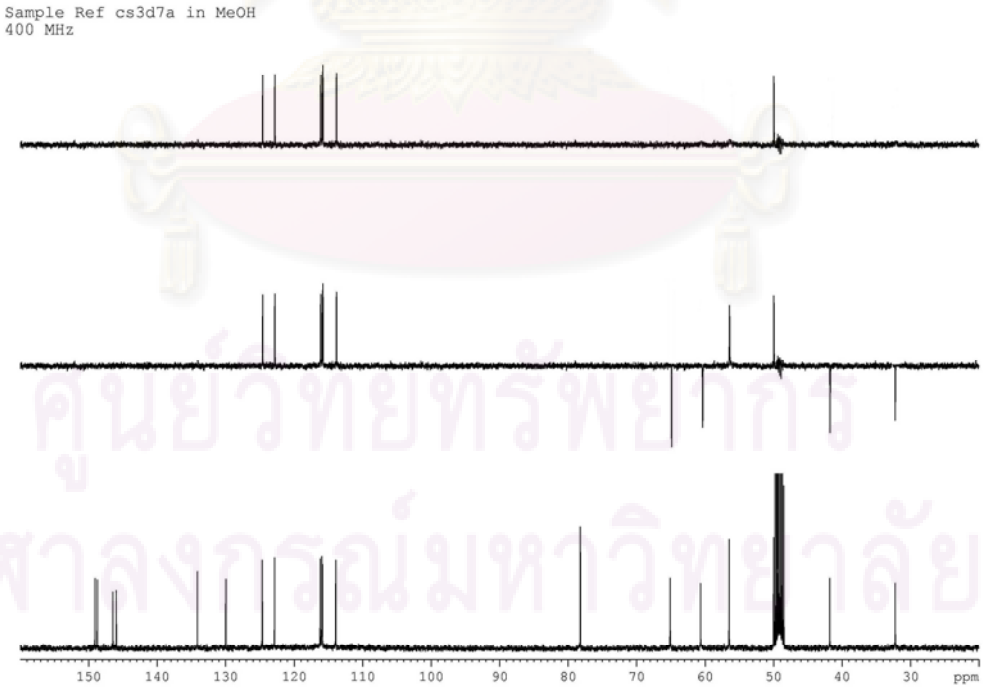

Figure 124 ^{13}C-NMR (100 MHz) and DEPT spectra of compound CS4 (MeOH-d_4)

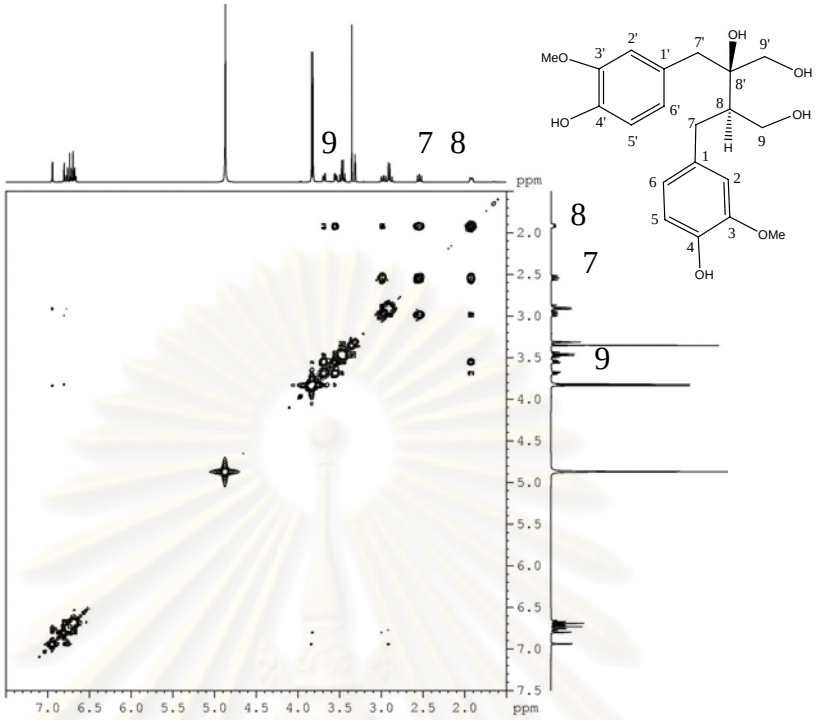

Figure 125 ^{1}H-^{1}H COSY spectrum of compound CS4 (MeOH-d_4)

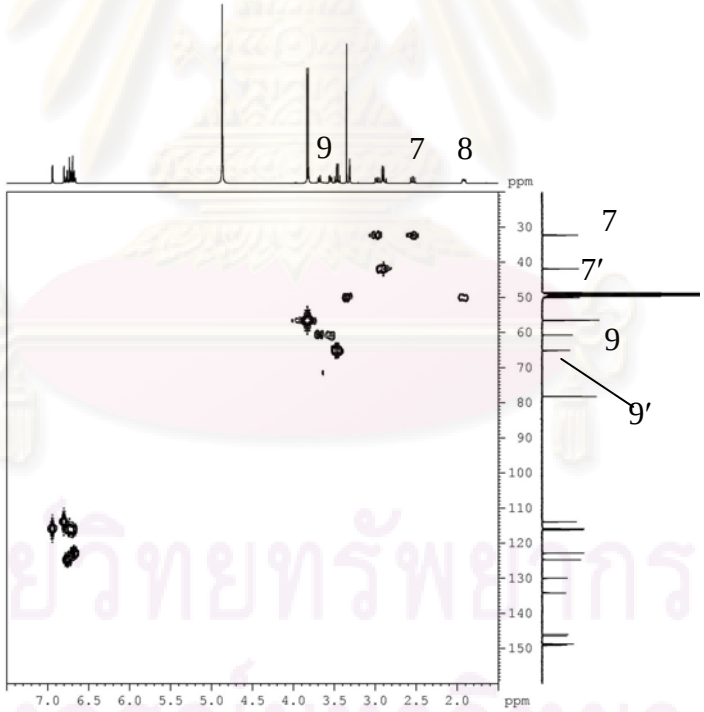

Figure 126 HMQC spectrum of compound CS4 (MeOH-d_4)

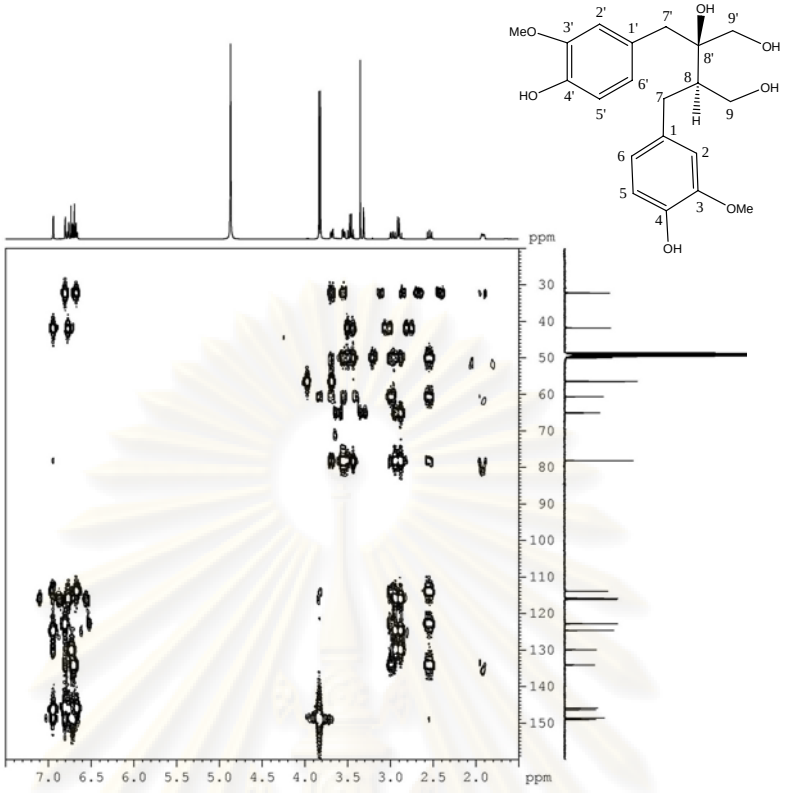

Figure 127 HMBC spectrum of compound CS4 (MeOH-d_4)
[δ_H 1.5-7.5 ppm, δ_C 20-160 ppm]

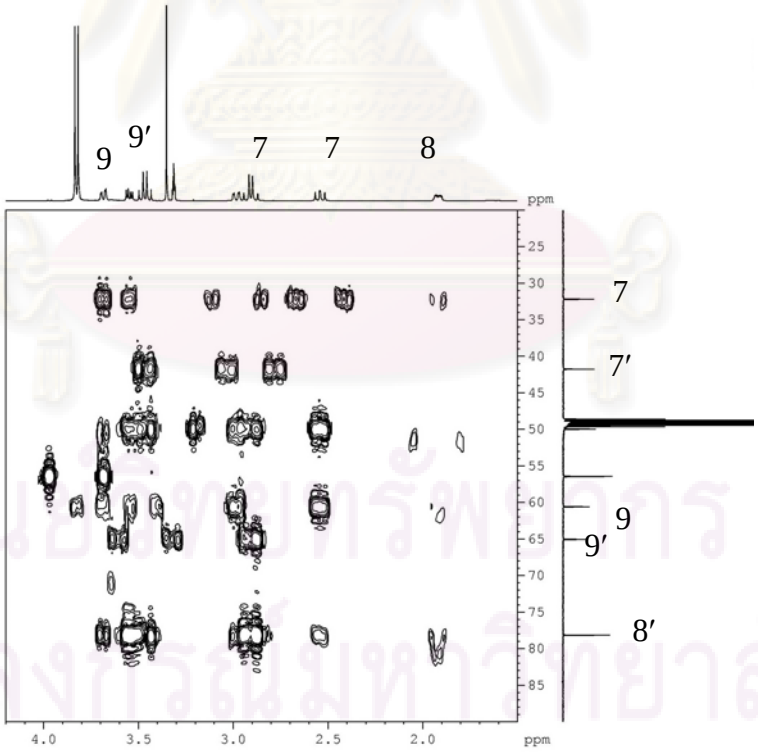

Figure 128 HMBC spectrum of compound CS4 (MeOH-d_4)
[δ_H 1.5-4.2 ppm, δ_C 20-90 ppm]

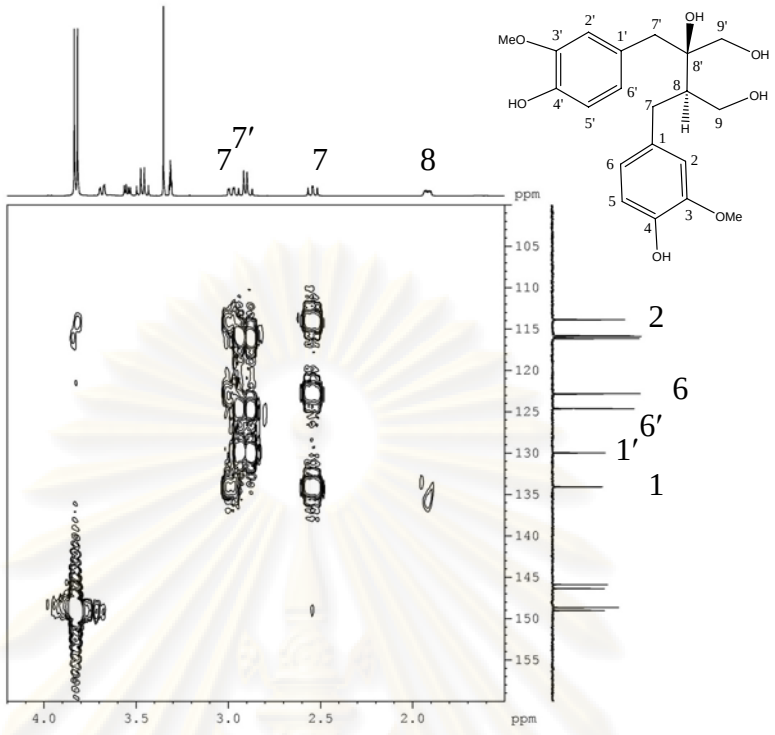

Figure 129 HMBC spectrum of compound CS4 (MeOH-d_4)
[δ_H 1.5-4.2 ppm, δ_C 100-160 ppm]

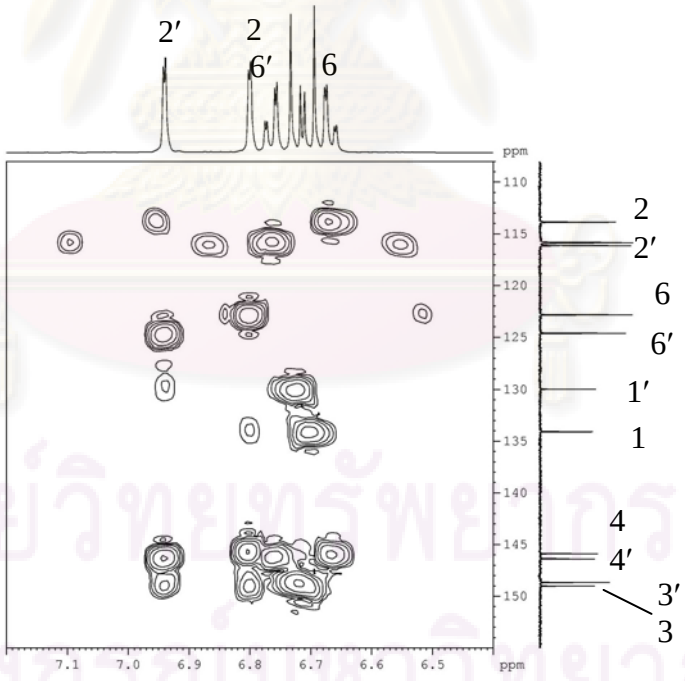

Figure 130 HMBC Spectrum of compound CS4 (MeOH-d_4)
[δ_H 6.4-7.2 ppm, δ_C 98-155 ppm]

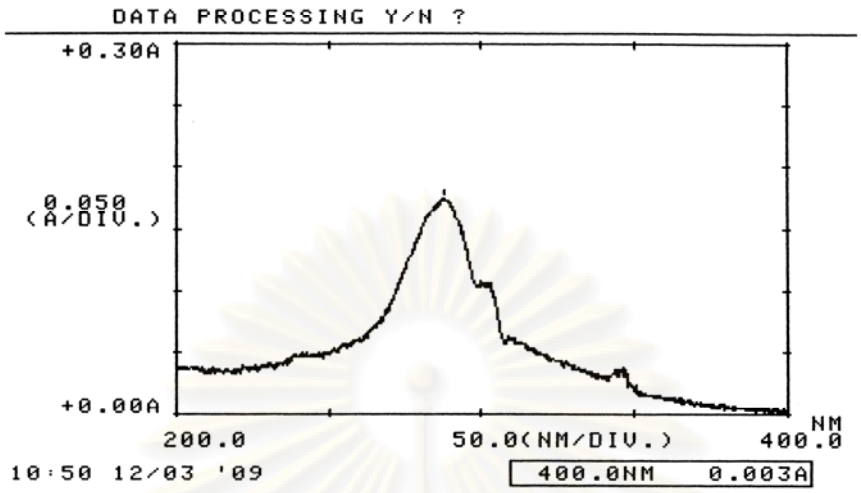

Figure 131 UV spectrum of compound CS5 (methanol)

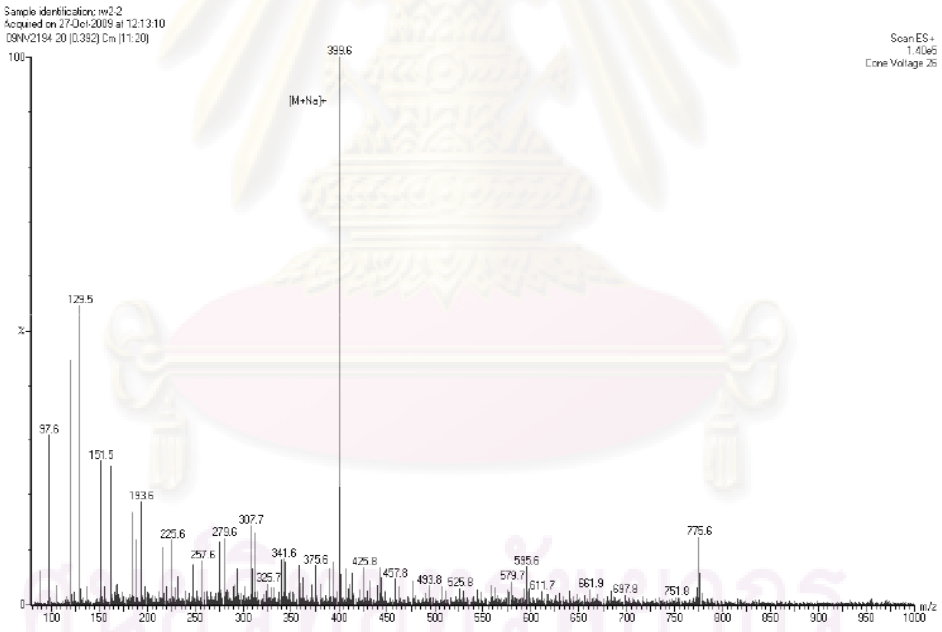

Figure 132 ESI mass spectrum of compound CS5

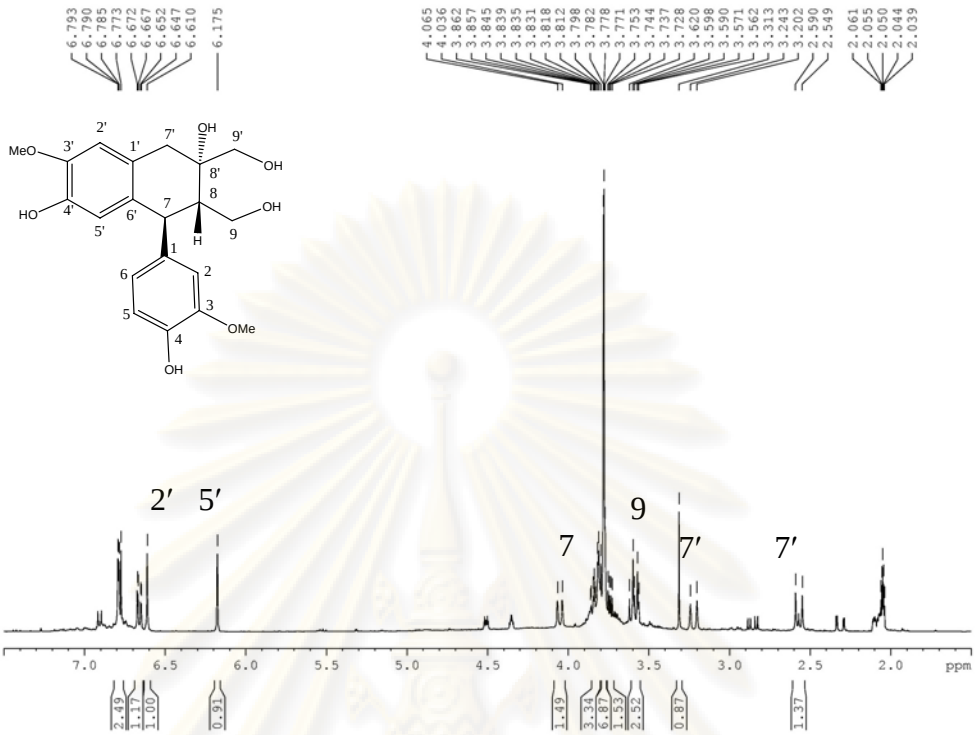

Figure 133 ^{1}H-NMR (400 MHz) spectrum of compound CS5 (acetone-d_6)

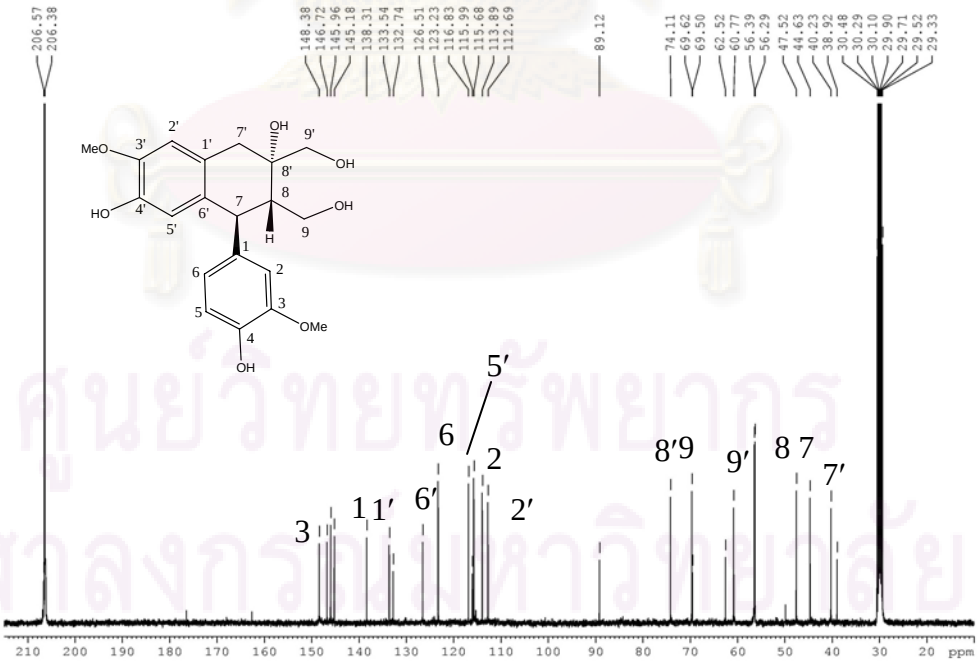

Figure 134 ^{13}C-NMR (100 MHz) spectrum of compound CS5 (acetone-d_6)

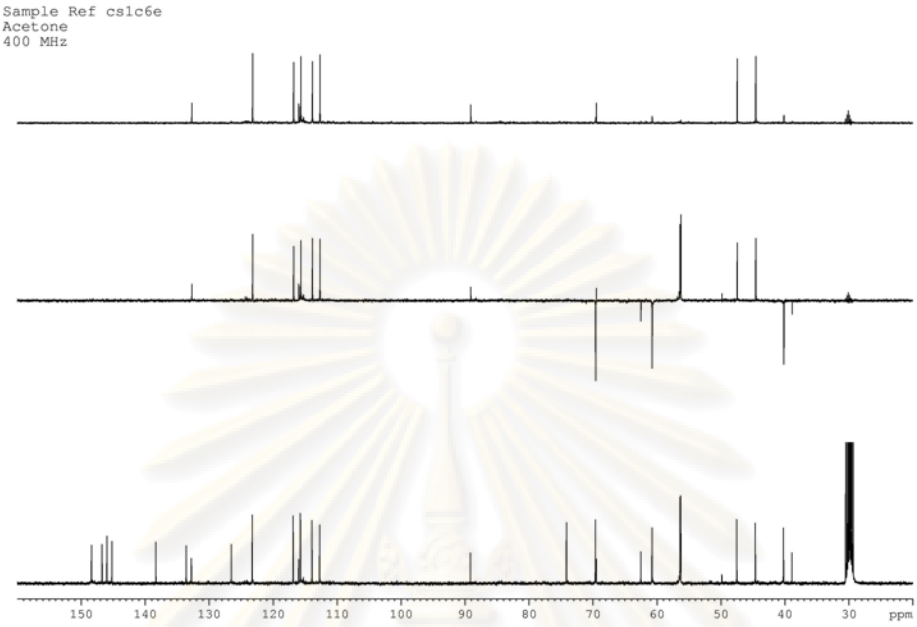

Figure 135 ^{13}C-NMR (100 MHz) and DEPT spectra of compound CS5 (acetone-d_6)

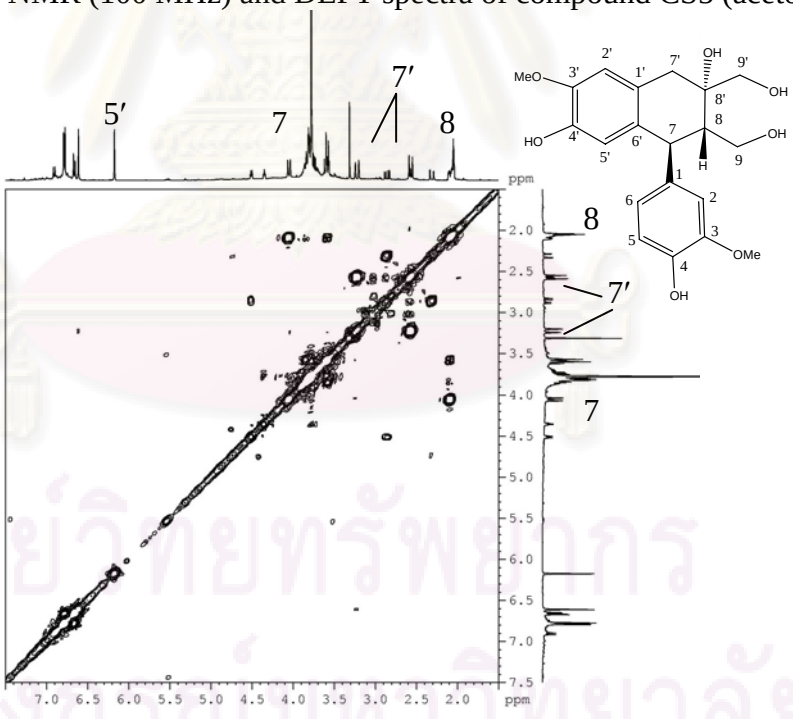

Figure 136 ^{1}H-^{1}H COSY spectrum of compound CS5 (acetone-d_6)

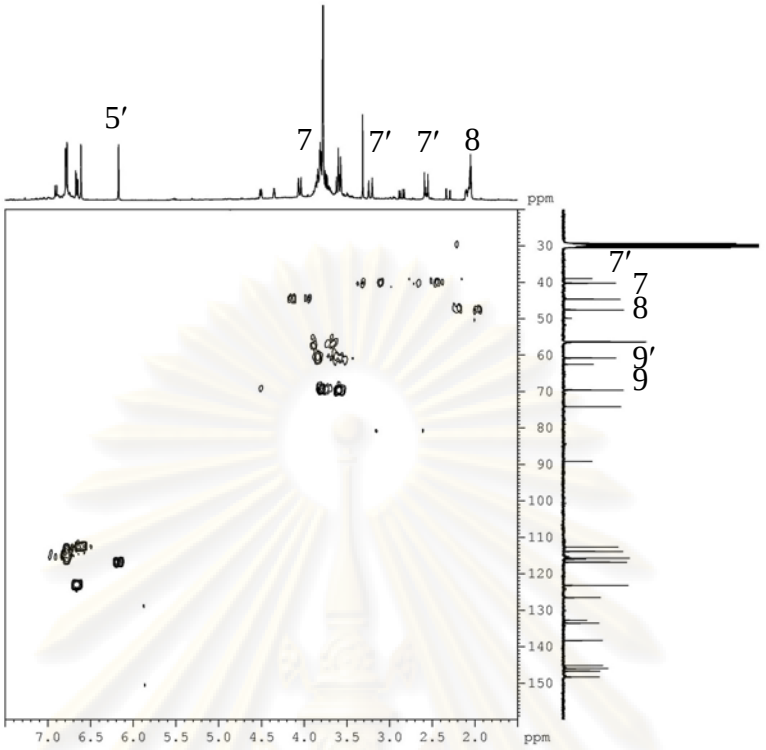

Figure 137 HMQC spectrum of compound CS5 (acetone-d_6)

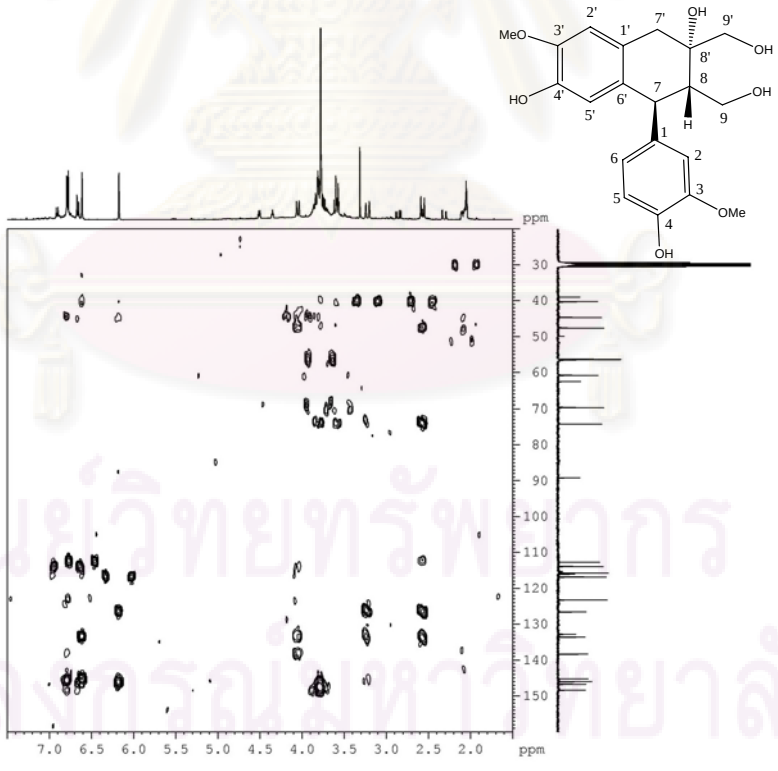

Figure 138 HMBC spectrum of compound CS5 (acetone-d_6)
[δ_H 1.5-7.5 ppm, δ_C 20-160 ppm]

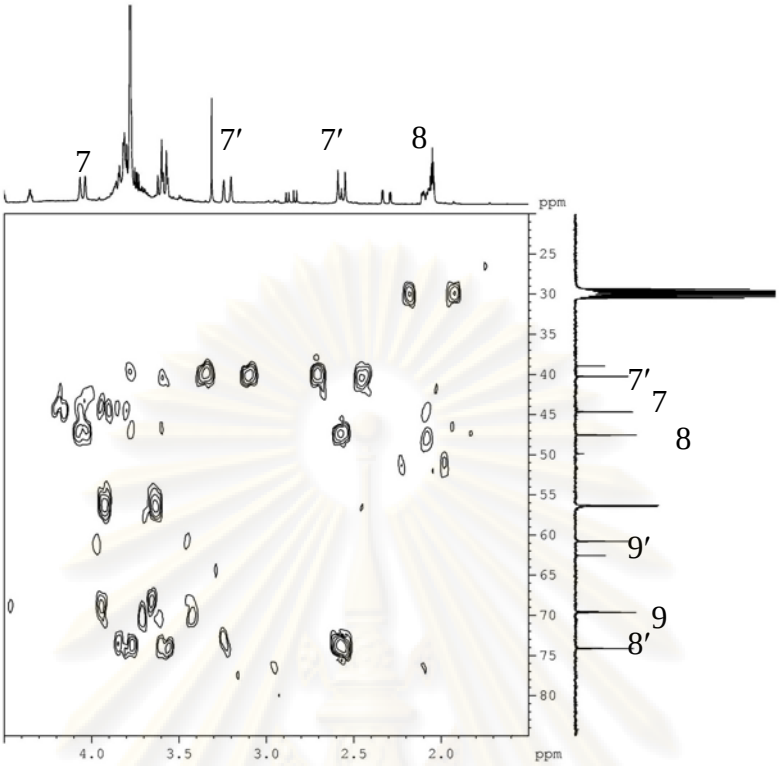

Figure 139 HMBC spectrum of compound CS5 (acetone-d_6) [δ_H 1.5-4.5 ppm, δ_C 20-85 ppm]

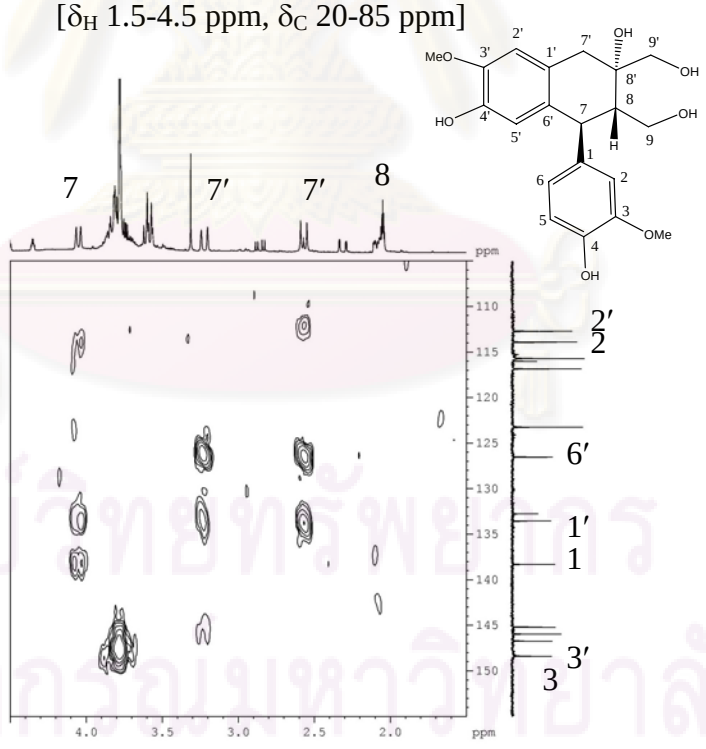

Figure 140 HMBC spectrum of compound CS5 (acetone-d_6) [δ_H 1.5-4.5 ppm, δ_C 105-155 ppm]

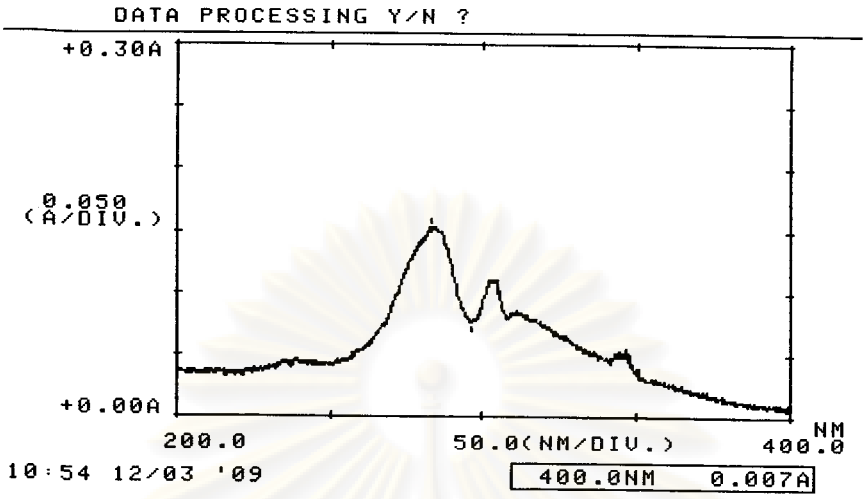

Figure 141 UV spectrum of compound CS6 (methanol)

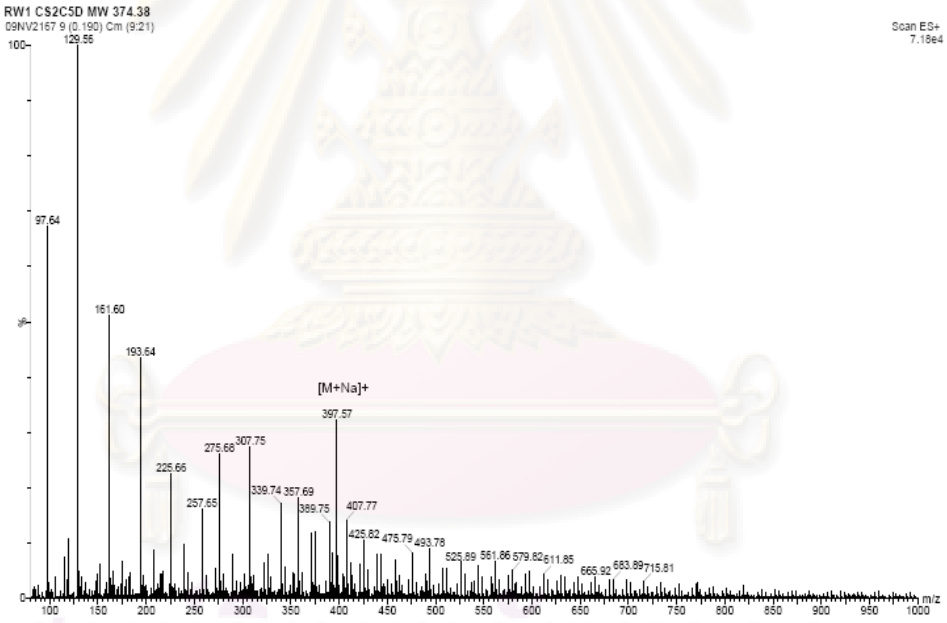

Figure 142 ESI mass spectrum of compound CS6

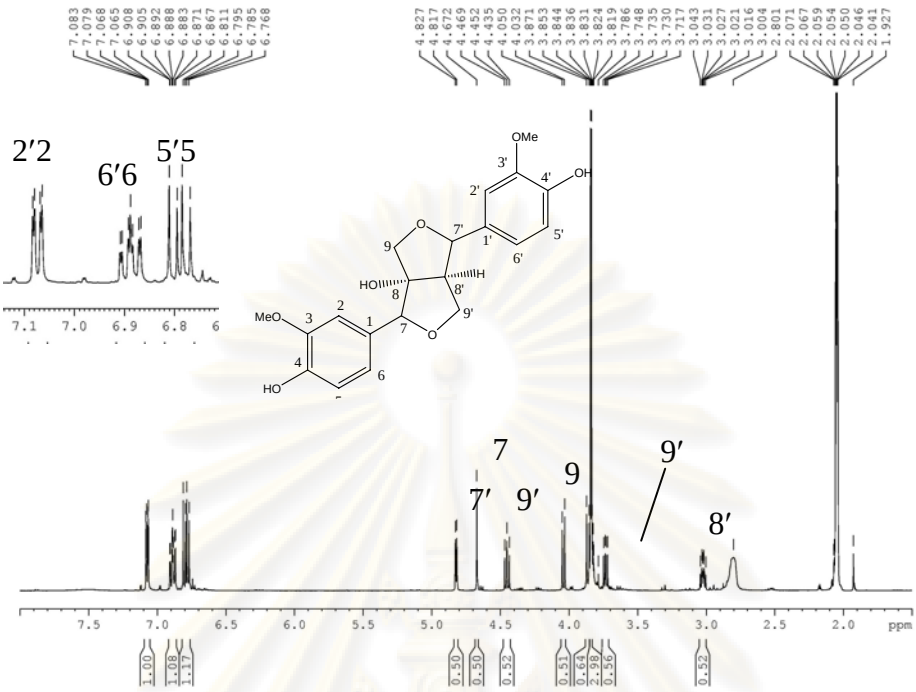

Figure 143 ^{1}H-NMR (500 MHz) spectrum of compound CS6 (acetone-d_6)

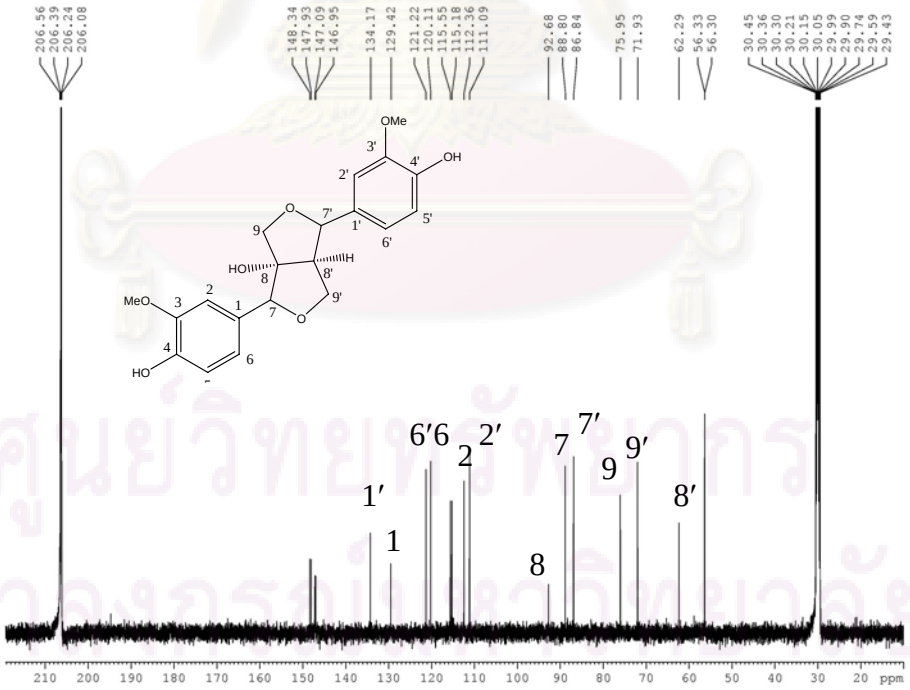

Figure 144 ^{13}C-NMR (125 MHz) spectrum of compound CS6 (acetone-d_6)

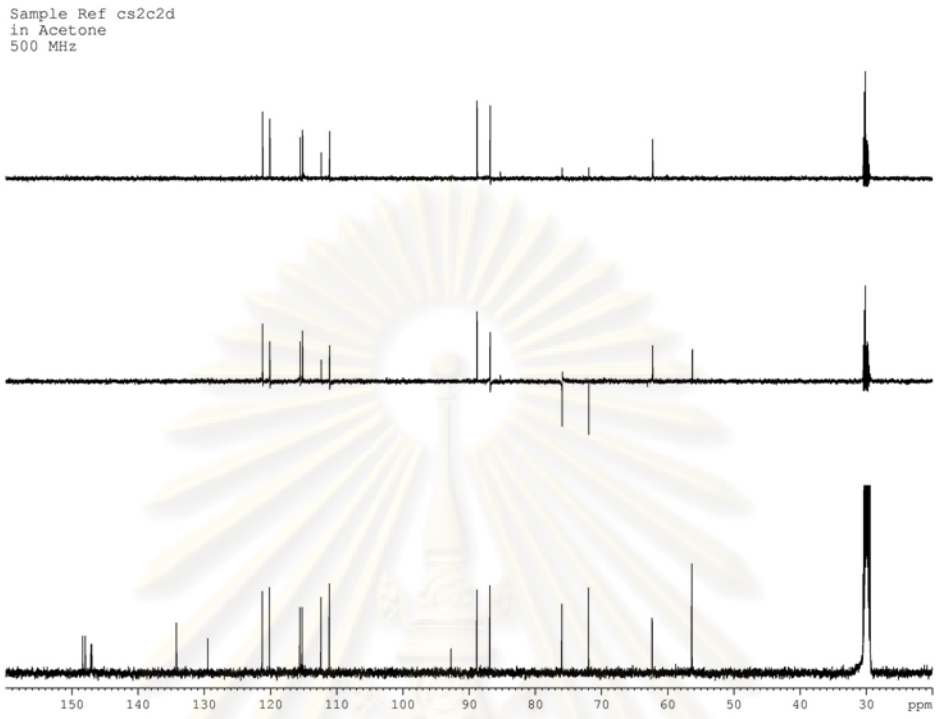

Figure 145 ^{13}C-NMR (125 MHz) and DEPT spectra of compound CS6 (acetone-d_6)

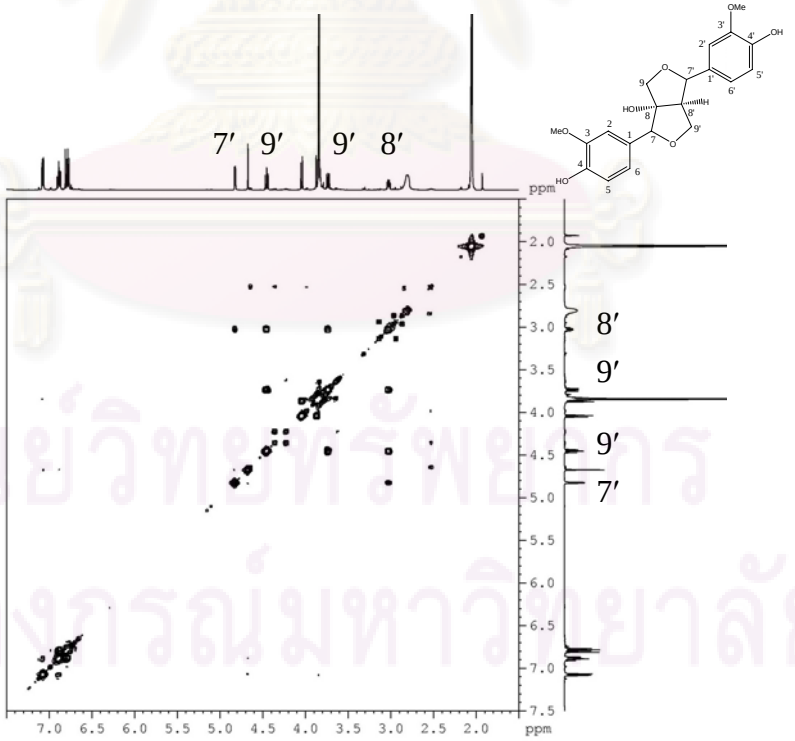

Figure 146 ^{1}H-^{1}H COSY spectrum of compound CS6 (acetone-d_6)

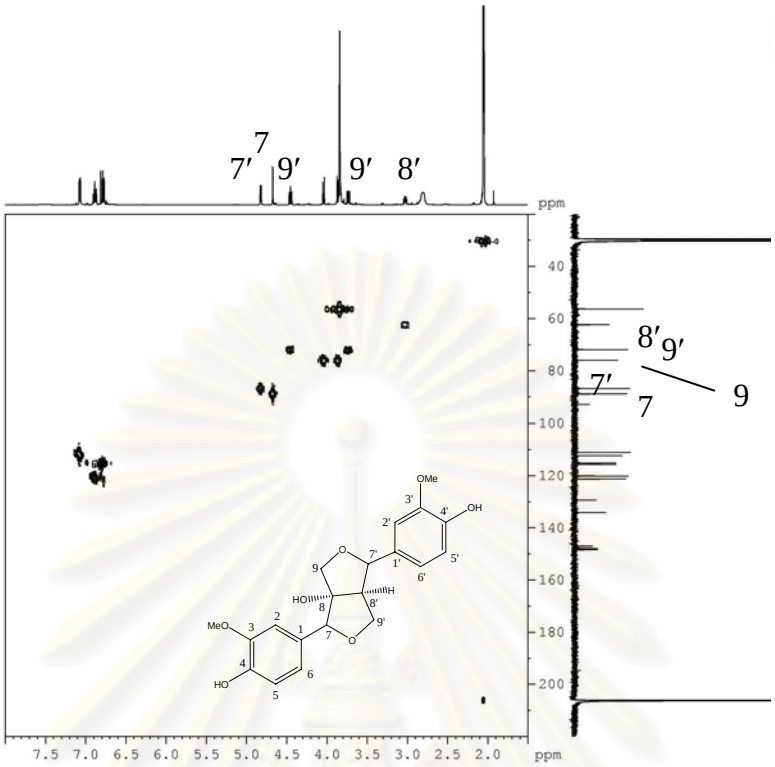

Figure 147 HMQC spectrum of compound CS6 (acetone-d_6)

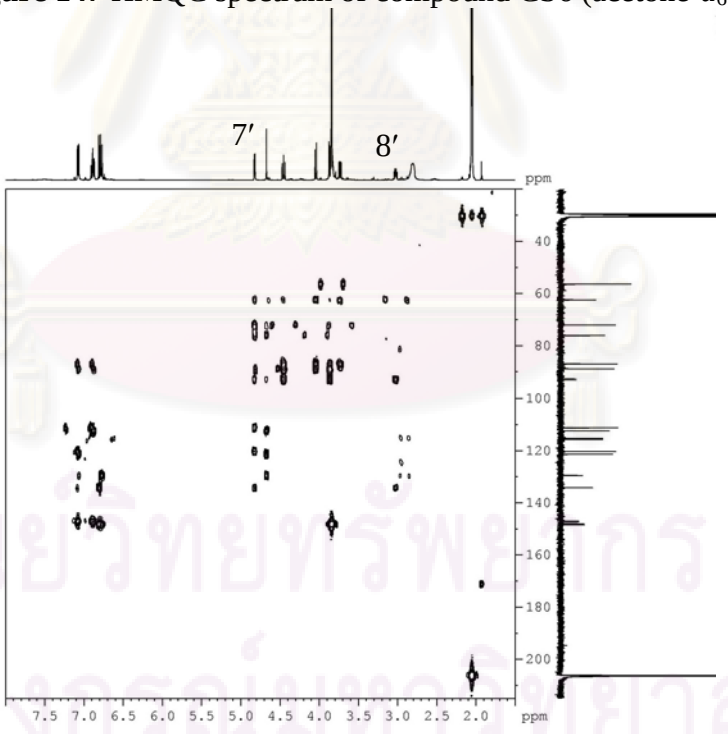

Figure 148 HMBC spectrum of compound CS6 (acetone-d_6) [δ_H 1.5-8 ppm, δ_C 30-210 ppm]

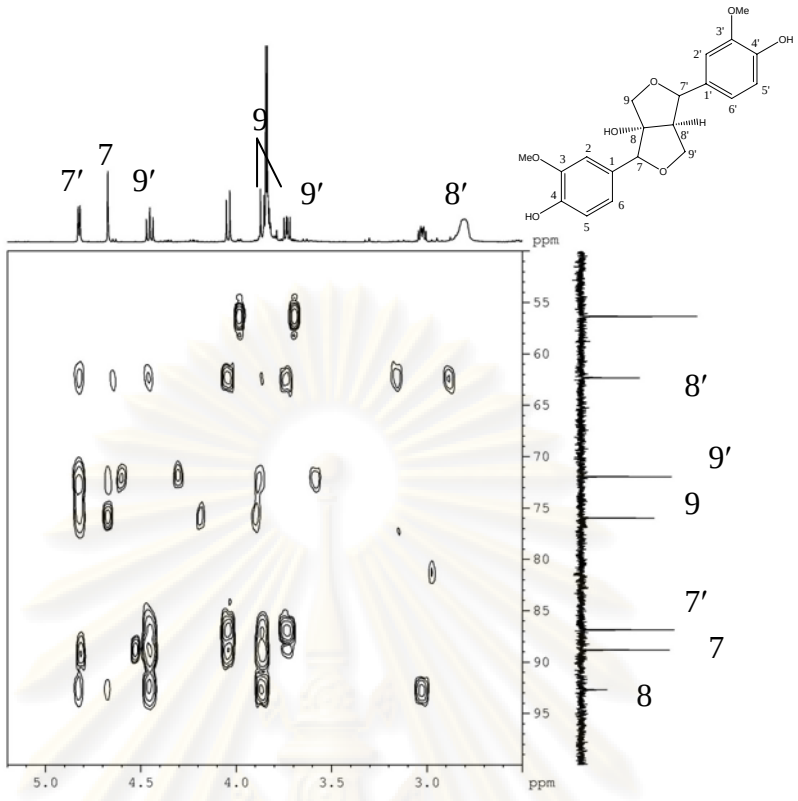

Figure 149 HMBC spectrum of compound CS6 (acetone-d_6)
[δ_H 2.5-5.2 ppm, δ_C 50-100 ppm]

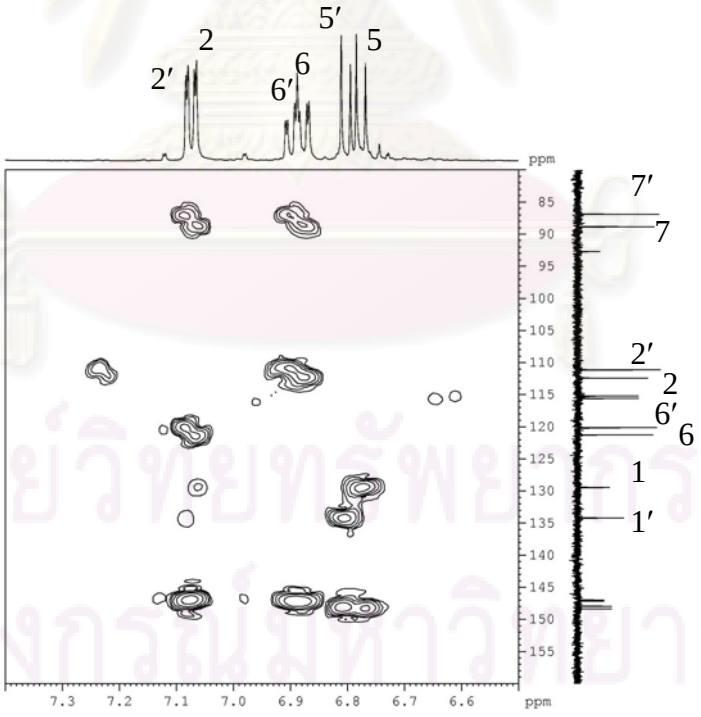

Figure 150 HMBC Spectrum of compound CS6 (acetone-d_6)
[δ_H 6.5-7.4 ppm, δ_C 80-160 ppm]

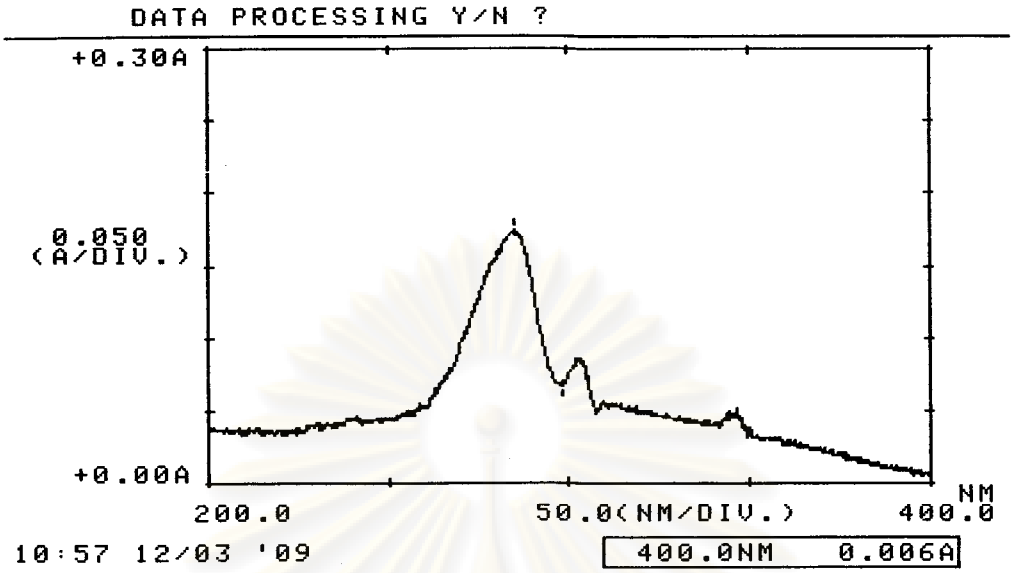

Figure 151 UV spectrum of compound CS7 (methanol)

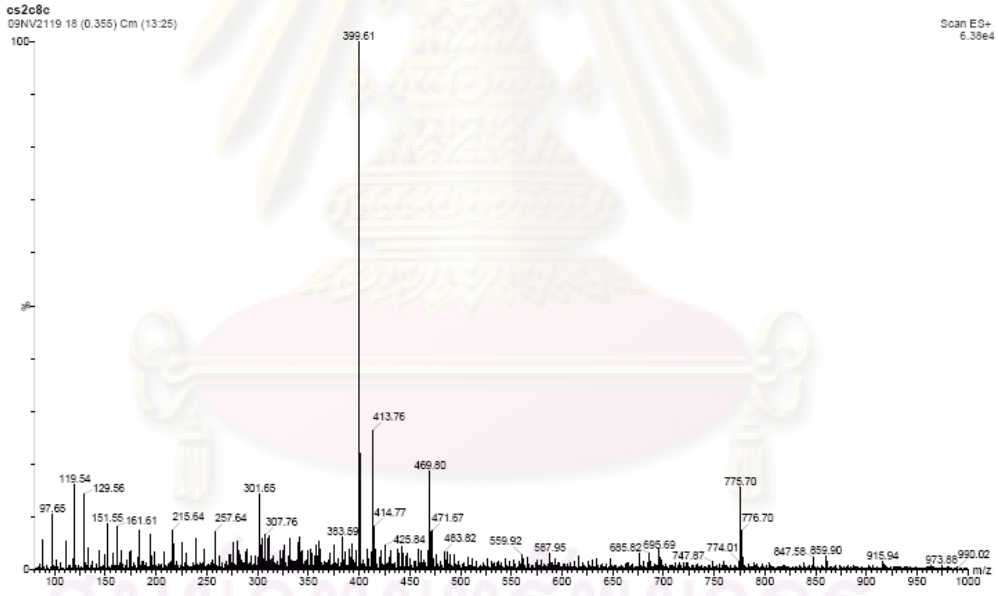

Figure 152 ESI mass spectrum of compound CS7

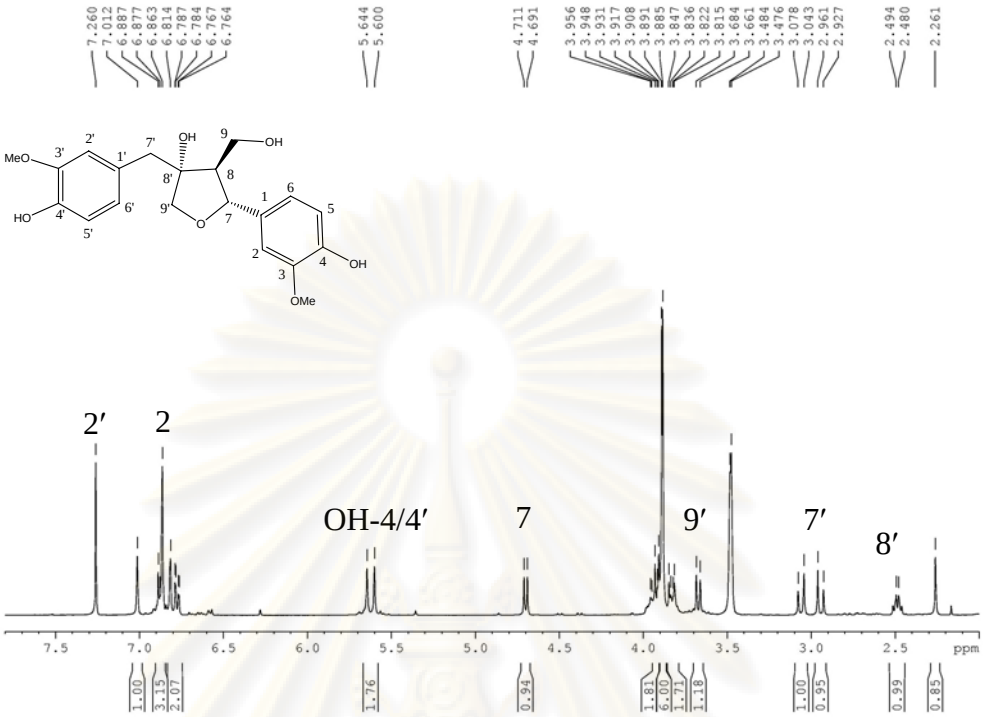

Figure 153 ^{1}H-NMR (400 MHz) spectrum of compound CS7 ($CDCl_3$)

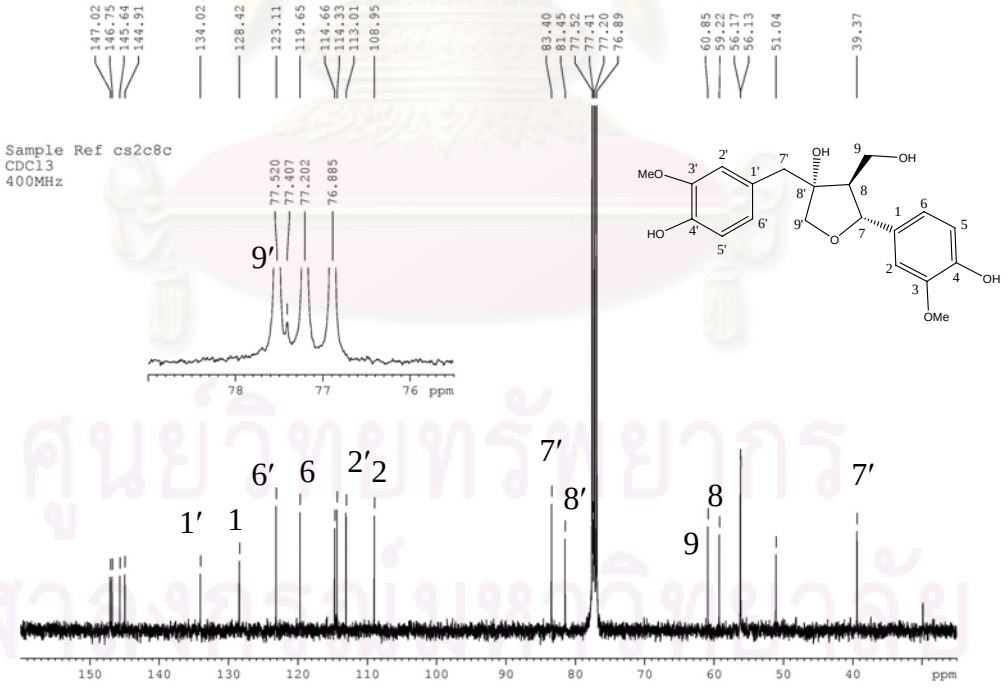

Figure 154 ^{13}C-NMR (100 MHz) spectrum of compound CS7 ($CDCl_3$)

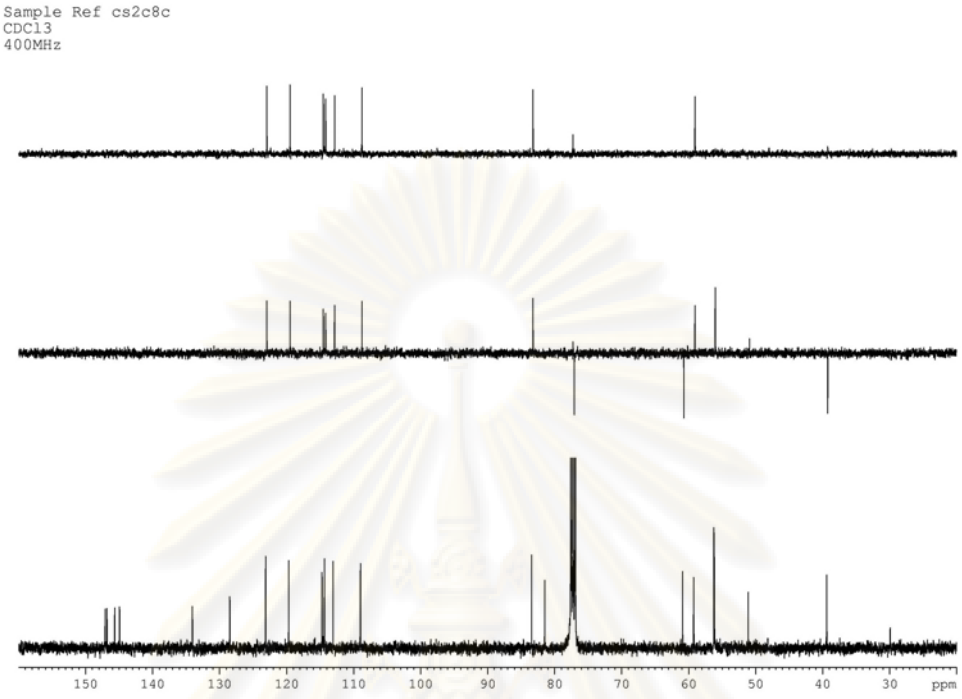

Figure 155 ^{13}C-NMR (100 MHz) and DEPT spectra of compound CS7 ($CDCl_3$)

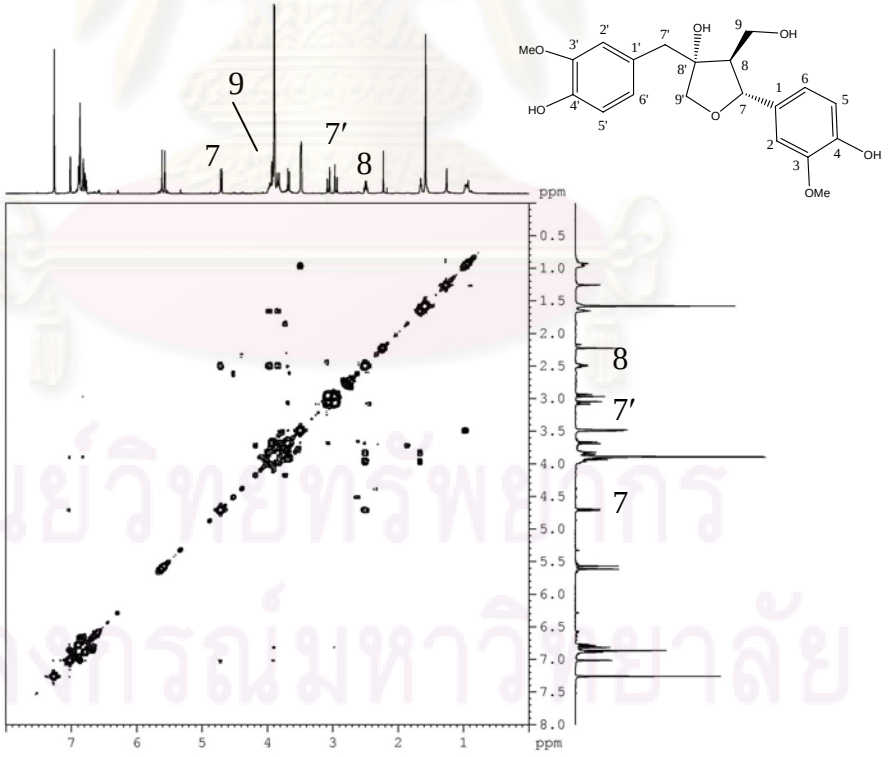

Figure 156 ^{1}H-^{1}H COSY spectrum of compound CS7 ($CDCl_3$)

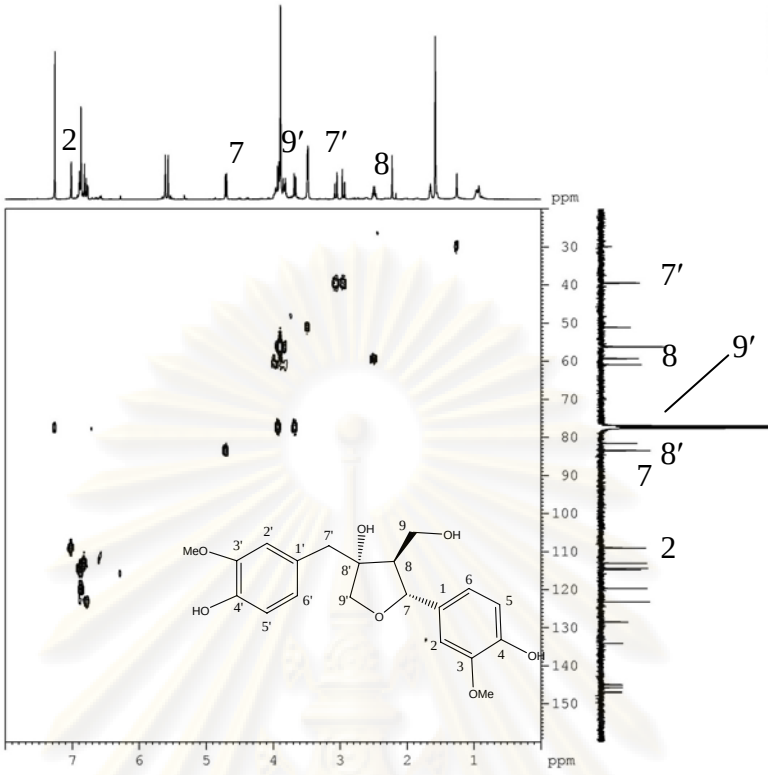

Figure 157 HMQC spectrum of compound CS7 ($CDCl_3$)

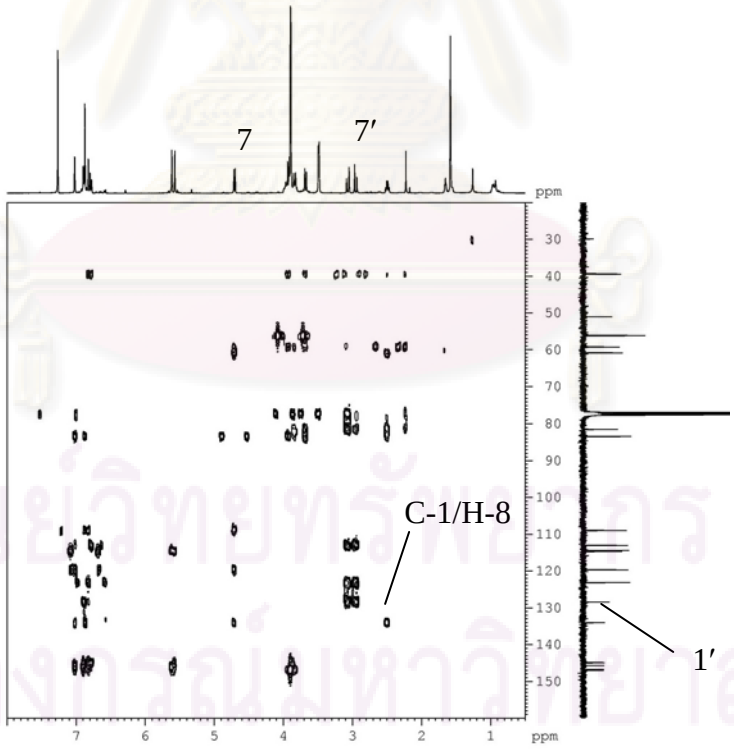

Figure 158 HMBC spectrum of compound CS7 ($CDCl_3$)
[δ_H 0.5-8 ppm, δ_C 20-160 ppm]

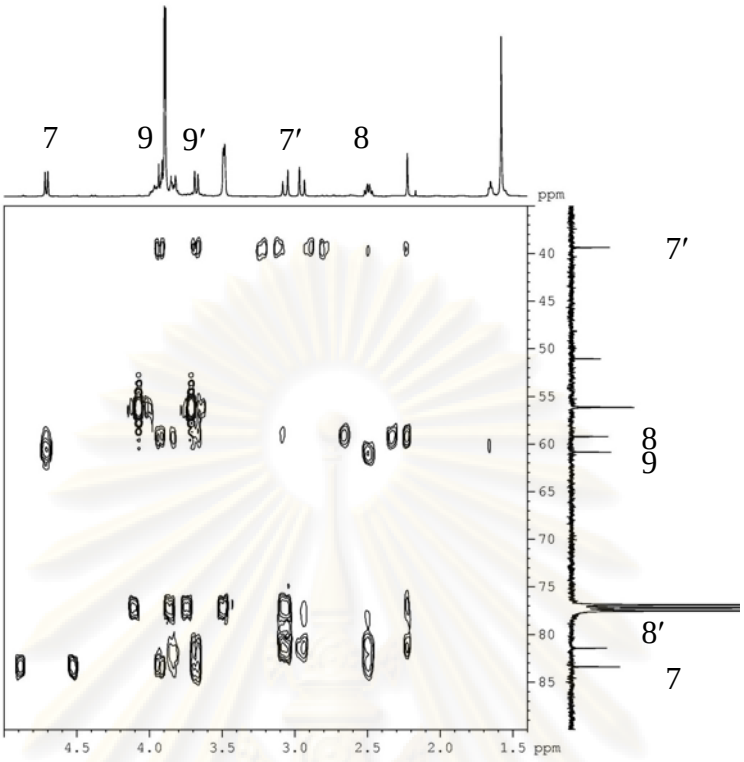

Figure 159 HMBC spectrum of compound CS7 ($CDCl_3$)
[δ_H 1.4-5 ppm, δ_C 30-90 ppm]

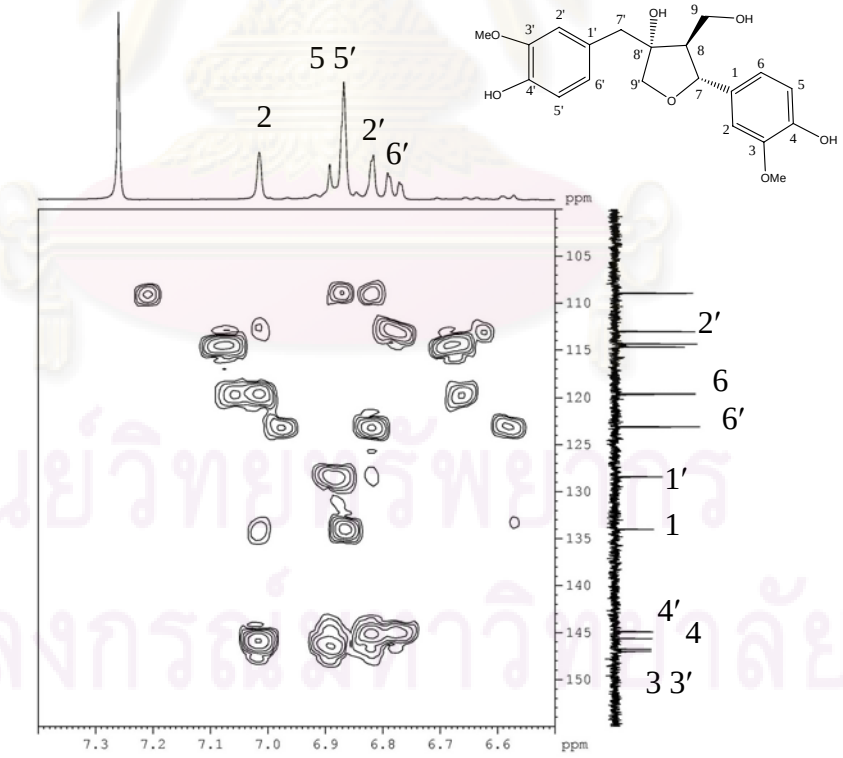

Figure 160 HMBC spectrum of compound CS7 ($CDCl_3$)
[δ_H 6.5-7.4 ppm, δ_C 100-155 ppm]

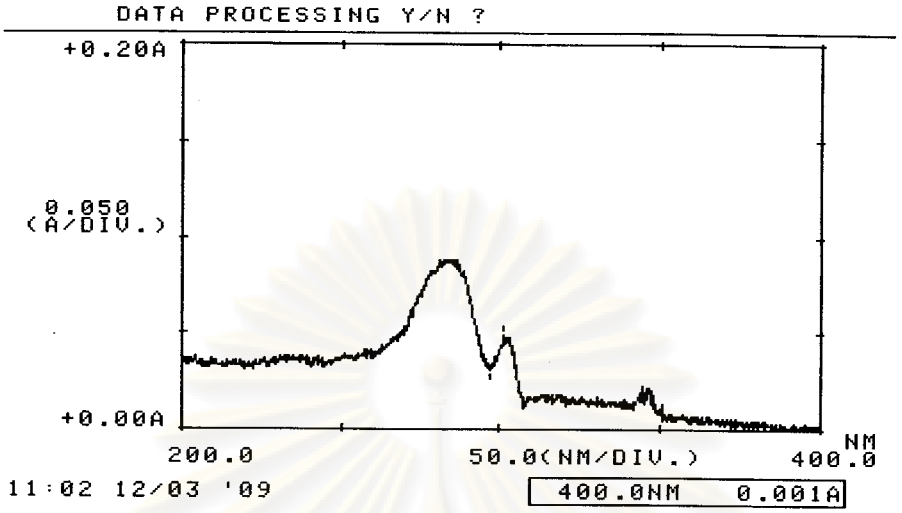

Figure 161 UV spectrum of compound CS8 (methanol)

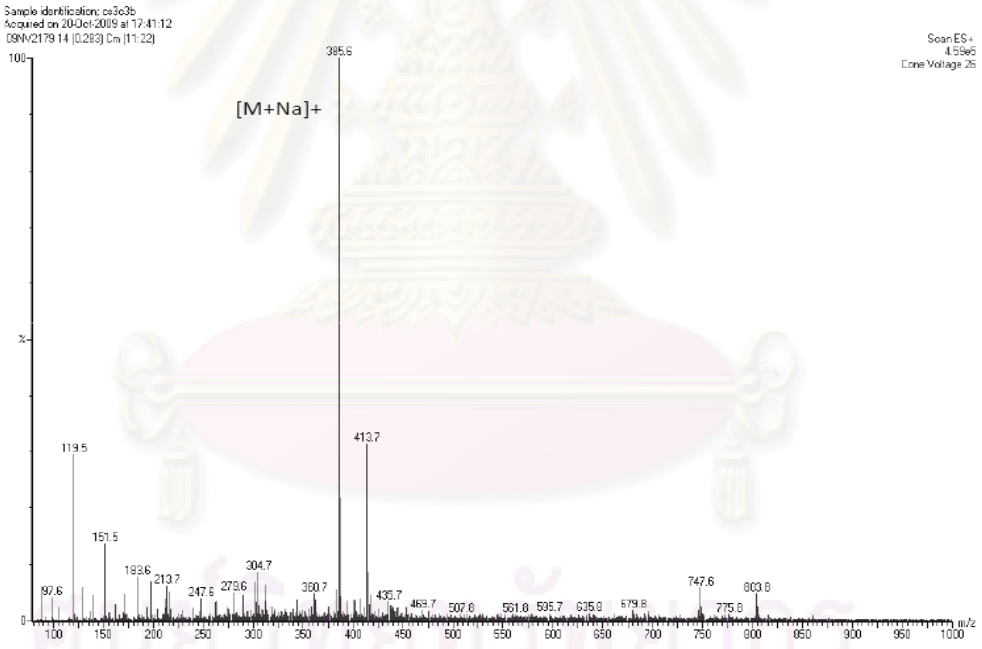

Figure 162 ESI mass spectrum of compound CS8

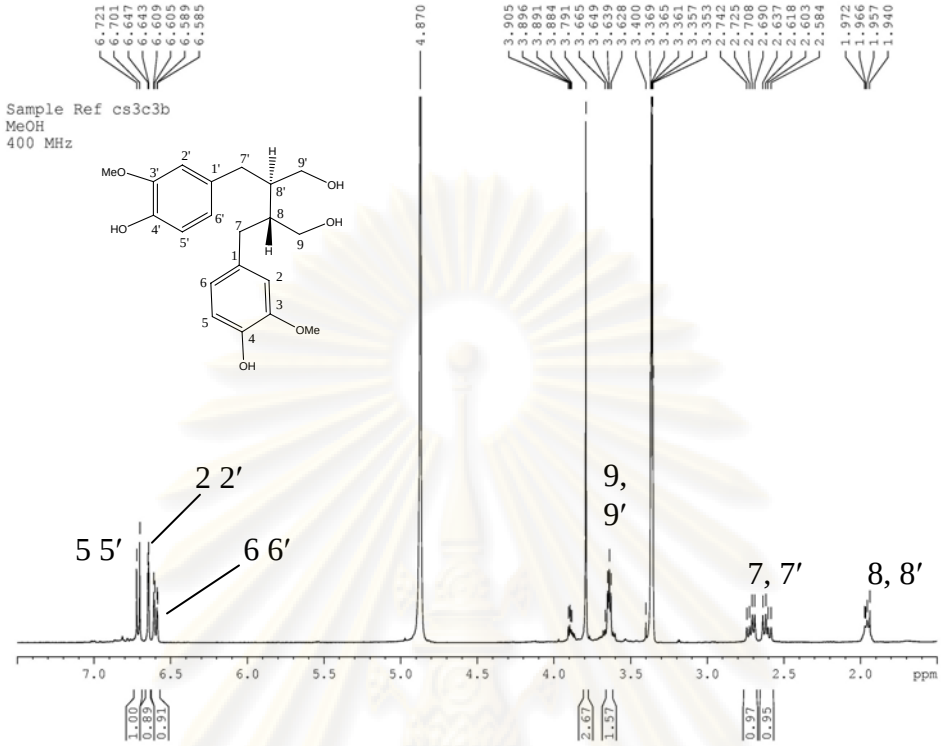

Figure 163 ^{1}H-NMR (400 MHz) spectrum of compound CS8 (MeOH-d_4)

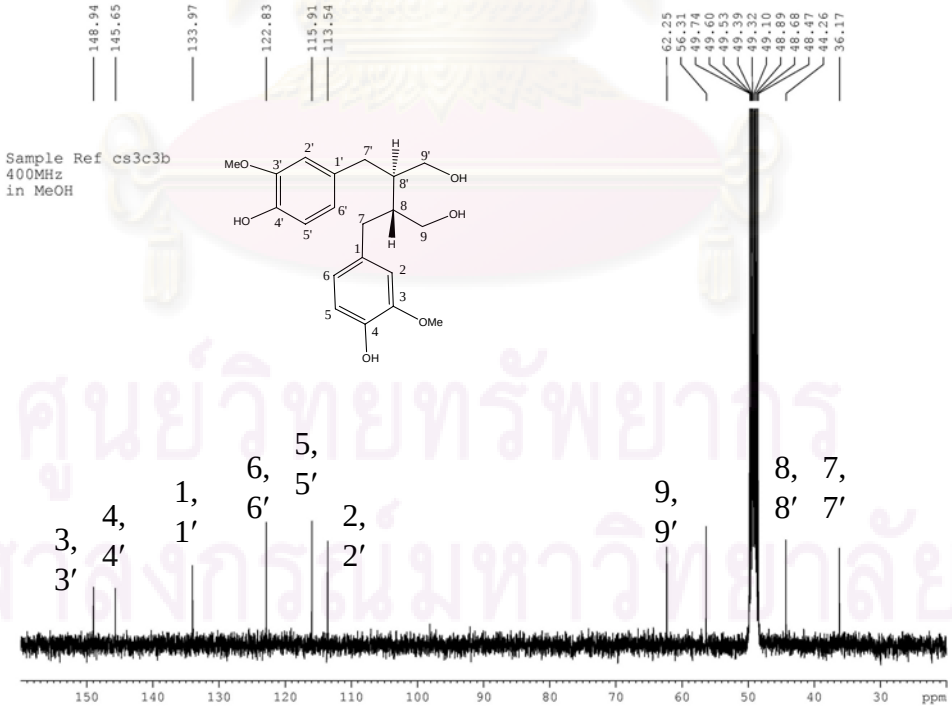

Figure 164 ^{13}C-NMR (100 MHz) spectrum of compound CS8 (MeOH-d_4)

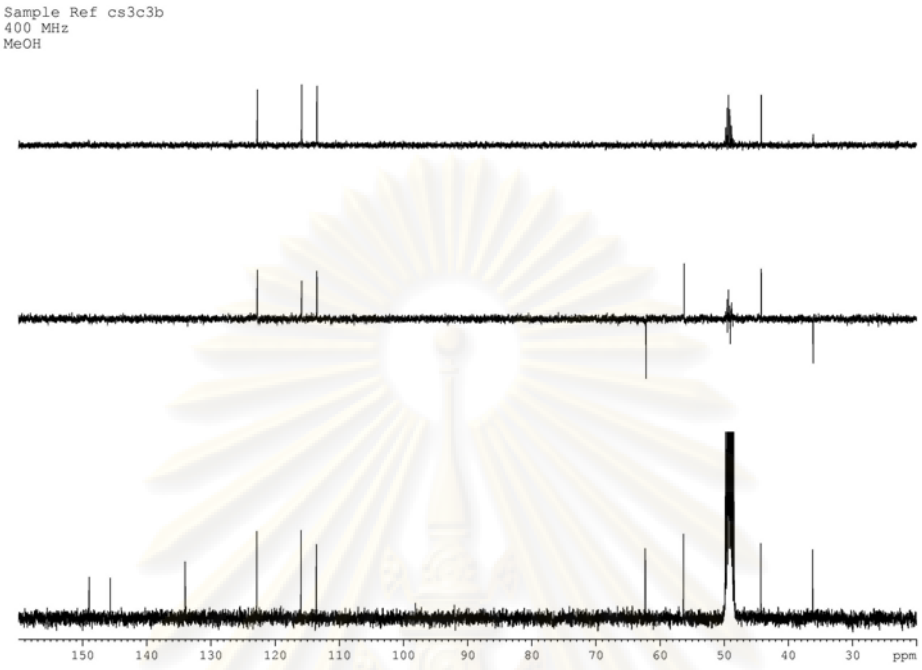

Figure 165 ^{13}C-NMR (100 MHz) and DEPT spectra of compound CS8 (MeOH-d_4)

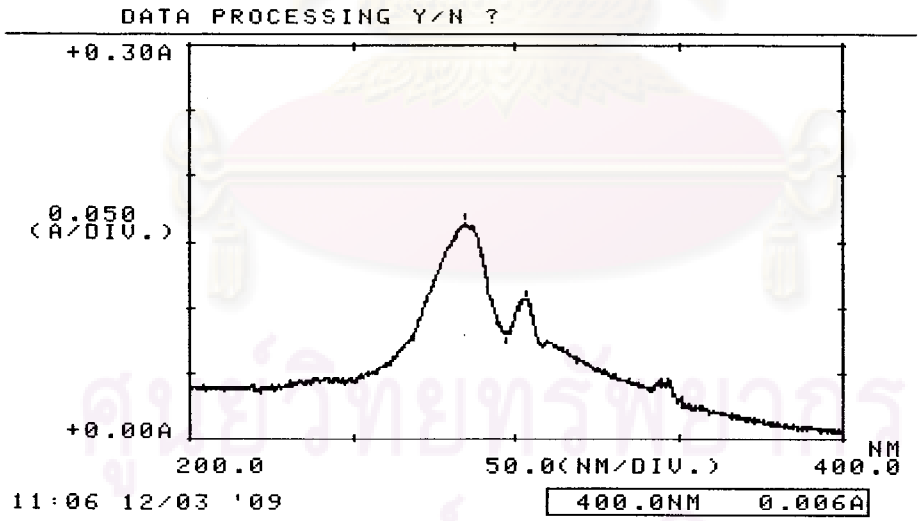

Figure 166 UV spectrum of compound CS9 (methanol)

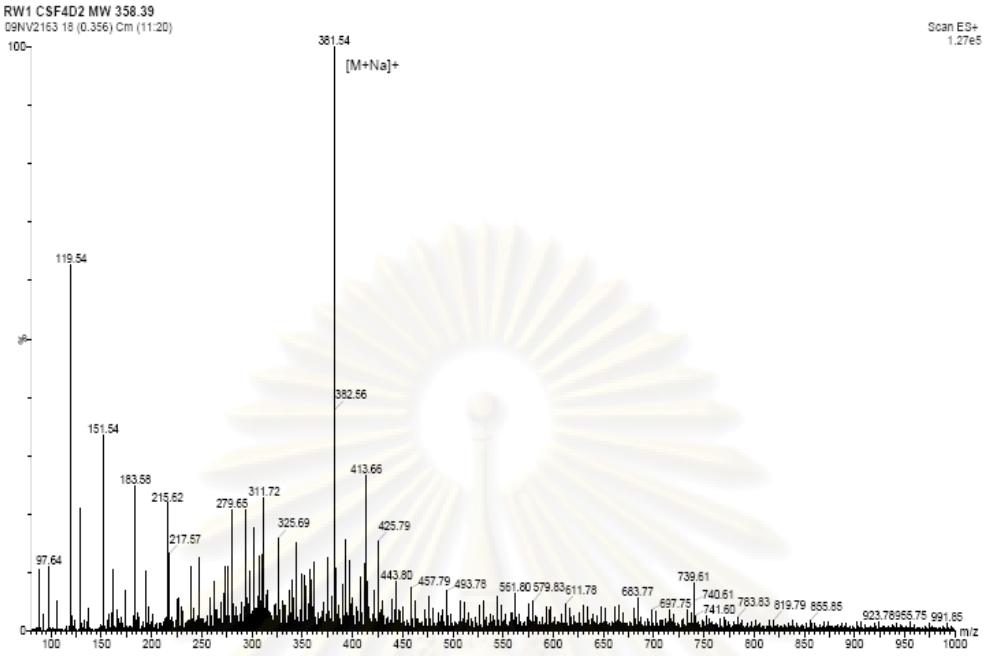

Figure 167 ESI mass spectrum of compound CS9

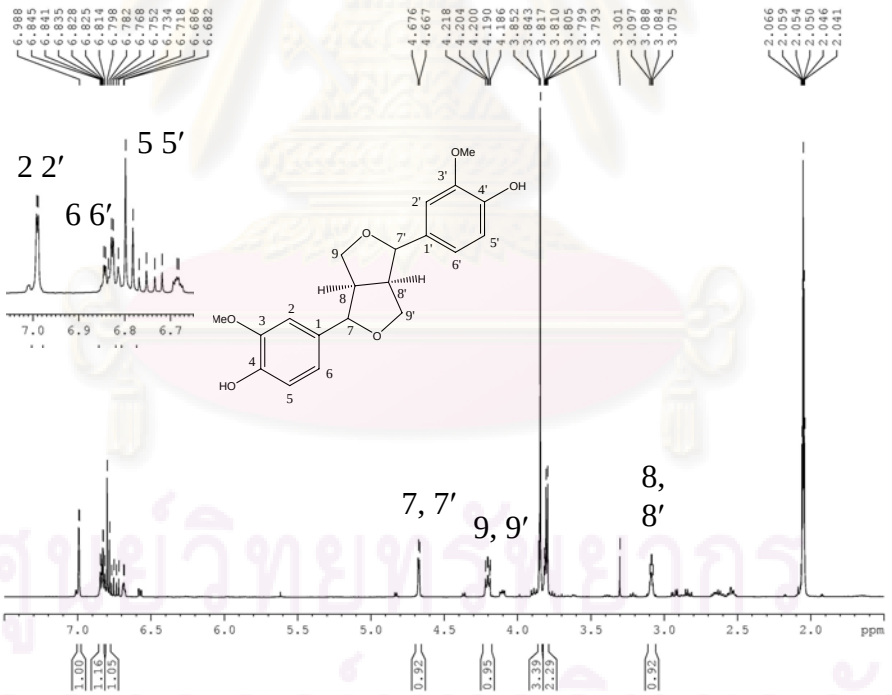

Figure 168 ^{1}H-NMR (500 MHz) spectrum of compound CS9 (acetone-d_6)

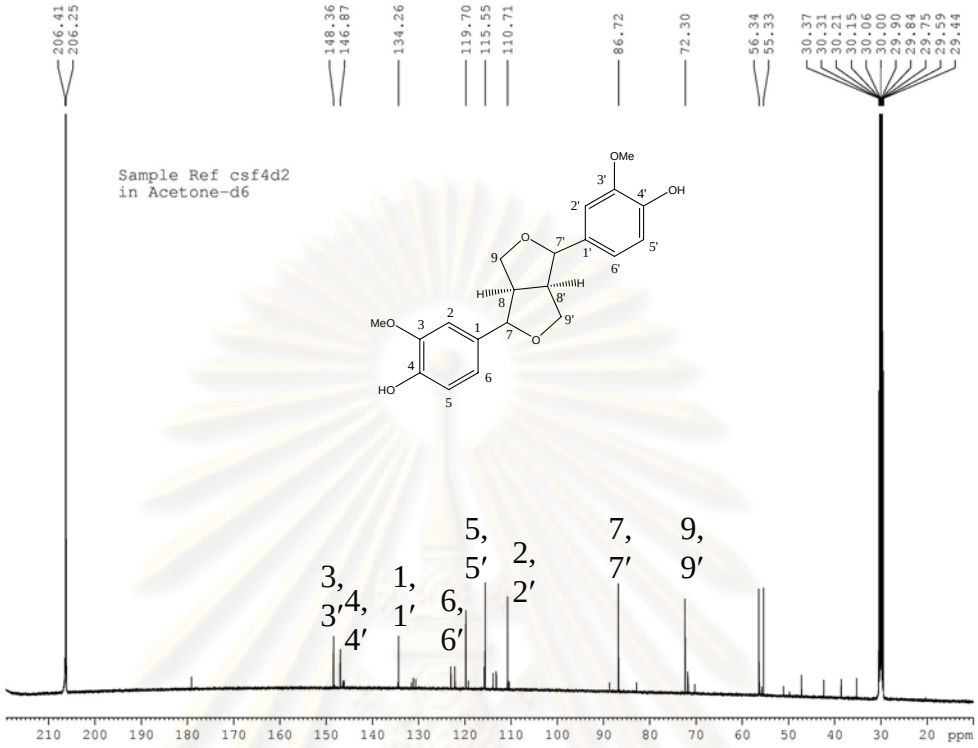

Figure 169 ^{13}C-NMR (125 MHz) spectrum of compound CS9 (acetone-d_6)

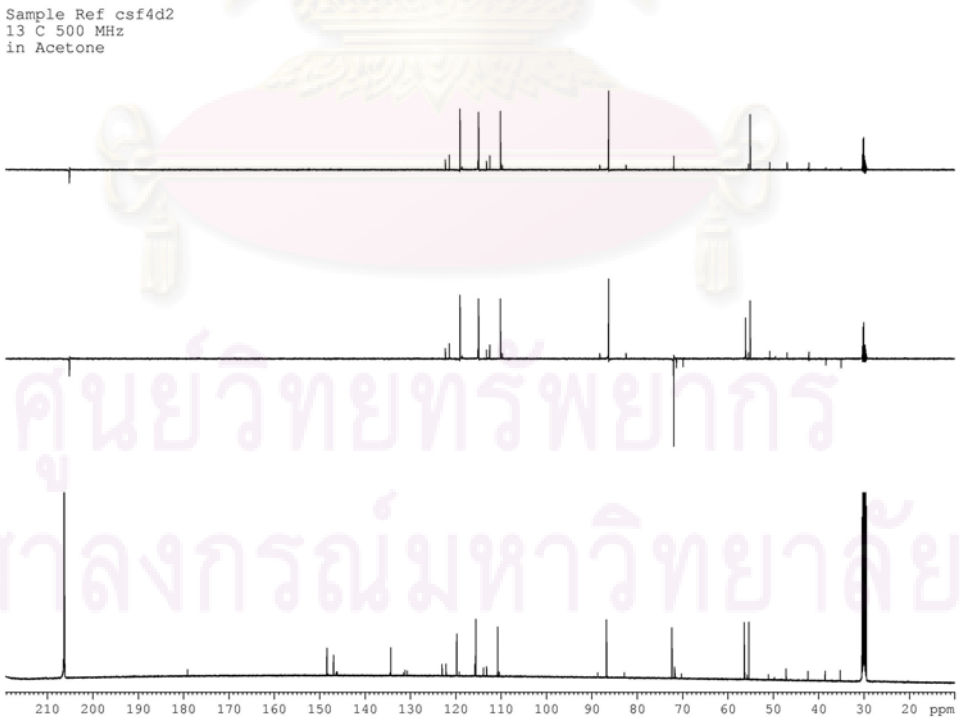

Figure 170 ^{13}C-NMR (125 MHz) and DEPT spectra of compound CS9 (acetone-d_6)

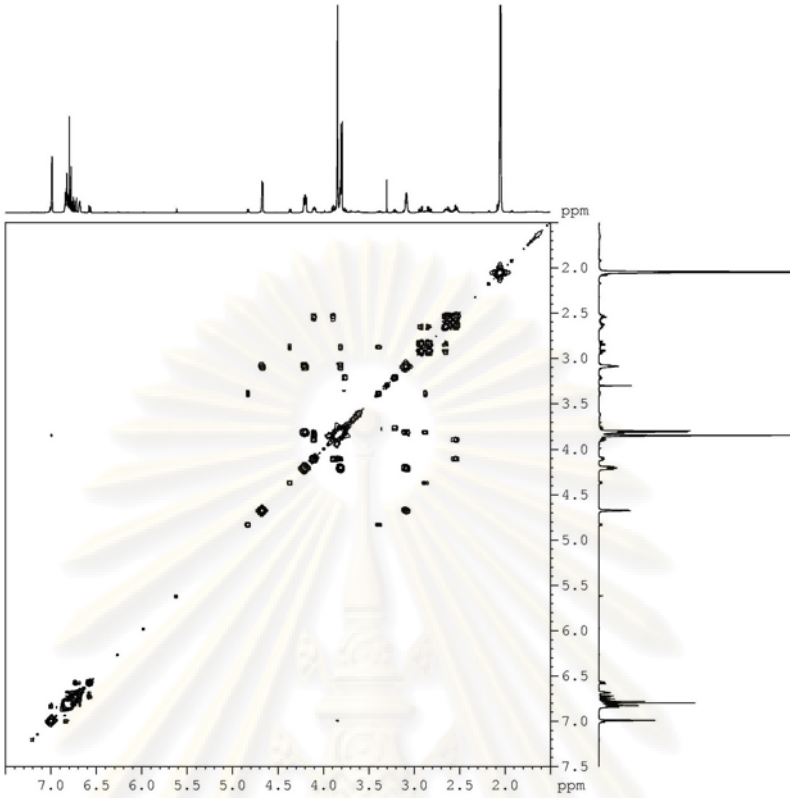

Figure 171 ^{1}H-^{1}H COSY spectrum of compound CS9 (acetone-d_6)

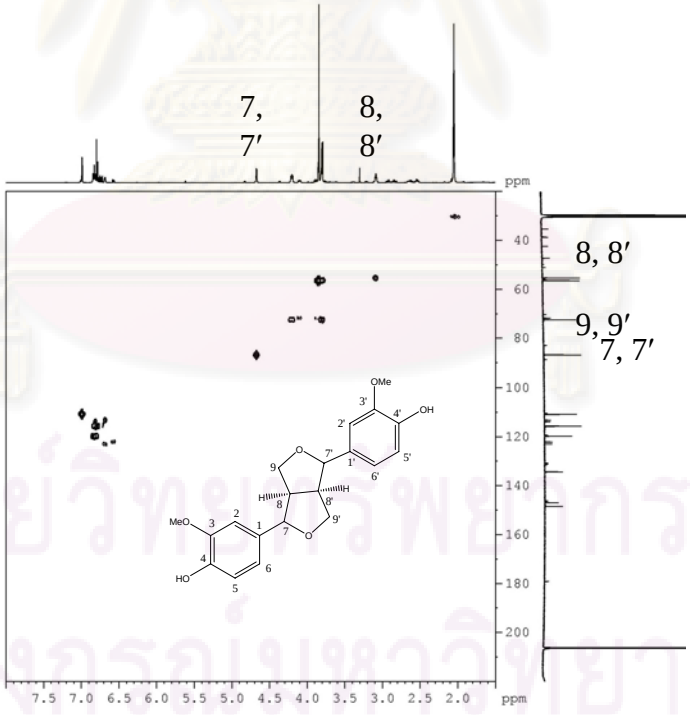

Figure 172 HMQC spectrum of compound CS9 (acetone-d_6)

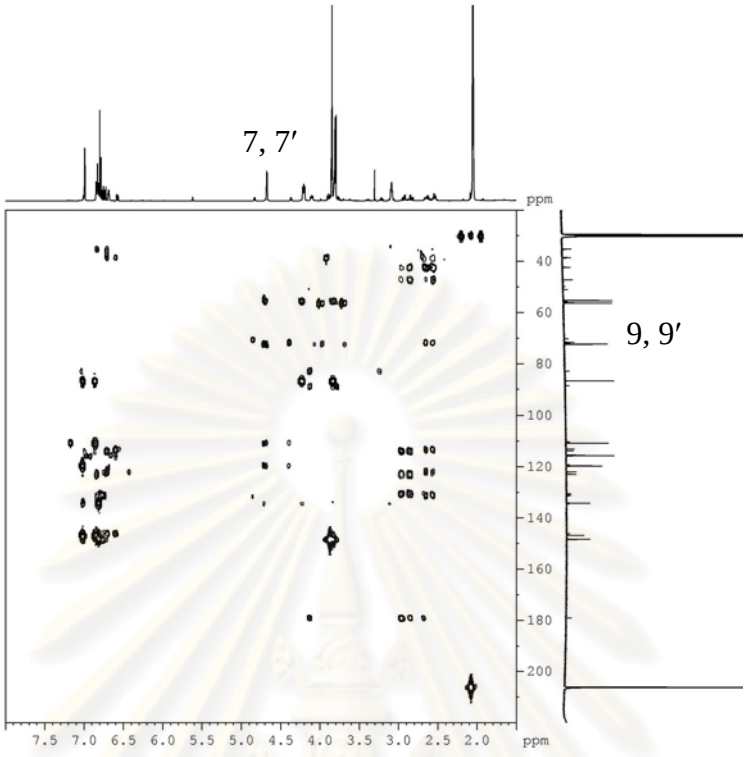

Figure 173 HMBC spectrum of compound CS9 (acetone-d_6) [δ_H 1.5-8 ppm, δ_C 30-210 ppm]

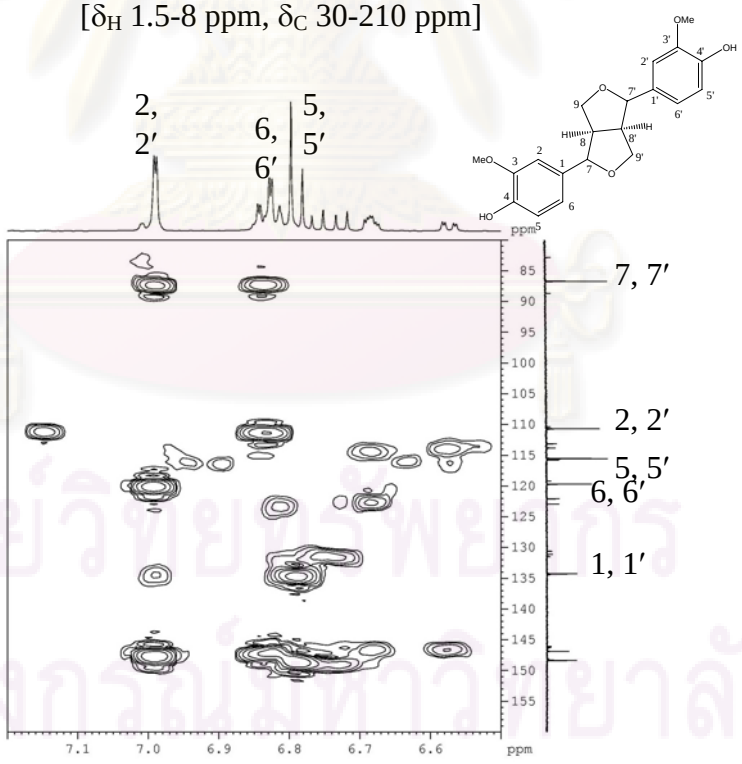

Figure 174 HMBC spectrum of compound CS9 (acetone-d_6) [δ_H 6.5-7.2 ppm, δ_C 80-160 ppm]

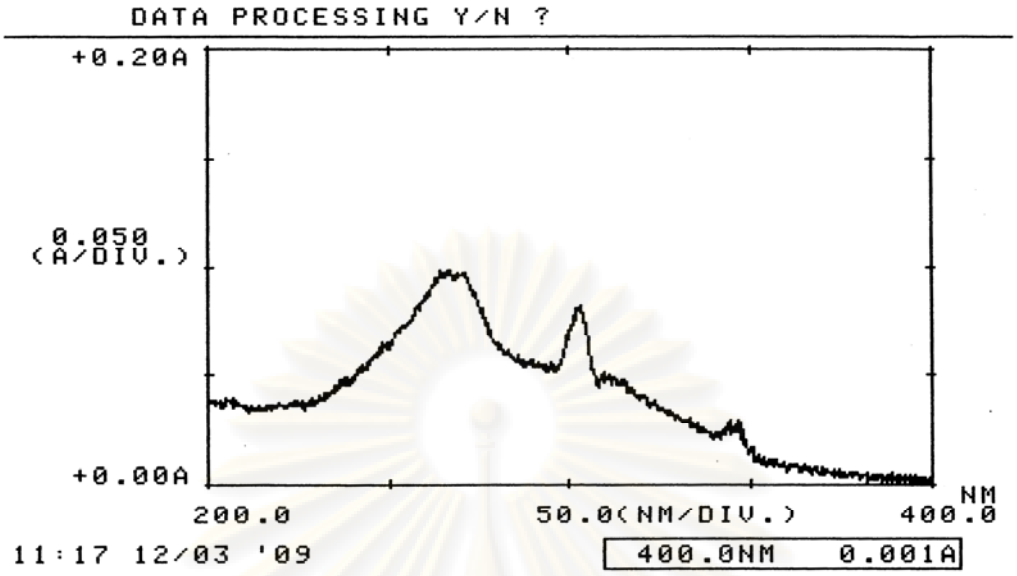

Figure 175 UV spectrum of compound CS10 (methanol)

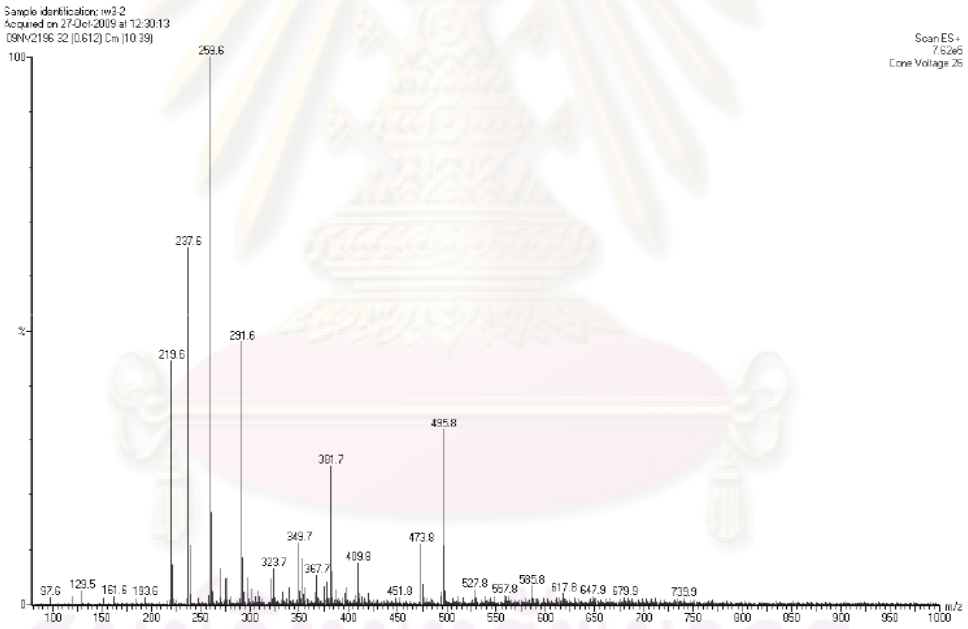

Figure 176 ESI mass spectrum of compound CS10

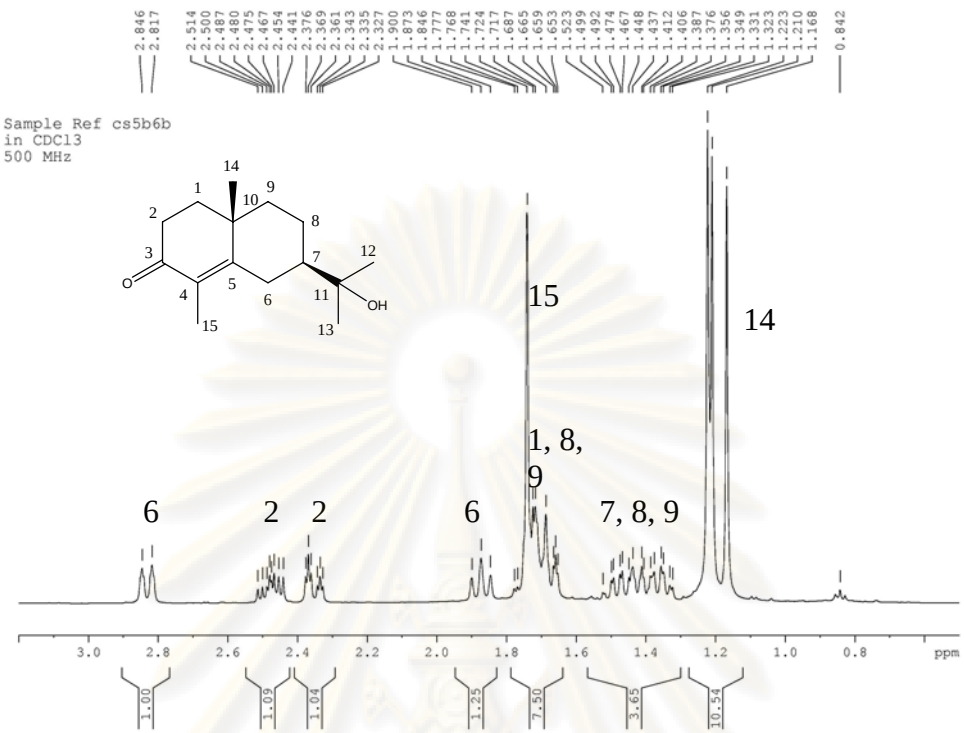

Figure 177 ^{1}H-NMR (500 MHz) spectrum of compound CS10 ($CDCl_3$)

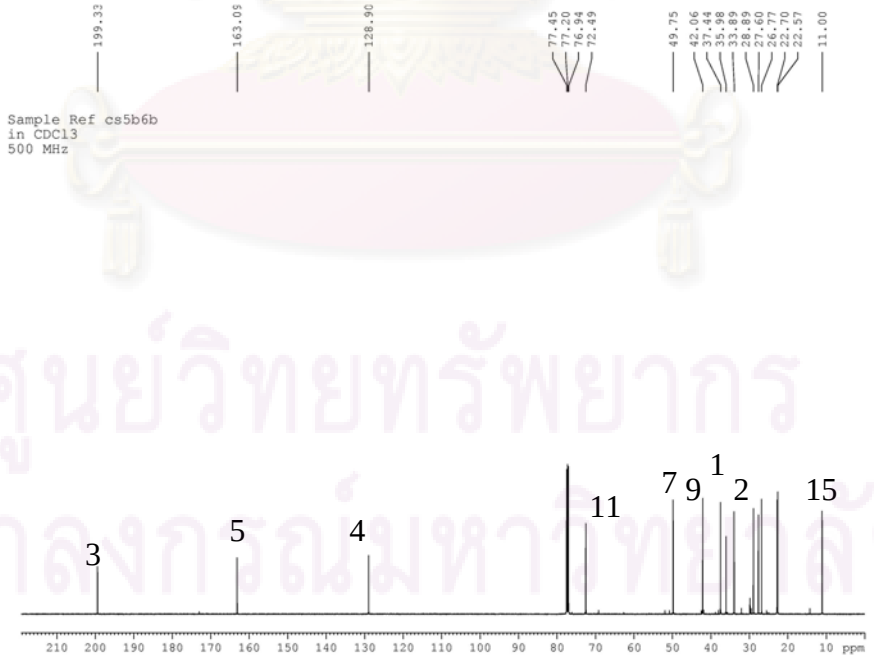

Figure 178 ^{13}C-NMR (125 MHz) spectrum of compound CS10 ($CDCl_3$)

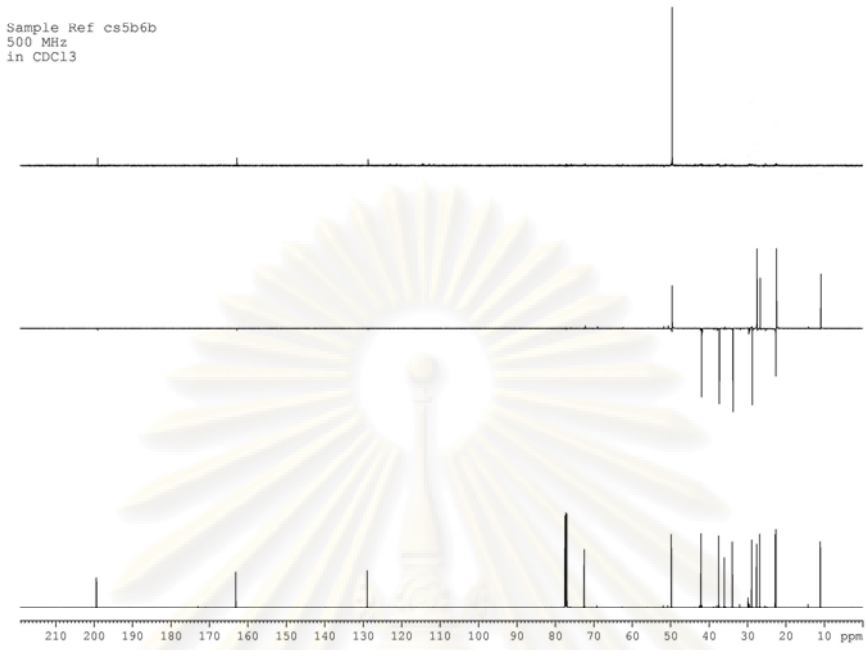

Figure 179 ^{13}C-NMR (125 MHz) and DEPT spectra of compound CS10 ($CDCl_3$)

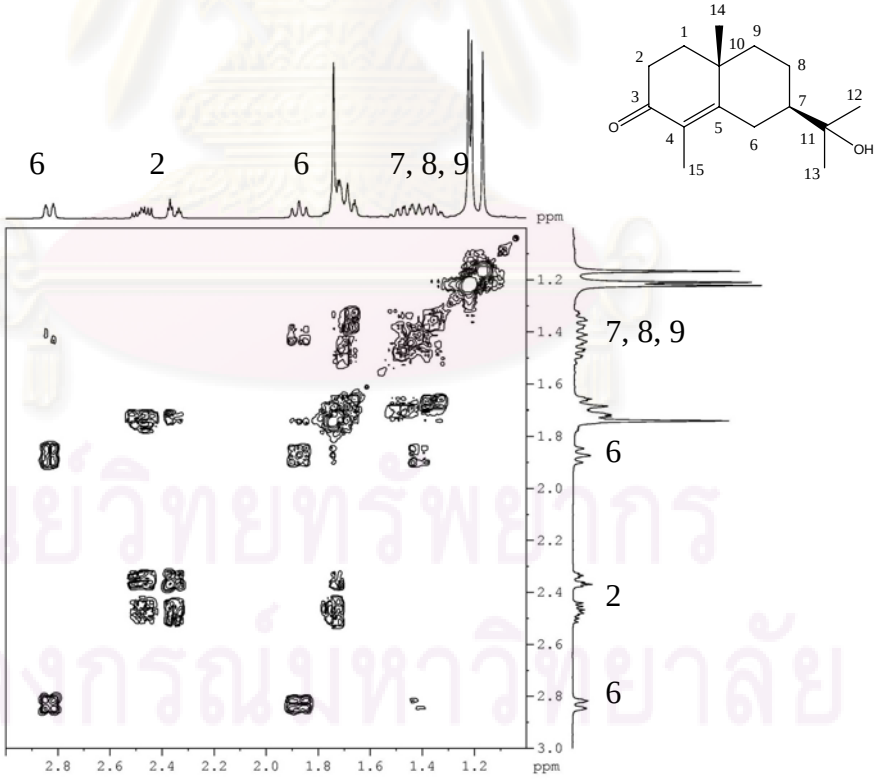

Figure 180 ^{1}H-^{1}H COSY spectrum of compound CS10 ($CDCl_3$)

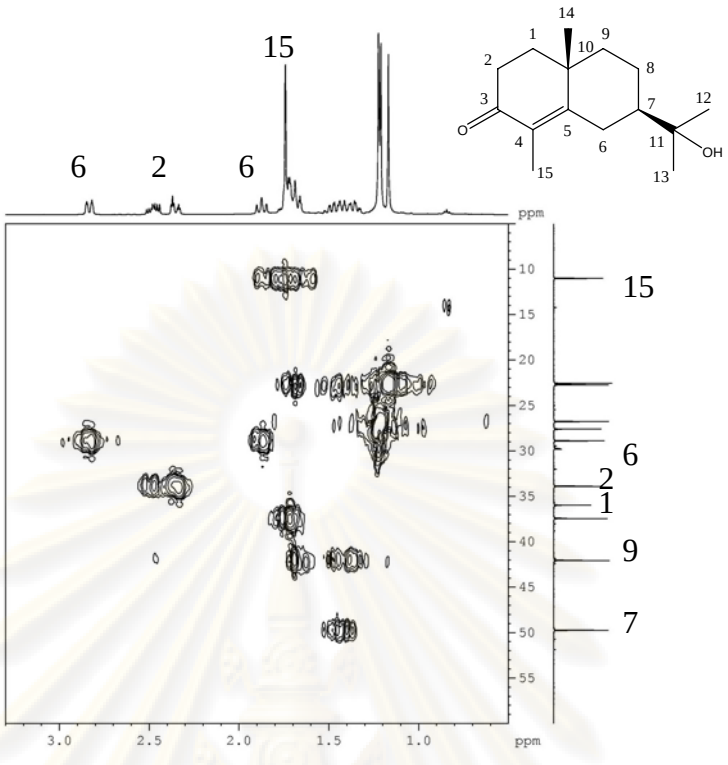

Figure 181 HMQC spectrum of compound CS10 ($CDCl_3$)

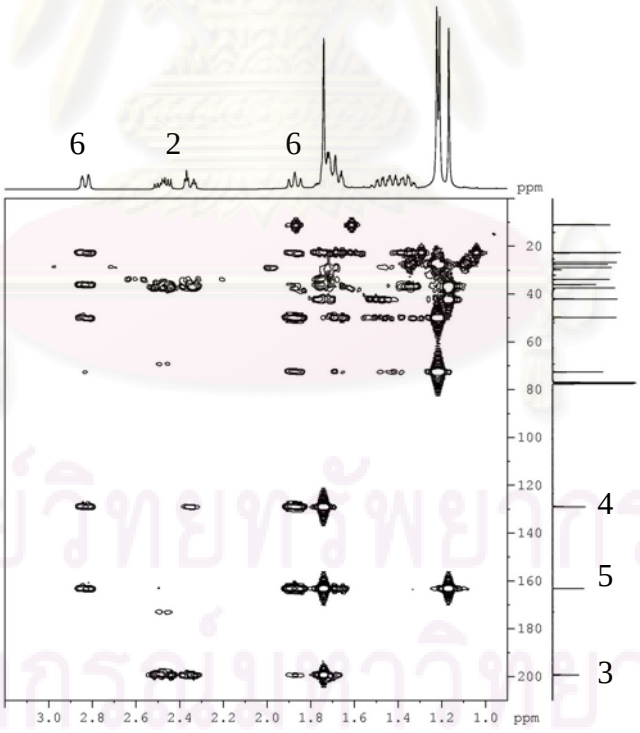

Figure 182 HMBC spectrum of compound CS10 ($CDCl_3$)
[δ_H 0.5-3.2 ppm, δ_C 10-210 ppm]

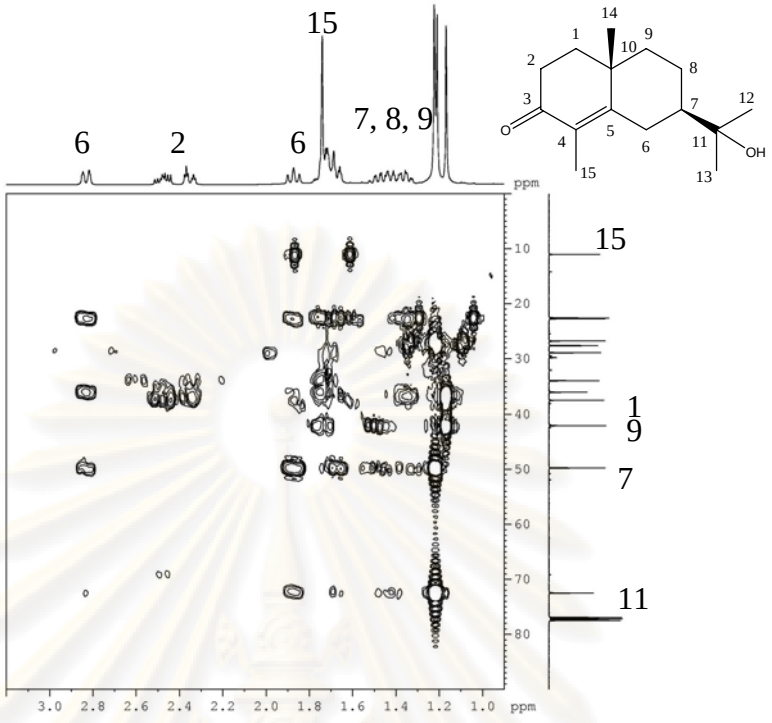

Figure 183 HMBC spectrum of compound CS10 ($CDCl_3$)
[δ_H 0.9-3.2 ppm, δ_C 5-90 ppm]

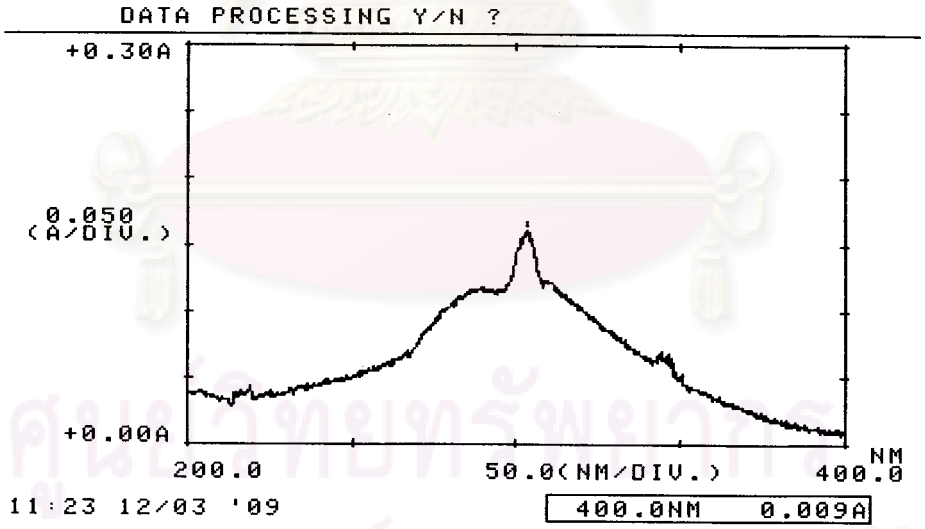

Figure 184 UV spectrum of compound CS11 (methanol)

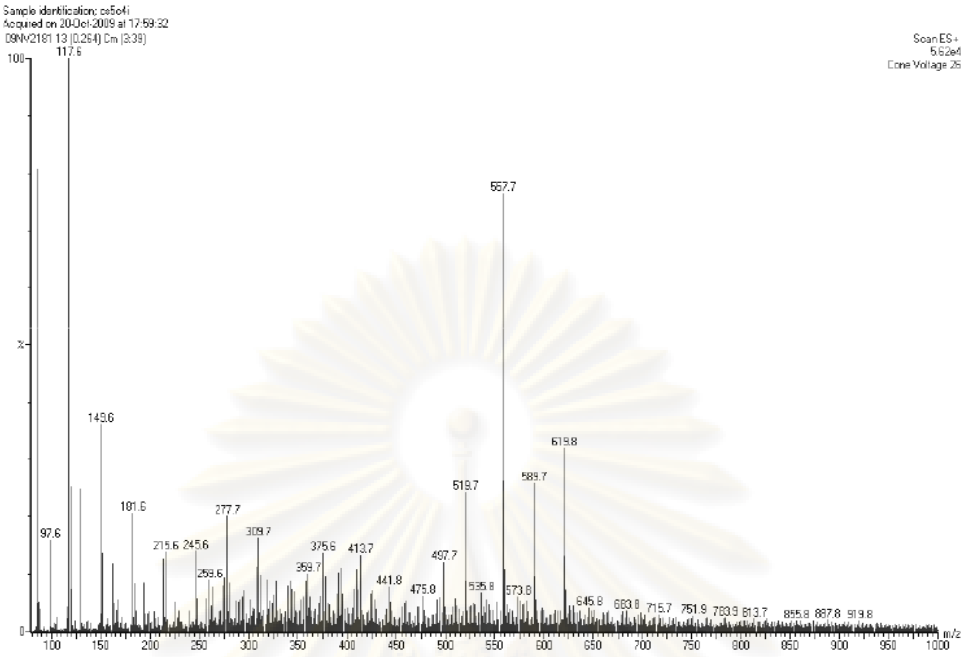

Figure 185 ESI mass spectrum of compound CS11

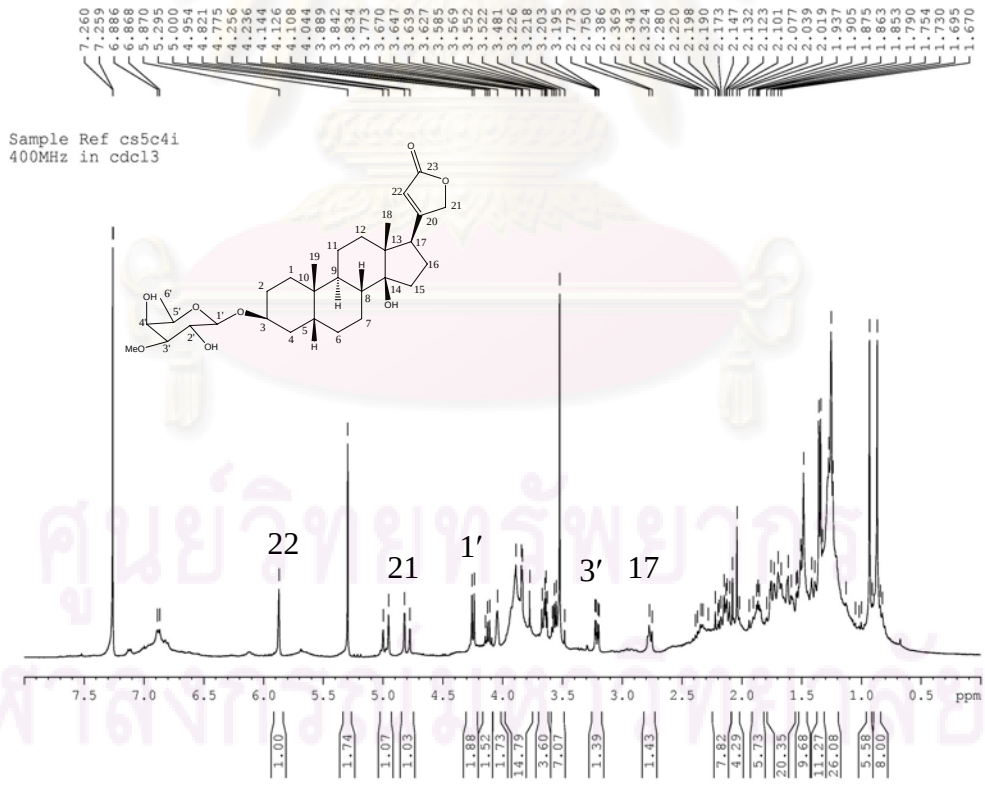

Figure 186 ^{1}H-NMR (400 MHz) spectrum of compound CS11 ($CDCl_3$)

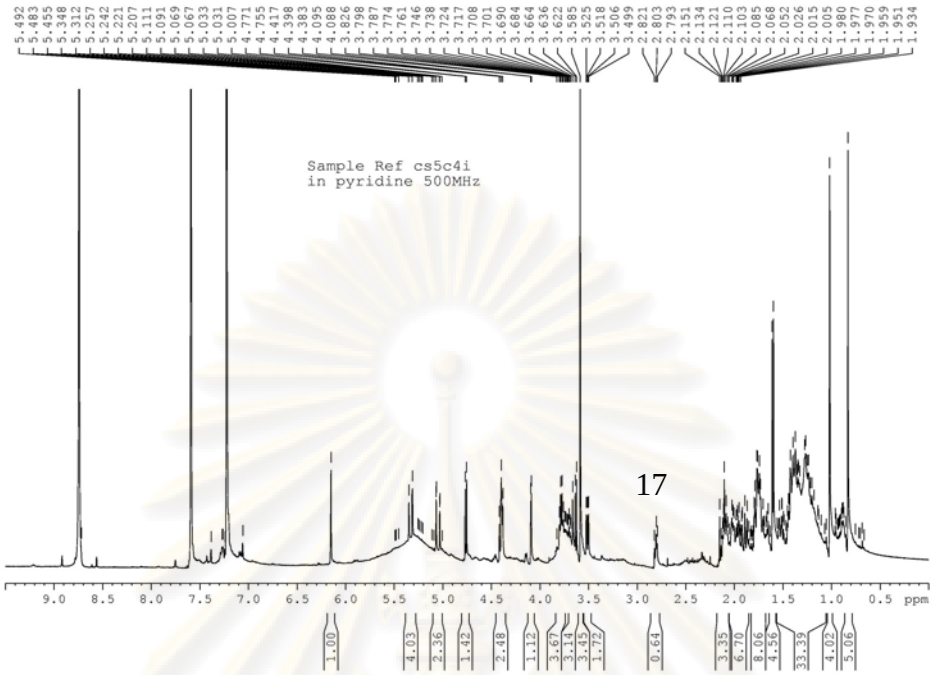

Figure 187 ^{1}H-NMR (500 MHz) spectrum of compound CS11 (pyridine-d_5)

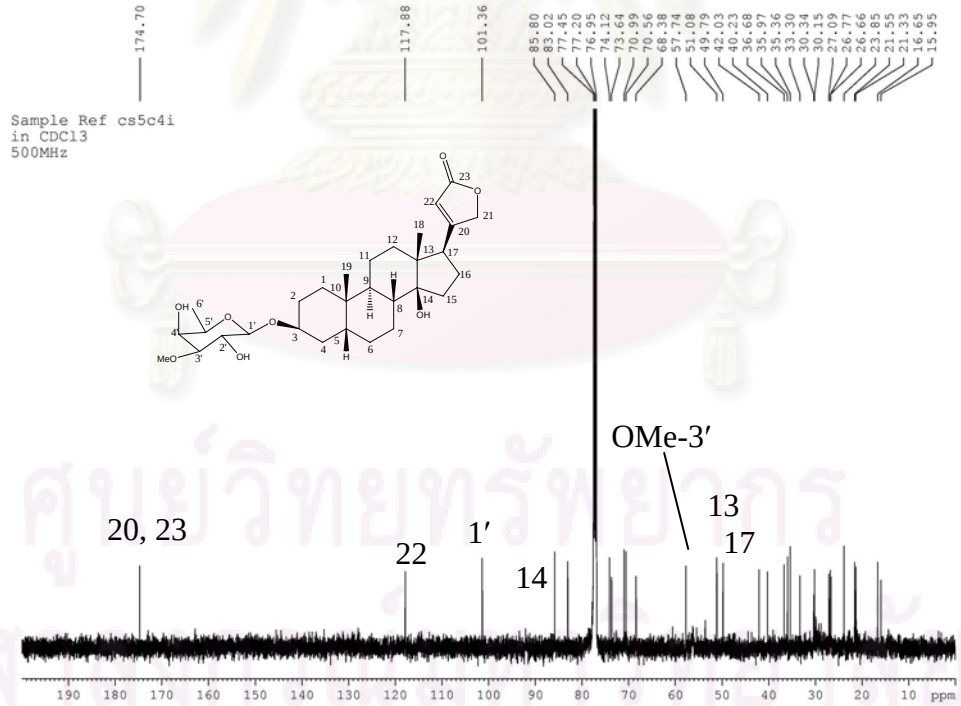

Figure 188 ^{13}C-NMR (125 MHz) spectrum of compound CS11 ($CDCl_3$)

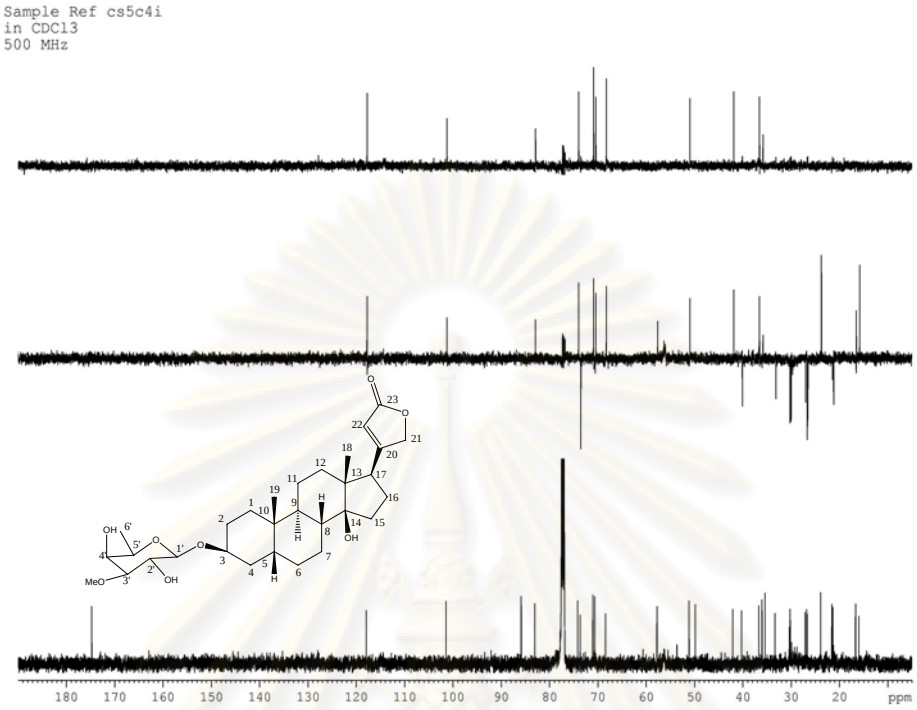

Figure 189 ^{13}C-NMR (125 MHz) and DEPT spectra of compound CS11 ($CDCl_3$)

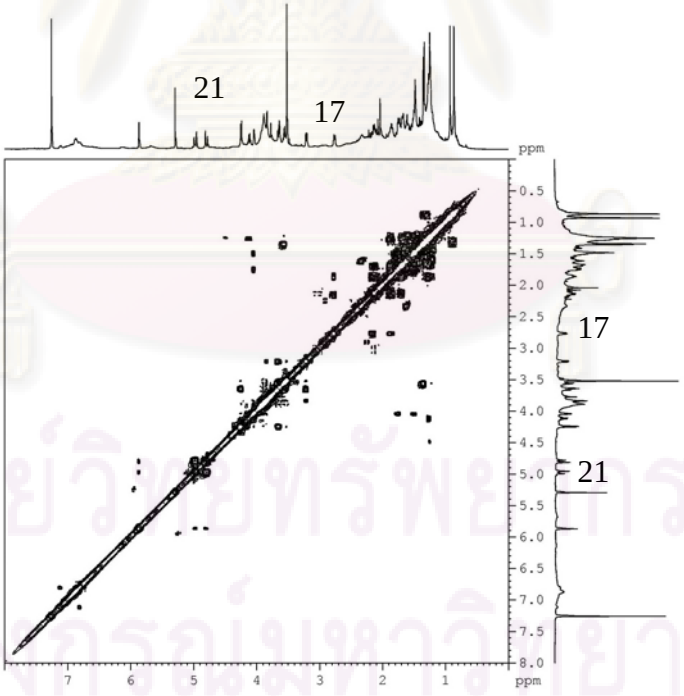

Figure 190 ^{1}H-^{1}H COSY spectrum of compound CS11 ($CDCl_3$)

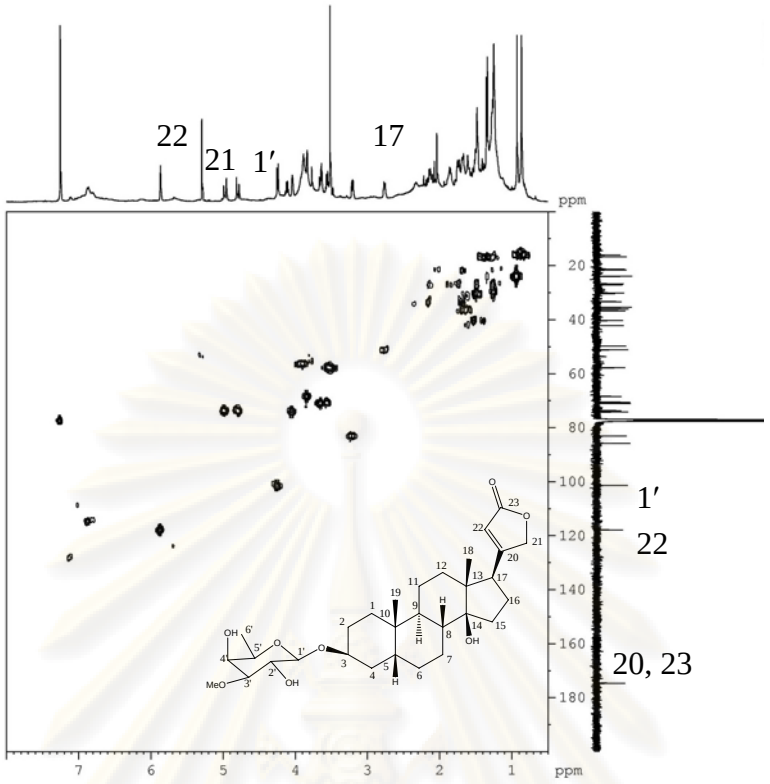

Figure 191 HMQC spectrum of compound CS11 ($CDCl_3$)

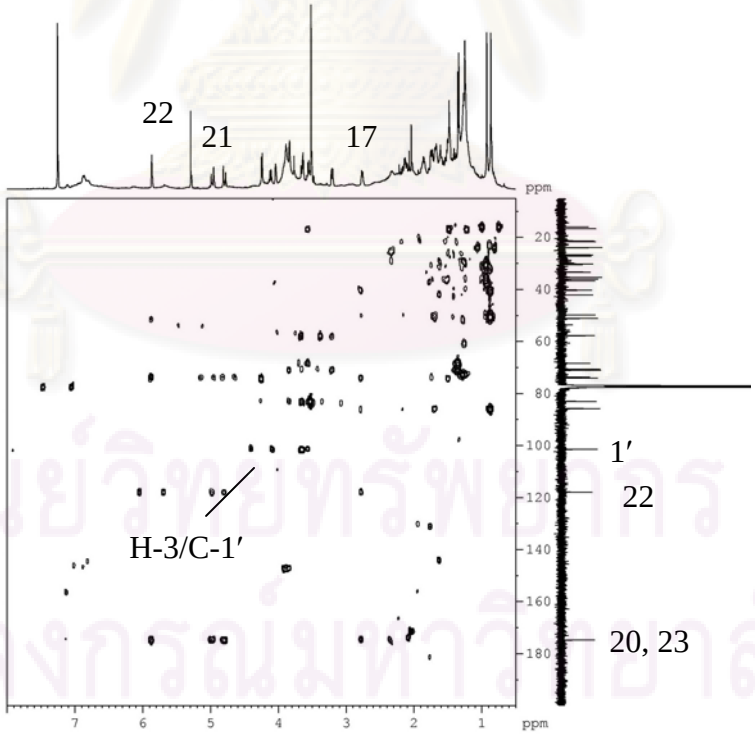

Figure 192 HMBC spectrum of compound CS11 ($CDCl_3$)
[δ_H 0.5-8 ppm, δ_C 10-190 ppm]

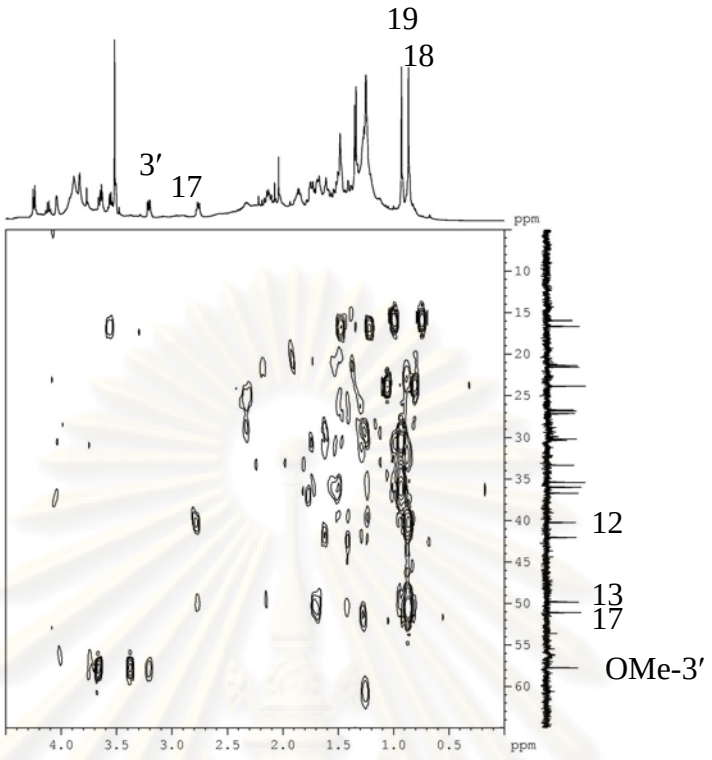

Figure 193 HMBC spectrum of compound CS11 ($CDCl_3$)
[δ_H 0-4.5 ppm, δ_C 5-70 ppm]

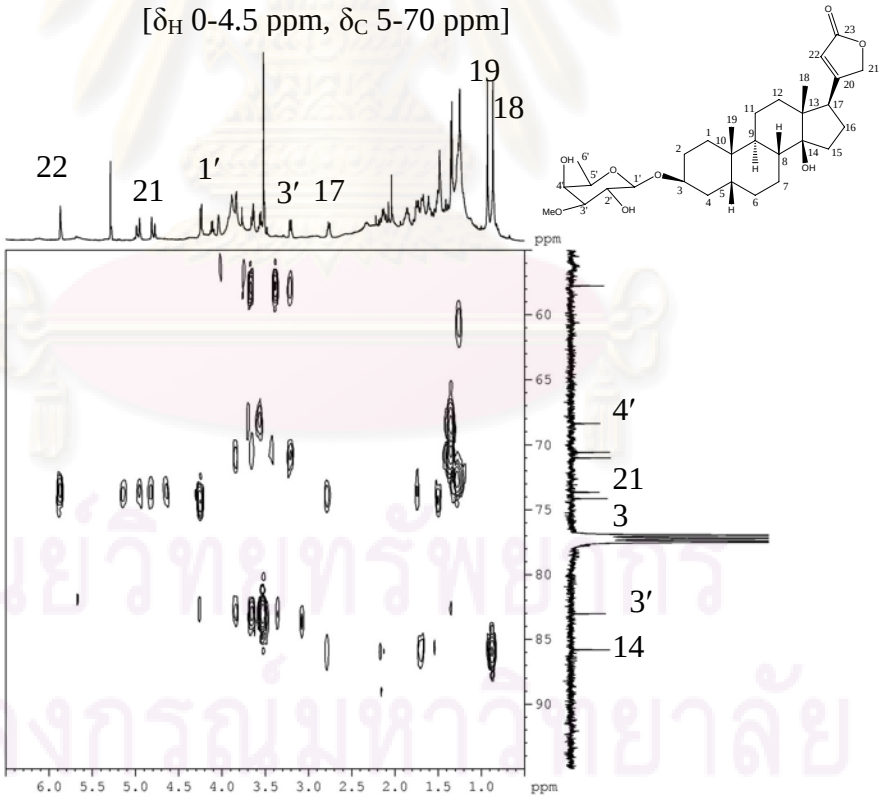

Figure 194 HMBC spectrum of compound CS11 ($CDCl_3$)
[δ_H 0.5-6.5 ppm, δ_C 55-95 ppm]

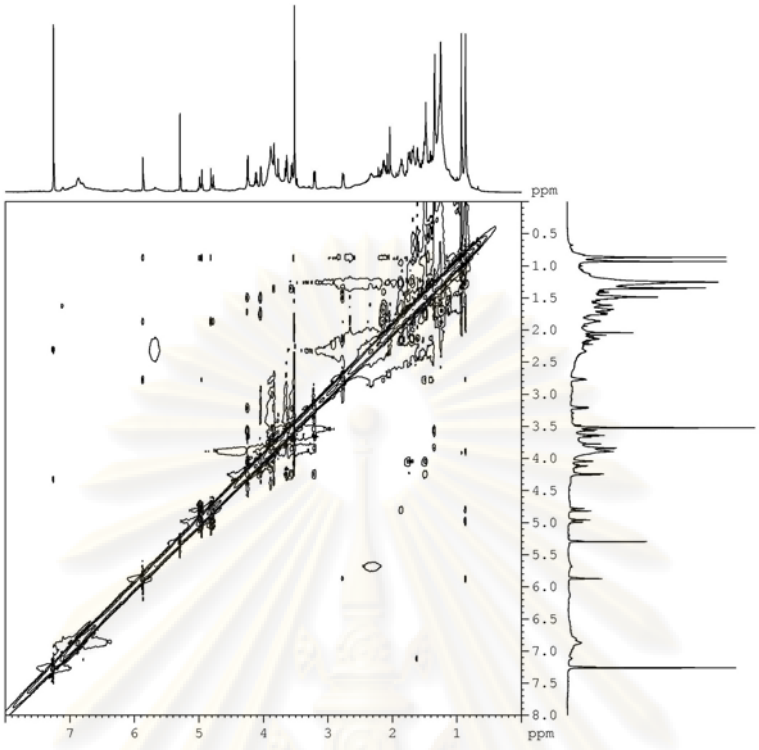

Figure 195 NOESY spectrum of compound CS11 ($CDCl_3$) [δ_H 0-8 ppm]

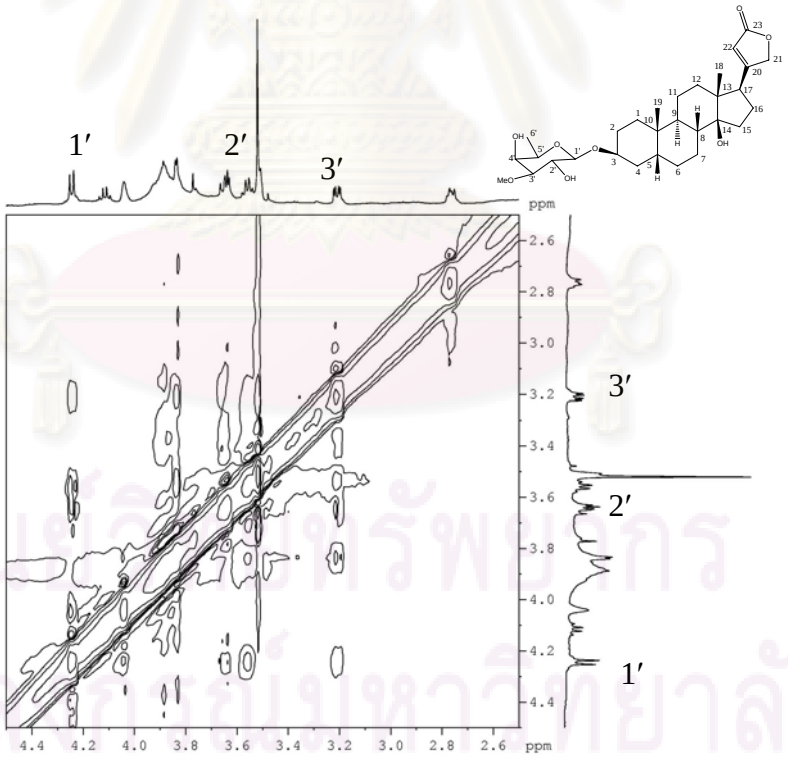

Figure 196 NOESY spectrum of compound CS11 ($CDCl_3$) [δ_H 2.5-4.5 ppm]

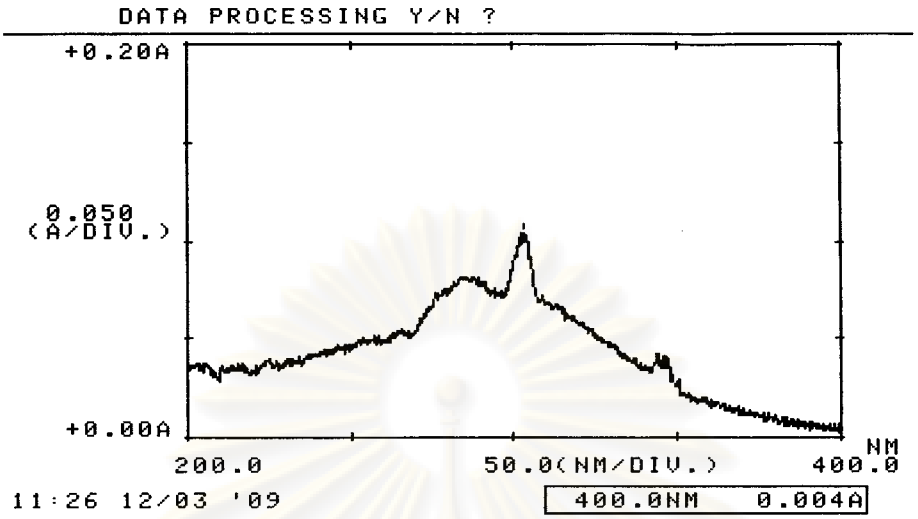

Figure 197 UV spectrum of compound CS12 (methanol)

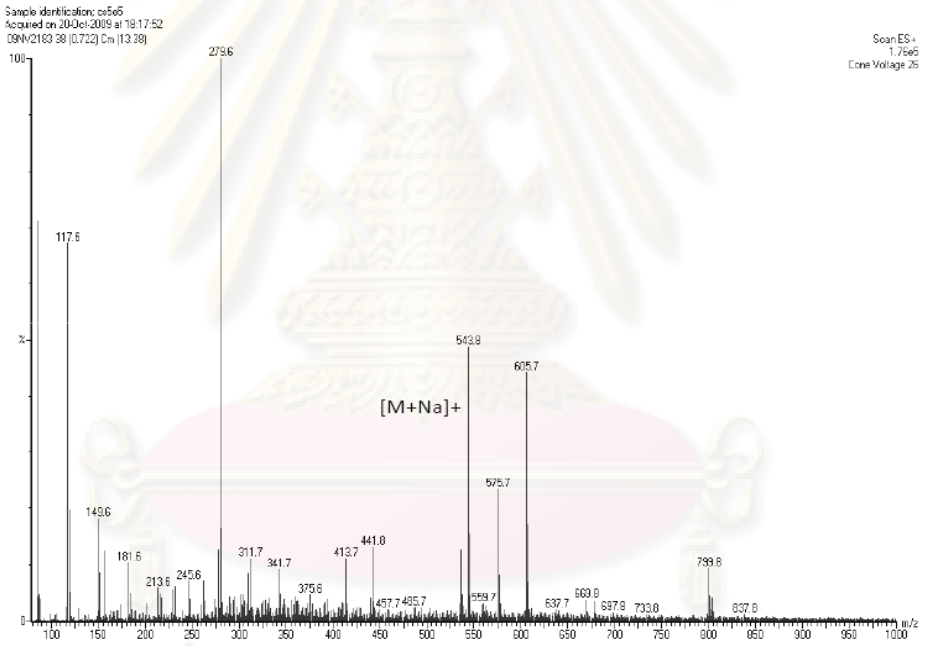

Figure 198 ESI mass spectrum of compound CS12

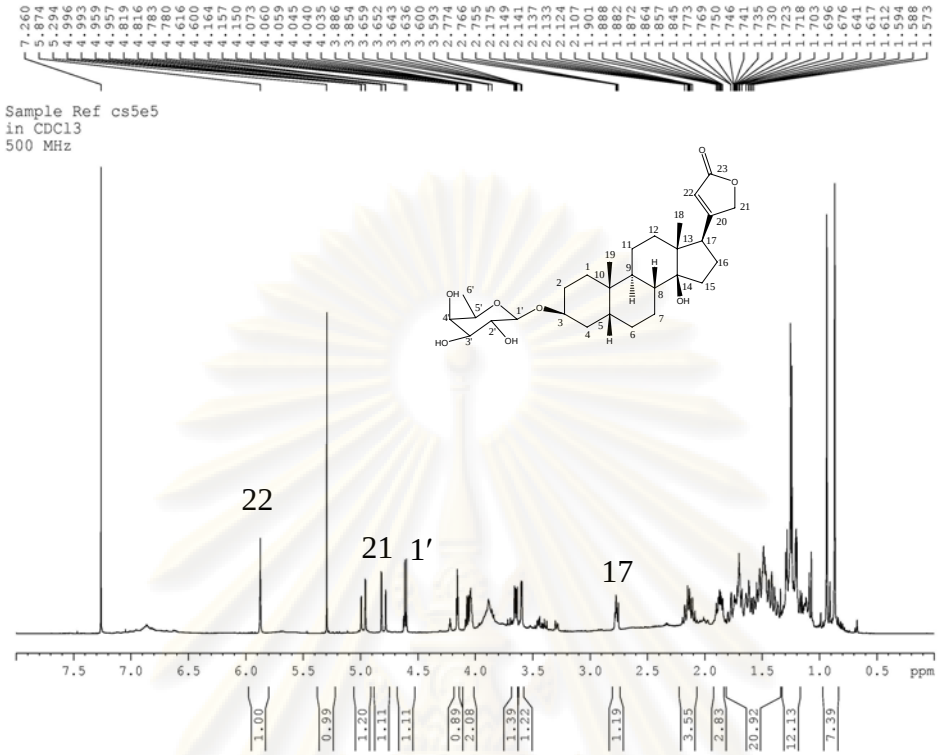

Figure 199 ^{1}H-NMR (500 MHz) spectrum of compound CS12 ($CDCl_3$)

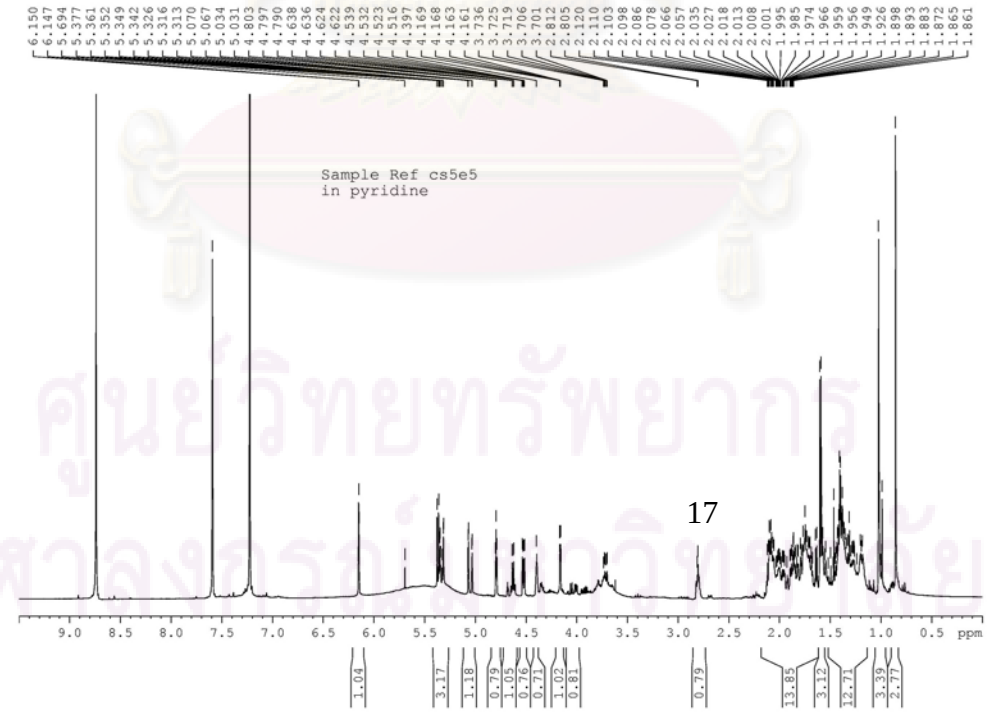

Figure 200 ^{1}H-NMR (500 MHz) spectrum of compound CS12 (pyridine-d_5)

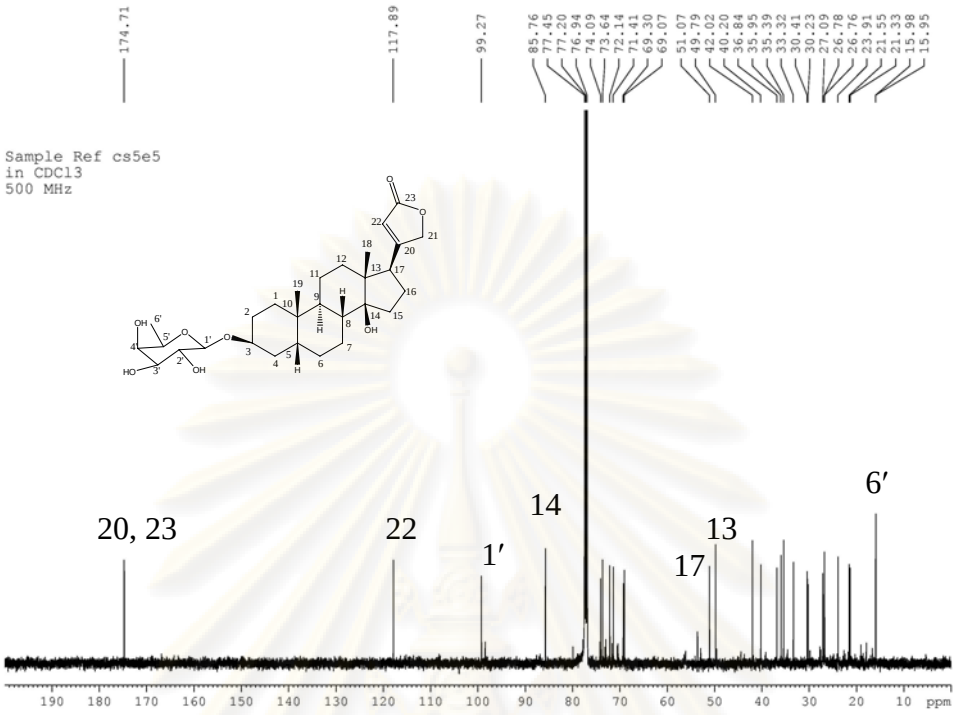

Figure 201 ^{13}C-NMR (125 MHz) spectrum of compound CS12 ($CDCl_3$)

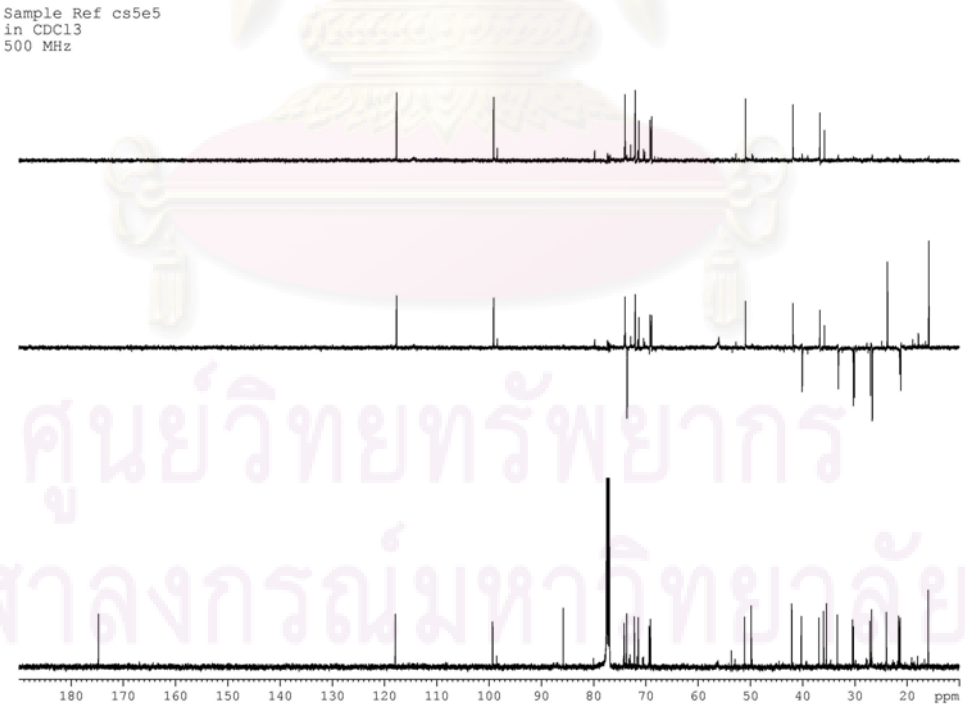

Figure 202 ^{13}C-NMR (125 MHz) and DEPT spectra of compound CS12 ($CDCl_3$)

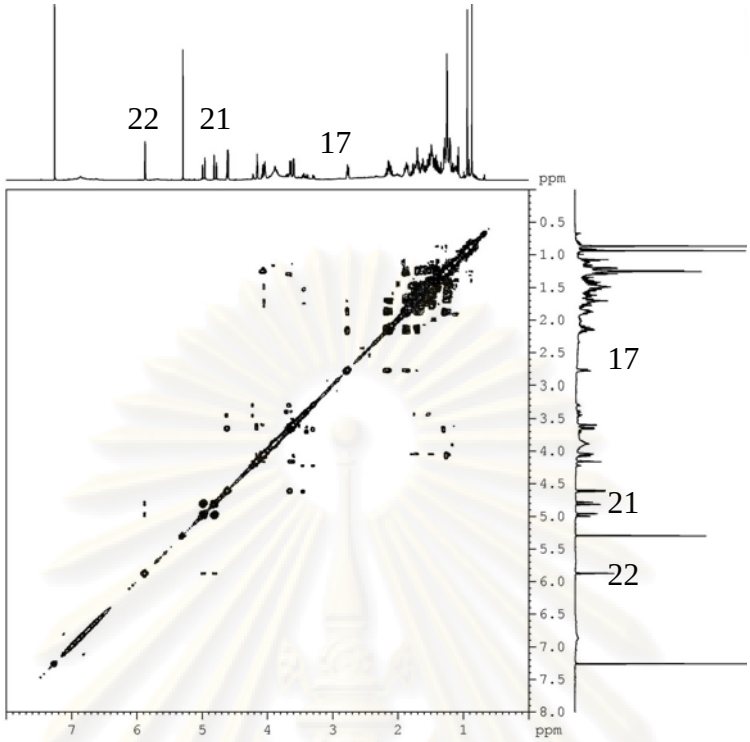

Figure 203 ^{1}H-^{1}H COSY spectrum of compound CS12 ($CDCl_3$)

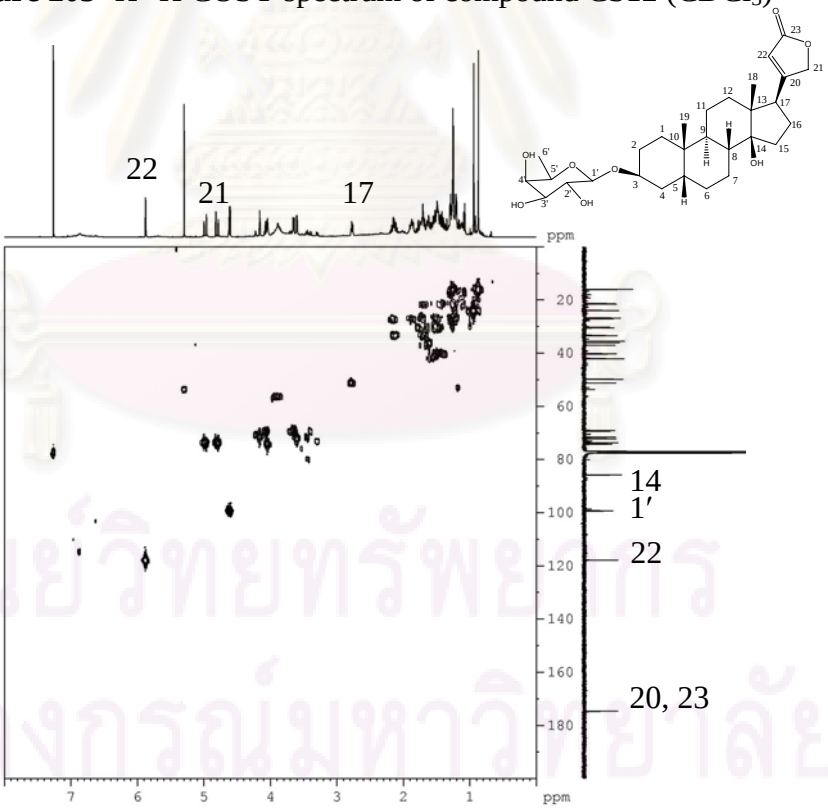

Figure 204 HMQC spectrum of compound CS12 ($CDCl_3$)

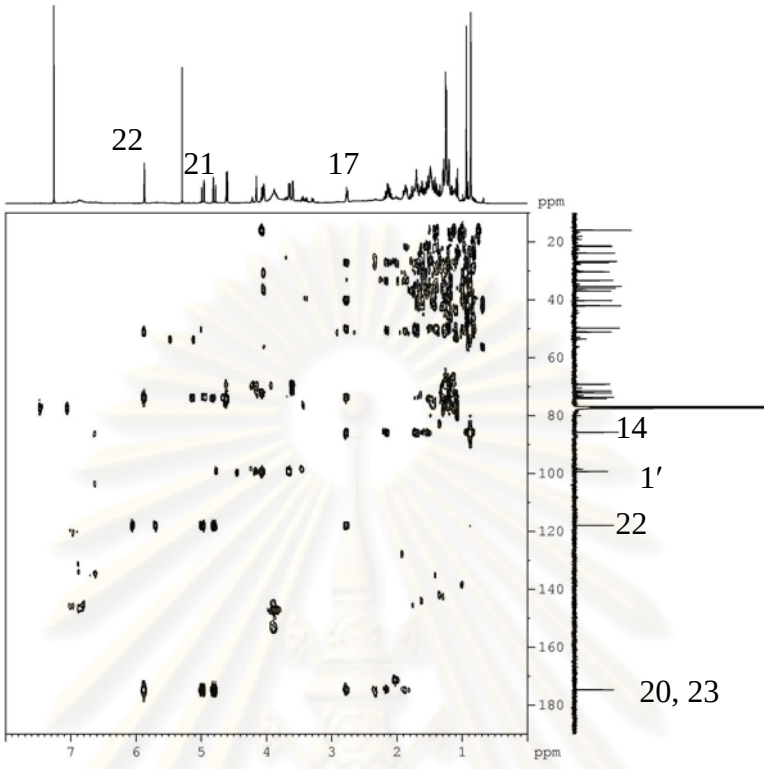

Figure 205 HMBC spectrum of compound CS12 ($CDCl_3$)
[δ_H 0-8 ppm, δ_C 10-190 ppm]

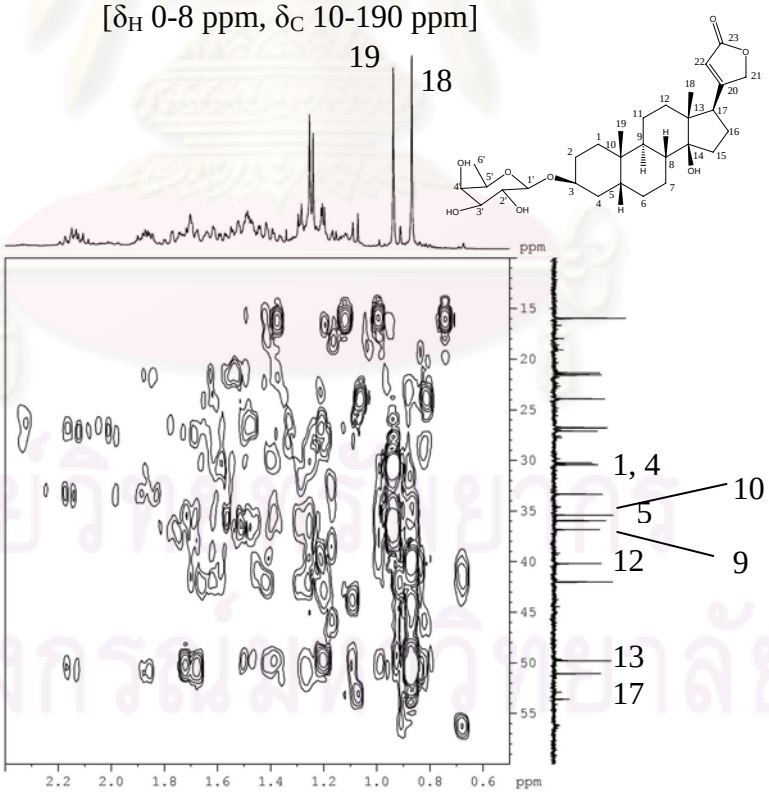

Figure 206 HMBC spectrum of compound CS12 ($CDCl_3$)
[δ_H 0.5-2.4 ppm, δ_C 10-60 ppm]

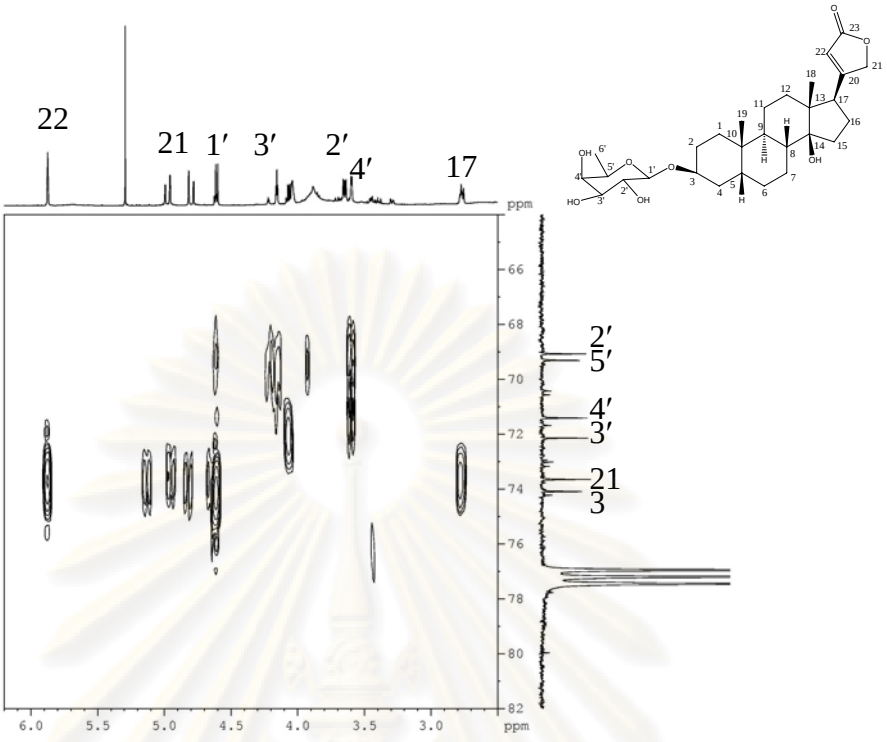

Figure 207 HMBC spectrum of compound CS12 ($CDCl_3$)]
[δ_H 2.5-6.2 ppm, δ_C 64-82 ppm]

VITA

Miss Ruchira Wangteeraprasert was born on February 25, 1982 in Bangkok, Thailand. She received her Bachelor's degree of Science in Pharmacy in 2004 from the Faculty of Pharmaceutical Sciences, Chulalongkorn University, Thailand. She was awarded a 2005 Royal Golden Jubilee Scholarship from the Thailand Research Fund and the 90th Anniversary Chulalongkorn University (Ratchadaphiseksomphot) Endowment Fund.

Publications

1. Wangteeraprasert, R., and Likhitwitayawuid, K. 2008. A new rotenoid from *Derris malaccensis*. Heterocycles 75: 403-406.
2. Wangteeraprasert, R., and Likhitwitayawuid, K. 2009. Lignans and sesquiterpene glucoside from *Carissa carandas* stem. Helv. Chim. Acta 92: 1217-1223.

Poster Presentation

1. Wangteeraprasert, R., and Likhitwitayawuid, K. Rotenoids with free radical scavenging activity from *Derris malaccensis*. pp. 67. The Eighth Joint Seminar: Innovative Research in Natutal Products for Sustainable Development, February 3-4, 2009, Faculty of Pharmaceutical Sciences, Chulalongkorn University, Bangkok.